



Probing transcriptional specificities and fate potential of postnatal neural progenitors in the mouse forebrain

Guillaume Marcy

► To cite this version:

Guillaume Marcy. Probing transcriptional specificities and fate potential of postnatal neural progenitors in the mouse forebrain. *Neurons and Cognition [q-bio.NC]*. Université Paris sciences et lettres, 2018. English. NNT : 2018PSLEP070 . tel-02177211

HAL Id: tel-02177211

<https://theses.hal.science/tel-02177211>

Submitted on 8 Jul 2019

HAL is a multi-disciplinary open access archive for the deposit and dissemination of scientific research documents, whether they are published or not. The documents may come from teaching and research institutions in France or abroad, or from public or private research centers.

L'archive ouverte pluridisciplinaire **HAL**, est destinée au dépôt et à la diffusion de documents scientifiques de niveau recherche, publiés ou non, émanant des établissements d'enseignement et de recherche français ou étrangers, des laboratoires publics ou privés.

THÈSE DE DOCTORAT

*de l'Université de recherche Paris Sciences et Lettres
PSL Research University*

Préparée à l'École Pratique des Hautes Études

Etude des Spécificités Transcriptionnelles et de la Compétence des Progéniteurs Neuraux Postnataux du Cerveau Antérieur chez la Souris

École doctorale de l'EPHE – ED 472

Spécialité : *NEUROSCIENCES*

Soutenue par :

Guillaume MARCY

le 19 décembre 2018

Dirigée par :

Giovanni STEVANIN

Olivier RAINETEAU

COMPOSITION DU JURY :

M. Giovanni STEVANIN
Université PSL EPHE Paris
Directeur

M. Olivier RAINETEAU
Université Lyon 1
Co-directeur

Mme Ana MARTIN-VILLALBA
German Cancer Research Center (DKFZ)
Rapporteure

M. Marc-André MOUTHON
Université Paris XI
Rapporteur

Mme Nadine MESTRE-FRANCES
Université de Montpellier
Présidente du Jury



École Pratique
des Hautes Études



Probing Transcriptional Specificities and Fate Potential of Postnatal Neural Progenitors in the Mouse Forebrain

Guillaume MARCY

PhD Thesis

Thesis Director: Dr. Giovanni STEVANIN

Thesis Co-Director: Dr. Olivier RAINETEAU

University Paris Sciences et Lettres

Doctoral School of EPHE – ED 472

Stem Cell and Brain Research Institute, Bron, France

Laboratory unit Inserm U1208 Team Postnatal Forebrain Development and Plasticity

Ecole Pratique des Hautes Etudes Neurogenetics Department

Public Defense on Wednesday, December 19th 2018

Reviewer: Pr. Ana MARTIN-VILLALBA

Reviewer: Dr. Marc-André MOUTHON

President: Dr Nadine MESTRE-FRANCES

Supervisor: Dr. Giovanni STEVANIN

Co Supervisor: Dr. Olivier RAINTEAU

Résumé

Pendant le développement, la coordination remarquable d'évènements moléculaires et cellulaires mène à la production du cortex cérébral qui orchestre les fonctions sensori-motrices et cognitives. Son développement s'effectue par étapes : les cellules gliales radiaires (RGs) – les cellules souches neurales (NSCs) du cerveau en développement – et les cellules progénitrices de la zone ventriculaire (VZ) et de la zone sous ventriculaire (SVZ) génèrent séquentiellement des vagues distinctes de nouveaux neurones qui formeront les différentes couches corticales. Autour de la naissance, les RGs changent de devenir et produisent des cellules gliales. Cependant, une fraction d'entre elles persiste tout au long de la vie dans la SVZ qui borde le ventricule, perdant au passage leur morphologie radiale. Ces NSCs produisent ensuite les différents sous types d'interneurones du bulbe olfactif ainsi que des cellules gliales en fonction de leur emplacement d'origine et de leur localisation dans la SVZ périnatale.

Ces observations soulèvent d'importantes questions non résolues sur 1) le codage transcriptionnel régulant la régionalisation de la SVZ, 2) le potentiel des NSCs postnatales à la régénération cellulaire et à la réparation cérébrale, et 3) la relation de lignage et les spécificités transcriptionnelles entre les NSCs et leur descendants.

Mon travail de doctorat s'est construit à partir d'une étude transcriptionnelle des différents microdomaines de la SVZ postnatale. Cette étude surlignait le haut degré d'hétérogénéité transcriptionnelle entre les NSCs et les progéniteurs et identifiait des régulateurs transcriptionnels clés soutenant la régionalisation de la SVZ. J'ai développé des approches bio-informatiques pour explorer ces banques de données et connecté l'expression de facteurs de transcription avec la génération régionale de lignages neuraux distincts. J'ai ensuite développé un modèle d'ablation ciblée qui peut être utilisé pour étudier le potentiel régénératif des progéniteurs postnataux dans divers contextes. Finalement, j'ai participé au développement d'une procédure pour explorer et comparer des populations sélectionnées de progéniteurs pré et postnataux à l'échelle de la cellule unique.

Objectif 1 : *Des expériences de transcriptomique ainsi que de cartographie ont été réalisées pour étudier la relation entre l'expression régionale de facteurs de transcription par les NSCs et l'acquisition de leur devenir dans des lignages neuraux distincts. Nos résultats suggèrent un engagement précoce des NSCs à produire des types cellulaires définis selon leur localisation spatiale dans la SVZ et identifient la protéine HOPX comme un marqueur d'une sous population biaisé à générer des astrocytes.*

Objectif 2 : *J'ai mis au point un modèle de lésion corticale qui permet l'ablation ciblée de neurones de couches corticales définies pour étudier la capacité régénérative et la spécification appropriée des progéniteurs corticaux postnataux. Une analyse quantitative des régions adjacentes, incluant la partie dorsale de la SVZ, a révélé une réponse transitoire de populations de progéniteurs définis.*

Objectif 3 : *Nous avons développé une lignée de souris transgénique nommée Neurog2^{CreERT2Ai14}, qui permet le marquage de façon conditionnelle de cohortes de progéniteurs glutamatergiques et de leurs descendants. Nous avons utilisé des approches de cartographie et montré qu'une large fraction de ces progéniteurs persiste dans le cerveau antérieur postnatal après la fermeture de la période de neurogénèse corticale. Ils ne s'accumulent pas pendant le développement embryonnaire mais sont produits par des RGs qui persistent après la naissance dans la SVZ et qui continuent de générer des neurones corticaux, bien que l'efficacité soit faible. Le séquençage d'ARN sur cellule unique a révélé une dérégulation transcriptionnelle qui corrèle avec le déclin progressif observé in vivo de la neurogénèse corticale.*

Ensemble, ces résultats soulignent le potentiel des études transcriptomiques à résoudre mais aussi à soulever des questions fondamentales comme les changements transcriptionnels intervenant dans une population de progéniteurs au cours du temps et participant aux changements de leur destinée. Cette connaissance sera la clé du développement d'approches novatrices pour recruter et promouvoir la génération de types cellulaires spécifiques, incluant les sous-types neuronaux dans un contexte pathologique.

Abstract

During development, a remarkable coordination of molecular and cellular events leads to the generation of the cortex, which orchestrates most sensorimotor and cognitive functions. Cortex development occurs in a stepwise manner: radial glia cells (RGs) - the neural stem cells (NSCs) of the developing brain - and progenitor cells from the ventricular zone (VZ) and the subventricular zone (SVZ) sequentially give rise to distinct waves of nascent neurons that form cortical layers in an inside-out manner. Around birth, RGs switch fate to produce glial cells. A fraction of neurogenic RGs that lose their radial morphology however persists throughout postnatal life in the subventricular zone that lines the lateral ventricles. These NSCs give rise to different subtypes of olfactory bulb interneurons and glial cells, according to their spatial origin and location within the postnatal SVZ.

These observations raise important unresolved questions on 1) the transcriptional coding of postnatal SVZ regionalization, 2) the potential of postnatal NSCs for cellular regeneration and forebrain repair, and 3) the lineage relationship and transcriptional specificities of postnatal NSCs and of their progenies.

My PhD work built upon a previously published comparative transcriptional study of defined microdomains of the postnatal SVZ. This study highlighted a high degree of transcriptional heterogeneity within NSCs and progenitors and revealed transcriptional regulators as major hallmarks sustaining postnatal SVZ regionalization. I developed bioinformatics approaches to explore these datasets further and relate expression of defined transcription factors (TFs) to the regional generation of distinct neural lineages. I then developed a model of targeted ablation that can be used to investigate the regenerative potential of postnatal progenitors in various contexts. Finally, I participated to the development of a pipeline for exploring and comparing select populations of pre- and postnatal progenitors at the single cell level.

Objective 1: *Transcriptomic as well as fate mapping were used to investigate the relationship between regional expression of TFs by NSCs and their acquisition of distinct neural lineage fates. Our results supported an early priming of NSCs to produce defined cell types depending of their spatial location in the SVZ and identified HOPX as a marker of a subpopulation biased to generate astrocytes.*

Objective 2: *I established a cortical lesion model, which allowed the targeted ablation of neurons of defined cortical layers to investigate the regenerative capacity and appropriate*

specification of postnatal cortical progenitors. Quantitative assessment of surrounding brain regions, including the dorsal SVZ, revealed a transient response of defined progenitor populations.

Objective 3: *We developed a transgenic mouse line, i.e. Neurog2^{CreERT2Ai14}, which allowed the conditional labeling of birth-dated cohorts of glutamatergic progenitors and their progeny. We used fate-mapping approaches to show that a large fraction of Glu progenitors persist in the postnatal forebrain after closure of the cortical neurogenesis period. Postnatal Glu progenitors do not accumulate during embryonal development but are produced by embryonal RGs that persist after birth in the dorsal SVZ and continue to give rise to cortical neurons, although with low efficiency. Single-cell RNA sequencing revealed a dysregulation of transcriptional programs, which correlates with the gradual decline in cortical neurogenesis observed in vivo.*

Altogether, these data highlight the potential of transcriptomic studies to unravel but also to approach fundamental questions such as transcriptional changes occurring in a population of progenitors over time and participating to changes in their fate potential. This knowledge will be key in developing innovative approaches to recruit and promote the generation of selected cell types, including neuronal subtypes in pathologies.

Acknowledgments

Here, I would like to share my thanks to all the people who have participated one way or another to this PhD work. Basic Research is so psychologically demanding because of Up and Downs that team work, supports, encouraging words, kindness are necessary and I wouldn't have enough words to thank all of you enough for that. It wouldn't have been possible without you!

This work was performed at the SBRI between October 2014 and December 2018 and my first thanks are to **Oliver Raineteau**. Thank you for recruiting me in 2013! It was a pleasure to help setting up the lab. My sincere gratitude to you for accepting me up into the PhD program despite the high concentration of PhD students at the same time. You were not obliged to do that. I will always be thankful for that. I have to apologize for the extra work that this created to you, especially from my “pathology” of starting everything at the last minute... I, on the personal side, really appreciated working with you, discussing, sharing and the relationship based on trust. I am, on the work side, grateful for your supervision, advices, patience and general support and will always be impressed by your . Hope this will continue as long as possible. Many thanks!

Then, I can't be grateful enough as well to **Giovanni Stevanin**. You understood my curriculum and accepted to defend my PhD application and supervise me always in a kind way. It won't have been possible without you and was lucky to meet you. Thank you for pushing me up, your optimism and advices, and to give me the chance to explore new opportunities in teaching. Many thanks!

I would like to express my thankfulness to the jury members, **Ana Martin-Villalba**, **Nadine Mestre-Frances** and **Marc-André Mouthon**. I know that the end of the year is always a heavy period so thank you so much for accepting this invitation and sacrificing your time in evaluating my work. I really appreciate it and am honored by your presence. Thanks.

I also have a thought to **Denis Jabaudon** who participated to my yearly committee. Thank you for your support, inputs and encouragements. And thank you for sharing protocols and expertise.

My gratitude goes to all the past and current lab members. Thank you for the great atmosphere you created, your friendship and the funny moments we've shared. I still think that you all were a bit crazy (me being normal) but it is good to be crazy. Wish you all, all the best! It was good to leave "abroad in France" (Switzerland, Holland, Vendée and France origins! What a good mix and good image for Europe!) I have a special thanks to **Stefan Zweifel** and **Vanessa Donega**, because we have shared projects and all the up and downs that go with it. Finally we made it through, congrats! Thank you Dr. Stefan for your friendship and your refreshing personality. I was impressed by your creativity, your meticulous way of work and the way you managed all the things during your last months. I wish I could be as good as you regarding that. Didn't honor my drinking evening with you. Hope that in the near future I can honor my promise. Geil! (I think I understood it means awesome...). Dr. Vanessa, well, I really appreciated working with you. Thanks for all the help, you were always available and enthusiastic. I could always count on you. Thanks for the discussions we had on everything, it was really nice to share things of life in general with you. I may apologize for the 2 fingers you lost while I was cutting the mouse tails. But the vision declines when you get older you know... And also for the StarWars spoilers. May the force be with you. Thank you Dr. **Elodie Gaborieau** for your refreshing and enthusiastic personality which brought fun in the office. Thanks for the easy way it was to work with you. I must say you impressed me the way you finished up the thesis and the papers. It was really an amazing job so wish you to find the right direction that make you happy now. I can't forget **Quentin Lo Giudice** who basically saved my life with bioinformatics (ha the geeks...). I don't really have words to express my gratitude for the contribution you made. And I don't forget that you saved my computer!! You showed me so many things and it was so pleasant to work with such a great person. Can't wait to assist to your thesis defense in Geneva! I also would like to thank **Charlotte Verrier**, who was a very great technician student, for the quality work you made, **Pierre Marijon** for establishing bioinformatics tools and Diane Angonin. My last words will go to **Louis Foucault**, our new PhD student. I wish you all the best and am really glad to continue working with you. Easy going, nice and always showing the desire to learn. It's impressive! Good luck! I may teach you how to fly in the future because it's definitely your weakness... I also have thoughts to **Kaz**, a previous postdoc in Olivier's former lab who taught me and provided me with a lot of information and advice at the beginning of the different projects.

I would like to thank all the different people that I knew before or those I learnt to know over the last years at the SBRI who helped me and encouraged me. I have worked here during 6 years from 2003 to 2009 so it's with a particular emotion that I am turning the page of this part of my life here. It is great to work with you and can't cite and thank all of you here. Still, my thankfulness to **Colette Dehay** and **Henry Kennedy** for their support, **Chandara Nay** and **Jennifer Beneyton** for their administrative support and to **all the animal facility technicians** for their help. I would like to thank some people outside SBRI for their technical assistance, expertise and contribution: people from **ProfilExpert** and **Isabelle Durand**.

The last but not the least, I have no doubt when I am saying that you helped me to hold when things are not working and that it would have been so much more difficult without you. You are always here to give me more strength and self-confidence and to push me forward. Thank you for being in my life and thank you for the sacrifice you made, professionally and personally, to allow me to concentrate to finish this up. My forever thank to you **Irène**. And of course, how can I not say a word on my **two little monsters**. I wasn't sure if I would thank you kids because you didn't really help me to rest and relax!! but only you can transform the worse day ever into peanuts by a simple look or smile which make me realizing what's really important in life. Love you and hope you will be proud of me because it's a bit for you that I was doing it.

Long Résumé

Une activité germinale persiste dans le cerveau postnatal des mammifères dans des niches spécialisées, à savoir le gyrus denté (DG) de l'hippocampe et la zone sous-ventriculaire (SVZ) qui entoure le ventricule latéral (LV). Les cellules souches neuronales (NSCs) de la SVZ postnatale se divisent et donnent naissance à des progéniteurs transitoires (TAPs) qui génèrent des neuroblastes migrant via la voie de migration rostrale (RMS) vers le bulbe olfactif (OB), où ils se différencient en neurones. La SVZ génère en outre des progéniteurs gliaux qui envahissent le parenchyme local. Récemment, de plus en plus de preuves ont mis en évidence la nature hétérogène de la SVZ postnatale en ce qui concerne ses différents microdomaines générant des lignages neuraux distincts. Par exemple, les progéniteurs des neurones GABAergiques sont principalement dérivés de la SVZ latérale (ISVZ), tandis que la production des progéniteurs des neurones glutamatergiques est limitée à la SVZ dorsale (dSVZ). De plus, des oligodendrocytes postnatals sont générés à partir de la dSVZ.

Cette hétérogénéité a pour origine le développement embryonnaire précoce et est intrinsèquement codée par l'expression de facteurs de transcription (TFs) spécifiques. Ainsi, l'expression régionalisée de TFs enrichis dans des régions du cerveau antérieur embryonnaire persiste dans les microdomaines correspondants de la SVZ postnatale. Nous avons récemment décrit les hétérogénéités transcriptionnelles des différentes populations de cellules contenues dans la SVZ postnatale. Ainsi, un nombre élevé et inattendu de transcrits (1900) étaient exprimés de manière différentielle dans des NSCs et TAPs isolés à partir de microdomaines définis de la SVZ. Nous avons observé que l'hétérogénéité transcriptionnelle observée entre les NSCs latérales et dorsales (dNSCs et INSCs) était due à l'expression de facteurs de transcription. Notamment, la protéine HOPX a été identifiée avec une expression abondante spécifiquement dans les dNSCs. HOPX est une petite protéine atypique (73 acides aminés) de la famille homeobox dépourvue de sites de liaison à l'ADN. L'expression d'Hopx est minimale au jour embryonnaire 14,5 (E14,5) et atteint un pic autour d'E16,5 avec un gradient rostromédial à caudolatéral. La protéine HOPX est exprimée dans les cellules souches du gyrus denté de l'hippocampe chez l'adulte, alors qu'elle est décrite comme étant systématiquement absente de la SVZ adulte. De plus, HOPX a récemment fait l'objet d'une attention croissante en raison de son expression dans les NSCs quiescentes, dans les astrocytes matures du DG de la souris adulte (Li et al., 2015), ainsi que dans les cellules de la glie radiaire externe (oRG) du cerveau humain en développement (Pollen et al., 2015; Thomsen et al., 2015a).

Dans mon **premier chapitre expérimental**, des approches transcriptomiques et de cartographie du devenir cellulaire ont été utilisées pour explorer la relation entre l'expression régionale de facteurs de transcription par des cellules souches neurales (NSCs) et leur spécification dans des lignages neuraux définis. En particulier, nous avons caractérisé le lignage et le profil d'expression spatio-temporelle d'HOPX dans la SVZ postnatale. J'ai développé en collaboration avec Q. Lo Giudice un outil bio-informatique appelé Heatmap Generator qui vise à combiner et à comparer des ensembles de données de transcription publiés afin de réaliser une méta-analyse. J'ai également effectué des expériences histologiques ainsi qu'une méta-analyse d'une expérience de séquençage d'ARN sur cellule unique récemment publiée. Nos résultats démontrent un amorçage précoce des NSCs pour la genèse de types cellulaires définis en fonction de leurs localisations spatiales dans la SVZ et identifient HOPX comme marqueur d'une sous-population amorcée vers un destin astrocytaire.

Dans cette étude, les TFs qui régulent des lignages neuronaux distincts ont été caractérisées pour leur enrichissement dans des microdomaines spécifiques de la SVZ. En sélectionnant l'un de ces transcrits, nous montrons que les NSCs se distinguent spatialement et qu'elles sont amorcées dans la différenciation vers des destins neuronaux spécifiques. Nos résultats identifient Hopx comme un gène révélant une hétérogénéité accrue de la SVZ dorsale (dSVZ) régulant certains aspects de l'astrogenèse.

La diversité des sous-types de neurones générés par les NSCs de la SVZ après la naissance est beaucoup plus grande qu'on ne le pensait. Le concept de régionalisation de la SVZ, dans lequel la genèse de lignées neuronales distinctes est régulée spatialement et temporellement, est de plus en plus étudié. Les NSCs situées dans les microdomaines SVZ proviennent de régions spécifiques du cerveau antérieur en développement (Fuentealba et al., 2015a) et génèrent une grande diversité de cellules neurales, y compris des sous-types neuronaux, en fonction de l'expression de programmes de transcription spécifiques. En conséquence, l'expression des TFs est directement corrélée à l'acquisition de destins neuronaux définis, un concept qui a été exploré dans cette première étude.

Nous avons tiré parti du transcriptome du génome entier des NSCs postnatales spécifiques aux différentes régions de la SVZ, récemment décrit (Azim et al., 2015). Une méta-analyse des TFs exprimés dans les NSCs latérales et dorsales avec des jeux de données de sous-populations neuronales et gliales isolées à partir du cerveau antérieur (Cahoy et al., 2008) a mis en évidence des réseaux transcriptionnels correspondant aux

lignages dérivés des NSCs de chaque micro-domaines. Nous démontrons ainsi que l'expression précoce de TFs spécifiques amorcent les NSCs dans un destin spécifique. Une tel amorçage précoce est corroboré par un séquençage de l'ARN en cellule unique des NSCs de la SVZ adulte (Llorens-Bobadilla et al., 2015). L'identification de marqueurs de NSCs régionalisées, tels que HOPX, facilitera grandement l'exploration de l'hétérogénéité spatiale et de la nature restreinte des NSCs lors de la génération de lignées neuronales spécifiques. En utilisant deux approches distinctes, nous démontrons que l'expression d'HOPX est limitée à une sous-population de NSCs dorsales (dNSCs) alors que son expression est minimale dans les NSCs latérales (INSCs). De plus, nos résultats impliquent une association d'HOPX dans le lignage astroglial. De même, au stade embryonnaire 17.5 (E17.5), l'ARNm d'Hopx est confiné (20%) à une sous-population de cellules gliales radiaires (RGCs) – les cellules souches du cerveau en développement – (20%) caractérisée par un enrichissement en marqueurs astrocytaires issus des astrocytes de la SVZ adulte. Ceci est en corrélation avec la cartographie récente réalisée de manière clonale, du destin des RGCs suggérant une transition neurogénique à gliogénique en grande partie incomplète, dans la mesure où seulement une fraction des RGCs (estimée à environ 1/6) produit des cellules gliales. Il est important de noter, bien que l'expression d'HOPX soit observée dans une sous-population de NSCs produisant principalement des astrocytes, HOPX ne peut pas être considérée comme un marqueur astrocytaire général. En effet, l'expression d'HOPX est limitée dans l'espace et est donc susceptible d'être associée à la génération d'une sous-population d'astrocytes. Des études de cartographie de lignage ont révélé que les astrocytes sont localement produits selon le site embryonnaire d'origine dans la zone ventriculaire (Tsai et al., 2012). En outre, l'analyse transcriptomique d'astrocytes isolés de différentes régions du cerveau révèle une expression hétérogène de plusieurs marqueurs astrocytaires. Par exemple, HOPX s'est avéré être enrichi dans les astrocytes du cerveau antérieur dorsal (cortex et hippocampe) et faiblement exprimé dans les astrocytes des régions sous-corticales (thalamus et hypothalamus; Morel et al., 2017). L'hétérogénéité des astrocytes dans le CNS a récemment été décrite comme influençant la synaptogenèse et la maturation neuronale via la sécrétion de plusieurs protéines de la matrice extracellulaire (Eroglu et Barres, 2010). De plus, la densité d'astrocytes varie considérablement entre les régions du cerveau (Azevedo et al., 2009). Le rôle d'HOPX dans l'acquisition des propriétés et / ou la régulation des densités des astrocytes régionaux reste à explorer.

Les mécanismes par lesquels HOPX assure ses fonctions restent largement inconnus. HOPX est un TF atypique qui ne se lie pas directement à l'ADN, mais module d'autres TFs et / ou effecteurs de voies de signalisation au niveau post-transcriptionnel. Une interaction

d'HOPX avec SRF a été démontrée au cours du développement cardiaque (Shin et al., 2002), mais il est peu probable qu'elle se produise dans la SVZ où l'expression de SRF reste faible (données non présentées). Une fonction plus probable d'HOPX est la modulation des voies de signalisation dorsalement actives, telles que les voies BMP et WNT (voir aussi Azim et al. 2014; Azim et al. 2017), qui ont été démontrées comme raffinant l'astrogenèse avec la neurogenèse au cours de corticogenèse (Gross et al., 1996; Takizawa et al., 2001; Tiberi et al., 2012). Une action réciproque entre BMP et WNT a été rapportée dans plusieurs populations de progéniteurs (He et al., 2004; Plikus et al., 2008; Kandyba et al., 2013; Genander et al., 2014; Song et al., 2014). et peut être intégrée par l'expression d'HOPX, comme récemment démontré dans les cardiomyoblastes (Jain et al., 2015). Des études futures visant à manipuler l'activité de ces deux voies de signalisation chez les animaux HOPX KO pourraient nous permettre d'aborder ces questions et d'étudier le rôle de l'intégration du signal extrinsèque dans la spécification du lignage des populations de NSCs voisines.

Il est intéressant de penser que d'autres voies de signalisation peuvent influencer le profil d'expression d'HOPX et pourraient être impliquées dans son évolution chez les primates. Curieusement, l'expression d'HOPX dans la SVZ de souris suit la maturation spatio-temporelle des cellules épendymaires, ce qui peut limiter progressivement le contact des RGCs avec le liquide céphalorachidien (Mery et al., 2010). Ceci, combiné à l'expression d'HOPX dans les oRGCs, qui manquent de processus apicaux chez les primates, suggère qu'un signal inconnu sécrété par dans le liquide céphalo-rachidien pourrait réguler l'expression d'HOPX. En résumé, nos travaux démontrent que la dSVZ est beaucoup plus hétérogène qu'on ne le pensait auparavant en termes de ségrégation spatiale et d'amorçage précoce des NSCs lors de la génération de lignages neuronaux spécifiques. L'expression abondante du TF HOPX contribue à l'hétérogénéité intrarégionale de la dSVZ chez les rongeurs.

*Dans mon **deuxième chapitre expérimental**, des approches transcriptomiques et de cartographie du devenir cellulaire ont été utilisées pour étudier l'origine, les spécificités transcriptionnelles et la compétence des progéniteurs glutamatergiques (Glu) postnataux. J'ai établi le pipeline complet de l'isolement des progéniteurs Glu des souris Ng2^{Cre}2Ai14 - après optimisation des injections de tamoxifène - à l'analyse bioinformatique du séquençage d'ARN en cellule unique à l'aide du logiciel Seurat sous R. J'ai également effectué des manipulations génétiques in vivo sur des embryons ainsi que sur des animaux nouveau-nés pour aborder la question de l'origine et de la compétence des progéniteurs Glu. Nos résultats ont montré qu'une grande partie des progéniteurs Glu*

persistaient dans le cerveau antérieur postnatal après la fermeture de la période de neurogenèse corticale. Les progéniteurs postnataux Glu ne s'accumulent pas au cours du développement embryonnaire mais sont produits par des cellules gliales radiales embryonnaires qui persistent après la naissance dans la zone sous-ventriculaire dorsale (dSVZ) et continuent à donner naissance à des neurones corticaux, bien que l'efficacité soit faible. Le séquençage d'ARN sur cellule unique révèle une dérégulation des programmes transcriptionnels corrélée au déclin progressif de la neurogenèse corticale observé in vivo. Des manipulations génétiques et pharmacologiques montrent que les progéniteurs postnataux sont partiellement permissifs.

Au cours du développement cortical, les neurones glutamatergiques naissent de progéniteurs Glu situés dans la zone ventriculaire (VZ) et la zone sous-ventriculaire (SVZ) et s'assemblent pour former les circuits sous-jacents aux fonctions cognitives. Comme décrit précédemment, il est généralement admis que la période de neurogenèse corticale s'achève autour du jour embryonnaire (E) 17,5 chez la souris, les progéniteurs neuronaux changeant alors de destin pour produire des astrocytes (Li et al., 2012). Cependant, une fraction importante des progéniteurs neuronaux ne change pas de destin. Par exemple, une population de progéniteurs subsistant dans la SVZ postnatale contribue à la neurogenèse du bulbe olfactif et à la gliogenèse parenchymateuse tout au long de la vie (Doetsch et al., 1999b). Certains au moins de ces progéniteurs proviennent de cellules de la glie radiale (RGCs) embryonnaires, cyclant lentement ou en quiescence, qui se divisent entre E13.5 et E15.5 (Fuentetaja et al., 2015b; Furutachi et al., 2015). L'analyse de la cartographie de leur destinée a montré qu'elles donnaient lieu à des lignages neuronaux et / ou gliaux distincts, en fonction de leur localisation dans la SVZ (Fiorelli et al., 2015). Étonnamment, plusieurs études suggèrent la persistance des progéniteurs Glu dans la SVZ dorsale (dSVZ) jusqu'au début de l'âge adulte (Brill et al., 2009; Winpenny et al., 2011). Nous avons utilisé des souris Neurog2^{CreERT2} / tdTom pour marquer de manière permanente et spécifique des cohortes synchrones de progéniteurs prénatux et postnataux Glutamatergiques afin d'étudier leurs relations de lignage et leurs spécificités transcriptionnelles. Nos résultats montrent que les progéniteurs Glu continuent à être produits après la fermeture de la période de neurogenèse corticale. Le séquençage d'ARN sur cellule unique (scRNA-seq) révèle que les progéniteurs postnataux Glu présentent une dérégulation des gènes impliqués dans le métabolisme, la différenciation et la migration, parallèlement à un déclin rapide de leur capacité à migrer et à se différencier. Nos données suggèrent que cette dérégulation de la transcription chez les progéniteurs de Glu postnataux pourrait résulter d'une diminution de la méthylation de la N6-méthyladénosine (m6A) de certains gènes proneuronaux. Néanmoins, les progéniteurs postnataux Glu

restent partiellement permissifs aux manipulations pharmacologiques et génétiques ce qui suggère qu'ils pourraient être recrutés pour une réparation corticale.

La période périnatale a longtemps été considérée comme une période de gliogenèse corticale exclusive associée à la maturation des neurones nés pendant le développement embryonnaire et à leur intégration dans des circuits fonctionnels. Cette vision est actuellement contestée par la démonstration de la neurogenèse dans des régions corticales spécifiques. Ainsi, les progéniteurs GABAergiques s'accumulent dans la substance blanche postnatale précoce et donnent naissance à une sous-population d'interneurones interstitiels corticaux (Frazer et al., 2017). De plus, il a été démontré que la migration des interneurones dans le cortex frontal persistait tôt après la naissance chez les rongeurs (Inta et al., 2008; Le Magueresse et al., 2012), ainsi que chez les bébés humains (Nogueira et al., 2003). 2017).

Nos résultats révèlent que cette neurogenèse persistante ne se limite pas à la lignée GABAergique mais inclut également les neurones de la lignée glutamatergique. En effet, notre travail identifie une petite population de neurones corticaux Satb2/Cux1⁺ générés à la naissance. Les neurones survivants développent des épines et des projections axonales intracorticales, favorisant ainsi leur intégration dans les réseaux corticaux. Nos résultats indiquent en outre que ces neurones proviennent d'une large population palliale de RGCs qui ne basculent pas vers l'astrogenèse et persistent dans la dSVZ. Ces résultats sont en accord avec des expériences MADM suggérant que seulement 1 cellule neurogénique radiaire sur 6 produit des cellules gliales (Gao et al., 2014a). Nos résultats soulignent un déclin rapide de la capacité des progéniteurs Glu à se différencier et à migrer, contribuant ainsi à la fermeture de la période de neurogenèse corticale.

Nos données de scRNAseq ont mis en lumière les mécanismes à l'origine de cette perte progressive du pouvoir neurogène. Les changements épitranscriptomiques apparaissent comme des mécanismes clés dans la médiation du contrôle temporel sur la progression du lignage. La modification de l'ARNm m6A est la modification la plus répandue dans les cellules eucaryotes (Desrosiers et al., 1974) et a récemment été suggérée dans la régulation de la corticogenèse (Yoon et al., 2017). Nos résultats identifient cette méthylation comme un mécanisme possible conduisant à la dérégulation de la transcription que nous observons chez les progéniteurs Glu postnataux. Outre ces modifications épitranscriptomiques, l'analyse KEGG met en évidence les changements de plusieurs voies de signalisation clés, telles que celles impliquées dans l'astrogenèse (comme les voies de signalisation Jak-Stat et Notch; Rowitch & Kriegstein 2010),

suggérant qu'elles peuvent affecter simultanément le potentiel de différenciation des progéniteurs de Glu. Une autre voie de signalisation dérégulée est la voie de signalisation Wnt. Ceci est en accord avec une étude précédente décrivant une augmentation progressive de l'activité de GSK3 β à partir de E15.5 et se traduisant par la phosphorylation de Neurog2, effecteur du lignage neuronal glutamatergique, affectant ainsi son activité (Li et al., 2012). Parallèlement à une activité transcriptionnelle réduite de Neurog2, 64% de ses gènes cibles (Gohlke et al., 2008) sont régulés négativement à P2, alors que 2% seulement sont régulés à la hausse, malgré la persistance de l'expression de Neurog2.

Il est important de noter que les progéniteurs postnataux Glu semblent toujours être permissifs à la manipulation intrinsèque/extrinsèque. Nous montrons que leur prolifération et migration Glu peuvent être favorisées par des manipulations génétiques ou pharmacologiques. Nos expériences révèlent toutefois que ces manipulations ne sont pas suffisantes pour favoriser la survie à long terme des neurones, ce qui suggère que le cortex n'est pas permissif à l'intégration de ces neurones nouveau-nés dans des conditions physiologiques. Cependant, des observations récentes suggèrent que la permissivité de l'environnement pourrait être accrue après une lésion, comme après une hypoxie chronique néonatale, où une neurogenèse corticale de novo a été observée (Fagel et al., 2009; Bi et al., 2011; Falkner et al., 2011). , 2016; Azim et al., 2017). Il est probable que nos résultats fourniront des informations importantes pour orienter les recherches futures dans ce contexte.

Les régions germinales ne sont pas homogènes, mais très hétérogènes, avec des différences de transcription conduisant à la production de lignées cellulaires divergentes. Récemment, notre laboratoire a contribué à résoudre cette hétérogénéité en démontrant un niveau inattendu d'hétérogénéité transcriptionnelle entre la zone sous-ventriculaire dorsale et latérale du cerveau antérieur de la souris postnatale, ainsi que dans leurs cellules souches neurales et leurs progéniteurs (Azim et al. 2015). Dans le premier chapitre de ma thèse, mes résultats ont contribué à décrire et à discuter un nouveau niveau d'hétérogénéité régionale et spécifique à la lignée dans la SVZ dorsale basée sur l'expression de *Hopx* (**chapitre 1**). Ces travaux soutiennent la coexistence de NSCs biaisés vers un lignage, les NSCs voisines exprimant des facteurs de transcription distincts qui influencent leurs comportements respectifs et les guident tout au long de l'acquisition de différents destins.

Dans le deuxième chapitre de ma thèse, j'ai poursuivi l'exploration de l'hétérogénéité régionale et spécifique à la lignée de la SVZ dorsale en caractérisant les progéniteurs des

neurones glutamatergiques corticaux (c.-à-d. Les progéniteurs Glu) dont il a déjà été montré qu'ils persistaient après la naissance (Donega et al., 2018a). On pense généralement que les progéniteurs de neurones glutamatergiques corticaux changent de destin avant la naissance pour produire des astrocytes. Mes résultats montrent que ce changement est en grande partie incomplet et qu'une grande partie des progéniteurs Glu continue à être produite dans le cerveau antérieur postnatal après la fermeture de la période de neurogenèse corticale. Le séquençage d'ARN sur cellule unique révèle toutefois une dérégulation transcriptionnelle profonde aux stades postnataux, ce qui est en corrélation avec le déclin progressif de la neurogenèse corticale observé *in vivo* (chapitre 2).

Pris ensemble, mon travail de thèse illustre l'existence d'une profonde hétérogénéité des NSCs dans la SVZ postnatale, qui peut être explorée du niveau régional au niveau cellulaire. Cela met également en évidence l'intérêt des études transcriptionnelles pour explorer la diversité de l'hétérogénéité des NSCs à ces différentes échelles. Il démontre enfin la nécessité de l'analyse clonale en histologie et de la transcriptomique unicellulaire pour éclairer de manière plus approfondie notre compréhension de l'activité germinative du cerveau antérieur aux moments pré et postnataux. Dans la discussion générale de ce manuscrit de thèse, je passe en revue la contribution récente des approches unicellulaires, y compris les travaux décrits dans cette thèse, sur la progression du lignage et des compétences des progéniteurs neuraux tout au long du développement pré et postnatal (revue concise soumise et en cours de révision). Enfin, je conclus en examinant l'implication de ces résultats dans la réparation du CNS et en proposant un nouveau modèle expérimental pour étudier la compétence des progéniteurs neuronaux postnataux dans la régénération de sous-types neuronaux définis à la suite d'une lésion cérébrale.

List of Abbreviations

AC	<i>anterior commissure</i>
AH	<i>anti Hem</i>
Aldh1l1	<i>aldehyd dehydrogenase</i>
ANR	<i>anterior neural ridge</i>
BLBP	<i>brain lipid-binding protein</i>
BMP	<i>bone morphogenetic protein</i>
BrdU	<i>5-bromo-2'-deoxyuridin</i>
CB	<i>calbindin</i>
CC	<i>corpus callosum</i>
CGE	<i>caudal ganglionic eminence</i>
CH	<i>cortical hem</i>
CNS	<i>central nervous system</i>
CoPNs	<i>commissural PNs</i>
CP	<i>cortical plate</i>
CPNs	<i>callosal PNs</i>
CR	<i>calretinin</i>
CSF	<i>cerebrospinal fluid</i>
CTPNs	<i>corticotectal PNs</i>
Ctrl.	<i>control</i>
DCX	<i>doublecortin</i>
dEPO	<i>dorsal electroporation</i>
DG	<i>dentate gyrus</i>
dIEPO	<i>dorso-lateral electroporation</i>
dINSC	<i>dorso-lateral neural stem cell</i>
dISVZ	<i>dorso-lateral subventricular zone microdomain</i>
dmEPO	<i>dorso-medial electroporation</i>
dmNSC	<i>dorso-medial neural stem cell</i>
dmSVZ	<i>dorso-medial subventricular zone microdomain</i>
dNSC	<i>dorsal neural stem cell</i>
dpe	<i>days post electroporation</i>
dSVZ	<i>dorsal subventricular zone microdomain</i>
DT	<i>diphtheria toxin</i>
DTR	<i>diphtheria toxin receptor</i>
EGFR	<i>epidermal growth factor receptor</i>
EPO	<i>electroporation</i>
FACS	<i>fluorescence activated cell sorting</i>
FGF	<i>fibroblast growth factors</i>
GFAP	<i>glial fibrillary acidic protein</i>
GFP	<i>green fluorescent protein</i>
GL	<i>glomerular layer</i>
GLAST	<i>glutamate aspartate transporter</i>
Glu	<i>glutamatergic</i>
IFC	<i>integrated fluidic circuits</i>
IN	<i>inhibitory neuron</i>

IPC	<i>intermediate progenitor cell</i>
IUE	<i>in utero electroporation</i>
LGE	<i>lateral ganglionic eminence</i>
LIF	<i>leukemia inhibitory factor</i>
INSC	<i>lateral neural stem cell</i>
ISVZ	<i>lateral subventricular zone microdomain</i>
LV	<i>lateral ventricle</i>
MADM	<i>mosaic analysis with double markers</i>
MAP2	<i>microtubule-associated protein-2</i>
MGE	<i>medial ganglionic eminence</i>
mSVZ	<i>medial subventricular zone microdomain</i>
NECs	<i>neuroepithelial stem cells</i>
NeuN	<i>neuronal nuclei</i>
NP	<i>neural progenitor</i>
NSC	<i>neural stem cell</i>
OB	<i>olfactory bulb</i>
Olig2	<i>oligodendrocyte transcription factor 2</i>
OPC	<i>oligodendrocyte precursor cell</i>
oRG	<i>outer radial glia</i>
PCA	<i>principal Component Analysis</i>
PN	<i>projection Neuron</i>
POA	<i>preoptic area</i>
PPI	<i>proteinprotein interaction</i>
Prog	<i>progenitor</i>
PSA-NCAM	<i>polysialylated-neural cell adhesion molecule</i>
PV	<i>parvalbumin</i>
qNSCs	<i>quiescent NSCs</i>
qPCR	<i>quantitative polymerase chain reaction</i>
RG	<i>radial glia</i>
RMS	<i>rostral migratory stream</i>
S100β	<i>s100 calcium-binding protein B</i>
SCDE	<i>single-cell differential expression</i>
scRNA-seq	<i>Single cell RNA sequencing</i>
SCZ	<i>subcallosal zone</i>
SGZ	<i>subgranular zone</i>
Shh	<i>sonic hedgehog</i>
SST	<i>somatostatin</i>
St	<i>striatum</i>
SVZ	<i>subventricular zone</i>
Tam	<i>tamoxifen</i>
TAP	<i>transient amplifying progenitor</i>
Tbr2	<i>T-box brain protein 2</i>
TF	<i>transcription factor</i>
TH	<i>tyrosine hydroxylase</i>
t-SNE	<i>distributed stochastic neighbour embedding</i>
VZ	<i>ventricular zone</i>

List of Figures

1.1.1. Figure 1: Cerebral cortex development and morphogens expression	1
1.1.1. Figure 2: Neural progenitor subtypes and neurogenic phases during cerebral cortex development in mice	3
1.1.2. Figure 3: The genetics of early pallial patterning	5
1.1.3. Figure 4: Schematic representation of the major neocortical interneuron subtypes	7
1.1.4. Figure 5: Schematic illustration of the six horizontal layers characteristic of the cerebral neocortex	9
1.2.1. Figure 6: The SVZ replenishes olfactory interneurons throughout life	12
1.2.2. Figure 7: Cellular composition of the ventricular–subventricular zone (SVZ)	14
2.3. Figure 8. A Meta-Analysis of TFs Enrichment in dNSCs Highlights Their Association with Distinct Neural Lineages	39
2.3. Figure 9. HOPX Exhibits a Complex Spatial and Temporal Expression Pattern within the SVZ Where it Labels a Subpopulation of dNSCs	41
2.3. Figure 10. Lineage-Specific Markers Highlight Acquisition of Divergent Cell Fates by NSCs Located in Different dSVZ Subdomains	43
2.3. Figure 11. Conditional Fate Mapping Reveals HOPX-Expressing NSCs Are Biased to Generate Astrocytes	45
2.3. Figure 12. Single-cell RNA Sequencing Meta-analysis Reveals Hopx-expressing RGCs Share Transcriptional Features with Adult Astrocytes	47
2.5. Figure S1. Analysis of TFs Enriched in Regionally Separated NSC Population. Related to Figure 8	51
2.5. Figure S2. Spatial Heterogeneity of Hopx Expression at P4. Related to Figure 9	52
2.5. Figure S3. Confirmation of Lineage Specificity of Selected Transcripts using the Dataset from the Barres Group. Related to Figure 10	53
2.5. Figure S4. Hopx and Astrocytic Markers Identified by Zywitzka et al. Identify a Subpopulation of “Astrogenic” RGCs at E17.5. Related to figure 12	54
3.3. Figure 13. Neurog2 ^{CreERT2} /tdTom Mice Allow Fate Mapping of Birth-Dated Cohorts of Glu Progenitors and Reveal Their Persistence at Postnatal Stages	62
3.3. Figure 14. Postnatal Glu Progenitors Originate from a Pool of Slow-Cycling RGCs that Accumulate in the SVZ during Corticogenesis	65
3.3. Figure 15. Dysregulation of Neurogenic Transcriptional Coding in Postnatal Glu Progenitors	67

3.3. Figure 16. <i>Partial Rescue of Impaired Migration and Differentiation of Postnatal Glu Progenitors by Pharmacological and Genetic Manipulations</i>	69
3.4. Figure S5. <i>Related to Figure 13. Neurog2Creert2/tdTom transgenic mouse line allows detailed analyses of cell morphology</i>	72
3.4. Figure S6. <i>Related to Figure 13. Postnatal Glu progenitors mainly give rise to glutamatergic projection neurons of sensory cortical regions</i>	73
3.4. Figure S7. <i>Related to Figure 13. Neurog2Creert2/tdTom mice reveal a late wave of corticogenesis early postnatally</i>	74
3.4. Figure S8. <i>Related to Figure 13. Postnatally born glutamatergic neurons develop intracortical projections and dendritic spines</i>	75
4.2. Figure 17. <i>The periventricular germinal niche at pre- and postnatal timepoints</i>	85
4.2. Figure 18. <i>A unifying scheme of pre- and postnatal germinal activity, integrating single cell findings discussed in this review</i>	91
4.3. Figure 19: <i>Specific Targeting of Layer IV Cortical Neurons induces fast and efficient neuronal ablation</i>	96
4.3. Figure 20: <i>Targeted cortical ablation induces progenitor responses within the dSVZ</i>	98

Table of Contents

1. <i>Regional Heterogeneity and Competence of Neural Stem Cells Throughout Development and Postnatal Life</i>	1
1.1. <i>The Developing Forebrain Generates Neuronal Diversity</i>	1
1.1.1 <i>Diversity of the Progenitors during Cortical Neurogenesis</i>	1
1.1.2 <i>Regionalization of the Developing Brain</i>	4
1.1.3. <i>Basic Principles of Cortical Organization</i>	6
1.1.4. <i>Molecular Diversity of Anatomically Defined PNs</i>	8
1.2. <i>Germinal Activity Persists in the Postnatal SVZ</i>	11
1.2.1. <i>The Postnatal Niche</i>	11
1.2.2. <i>The Radial Glia Origin of Type B1 Cells:</i>	13
1.2.3. <i>Type B1 Cells: A Specialized Astrocyte</i>	13
1.2.4. <i>Regionalization and heterogeneity of Postnatal SVZ NSCs</i>	15
1.2.5. <i>Regionalization also applied to gliogenesis</i>	17
1.2.6. <i>Signals from the CSF and the niche act in concert to regulate NSCs activity and regionalization throughout pre- and postnatal life</i>	18
1.3. <i>Transcriptional correlates of SVZ NSCs regionalization</i>	25
1.4. <i>Objectives of the PhD thesis</i>	27
2. <i>Experimental Chapter 1: HOPX Defines Heterogeneity of Postnatal Subventricular Zone Neural Stem Cells</i>	31
2.1. <i>Introduction</i>	32
2.2. <i>Experimental procedures</i>	33
2.3. <i>Results</i>	38
<i>Hopx Is Enriched in NSCs of the dSVZ and in Cells of the Astrocytic Lineage.</i>	38
<i>HOPX Expression Reveals Intraregional Heterogeneity within the dSVZ</i>	40
<i>The dSVZ Is Defined by Microdomains with Distinct Lineage Outputs</i>	42
<i>HOPX-Expressing dNSCs Are Biased to Acquire an Astroglial Fate</i>	44

<i>Hopx</i> -expressing RGCs are Present in the Late Developing pallium and Share Transcriptional Features with adult Astrocytes	46
2.4. Discussion	48
2.5. Supplementary Figures.....	51
3. Experimental Chapter 2: Transcriptional Dysregulation in Postnatal Glutamatergic Progenitors Contributes to Closure of the Cortical Neurogenic Period	55
3.1. Introduction.....	56
3.2. Experimental Procedures	56
3.3. Results	61
Fate Mapping of Birth-Dated Cohorts of Glutamatergic Neurons.....	61
A Large Population of Glu Progenitors Persist in the Postnatal SVZ	63
ScRNA-Seq Reveals Transcriptional Dysregulation in Postnatal Glu Progenitors ..	64
Postnatal Glu Progenitor Differentiation Can Be Partially Rescued	68
3.4. Discussion	69
3.4. Supplementary Figures.....	72
4. General Discussion	79
4.1. Summary and Opened Questions.....	79
4.2. Contributions of Single cell Approaches to Probe Neural Progenitor's Heterogeneity and Dynamics.....	80
4.2.1. Clonal Techniques in Histology and Transcriptomic	80
4.2.2. Contributions of Single Cell Approaches to Probe Spatial Identity Specification	82
4.2.3. Contributions of Single cell Approaches to Probe Temporal Identity Specification	86
4.2.4. Contributions of Single cell Approaches to Probe Adult NSCs Origin and Biology	88
4.3. Implication for Brain Repair.....	92
4.3.1 Are embryonic and Postnatal/adult NSCs Representing Distinct Populations in term of Diversity and Competence?	92

4.3.2. Targeted Neuronal Ablation as a Model to Study Competence of Postnatal NSCs for Cortical Repair	93
5. Annexes	101
6. References.....	124
7. CV.....	143
8. List of Publications	144
9. Additional Publications	145

INTRODUCTION

1. Regional Heterogeneity and Competence of Neural Stem Cells Throughout Development and Postnatal Life

The central nervous is a tissue of exquisite complexity. It forms in a stepwise manner during embryonic development from a population of specialized cells within the ectoderm. Here I describe its gradual development and complexification over time, with a special emphasis on the forebrain and of the cortex, the regions of interest of this PhD work. Germinal activity does not sharply stop at birth, but persists within the subventricular zone of the lateral ventricle. In a second part of the introduction, I describe the transformation of this germinal region at postnatal stages. I finally describe its specificities and similarities compared to its embryonic counterpart, both in term of cellular and regional organization, which were both explored further during my PhD.

1.1. The Developing Forebrain Generates Neuronal Diversity

The neocortex is by far one of the most complex regions of the mammalian brain, characterized by a remarkably diversity of neuronal and non-neuronal cell types, whose spatial and temporal coordinated development and function guarantee the execution of high-order cognitive, sensory, and motor behaviors. Decoding its heterogeneity have been at the core of neuroscientists' work for decades. In this first part of the introduction I would like to introduce some of the key aspects of its organization and development.

1.1.1 Diversity of the Progenitors during Cortical Neurogenesis

*Once neurulation is completed, the neural tube forms three primary vesicles, namely the forebrain, the midbrain and the hindbrain (**Figure 1A**). The forebrain rapidly evolves in further subdivisions to form secondary vesicles including the telencephalon. Its dorsal part becomes the pallium where the cerebral cortex derives.*

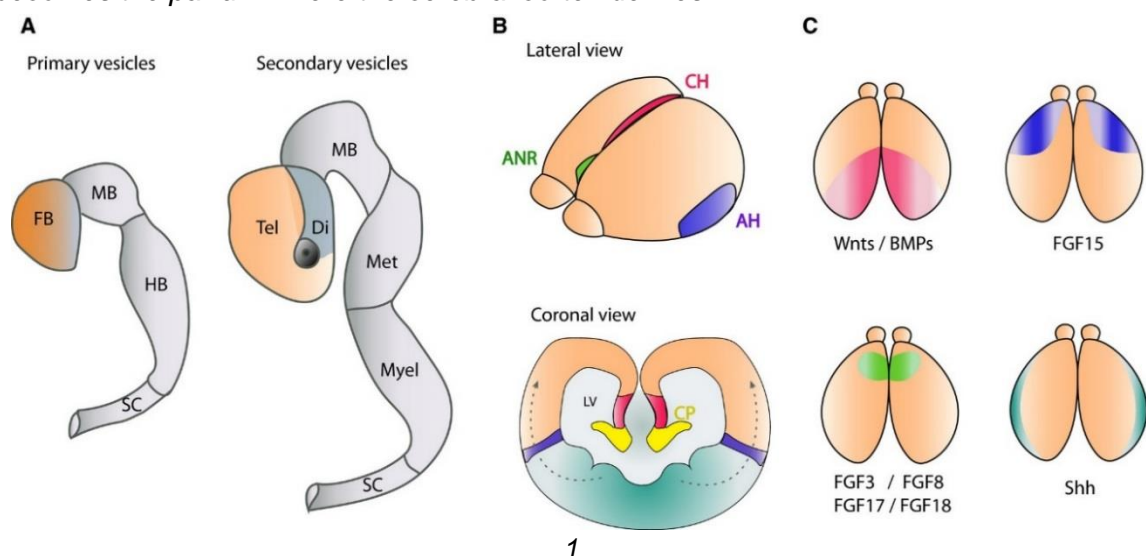


Figure 1: Cerebral cortex development and morphogens expression. (A) The rostral part of the neural tube evolves rostrally into the primary forebrain (FB), midbrain (MB) and hindbrain (HB) vesicles while the caudal part gives the spinal cord (SC). The secondary vesicles telencephalon (Tel), diencephalon (Di), metencephalon (Met) and myelencephalon (Myel) develop from the primary vesicles. **(B)** The anterior neural ridge (ANR), cortical hem (CH) and anti-hem (AH) are secreting centers. ANR secretes FGFs, CH secretes Wnts/BMPs and AH secretes FGF15 morphogens in the telencephalon. Shh is mainly present in the ventral part of the telencephalon, where ganglionic eminences are specified and generate interneurons that follow dorsal tangential path to invade the developing cortex. All morphogens are also found in the CSF secreted by choroid plexus (CP) and filling the lateral ventricles (LV). **(C)** Morphogens gradients in the dorsal telencephalon. Illustration from Agirman et al., 2017.

At the end of the neural tube closure, the neuroepithelium is composed of neuroepithelial stem cells (NECs), the earliest progenitors of the cortex. They are organized in a pseudostratified neuroepithelium because their nuclei migrate up and down the apical-basal axis during the cell cycle. NECs show typical epithelial features and are highly polarized along their apical-basal axis. These cells initially expand their pool by successive symmetric proliferative divisions and later divide asymmetrically to generate radial glial cells (RGCs) that sit in the ventricular zone (VZ) of the dorsal part of the telencephalon, the most apical cell layer that lines the ventricles. During this process, NECs lose some of their epithelial traits to acquire astroglial hallmarks. For example, in contrast to NECs, RGCs show several astroglial properties such as the presence of glycogen granules and the expression of astrocytic proteins like GLAST, S100 β , GFAP, Vimentin and BLBP. This transition marks the onset of neurogenesis in mice and occurs throughout most of the brain between embryonic days 10 (E10.5) and E12.5.

RGCs maintain a bipolar morphology with apical and basal processes (Figure 2A) and produce most of the neurons in the brain, either directly or indirectly (Haubensak et al., 2004; Miyata, 2004; Noctor et al., 2004). Cortical neurogenesis which extends from E10.5 to E18.5 in mice is followed by the gliogenesis period, which terminates after birth. At early stage of corticogenesis, RGCs in the pallium divide asymmetrically to self-renew and generate a projecting neuron. This process is defined as direct neurogenesis. As corticogenesis proceeds, RGCs give rise to intermediate progenitors (IPs) that delaminate from the apical surface to invade the subventricular zone (SVZ) (Figure 2B). Contrary to RGCs, IPs divide symmetrically to give birth to two identical neurons following further round of cell division. This process is defined as indirect neurogenesis and is critical to increase the number of neurons that are generated from a given number of RGCs (Haubensak et al., 2004). IPs differ from RGCs in terms of genes they express. For

example, they specifically express the genes that encode the transcription factor *Tbr2* (Englund, 2005). Newborn neurons generated directly or indirectly from RGCs migrate to reach the cortical plate (CP). Early born neurons move basally through somal translocation and integrate the deep layers of the cortex (Tabata et al., 2009). In contrast, later born neurons transit through multiple morphologies and use the processes of RGCs as a scaffold for their locomotion towards the upper cortical layers (Evsyukova et al., 2013; Hippenmeyer, 2014). Cortical layering occurs in an 'inside-out' fashion whereby earlier born neurons populate deep layers and later born neurons progressively occupy upper layers (Angevine and Sidman, 1961). These successive waves produce six layers in the neocortex.

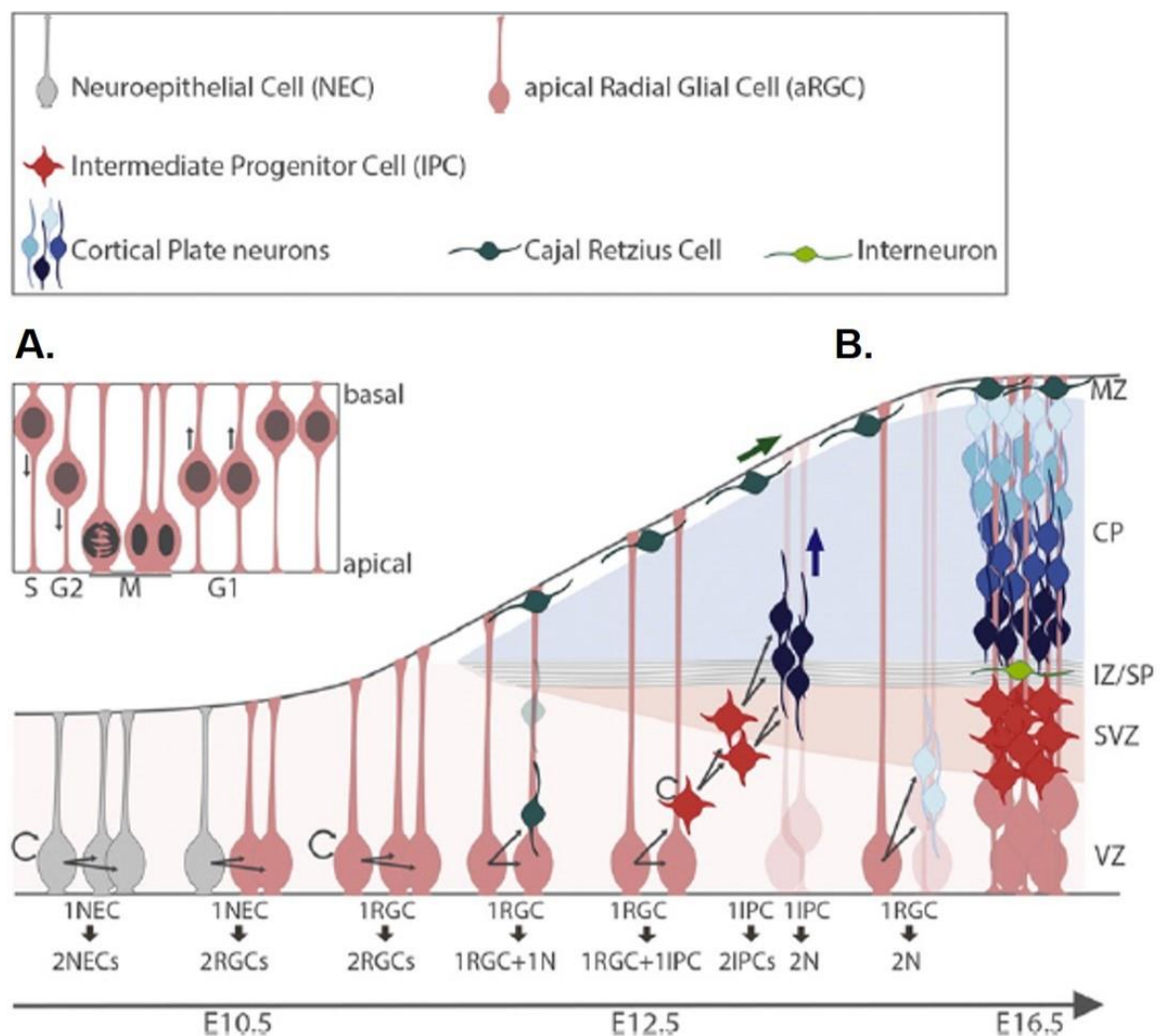


Figure 2: Neural progenitor subtypes and neurogenic phases during cerebral cortex development in mice. (A) RGCs maintain a bipolar morphology with apical and basal processes. (B) Sequential steps of neurogenesis in the mouse: neuroepithelial cells (NECs, grey) self-renew by symmetric division, then turn into apical radial glial cells (RGCs, pink) that divide either symmetrically to self-renew, or asymmetrically to give rise first to primary neurons including Cajal–Retzius cells (dark green) (direct neurogenesis) which migrate to the cortical surface to form the marginal zone (MZ), and to intermediate progenitor cells (IPC) at E12.5 and onwards; IPCs populate the subventricular zone (SVZ) and generate cortical layer neurons (dark to light blue), which migrate along the basal process of RGCs through the intermediate zone or subplate (IZ/SP) towards their destined layer. At later stages, some RGCs can undergo final symmetric divisions generating two neurons or switch to gliogenesis. Illustration adapted from Jiang and Nardelli, 2015.

1.1.2 Regionalization of the Developing Brain

Within the telencephalon, a dorso-ventral polarity rapidly develops leading to the emergence of the pallium at its dorsal part. This is due to the reciprocal action of transcription factors and morphogens secreted by three signaling centers, the cortical hem (CH) in the mediodorsal region, the anti-hem (AH) in the lateral aspect, and the anterior neural ridge (ANR) in the anteromedial region (Figure 1B and 1B). These patterning molecules diffuse in complementary gradients and induce expression of regionally defined transcription factors (TFs). Some of the main TFs involved in the regionalization of the embryonic pallium are presented here. Some of these morphogens and their role in neural stem cell activity are covered in more details in part 1.3.5. of this introduction.

The early forebrain patterning in mouse embryo is established around E8.5. Otx2 first establishes the forebrain and midbrain territories (Inoue et al., 2012). Then, Emx2 and Pax6 functions redundantly to establish the caudal forebrain, which contributes to the medial pallium, ventral pallium and diencephalon while Six3 establishes the rostral forebrain domain (Lagutin et al., 2003) (Figure 3). The expression of Fgf8 in the anterior neural ridge induces Foxg1 in the Six3-expressing domain and establishes the dorsal pallium and subpallium (Kobayashi et al., 2002; Lagutin et al., 2003). The boundary between the pallium and subpallium is regulated by cross-repression between Gli3 and Shh, and Fgf8 expression (Gutin, 2006). Through these interactions, the border between the Pax6⁺ pallium and the Nkx2.1⁺ subpallium is first established around E9.5 (Shimamura and Rubenstein, 1997), which is subsequently replaced by a Pax6/Gsx2 boundary by E12.5 (Yun et al., 2001). After this, the entire pallium is defined by Pax6 expression in the progenitors and Tbr1 expression in the postmitotic neurons (Puelles et al., 2000), although Tbr1 is downregulated in many of the layers II–V neurons (Han et al., 2011). Emx1 further delineates an expression boundary between the dorsal and ventral pallium (Puelles et al.,

2000). Thus, excitatory glutamatergic projection neurons arise from progenitor cells of the *Emx1*-positive dorsal pallial area (Louvi et al., 2007), whereas the subpallium which includes the ganglionic eminences (GE) produces inhibitory interneurons (Hébert and Fishell, 2008; Moreno et al., 2009).

Following E9.5 several transcription factors have a clear regionalized expression pattern. This is particularly clear for markers of the pallium and the subpallium. Members of the *Dlx* family (Distal-less), namely homeobox genes *Dlx1*, *Dlx2* (Bulfone et al., 1993), *Dlx5* and *Dlx6* (Simeone et al., 1994) are enriched in the ganglionic eminences of the subpallium and consistently absent from the pallial domain. Other ventrally enriched genes are *Nkx2*, *Nkx6.2*, *Gsx1* and *Gsx2* (Zhong et al., 2008; Zhong and Holland, 2011).

On the other hand, homeobox genes *Emx1*, *Emx2* and *Pax6* show restricted expression to the pallium as well as the T-box transcription factors *Tbr1* and *Tbr2* (also referred as *Eomes*) (Bulfone et al., 1995; Bulfone et al., 1999), as well as the bHLH transcription factor *Neurog2* (reviewed in Lee, 1997. Expression of these TFs antagonize a subpallial expression of the bHLH transcription factor *Mash1* (Casarosa et al., 1999).

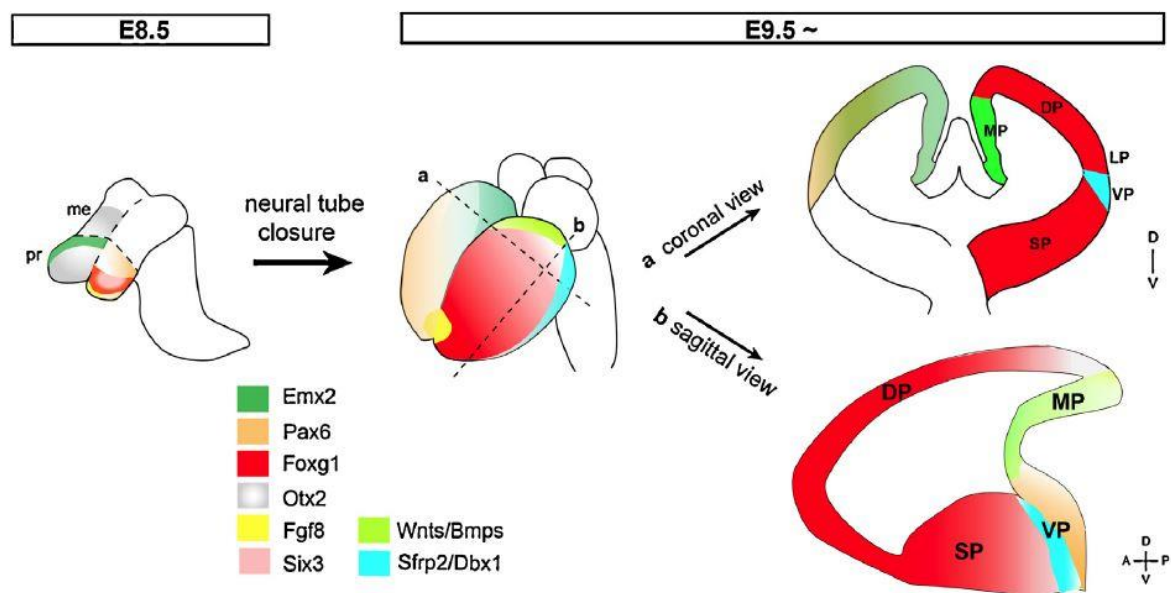


Figure 3: The genetics of early pallial patterning. Coronal view indicates spatial subdivisions of the pallium, where dorsal pallium lies between the medial and lateral/ventral pallium. In sagittal view, the medial and lateral/ventral pallium connects at caudal levels. DP, dorsal pallium; LP, lateral pallium; me, mesencephalon; MP, medial pallium; pr, prosencephalon; SP, subpallium; VP, ventral pallium. Adapted from (Kumamoto and Hanashima, 2014).

1.1.3. Basic Principles of Cortical Organization

Following embryonic development, the mouse neocortex consists of four primary areas: the somatosensory cortex (which processes sensory modalities, such as input from the vibrissae), the auditory cortex (which processes sound), the visual cortex (which processes the sense of sight), and the motor cortex (which outputs information to control fine motor behavior) (Rash and Grove, 2006) (**Figure 5A**). These primary cortical areas occupy most of the cortical surface, unlike in humans where secondary or associative cortical areas are more developed. The cortex displays unique cytoarchitectural characteristics, which are the result of the organization and composition of the different cell types and circuits and vary in an area-specific manner. The neocortex is organized into six horizontal layers, historically defined as supragranular (layer I/II–III), granular (layer IV), and infragranular (layers V and VI). Layers contain different classes of neurons and vary in thickness and tissue architecture depending on their areal identity (Greig et al., 2013). Neurons can be classified in excitatory glutamatergic projection neurons (PNs) (also referred as pyramidal neurons) and GABAergic inhibitory interneurons (INs).

GABAergic inhibitory interneurons

Inhibitory INs are approximately 20–30% of the total number of cortical neurons and are often referred to as ‘short axons neurons’, although several long projecting INs have been recently traced (Tremblay et al., 2016). Aspiny INs are the main inhibitory component of neocortical circuits, finely modulating projection neuron activity by regulating both synaptic function and the timing of action potential generation (Kepecs and Fishell, 2014). Generated from the ventral forebrain progenitors located in medial and caudal ganglionic eminences (MGE and CGE), as well as in the preoptic area (POA), inhibitory INs reach their final destinations in the appropriate cortical layer through a highly coordinated process of tangential migration and radial dispersion in the cortex. The MGE has long been regarded as a primary source of cortical interneuron population in mice (~ 60%) (Butt et al., 2005) while the CGE has been shown to be the second-greatest contributor of interneuron progenitors, producing approximately 30% of all cortical interneurons (Anderson et al., 2001). Cortical GABAergic INs are very diverse; they contain subtypes that differ in morphology, molecular identity, firing properties, and patterns of local connectivity (Wamsley and Fishell, 2017). Although it is far from being an accurate representation, neocortical interneurons can be largely classified into several cardinal groups based on the expression of key molecular markers (Tremblay et al., 2016), which include: parvalbumin (PV), somatostatin (SST) produced mainly by MGE, vasoactive intestinal peptide (VIP), serotonin receptor 3a (5HT3aR), calretinin (CR) produced by CGE

and others. PV- and SST-positive INs are primarily found in the deep layers of the cortex, and 5HT3aR-positive INs preferentially populate the upper layers (Rudy et al., 2011) (Figure 4). However, compared with PNs, the laminar distribution of the molecularly distinct IN groups is much less precise.

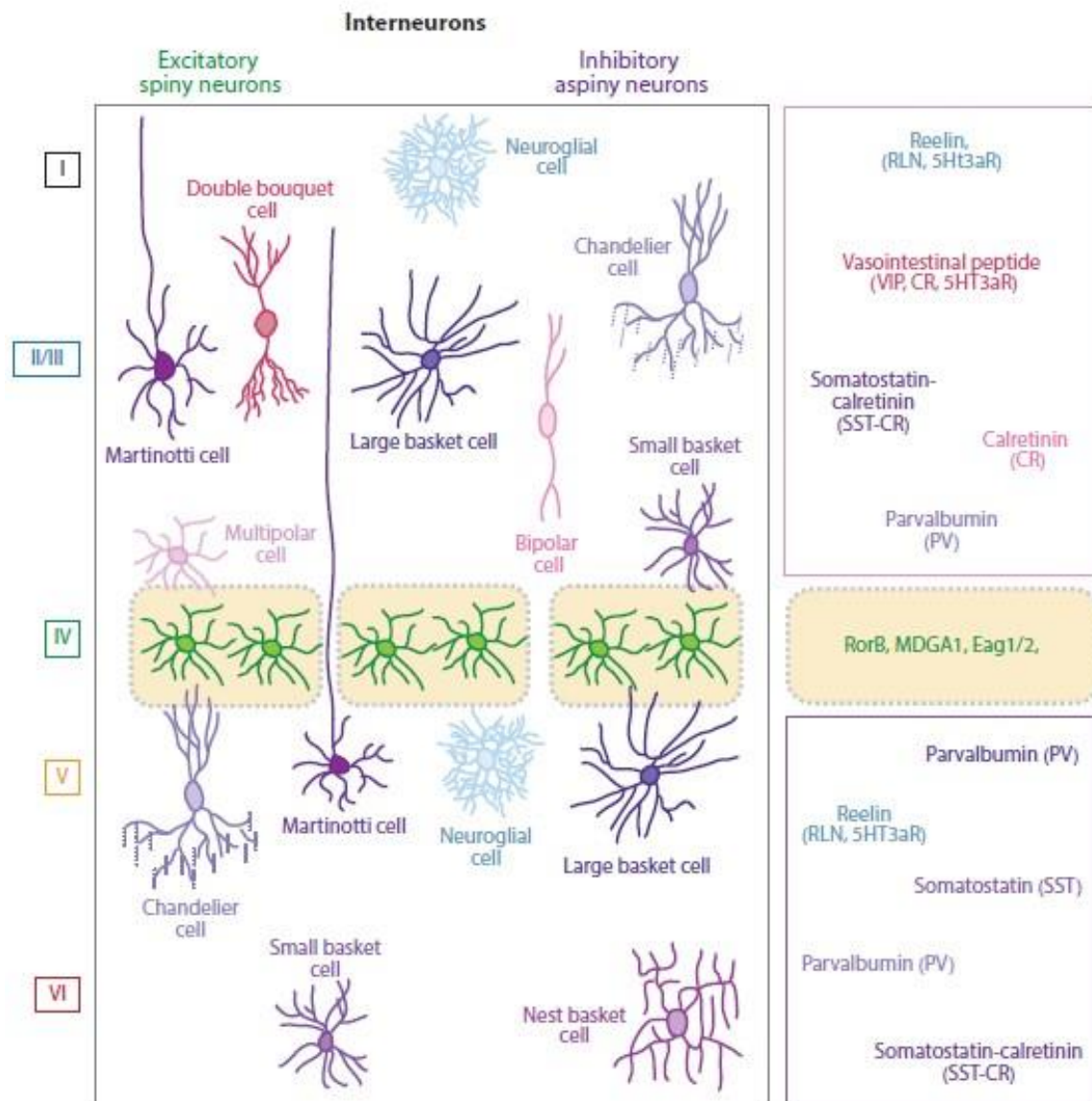


Figure 4: Schematic representation of the major neocortical interneuron subtypes. Schematic representation of the distinct interneuron classes within the six cortical layers. Excitatory spiny interneurons display mainly stellate and pyramidal morphology and are primarily located in the intragranular layer IV of the somatosensory cortex (barrel cortex, shown in the yellow boxes). In contrast, each cortical layer contains different types of inhibitory interneurons with different morphologies and molecular identities. (molecular markers are listed on right). Illustration from Lodato and Arlotta, 2015.

Glutamatergic projection neurons

On the other hand, PNs are excitatory glutamatergic neurons and make up the vast majority of neurons of the cortex population (approx. 80%). They connect the cerebral cortex to its distal intracortical, subcortical, and subcerebral targets through their long axonal projections. PNs are generated from dorsal forebrain progenitors and can be broadly classified into intracortical and corticofugal neurons. Intracortical PNs are present in all six layers, but they are predominantly represented in the upper layer II/III and can be further divided into associative and commissural PNs (CoPNs) (**Figure 5BC**). PNs that project their axons either to targets in the same hemisphere or to different layers of the same area or column are called associative PNs (Molyneaux et al., 2007). By contrast, CoPNs project their axons to targets located in the opposite hemisphere, usually in a topographic manner, through one of two major fiber commissures: the corpus callosum (CC) or the anterior commissure (AC). However most CoPNs connect through the CC and are known as callosal PNs (CPNs). Corticofugal PNs are primarily located in the deep layers and send their axons to distal targets outside of the cortex and include all corticothalamic, corticopontine, corticotectal and corticospinal neurons. Corticothalamic PNs are a heterogeneous population of PNs located in layer VI that project to different nuclei of the thalamus to modulate incoming sensory information. Subcerebral PNs reside in layer Vb across multiple areas and project their axons to distinct targets below the brain, predominantly to the pons and other nuclei of the brainstem, in which case they are called corticopontine PNs; to the superior colliculus, in which case they are called corticotectal PNs (CTPNs); and to the spinal cord, in which case they are called corticospinal motor neurons (CSMNs) (Molyneaux et al., 2007).

1.1.4. Molecular Diversity of Anatomically Defined PNs

Nevertheless, the full picture of PNs types is incomplete as some of them do not fit into these classical classes (Cederquist et al., 2013). Several studies have however recently tackled this problem by using single cell resolution approaches (Zeisel et al., 2015; Han et al., 2018). The authors revealed an additional level of diversity of intracortical PNs, which collectively with previous studies (Molyneaux et al., 2015), provide PN class-specific signature genes. Examples are *Fezf2*, *Cntn6*, *Cad13*, *Ctip2*, *Cry-mu*, *Igfbp4* and *Ldb2* for layer V and CSMNs, and *Cux2*, *Svet1*, *Lhx2*, *Mef2c*, *Inhba*, *Btg1*, *Lpl*, *Cited2*, and *PlexinD1* for CPNs (Arlotta et al., 2005; Molyneaux et al., 2009, 2015; Lodato et al., 2014). *Sox5*, *Tle4*, *FoxP2* are specifically expressed in corticothalamic PNs of layer VI. Molecular differences also allow distinguishing between more closely related classes. Several important conclusions can be drawn from those profiling studies. First, the identity of a

defined neuronal population relies on the expression of multiple class-specific genes rather than the expression of specific single genes. Second, it implies also that laminar coordinates of a neuron do not fully define its class-specific identity. Third, transcriptional profiling suggests a higher degree of heterogeneity within PN subtypes than what it looks like from their connectivity pattern. For example the expression of *Cux2*, *Ptn*, *EphA3* and *Nnmt* parcellate CPNs (Molyneaux et al., 2009, 2015). Finally, class-specific profiles of gene expression are temporally dynamic, changing dramatically during neuronal maturation.

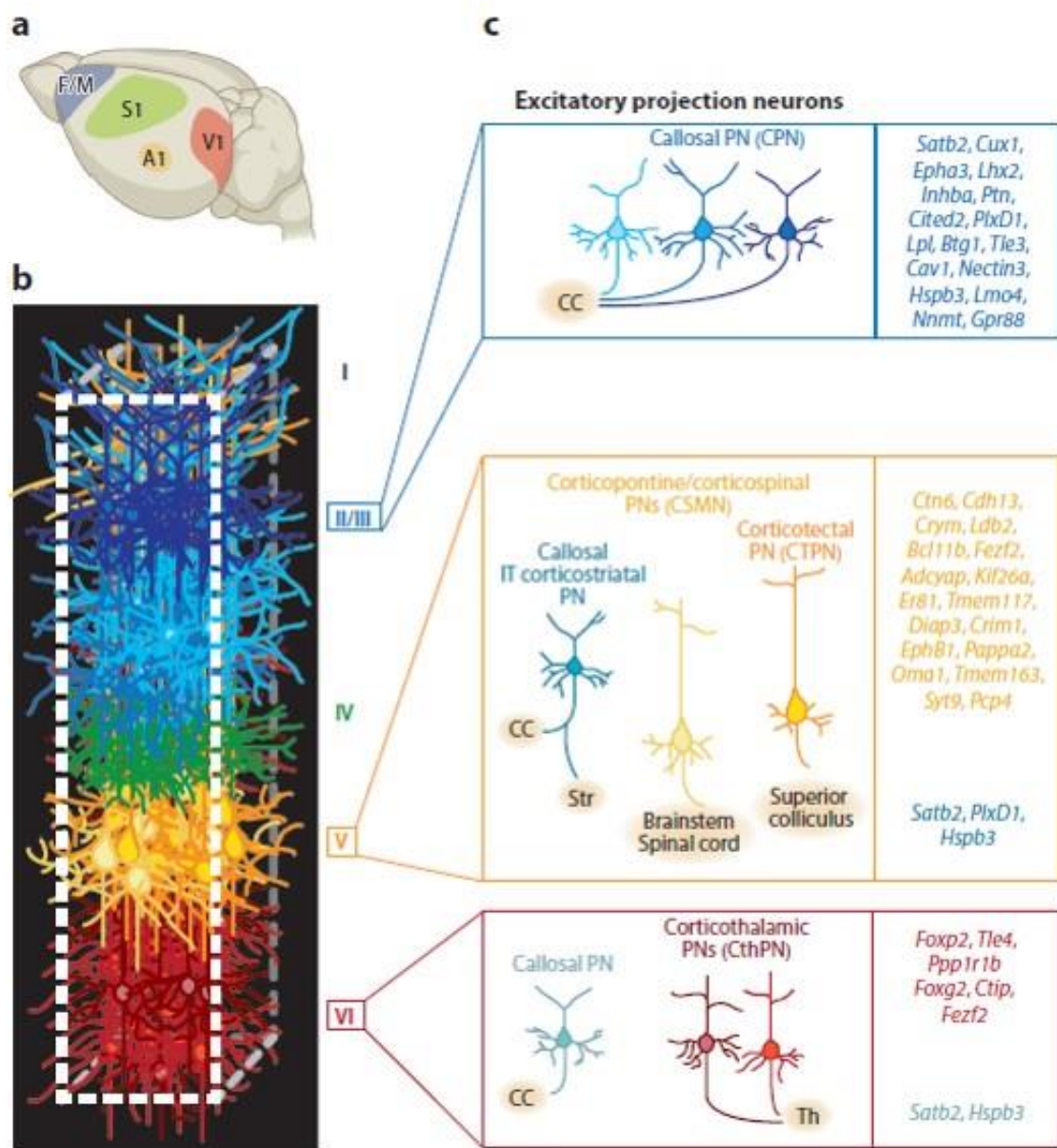


Figure 5: Schematic illustration of the six horizontal layers characteristic of the cerebral neocortex. (A) Schematic representation of primary neocortical areas. (B) Cortical columns contain horizontally arranged layers with very diverse neuronal compositions. (C) Layer II/III contains different classes of commissural neurons, primarily of distinct CPN identities. Layer V contains CPNs, often maintaining distinctive collaterals to the striatum and different classes of subcerebral PNs that connect to the brainstem, spinal cord, and superior colliculus. Layer VI has different classes of CThPNs, connecting to separate thalamic nuclei, and CPNs that connect through the CC. Cortical PN subtypes express unique gene signatures that in specific combinations identify each class (listed on right). Abbreviations: A1, auditory cortex; CC, corpus callosum; CPN, callosal projection neuron; CTPN, corticotectal projection neuron; CThPN, corticothalamic; F/M, frontal/motor cortex; IN, interneurons; IT, intratelencephalic; PN, projection neuron; S1, somatosensory cortex; Th, thalamus; V1, visual cortex. Illustration from Lodato and Arlotta, 2015.

With the recent advance of single-cell transcriptomics, it is now possible to tackle the fundamental problem of neuronal diversity at the necessary resolution of individual cells. Single-cell RNA sequencing technology (scRNA-Seq) had opened new avenue for cell type classification and unbiased discovery of cell types (Macosko et al., 2015; Zeisel et al., 2015; Tasic et al., 2016). The first unbiased sampling of mouse primary somatosensory cortex from Zeisel and colleagues allowed the identification of 7 excitatory and 16 inhibitory neuronal cell types that correctly fitted the already identified molecularly-defined classes. However, they used an unbiased approach, in which a heterogeneous mixture of cells from all cortical layers was subjected to scRNA-Seq without a priori selection, whereas Tasic and colleagues combined scRNA-Seq with reporter mice to generate a most complete description of cortical neurons although in a more restricted area of the adult mouse cortex (i.e. the primary visual cortex). The limit of the former study is the under sampling of rare and fragile neurons due to unbiased tissue isolation and single cell dissociation. As a result, it favors the most common types of neurons at the expense of the most fragile ones. In the later study, the authors purified and sequenced specific subsets of cortical neurons using transgenic mouse lines. They identified 19 excitatory and 23 inhibitory neuronal cell types. More and more elegant and pioneered studies are recently emerging such as integrative approaches of multidimensional profiling to draw a more complete cell-type atlas in the mouse cerebral cortex. Activity-induced transcriptional states and electrophysiological features followed by scRNA-Seq (P. Hu et al. 2017; Chevée et al. 2018; Fuzik et al. 2016) are novel strategies that will deepened our understanding of the cortical cellular composition.

1.2. Germinal Activity Persists in the Postnatal SVZ

Germinal activity does not stop sharply at birth, but persists in the vicinity of the lateral ventricles. In this region, RGCs change their morphology to gradually transform into postnatal, then adult NSCs (also named Type B1 cells). They continue proliferating to give rise to both glial cells and neurons. Interestingly, although major differences exist in the cellular composition and organization of the SVZ when compared to its embryonic counterpart, significant similarities are also evidenced. In particular the regionalization of postnatal/adult NSCs is inherited from early development, leading to the local production of defined progenitor populations. Unraveling the signaling pathway and transcriptional correlates of this regionalization has become an active area of research.

1.2.1. The Postnatal Niche

*The postnatal and adult mouse brain contains several hundreds (estimated to ~1200 in young adult mice) of NSCs distributed along the lateral ventricle walls (Ponti et al., 2013). These SVZ NSCs are named type B1 cells in adult animals and share characteristics with brain astrocytes such as the expression of several glial markers including the glial-fibrillary acidic protein (GFAP), glutamate aspartate transporter (GLAST), and brain lipid-binding protein (BLBP); morphology, and ultrastructure (Paterson et al., 1973; Doetsch et al., 1997a, 1999a). Type B1 cells are heterogeneous and exists in a quiescent (qNSCs) or activated state (aNSCs) (Codega et al., 2014; Mich et al., 2014). These cardinal features underline molecular and cellular differences, which have implications on disease and repair ability. For instance, it is important to understand the molecular specificities and mechanisms controlling the induction of these two ground states to be able to use adult NSCs in therapy without depleting them. Activated type B1 cells give rise to transit amplifying progenitors (type C cells), which generate neuroblasts (type A cells) that migrate to the OB. Type A cells move along as chains, which are ensheathed by GFAP positive cells (Lois 1996; Lois et al. 1996; Wichterle et al. 1997) (**Figure 6**). This neuroblast chain migration defines the rostral migratory stream (RMS) that originates at the anterior tip of the SVZ (Doetsch and Alvarez-Buylla, 1996). Inside the OB, neuroblasts then migrate radially from the RMS to invade the distinct OB layers where they differentiate into distinct interneuron subtypes. They become integrated into functional circuits replacing throughout life the older cells. This has been suggested to be important for neuronal plasticity and the processing of olfactory information (Cecchi et al., 2001; Petreanu and Alvarez-Buylla, 2002; Wachowiak and Shipley, 2006; Imayoshi et al., 2008; Lledo et al., 2008; Sakamoto et al., 2014). The transcription factors *Ascl1* and *Dlx2* are used as markers of type C cells*

whereas doublecortin (DCX) and polysialylated neural- cell-adhesion molecule (PSA-NCAM) are expressed by type A cells (Doetsch et al., 1997b). Type B1 cells also give rise to oligodendrocytes for the corpus callosum but in a much lower magnitude as compare to OB neurogenesis (Menn et al., 2006). Brain injury has also been suggested to induce the SVZ to produce astrocytes that migrate to the injury site (Benner et al., 2013). Nonetheless, it is still unclear whether type B1 cells are multipotent and, thus, able to generate both neurons and glial cells. To address this question, Ortega and colleagues isolated single activated NSC *in vitro* and performed live imaging to continuously track them. Their results reveal that while aNSCs can give rise to both astrocytes and neurons, none were capable of giving rise to both oligodendroglia and neurons (Ortega et al., 2013). While single cell lineages tracing studies were later performed *in vivo* (Calzolari et al., 2015), the use of a *Glast* promoter to induce recombination in a small number of NSCs prevented the authors to conclude on the multipotency of adult NSCs. Indeed, *Glast* is active in NSCs, but also in glia cells surrounding the lateral ventricle.

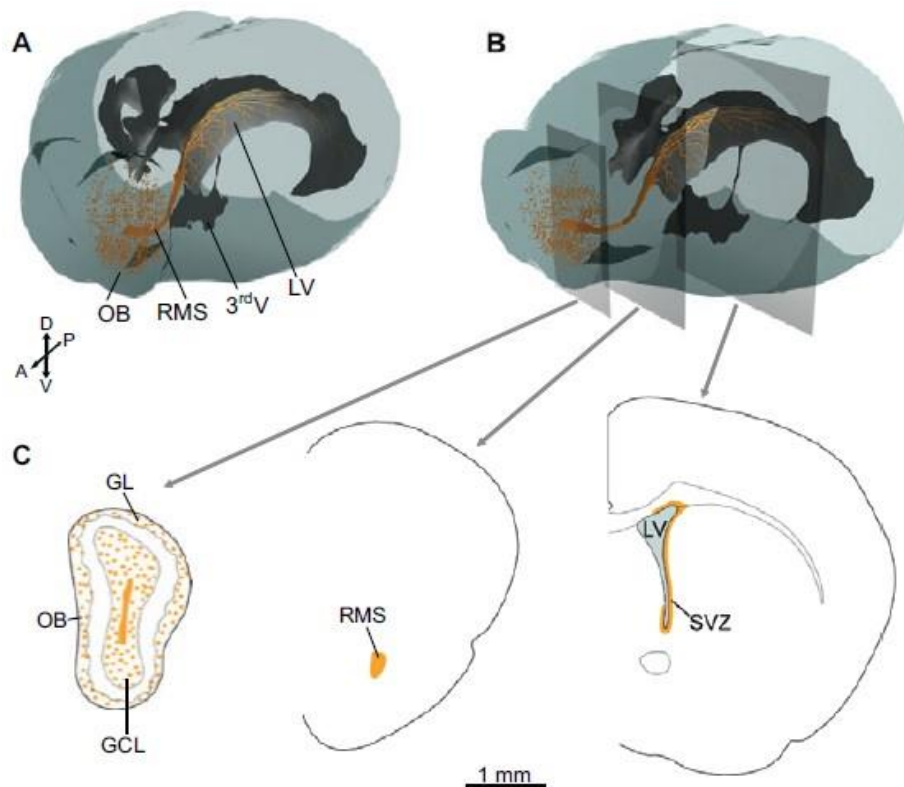


Figure 6: The SVZ replenishes olfactory interneurons throughout life. Schematic depiction of the neurogenic process along the entire extent of the ventricular system of the neonatal/adult rodent forebrain. **(A)** 3D representation of SVZ neurogenesis. Neural stem cells (NSCs) are located in the walls of the lateral ventricle (LV) and generate an irregular network of migratory neuroblasts (orange) that converge into the rostral migratory stream

(RMS). Upon arrival at the olfactory bulb (OB), the neuroblasts migrate radially to reach their final destination and mature into GABAergic neurons (granule cells and periglomerular neurons) and a minor population of glutamatergic neurons in the granule cell layer (GCL) or the glomerular layer (GL). **(B)** Sectioning planes through the OB, RMS and LV show the distribution of newly generated neuroblasts in these three forebrain compartments. Illustration from Fiorelli et al., 2015.

1.2.2. The Radial Glia Origin of Type B1 Cells:

Type B1 cells and embryonic radial glia share both spatial and morphological similarities. The ventricular contact of type B1 cells, their long-term neurogenic potential, and their unique apical process containing a primary cilium suggest the direct lineage relationship of the two cell types. The original and prevailing model suggested that radial glia transform into B1 cells during the first postnatal weeks, after they have produced the neurons and glial cells of the forebrain (Kriegstein and Alvarez-Buylla, 2009). This simple view has recently been challenged by lineage tracing studies (Fuentealba et al., 2015a; Furutachi et al., 2015). The authors of these studies show that postnatal B1 cells are indeed derived from embryonic NSCs that produce also neurons and glia for other forebrain regions (including cortex, striatum, and septum), but also reveal that the lineage progression of NSCs is not linear. Indeed, their results demonstrate that a subpopulation of radial glial cells, bifurcates from the main population during embryogenesis (i.e. between E13 and E15), and enter quiescence. At postnatal stages, these cells appear to reactivate gradually. These new findings suggest that the lineage for postnatal NSCs is not linear, but bifurcates in the embryo. I will come back on their origin in more details in the general discussion of this manuscript.

1.2.3. Type B1 Cells: A Specialized Astrocyte

*Type B1 cells are located within the ventricular epithelium which form a tight barrier of multiciliated ependymal cells to separate the brain parenchyma from the ventricle lumen. Type B1 cells make direct contact with the ventricle by extending a thin cellular process in-between ependymal cells (Doetsch et al., 1999b) (**Figure 7**). These apical processes contain each a primary cilium and tend to cluster together at the center of a rosette of ependymal cells in a repeating “pinwheel” pattern. The integrity of the ependymal cell layer as well as the primary cilium and apical contact with the CSF of type B1 cells, are primordial for the maintenance of SVZ germinal activity and neurogenesis. Similarly to*

embryonic NECs and RGCs this cellular structure likely transduces signaling molecules present within the CSF. For instance, *Shh*, *Wnts*, retinoic acid (RA), and BMPs are all found in CSF (Huang et al., 2010; Lehtinen and Walsh, 2011; Lehtinen et al., 2011), and these factors regulate SVZ neurogenesis.

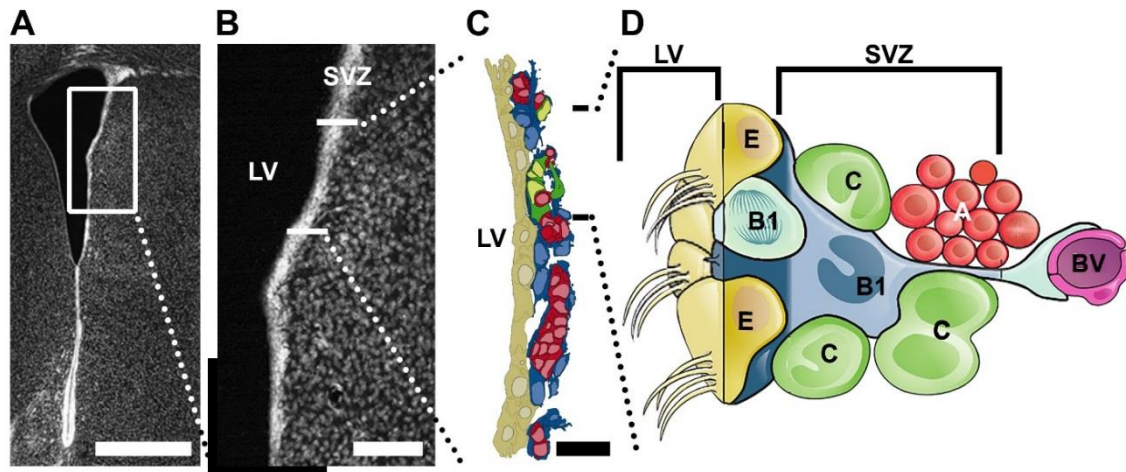


Figure 7: Cellular composition of the ventricular-subventricular zone (SVZ). (A+B): Representative micrographs of the SVZ (A) and the higher magnification of the lateral microdomain (B) show the zone of interest to illustrate the SVZ cytoarchitecture. (C+D): Ciliated ependymal cells (E; yellow) align the LV and isolate the lumen from the proliferative SVZ. NSC (type B1; blue) give rise to type C cells (green) which generate migrating neuroblasts (type A; red) (illustrations were modified from Doetsch et al., 1997 and Tong and Alvarez-Buylla, 2014). Scale bars: A = 500 μ m; B = 100 μ m; C = 20 μ m. Abbreviations: BV, blood vessel; LV, lateral ventricle; SVZ, subventricular zone.

Due to their dynamics, state of activation and close lineage relationship with brain astrocytes, the identification of type B1 cells markers remains a major challenge since several decades. Several cell surface markers or transcription factors have been identified, but are not exclusively expressed in Type B1 Cells. For instance, GFAP is expressed by many astrocytes that are not neurogenic and reside outside of the SVZ. The CD133 or Prominin-1 cell-surface marker has been used to enrich for SVZ NSCs, but expression of CD133 is variable in type B1 cells and is also prominently expressed on ependymal cells (Mirzadeh et al., 2008; Beckervordersandforth et al., 2010). LewisX (LeX) or CD15, is a cell-surface carbohydrate antigen that has also been found on SVZ NSCs, but this marker is also present on many non-GFAP-expressing cells as well as in some type A cells (Capela and Temple, 2002; Imura et al., 2006; Shen et al., 2008; Obermair et al., 2010). The epidermal growth factor receptor (EGFR) is found on “activated” type B1 cells, but

remains highly expressed in type C cells (Pastrana et al., 2009). Similarly, GLAST is found in both type B1 cells and some type C cells, as well as in some mature non-neurogenic astrocytes. Although high levels of *Id1* have been found in type B1 cells, this transcription factor is present at lower levels in type C cells (Nam and Benezra, 2009). Finally, VCAM1 has been found to be expressed on the apical process of type B1 cells and shown to play a critical role in NSC maintenance (Kokovay et al., 2012).

These patterns of protein expression demonstrate the difficulty of identifying unique marker of adult NSCs. As a consequence, identification of type B1 cells relies on multiple markers which combined and/or differential expression, allows identifying and FAC-sorting adult NSCs. While many of these protocols rely on the use of transgenic animals, Daynac and colleagues established a FACS protocol based on a combination of cell surface markers to isolate type B1 cells from their progenies and to distinguish the quiescent and activated state. They used LeX combined with an anti-CD24 antibody to label neuroblasts and a fluorescent EGF to label EGFR on actively proliferating cells (Daynac et al., 2014). They described 6 cell populations: the type C neuroblast cells as $CD24^+LeX^-EGFR^-$, the immature neuroblasts as $CD24^+LeX^-EGFR^+$, the TAPS as $CD24^-LeX^-EGFR^+$, the activated NSCs as $CD24^-LeX^+EGFR^+$ and finally the Lex^{bright} ($CD24^-LeX^+EGFR^-$) as the quiescent NSCs. Isolation of the two cell populations allowed the transcriptional identification of distinct molecular signatures in quiescent and activated NSCs (Morizur et al., 2018). This, together with a previous study based on the use of alternative markers (Codega et al., 2014), reveal specific interactions of NSCs with their microenvironment during quiescence.

Thanks to advances of sequencing technologies, a recent single cell transcriptomic study revealed additional insights in the molecular profiles of adult NSCs (Llorens-Bobadilla et al., 2015) by describing in exquisite details their sequential pattern of activation. It demonstrated that qNSCs can be divided into 2 further subpopulations: a dormant state (qNSC1) preceding a primed-quiescent state (qNSC2) which can be identified based on *Glast* expression level. Indeed, $Prom1^+EGFR^-Glast^{+low}$ or $Glast^{+high}$ can distinguish qNSC2 from qNSC1, respectively. Moreover, the authors described CD9 as new marker of NSCs versus mature parenchymal astrocytes.

1.2.4. Regionalization and heterogeneity of Postnatal SVZ NSCs

Three regions of the developing forebrain contribute to the formation of the lateral ventricular walls, and therefore to the formation of the SVZ: i.e. the septum, the pallium and the ganglionic eminences, that contribute to the medial, dorsal and lateral SVZ,

respectively. This results in NSCs of different embryonic origin being distributed within all the 3 walls of the postnatal lateral ventricles. Accumulating evidences have proven that their origin (and therefore their location) drives their specification in defined interneuron subtypes in the OB (Merkle et al., 2007a; Alvarez-Buylla et al., 2008; Fiorelli et al., 2015). Thanks to viral infection, genetic fate mapping or targeted electroporation, several landmark experiments revealed that CR⁺ [expressing calretinin] PGCs are preferentially generated by the medial SVZ NSCs (Merkle et al., 2007a; Young et al., 2007; Fernández et al., 2011; Fiorelli et al., 2015). Superficial GCs, tyrosine hydroxylase (TH)-expressing PGCs and a small number of glutamatergic juxtglomerular cells are generated by NSCs in the dorsal SVZ (Merkle et al., 2007a; Young et al., 2007; Brill et al., 2009; Fernández et al., 2011; de Chevigny et al., 2012). In contrast, deep GCs as well as CB⁺ [expressing calbindin] PGCs preferentially originate from NSCs of the lateral wall (Merkle et al., 2007a; Young et al., 2007; Fernández et al., 2011). A subsequent study has more recently revealed an extra level of heterogeneity by identifying the site of origin of additional, rare, subtypes of interneurons (Merkle et al., 2014). Moreover, it is worth mentioning that rostral and medial/dorsal localization primes NSCs to generate neurons that populate more superficial layers of the OB, whereas a caudal and lateral origin correlates with deeper fates (Fernández et al., 2011; de Chevigny et al., 2012; Fiorelli et al., 2015).

Taken together, these observations underline that NSCs are not a homogenous population and that their regional specification in defined interneuron subtypes originates from early embryonic development (Willaime-Morawek et al., 2006; Kohwi et al., 2007; Ventura and Goldman, 2007; Young et al., 2007; Willaime-Morawek and Van Der Kooy, 2008; Fuentealba et al., 2015b). Indeed, the embryonic NSCs of the septum, the MGE, the LGE and the neocortex generate NSCs that respectively populate the medial, ventral, lateral and dorsal areas of the adult SVZ. A small level of mixing appears to exist between specific walls. Indeed a degree of NSCs migration has been reported between defined SVZ, such as dorsal/pallial NSCs which have been described to migrate into the lateral SVZ at perinatal timepoints to ventral markers (Willaime-Morawek et al., 2006). Therefore, OB neuronal diversity emerges from a broad postnatal germinal zone, organized in microdomains that relate to the major subdivisions of the telencephalon. It is likely that molecular patterning of each subregion contribute to unique combinations of transcription factors. In agreement with their developmental origin, pallial markers (*Emx1*, *Pax6*, *Tbr2* (Eomes), *Tbr1*, *Neurog2*) are expressed in the dorsal most regions of the neonatal and adult LV, whereas subpallial (*Dlx1/2/5*, *Gsx1/2*, *Ascl1*, *Nkx2.1*, *Nkx6.2*) and septal (*Zic1/3*) markers are expressed in the lateral and medial walls of the LV, respectively (Kohwi et al., 2007; Winpenny et al., 2011; Azim et al., 2012a; López-Juárez et al., 2013; Merkle et al.,

2014). The expression pattern of these TFs can also vary significantly along the rostrocaudal extent of the SVZ, a characteristic recently described for *Zic1/3*, *Nkx6.2* and *Nkx2.1* in the most antero-ventral SVZ producing additional subtypes of OB neurons recently revealed (Merkle et al., 2014). A large number of region-specific TFs can be observed earlier during development (Flames et al., 2007), suggesting that a greater number of differentially expressed TFs might be observed in the SVZ at postnatal ages, which remain to be fully explored. Such intrinsic coding programs contribute to the OB neuronal diversity. For instance, different combinations of the expression of *Pax6*, *Dlx2* and *Meis2* drive the differentiation of NSCs toward *TH*⁺, *CB*⁺ or *CR*⁺ PGCs (Brill et al., 2008; Agoston et al., 2014). Other regionally expressed TFs, including *Etv1*, *Nurr1* (*Nr4a2*), *Sall3*, *Zic1/3* might be associated with the acquisition of defined neuronal fates (Díaz-Guerra et al., 2013).

1.2.5. Regionalization also applied to gliogenesis

Regionalization is not restricted to the production of distinct neuronal subtypes. Indeed, similar principle apply for macroglial cells, namely astrocytes and oligodendrocytes.

Astrocytes are generated towards the end of the embryonic development, following the period of neurogenesis. The classical model, is that RGCs switch fate and start to produce astrocytes precursors that migrate to the cortex and further amplify locally to associate with previously generated neurons in so called cortical columns (Ge et al., 2012; Magavi et al., 2012; Tabata, 2015). Recent studies indicate that astrocytes production is highly regionalized, with newborn astrocyte precursors migrating radially away from their region of origin (Tsai et al., 2012). Thus, cortical astrocytes derive from the *Emx1*-expressing pallial VZ, while striatal astrocytes derive from the *Dbx1*-expressing sub-pallial VZ. It is likely that these different origins reflect some phenotypic and functional heterogeneity of astrocytes present in distinct brain regions. Indeed, the densities and morphologies of astrocytes vary greatly between brain regions (Azevedo et al., 2009). Furthermore, astrocyte heterogeneity in the CNS has recently been described to influence neuronal synaptogenesis and maturation through secretion of several extracellular matrix proteins (Eroglu and Barres, 2010).

The other macroglia lineage, oligodendrocytes, were long believed to be generated by all RGCs, because of their presence in all regions of the forebrain (Richardson et al., 2006). Later studies have revealed that they are produced in 3 different temporal and spatial

waves. The first wave originates from the MGE around E12.5 and the medial part of the ventral forebrain, while the second is more laterally generated by the LGE around E15.5. The final third wave appears at perinatal ages from *Emx1*⁺ NSCs that reside in the dorsal SVZ microdomain (Kessaris et al., 2006). Interestingly, while oligodendrocytes formed by all 3 waves are rather homogeneously distributed throughout the forebrain at birth, their differential survival results in their heterogeneous distribution at later timepoint. As a result, ventral forebrain regions are mainly populated by oligodendrocytes generated from the first and second “ventral” waves, while dorsal forebrain regions including the corpus callosum are mainly populated by oligodendrocytes generated from the third “dorsal” (Kessaris et al., 2006).

Altogether, these observations indicate that regionalization is not restricted to neurogenesis but also embraces gliogenesis. The exact transcriptional mechanisms involved in the regional production and functional importance of glial cell heterogeneity remains however to be fully explored.

1.2.6. Signals from the CSF and the niche act in concert to regulate NSCs activity and regionalization throughout pre- and postnatal life

In the developing brain, morphogen signaling have a global influence on the organization and development of the cerebral cortex. RGCs harbor at their apical surface a primary cilium contacting the cerebrospinal fluid (CSF) within the ventricles (Cohen and Meiningner, 1987). This primary cilium acts like a sensor to probe extracellular signals secreted by the choroid plexus and initiate intracellular transduction of specific molecular pathways (Tasouri et al., 2013; Lepanto et al., 2016). The CSF composition changes during the corticogenesis period, as well as during postnatal life, and contains diffusible morphogens that act as key drivers of cortical development (Lehtinen et al., 2011; Silva-Vargas et al., 2016) including FGFs, *Shh*, transforming growth factor beta (*TGF-β*)/BMPs and Wnts.

Studies have shown that CSF from developing lateral ventricles (E17) is sufficient to stimulate progenitor proliferation and maintenance in neocortical explants and in neurosphere cultures (Lehtinen et al., 2011). Moreover, secreted factors from the lateral ventricle choroid plexus, a primary producer of CSF, directly and dynamically regulate multiple aspects of the behavior of adult NSCs, such as quiescence, and their progeny throughout the life of the animal (Silva-Vargas et al., 2016). In addition, the basal processes of RGCs contact meninges, which secrete regulatory factors for progenitor maintenance. β 1-integrins anchor RGC basal processes to the extracellular matrix, allowing exposure to meningeal-derived trophic signals that maintain progenitor survival

and proliferation (Radakovits et al., 2009). Lastly, on the striatal end of the SVZ, the basal processes of type B1 cells contact blood vessels at sites that lack unsheathing astrocytes or pericytes, facilitating direct access to circulating trophic factors (Tavazoie et al., 2008). This intricate constant cross talk between the vasculature and the SVZ has been further highlighted by coupling whole-mount preparation with automated 3D analysis of confocal images. Immediately underneath the ependymal cell layer the blood vessels form a dense plexus that is spatially associated with proliferating NSCs and type C progenitors (Shen et al., 2008; Tavazoie et al., 2008). An important component of blood vessels is the associated extracellular matrix, which forms extravascular structures named fractones. These fractones engulf astrocytic processes, as well as ependymal, microglial and progenitor cells, underlying their intimate association with the neurogenic niche and adding to the complexity of the NSC environment (Mercier et al., 2002; Shen et al., 2008). This specialized cytoarchitecture results in a unique microenvironment in which multiple signals act to maintain germinal activity in the adult brain (Ihrie and Álvarez-Buylla, 2011).

In addition to the CSF, the specialized cellular SVZ microenvironment, or “niche,” in which postnatal/adult NSCs reside play a key role in maintaining their activity and regionalization at postnatal stages. This is best illustrated by transplantation experiments. Homotopic grafts of SVZ cells give rise to large numbers of OB interneurons in the host mouse (Lois and Alvarez-Buylla, 1994). In contrast, SVZ cells transplanted to non-neurogenic brain regions produce few, if any neurons (Herrera et al., 1999) suggesting that SVZ cells are dependent on local environmental cues to promote neurogenesis. Heterotopic transplantation however do not support a direct role of the SVZ microenvironment in specifying distinct interneuron subtypes. For instance, NSCs isolated from the lateral SVZ that give rise to CB⁺ interneurons, in more dorsal SVZ regions fail to show re-specification in TH⁺ interneurons (Merkle et al., 2007b). It is also unclear if the SVZ niche provide signals for long term NSC self-renewal/maintenance. Transplantation experiments demonstrating the long-term self-renewal of NSCs are still lacking. Nevertheless, it is likely that fibroblast growth factor 2 (FGF-2) and epidermal growth factor (EGF), which are the principal mitogens used to maintain SVZ NSC under proliferation *in vitro*, likely play similar roles *in vivo*. Indeed, SVZ neurogenesis is reduced in mice null for either FGF-2 (Zheng et al., 2004) or the EGFR ligand-transforming growth factor α (TGF- α) (Tropepe et al., 1999). Interestingly, *in vitro* experiments suggested that local astrocytes can provide these proliferative signals for the SVZ niche (Morita et al., 2005). Other factors have been implicated in the regulation of the SVZ such as ciliary neurotrophic factor (CNTF) (Scott, 2006), Heparin-binding EGF (HB-EGF). Although most of these factors act on NSCs activation, those involved in maintaining NSCs quiescence remain to be fully explored.

I describe in more details below current knowledge on key diffusible and cell contact signaling pathways and on their role in NSCs activity and regionalization.

Sonic hedgehog

Shh is both a classical morphogen during development and a mitogenic factor for a variety of neural precursors (Ruiz i Altaba et al. 2003). Sonic hedgehog (Shh) is a diffusible protein that belongs to the hedgehog family members. In the developing forebrain, Shh is mostly secreted from the ventral telencephalon into the CSF (Echelard et al., 1993) (Figure 1C). Shh binding to its receptor Patched1 (Ptch1) at the primary cilium site induces a signaling cascade which leads to the activation of the downstream Gli2 and Gli3 transcription factors. They, in turn, activate numerous effectors including Gli1 and Nkx2.1 that participate to various aspects of ventral telencephalon specification including the generation of oligodendrocytes, astrocytes and GABAergic interneurons. The cortical interneurons invade the CP by tangential migration (Fuccillo, 2004). Their intracortical dispersion from the tangential migratory streams is controlled by a short primary cilium probing Shh signaling (Graef and Beimler, 1979). In contrast to the ventral telencephalon, the developing cortex shows limited sensitivity to Shh signaling whose physiological role remained unclear. However, changes (increase or decrease) affecting Shh signaling impair the generation of IPs and result in size modification of the dorsal telencephalon (Yabut et al., 2015; Wang et al., 2016) and prevent generation of the postnatal progenitors in the dentate gyrus (Han et al., 2008).

In the postnatal/adult SVZ, it appears that Shh has multiple roles and cells responding to Shh signaling express Gli1 transcription factor (Bai et al., 2002). Gli1⁺ cells produce OB interneurons and are found in ventral SVZ NSCs (Machold et al. 2003; Palma et al. 2005; Ihrie et al. 2011) but also in the dorsal domain producing cells of the oligodendroglial lineage (Tong et al., 2015). Shh mRNA is primarily detected in ventral forebrain neurons, suggesting that local expression of Shh activates Gli1 in the ventral SVZ (Ihrie et al., 2011). Conditional deletion of Shh in adult mice reduces the production of ventrally derived OB interneurons, suggesting that Shh activity underlies type B1 cell regional heterogeneity (Ihrie et al., 2011). Dorsal SVZ cells however appear to be resistant to Shh-pathway activation, suggesting that the regional identities of type B1 cells are epigenetically restricted. This may explain the absence of re-specification observed in heterochronic transplantation experiments, as previously discussed (Merkle et al., 2007c).

The Wnt/ β -catenin signaling pathway

*In neural development, the Wnt family of secreted signaling molecules plays multiple roles in stem cell maintenance, cellular proliferation, differentiation, migration, and axon guidance (Ille and Sommer, 2005; Harrison-Uy and Pleasure, 2012). Wnt ligands are secreted glycoproteins that bind to the receptors Frizzled and LRP 5/6 localized at the plasma membrane of APs inducing stabilization of the cytoplasmic β -catenin. Without signaling, activation β -catenin is degraded following its phosphorylation by GSK3 β . Once stabilized, β -catenin translocates into the nucleus and associates to TCF/LEF transcription factors family, which become activators and promote the transcription of downstream targets (Cadigan, 2012). The cortical hem of dorsomedial telencephalon secretes BMP and Wnt (2b, 3a, 5a, 7b, 8b) (**Figure 1C**) and regulates the patterning of the dorsoventral cerebral cortex (Caronia-Brown et al., 2014). Moreover, Wnt signaling plays a major role in the regulation of cortical development. During early corticogenesis, the increase of β -catenin induces proliferation of NECs by decreasing their cell cycle exit and by delaying the neurogenic (Hirabayashi, 2004; Wrobel et al., 2007). In contrast, later, it induces the expansion of the SVZ, the IPs pool and the neuronal output (Munji et al., 2011). The forced repression of the Wnt signaling pathway through genetic ablation of β -catenin during midgestation decreases Pax6 expression and leads to the depletion of APs, IPs and projection neurons, impairs oligodendrogenesis while increasing astroglialogenesis (Gan et al., 2014; Draganova et al., 2015). Indeed, Wnt signaling promotes the generation of oligodendrocyte progenitors by RGCs during late embryogenesis, while Shh supports the specification of ventrally derived oligodendrocyte progenitors (Langseth et al., 2010). Interestingly, these observations highlight the stage dependent activity of the canonical Wnt pathway. First it promotes self-renewal of NECs and RGCs and then promotes differentiation to IPs and finally induces oligodendrocyte differentiation from RGCs at the end of corticogenesis.*

In the postnatal SVZ, Wnt signaling is restricted to the dorsal-most microdomain, in NSCs and progenitors that generate oligodendrocytes and OB glutamatergic neurons (Azim et al., 2014). Genetic and pharmacological modulation approaches demonstrated that Wnt signaling regulates both proliferation and fate specification in the dSVZ (Azim et al., 2014). and identify canonical Wnts as the key dorsalizing factor in the postnatal SVZ, opposing ventrally localized Shh activity to determine dorso-ventral NSC fate (Backman et al., 2005). The highest functional Wnt activity defines the dSVZ-NSCs and their progeny, Tbr2⁺ NPs and Olig2⁺ OPs. Furthermore, Gli1 expression is not affected in dSVZ-NSCs providing further evidence that Wnt signaling exerts a direct dorsalizing effect on the postnatal SVZ. In the adult, increased β -catenin by expression of a stabilized form of this protein or

inhibition of the GSK3 β kinase, which is required for targeting β -catenin for degradation, increases the proliferation of Ascl1-expressing SVZ cells. This proliferation is also observed in the ISVZ of early postnatal brain but involves other signaling pathways as no induction of downstream Wnt target genes have been detected (Azim et al., 2014). In the early postnatal dSVZ, increase of β -catenin in NSCs produce more Tbr2 NPs at the expense of Dlx2 NPs. It is noteworthy that targeted genetic stimulation of β -catenin activity in NSCs of the ISVZ failed to induce Tbr2 expression. This non permissiveness of ISVZ-NSC appears to be a postnatal acquisition, since embryonic respecification of ventral NSCs can be achieved by expression of constitutively active β -catenin, resulting in partial expression of dorsally restricted markers in the ventral forebrain (most notably Ngn2) and a decrease in expression of ventral-restricted markers (Backman et al., 2005). Recently, Non canonical Wnt signaling regulates neural stem cell quiescence during homeostasis and after demyelination (Chavali et al., 2018).

Bone morphogenetic proteins

*Bone morphogenetic proteins (BMPs) are members of the TGF- β superfamily. BMPs (2, 4, 5, 6, 7) are secreted by the cortical hem and cooperate with Wnts to promote the dorsomedial patterning of the telencephalon (Furuta et al., 1997) (**Figure 1C**) and control midline development (Hébert et al., 2002). Without BMPs receptors, cortical progenitor specification is preserved and neurogenesis is maintained (Fernandes et al., 2007). In contrast, increase of BMP2/4 signaling during cortical development induces premature differentiation of RGCs into neurons (Shakèd et al., 2008). During gliogenesis stage, overexpression of BMP4 impairs the production of oligodendrocytes by RGCs at the expense of astrocytes (Gomes et al., 2003).*

BMPs also regulate adult brain germinal niches such as the SVZ. BMP signaling promotes astrocyte differentiation of cultured embryonic neural precursors at the expense of oligodendroglialogenesis and neurogenesis (Gross et al., 1996). Adult SVZ cells produce BMPs and their receptors (Peretto et al., 2002; Lim and Alvarez-Buylla, 2016). NOGGIN, a secreted BMP antagonist, is also locally expressed, most strongly in the ependymal cells. This locally derived BMP antagonist may contribute to the neurogenic niche. Downregulation of BMP signaling in NSCs impairs neurogenesis (Colak et al., 2008). Overexpression of BMP7 in the SVZ suppresses neurogenesis (Lim et al., 2000), and overexpression of Noggin from the ependymal suppresses local gliogenesis (Chmielnicki, 2004). Thus, a “balance” between BMP and their antagonists may control the levels of neurogenesis and gliogenesis from NSCs in adult brain niches. In embryonic stem cells, BMPs act in concert with leukemia inhibitory factor (LIF) to sustain self-renewal and

suppress differentiation (Ying et al., 2003). In the adult, it is possible that the level of their expression regulates the fate of type B1 cells into niche astrocytes or self-renewing stem cells. For example, overexpression of LIF promotes SVZ NSC self-renewal, expanding the population of NSCs in vivo while concomitantly decreasing OB neurogenesis (Bauer and Patterson, 2006).

Fibroblast growth factors

The fibroblast growth factors (FGFs) family is composed by 22 FGFs arranged into seven families (Mason, 2007). The signaling is mediated by four different tyrosine kinase receptors: FGFR1 to FGFR4 and promotes downstream activation of distinct pathways such as the Ras/Erk1/2 Map kinase, PI3-kinase, the Akt and the PKC pathways. The patterns of expression of the different FGFs are tightly regulated and contribute to the patterning of the cerebral cortex. At the cellular level, FGFs regulate timely differentiation of RGCs (Sahara and O'Leary, 2009). FGF receptors are expressed with specific spatial patterns along the progenitor region. However, absence of all FGFRs in the dorsal telencephalon leads to precocious neurogenesis, resulting in a reduced cortical surface area in both rostral and caudal parts (Kang et al., 2009). In addition, Notch related genes are downregulated in FGFR mutants and gain-of-function of Notch signaling can rescue the phenotype (Rash et al., 2013), suggesting that Notch lies downstream of FGFR signaling in the same pathway regulating cortical neurogenesis. Different FGF ligands can either promote progenitor differentiation or self-renewal (Raballo et al., 2000; Borello et al., 2008) therefore controlling in fine the normal growth of the brain. FGF signaling also participate to some extent to the differentiation of ventral progenitors independently of Shh signaling (Gutin, 2006). FGF signals, are required for the specification, survival, proliferation, and patterning of progenitor cells in the ventral telencephalon. Pharmacological inhibition of FGF signaling in embryos results in an increase in ventral apoptosis, loss of ventral gene expression, and ventral expansion of dorsal gene expression (Shinya et al., 2001). Thus, FGF signaling participates in patterning the telencephalon into ventral and dorsal domains, potentially via regulation of anti-hem signals/functions.

In the postnatal SVZ, FGF2 promotes NSC self-renewal, amplification of TAPs and subsequently OB neurons generation (Zheng et al., 2004; Azim et al., 2012b; Li et al., 2018). Further, direct administration of FGF2 into the lateral ventricle increased the generation of oligodendrocyte progenitors (OPCs) throughout the SVZ, both within the dSVZ and ectopically in the ISVZ and ependymal wall of the SVZ (Azim et al., 2012b).

Besides diffusible factors, other external factors arising from the direct cellular environment of NSCs influence their activity in a regional manner.

Notch signaling

*Notch signaling is activated by interactions between Notch receptors and their ligands. The mammalian Notch receptors (Notch1 - Notch4) are transmembrane proteins expressed on the cell surface as non-covalently linked heterodimers. The proteins comprise of an extracellular domain, which functions as the signal receiver and a transmembrane – intracellular domain that functions as the signal transducer. The extracellular domain contains epidermal growth factor (EGF)-like repeats, which are required for ligand binding (Zhang et al., 2018). The ligands of Notch signaling are transmembrane proteins that are present on the surface of neighboring cells. Such as IPs or neurons in the developing brain. There are five mammalian Notch ligands; Jagged1, Jagged2, Delta-like 1 (DLL1), DLL3 and DLL4, belonging to the Jagged and Delta-like families, respectively. As transmembrane ligands, they provide short-range signals. Notch in neural stem cells (NSCs) has been implicated in the maintenance of the undifferentiated and multipotent state (Lutolf et al., 2002; Nyfeler et al., 2005a; Mizutani et al., 2007; Ehm et al., 2010; Imayoshi et al., 2010; Basak et al., 2012), inhibition of neuronal differentiation and even terminal differentiation into an astrocyte lineage (Gaiano and Fishell, 2002). Once the ligand binds Notch receptor, the transcription of several genes, including the *Hairy enhancer of split (Hes)* genes, are initiated. *Hes* genes are basic-helix-loop-helix (bHLH) transcription factors that repress the expression of proneural genes, further ensuring RGCs stemness maintenance (Kageyama et al., 2008). *Hes* genes expression oscillate due to the negative feedback loop on their own promoter (Imayoshi et al., 2013). This characteristic pattern is critical for RGCs cell-cycle progression and a sustained *Hes* expression impairs neuronal generation (Baek, 2006). In contrast absence of *Hes1*, the key effector of the Notch signaling, leads to premature neurogenesis (Ishibashi et al., 1995). The crucial role of Notch signaling is underlined by various loss of function mutations in the embryo and in the adult. Conditional loss of Notch signaling in the embryo results in precocious differentiation of the RGCs and neurodevelopmental defects, including impaired survival as well as aberrant migration of progenitor cells (de la Pompa et al., 1997; Stump et al., 2002; Gratton et al., 2003). The RING finger E3 ubiquitin ligase *mind bomb 1 (MIB1)* is essential to activate Notch signaling (Itoh et al., 2003). Interestingly, *MIB1* is expressed in neurons and particularly in IPs, indicating that different progenitor populations can interact and mutually regulate each other to control the balance between self-renewal and neuronal differentiation in the mouse cortex (Yoon et al., 2008). A recent work provided evidence that during neurogenic divisions, *MIB1* is asymmetrically localized*

at the daughter centriole and then inherited by the future neuron, identifying the Notch regulator MIB1 as an intrinsic fate determinant (Tozer et al., 2017). Preventing MIB1 centrosomal association induces reciprocal Notch activation between sister cells and promotes symmetric divisions.

In postnatal/adult NSCs, Notch signaling suppresses neuronal differentiation and maintains precursor cell properties (Gaiano and Fishell, 2002). Notch1, Jagged1 and Delta1, are expressed in the adult SVZ (Stump et al., 2002; Nyfeler et al., 2005b; Givogri et al., 2006). In postnatal and adult SVZ cells, retrovirally transduced activated Notch prevents cell migration to the OB, suppresses neuronal differentiation, and decreases proliferation, creating an apparently more “quiescent” cell type (Chambers et al., 2001). Conversely, inactivation of canonical Notch signaling causes essentially all NSCs in the SVZ to differentiate into type C and A cells, leading to the eventual depletion of NSCs from this adult region (Imayoshi et al., 2010). Thus, Notch signaling is a critical component of type B1 cell maintenance. Interestingly, the ligands Jagged1 and Delta1 are expressed in type C and A cells (Givogri et al., 2006; Aguirre et al., 2010) (Givogri et al. 2006; Aguirre et al. 2010), which suggest a potential feedback regulation of the SVZ niche. Accumulation of newly born type A cells expressing Jagged1 or Delta1 may activate Notch signaling in type B1 cells, suppressing differentiation and potentiating self-renewal.

In the postnatal SVZ, regional differences in the composition of the extracellular matrix such as collagens, laminins or fibronectins and differential distribution of their receptors will likely contribute to the diffusion and exposition of these diffused molecules. Their role in NSCs activity and regionalization remains to be fully explored.

1.3. Transcriptional correlates of SVZ NSCs regionalization

As described above, a multitude of external factors (diffusible and cell-contact factors) act in concert to orchestrate NSCs activity and regionalization throughout pre- and postnatal development. Cross-talks exist at multiple levels in between these pathways resulting in the regional expression of define gene networks that regulate NSCs activity, as well as their production of distinct cell progenies (see for exemple Fiorelli et al., 2015; Azim et al., 2016). Understanding the transcriptional specificities of postnatal NSCs have proved to provide a wealth of information on their regional diversity.

Transcriptional profiling of NSCs have classically been performed on a population of cells (bulk analysis), even if recently developed RNA-sequencing approaches are now becoming more popular and provide additional information (see general discussion).

For bulk analysis, cell populations of interest are enriched by FACS, based on their expression of specific markers. Their mRNA is extracted then analyzed by microarrays, qPCR or RNA sequencing approaches. This approach gave deeper insights into transcriptional differences that exist in NSCs isolated from different regions, and/or at distinct stages of activation. Comparisons of transcriptional profiles of DG (Dentate Gyrus) and SVZ NSCs identified IGF2 to be highly enriched in the DG. In this region, IGF2 was shown to control the NSCs proliferation through AKT-signaling (Bracko et al., 2012). In the SVZ the early expression of neuronal markers in NSCs has been demonstrated, in agreement with an early priming of NSCs to differentiate into specific lineage. Further, the importance of cilia- and Ca-dependent pathways were emphasized (Beckervordersandforth et al., 2010). In another study, EGF receptor expression was used to isolate activated and quiescent NSCs from the SVZ. This allowed discovering multiple markers for these two stages and uncovered signaling pathways that may be targeted by small bioactive molecules to regulate NSCs activity (Codega et al., 2014).

We recently performed a similar transcriptional analysis to gain insight into the transcriptional correlates of SVZ NSCs. In order to probe heterogeneity of the postnatal SVZ, we microdissected its dorsal and lateral walls at different postnatal ages and isolated NSCs and their immediate progeny based on their expression of Hes5EGFP/Prominin1 and Ascl1-EGFP, respectively. Whole genome comparative transcriptome analysis revealed transcriptional regulators as major hallmarks that sustain postnatal SVZ regionalization. This comparative analysis, which was also applied to the NSCs and TAPs they contain, revealed the existence of an unsuspected heterogeneity in the postnatal SVZ, at both the regional and temporal levels (Azim et al., 2015). This was evidenced by the surprisingly high number of genes differentially expressed in the microdissected dorsal and lateral SVZ. Roughly, 30% of the genes were age-specific, whereas 30%–40% were shared by all three ages analyzed. Classification based on GO terms revealed the importance of transcription-related cues that were further abundant in NSCs. We identified several other transcriptional regulators aside from TFs. Those include chromatin modifiers, epigenetic modulators, downstream signaling mechanisms (nuclear), all of which could act in concert to dynamically regulate the diversity of neuronal and glial lineages generated by SVZ-NSCs during early postnatal life.

1.4. Objectives of the PhD thesis

Objectives of my PhD were twice.

First, *to explore further the transcriptional datasets of regionalized NSCs populations we have previously produced (Azim et al., 2015), by combining them with transcriptional datasets of specific neural lineages produced by others (Cahoy et al., 2008). To use such meta-analysis to explore differences in the lineage priming of regionalized NSC populations (Azim et al., 2017) and to identify new TFs associated with SVZ NSCs biased to acquire specific fate (see experimental chapter 1).*

Second, *to explore the origin, fate and transcriptional specificities of cortical progenitors that are still present in the dorsal-most domain of the postnatal SVZ, despite of the closure of the cortical neurogenic period. In particular, to develop a single-cell RNA-Sequencing approach to directly compare the transcriptome of this peculiar progenitor population at pre- and postnatal stages.*

To achieve these objectives, I acquired expertise in bioinformatics and developed all the scripts necessary to perform those studies. I also remained directly involved in the histology inherent to the completion of this work.

EXPERIMENTAL CHAPTERS

2. Experimental Chapter 1: HOPX Defines Heterogeneity of Postnatal Subventricular Zone Neural Stem Cells

This experimental chapter contains material published in the following manuscript, as well as original material that was not included in this publication

Stefan Zweifel, **Guillaume Marcy**, Quentin Lo Giudice, Deqiang Li, Christophe Heinrich, Kasum Azim, and Olivier Raineteau (2018) HOPX Defines Heterogeneity of Postnatal Subventricular Zone Neural Stem Cells. Stem Cell Reports, 11(3):770-783.

*In this chapter, transcriptomics and fate-mapping approaches were employed to explore the relationship between regional expression of transcription factors by neural stem cells (NSCs) and their specification in defined neural lineages. I developed in collaboration with Q. Lo Giudice a bioinformatic tool called Heatmap Generator (**see annexes for the complete script**), which aims at combining and comparing published transcriptional datasets in order to perform a meta-analysis. I also performed histology experiments as well as a meta-analysis of a recently published single-cell RNA sequencing experiment. The result supports the previous observation regarding the role of HOPX in the astrocytic lineage. Our results support an early priming of NSCs for the genesis of defined cell types depending on their spatial location in the SVZ and identify HOPX as a marker of a subpopulation primed toward astrocytic fates.*

N.B. experiments aimed at investigating the role of HOPX in SVZ NSCs by gain- and loss-of-function were all performed by S. Zweifel, and were therefore not included in this chapter (although they can be found in the published manuscript).

2.1. Introduction

Germinal activity persists in the postnatal mammalian brain in specialized niches, namely the dentate gyrus (DG) of the hippocampus and the subventricular zone (SVZ) that surrounds the lateral ventricle (LV). Neural stem cells (NSCs) of the postnatal SVZ divide and give rise to transient amplifying progenitors (TAPs) that generate neuroblasts, which migrate via the rostral migratory stream (RMS) into the olfactory bulb (OB), where they differentiate into neurons (Lois and Alvarez-Buylla, 1994). The SVZ additionally generates glial progenitors that invade the local parenchyma (reviewed in Azim et al. 2016). Recently, accumulating evidence has highlighted the heterogeneous nature of postnatal SVZ in respect to different microdomains generating distinct neural lineages. For example, progenitors of GABAergic neurons are predominantly derived from the lateral SVZ (ISVZ), while the genesis of glutamatergic neuron progenitors is restricted to the dorsal SVZ (dSVZ; Azim et al. 2012; reviewed in Fiorelli et al. 2015). Furthermore, postnatally derived oligodendrocytes are generated from the dSVZ (Kessaris et al., 2006).

This heterogeneity originates from early embryonic development (Fuentealba et al., 2015b) and is intrinsically encoded by expression of selected transcription factors (TFs). Therefore, TFs enriched in specific embryonic forebrain regions are persistent in their expression in corresponding microdomains of the postnatal SVZ. Examples of such TFs include EMX1 (pallium; dSVZ), GSX1/2 (lateral and medial ganglionic eminence; ISVZ), and ZIC1/3 (septum; medial SVZ; reviewed in Fiorelli et al. 2015). We recently resolved the transcriptional heterogeneities of different cell populations of the postnatal SVZ, in which an unexpected large number of transcripts (i.e. 1900) were differentially expressed in NSCs and TAPs sorted from defined SVZ microdomains. Intriguingly, most of the transcriptional heterogeneity observed between the dorsal and lateral NSCs (dNSCs and INSCs) was due to the expression of transcriptional cues. Notably, HOPX was identified with specific abundant expression in dNSCs (Azim et al., 2015). HOPX is a small (73 amino acids) atypical homeodomain protein that lacks DNA binding sites (Chen et al., 2002; Shin et al., 2002). Hopx expression is minimal at embryonic day 14.5 (E14.5) and peaks around E16.5 with a rostromedial to caudolateral gradient (Mühlfriedel et al., 2005). HOPX expression has been found in radial astrocytes of the adult DG, while it is described to be consistently absent from the adult SVZ (De Toni et al., 2008). Moreover, the expression of HOPX has recently received increasing attention due to its expression in quiescent NSCs, in mature astrocytes in the adult mouse DG (Li et al., 2015), as well as in outer radial glia (oRG) cells of the developing human brain (Pollen et al., 2015; Thomsen et al., 2015a).

Here, we used various approaches to further investigate the regionalization of the postnatal SVZ and of resident subpopulations of NSCs. In particular, we characterized the spatiotemporal and lineage- specific patterns of HOPX expression in the postnatal SVZ

2.2. Experimental procedures

Animals and Ethics

All animal experiments in Zurich were performed according to the Ethics Committee of the Veterinary Department of the Canton of Zurich (Approval ID 182/2011). Experiments in France were performed in accordance with European requirements 2010/63/ UE and have been approved by the Animal Care and Use Committee CELYNE (APAFIS #187 & 188). Mice used in this study were: OF1 wild-type (Charles Rivers; France), HES5:EGFP (Basak and Taylor, 2009), HOPX^{CreERT2} (Takeda et al., 2011) and Rosa-EYFP mice (Srinivas et al., 2001).

Plasmid Preparation and Electroporation

Plasmids used for electroporation are listed in the Supplemental Experimental Procedures. Plasmids were prepared and electroporated as previously described (Fernández et al., 2011). Immunohistochemistry Mice were sacrificed by an intraperitoneal overdose of pentobarbital followed by perfusion with Ringer's Lactate solution and 4% paraformaldehyde (PFA) dissolved in 0.1 M phosphate buffer (PB; pH 7.4). Brains were removed and postfixed for 12–48 hr at 4°C in 4% PFA and sectioned in 50-mm thick coronal serial sections. When necessary, antigen retrieval was performed for 20 min in citrate buffer (pH 6) at 80°C, then cooled for 20 min at room temperature and washed in 0.1 M PB. Immunostaining was performed as previously described (Azim et al. 2014, Azim et al., 2014)

Plasmids

The following plasmids were used in this study: pCX-GFP (kind gift of X Morin, ENS, Paris; France); pFloxPAdRed express (kind gift of Colette Dehay; INSERM U1208, Bron, France); pCAG-Cre (Addgene; 13775); pCMV-Hopx (Open Biosystems; MMM1013-202767606); pPB-CAG-EmGFP (VB161220-1119syh; VectorBuilder Inc., Cyagen Bioscience, Santa Clara, California, USA); pCMV-hyPBase (kind gift of Laura López-Mascaraque; Instituto Cajal, Madrid, Spain). Plasmids were purified using the EndoFree Plasmid Kit according to the manufacturer's protocol (Qiagen; 12362). Plasmids were re-suspended to a final concentration of 5 µg/µl. Dorsal electroporations were performed in

P1 to P2 (postnatal day 1 to 2) pups as previously described (Fernández et al., 2011). In Hopx^{CreERT2} animals subcutaneous tamoxifen (Tam; SIGMAAldrich; T5648) administration (1 mg per pup) was performed 2 to 3 hrs after electroporation.

Primary Antibodies for Immunohistochemistry

The following primary antibodies were used for immunohistochemical procedures: Rabbit anti-Hopx (1:400; Santa Cruz; sc-30216); Mouse anti-Hopx (1:400; Santa Cruz; sc-398703); Goat anti-DCX (1:500; Santa Cruz; sc-8066); Mouse anti-Olig2 (1:1500; Millipore; MABN50); Mouse anti-GFAP (1:500; Millipore; MAB3402); Chicken anti-GFP (1:1000; AVES LABS; GFP-1020); Rabbit anti-RFP (1:1500; MBL; PM005); Rabbit anti-S100 β (1:5000; SWANT); Chicken anti- β Gal (1:4000; Abcam; ab9361); Goat anti-Mcm2 (1:300; Santa Cruz; sc-9839); Mouse anti-Sox2 (1:100; Santa Cruz; sc-365823); Rabbit anti-Blbp (1:300; Millipore; ABN14). Blocking was done in TNB buffer (0.1 M PB; 0.05% Casein; 0.25% Bovine Serum Albumin; 0.25% TopBlock) with 0.4% triton-X (TNB-Tx). Sections were incubated over night at 4°C with gentle shaking the following primary antibodies in TNB-Tx. Following extensive washing in 0.1 M PB with 0.4% triton-X (PB-Tx), sections were incubated with appropriate secondary antibodies conjugated with Alexafluor 488, 555 or 647 (1:500; Life Technologies) for 2 hrs at room temperature. Sections were washed and counterstained with Dapi (1:5000; Life Technologies; D1306). To increase the signal from YFP and β Gal, biotinylated secondary antibodies (1:500; Jackson) were used in combination with DTAF conjugated streptavidin (1:250; Jackson) or a TSA amplification kit according to manufacturer's protocol (Life Technologies; T-20932), respectively.

Fluorescence-Activated Cell Sorting and qPCR

Hes5::EGFP (with C57BL/6 background) of the age P2-P4 were used for sorting for NSCs as previously described and using the exact same parameters (Azim et al. 2015). 4 to 5 animals of one litter was used for 1 "n" number. Microdissection of SVZ domains (dorso-medial; dorso-lateral and lateral) was performed in RNase free, sterile conditions. Microdissection of SVZ domains (dorso-medial; dorso-lateral and lateral) was performed in RNase free, sterile conditions. Tissues were dissociated using a trypsin-based Neural Dissociation Kit (Miltenyi Biotec, Bergisch Gladbach, Germany). For additional purification of the Hes5-EGFP population, an APC conjugated NSC antibody against the transmembrane-protein prominin-1 (1:100; ebiosciences) was applied for 15 mins at RT, before suspension was subjected to Fluorescence Activated Cell Sorting (FACS Aria III; BD Bioscience, Franklin Lakes, New Jersey, USA). Dead cells were excluded by forward and sideward scatter. Gating settings were gained using an EGFP- wildtype animal and a

prominin-1 isotype control conjugated to APC (rat anti-IgG; 1:100, ebiosciences). Brightest 30% of EGFP⁺ cells, which were *prominin-1*⁺ were collected directly into RNA lysis buffer and snap-frozen for further gene expression analysis. RNA extraction was performed using the RNeasy microkit (Qiagen; 74004) following manufacturer's guidelines. RNA amplification of 3 ng input material was done using the Nugene Pico Ovation WT kit (NuGen Technologies, Inc., San Carlos, CA) as described previously (Azim et al. 2015). qPCR was performed according to the procedures described elsewhere (Azim et al., 2012b, 2014)(Azim et al., 2012b, Azim et al., 2014b), with the Light Cycler 480 (Roche, Basel, Switzerland). All reactions were performed in duplicates or triplicates and GAPDH was used as reference gene. Primers used were custom made by Qiagen (EGFP, Eomes, Hopx, Pcnα, Sp8) or designed with the Primer Express 1.5 software and produced by Eurofins (Schönenwerd, Switzerland).

GAPDH: fw_CGTCCCGTAGACAAAATGGT, rv_TTGATGGCAACAATCTCCAC;
Aldh1l1: fw_CAGTAAACCTCCTGGCCAAA, rv_CCCTGTTTTCCCTACTTCCC;
Aqp4: fw_TGAGCTCCACATCAGGACAG, rv_TCCAGCTCGATCTTTTGGAC;
Dct: fw_GCATCTGTGGAAGGGTTGTT, rv_ACTCCTTCCTGAATGGGACC;
DCX: fw_CTGACTCAGGTAACGACCAAGAC, rv TTCCAGGGCTTGTTGGGTGTAGA;
Dlx2: fw_CTTCTTGAACCTTGGATCGGC, rv_AGACCCAGTATCTGGCCCTG;
Ebf1: fw_GGTGGAAGTCACACTGTCGTAC, rv_GTAACCTCTGGAAGCCGTAGTC;
Fgfr3: fw_ACAGGTGGTCATGGCAGAAGCT, rv_CTCCATCTCAGATACCAGGTCC;
Gli1: fw_CTCAAACCTGCCCAGCTTAACCC, rv_TGCGGCTGACTGTGTAAGCAGA;
Gli3: fw_CGAGAACAGATGTCAGCGAG, rv_TGAGGCTGCATAGTGATTGC;
Hes5: fw_GTAGTCCTGGTGCAGGCTCT, rv_AACTCCAAGCTGGAGAAGGC;
Id3: fw_GCGTGTCATAGACTACATCCTCG, rv_GTCCTTGAGATCACAAGTTCCG;
Lef1: fw_CGTCACACATCCCGTCAGATGTC, rv_TGGGTGGGGTGATCTGTCCAACG;
Olig1: fw_AGCAAGCTCAAACGTTGGTT, rv_GTTCTGTTTTTCAGGCTCGC;
Olig2: fw_GACGATGGGCGACTAGACA, rv_CAGCGAGCACCTCAAATCTA;
PDGFRα: fw_AGAAAATCCGATACCCGGAG, rv_AGAGGAGGAGCTTGAGGGAG;
Plp1: fw_GGGCCCCCTACCAGACATCTA, rv_TCCTTCCAGCTGAGCAAAGT;
Tcf7: fw_TGCCTTCAATCTGCTCATGCC, rv_GTGTGGAAGCTGCTGAAATGTTCCG;
Vax1: fw_CTCTACAGGCTGGAGATGGAGT, rv_GCTTAGTCCGCCGATTCTGGAA.

Meta-Analysis of Transcriptional Profiles

To generate the lists of TFs that are enriched in dNSCs and INSCs, we made use of previously published datasets (Cahoy et al., 2008; Azim et al., 2015), accessible on the Gene Expression Omnibus database (GEO: GSE60905 and GSE9566). We analyzed them on the “Gene Expression Omnibus” (<https://www.ncbi.nlm.nih.gov/geo/>) for transcripts that are differentially expressed between dNSCs and INSCs (≥ 1.8 fold enrichment and p -values $< 5\%$). Finally, we selected transcripts for transcription factor activity and regulation of transcription using “DAVID Analysis Wizard” (<https://david.ncicrf.gov/>). Lists of transcripts were analyzed for enrichments in the neuronal, astrocytic or oligodendrocytic lineage using the transcriptional dataset of the Barres group (Cahoy et al. 2008; GSE9566). Heatmaps were produced using a self-made R script “Heatmap Generator” which is described below.

Heatmap Generator

We developed a tool to combine different transcriptomic datasets available via the “Gene Expression Omnibus” (GEO) and generate heatmaps named HeatMap Generator. This tool is a self-made R script that can be run as a local application. The procedure involves to compile on the one hand the datasets of interest with their GSE references, and on the other hand the genes of interest. Both files should be saved as csv files with the same name and placed in a DataSet and Genes folders accordingly. Then the application GSEtoHeatmaps.sh can be launch. The software will interrogate the GEO database and generate heatmaps of pre-selected genes. The R script is provided as **Annex 1**.

Meta-Analysis of Single-Cell RNA Sequencing datasets

We analyzed the transcriptomes of embryonic cortical cells (E15.5 and E17.5) produced by Yuzwa et al. (Yuzwa et al. 2017, GEO: GSE107122.). The Seurat bioinformatic pipeline was used for the analysis as follow. We first created a “Seurat object” including cells expressing more than 100 genes and genes expressed in more than 2 cells. We next performed a Principal Components Analysis (PCA), using the `prcomp` function of R, after scaling and centering of the data across these genes. This ensured robust identification of the primary structures in the data. We identified statistically significant principal components and used the most significant genes for each of these PCs as input for t-Distributed Stochastic Neighbour Embedding (t-SNE, R package, “perplexity parameter” = 30). To identify clusters, a graph-based clustering approach was used. For the subclustering analysis of E17.5 RGCs only we used the astrocyte marker genes described in Zywitza et al. (Zywitza et al., 2018) as input for t-SNE. All the codes used to produce Figure 11 can be found in **Annex 2**.

Quantifications and Statistics

*Quantifications and Statistics Images were acquired using a Leica DM5500 epifluorescent microscope, a Leica TCS SPE II, and a TCS SP5 confocal microscope (Leica Microsystems, Wetzlar, Germany). Images were quantified using ImageJ-win64 or assembled as representative pictures with LAS X, ImageJ, and Photoshop (CS4). Statistical analysis was done with Microsoft Excel 2013 and GraphPad Prism 7. All data are shown as mean \pm SEM and statistical significance was calculated using the unpaired *t* test (in figures **p* < 0.05, ***p* < 0.01, ****p* < 0.001, *****p* < 0.0001).*

2.3. Results

Hopx Is Enriched in NSCs of the dSVZ and in Cells of the Astrocytic Lineage.

In a previous study, we examined the transcriptome of spatially distinct domains of the postnatal SVZ and revealed differential transcriptional networks in region-specific NSCs (Azim et al., 2015). This heterogeneity was explored further by analysis of TFs and transcriptional regulators (termed hereafter as TFs) as well as their association with defined neural lineages. Focusing on TFs only, 112 were differentially expressed between the regionalized subpopulations of NSCs (dNSCs: 61; INSCs: 51; **Figures 8A and S1A–S1C**). The expression of TFs enriched dorsally was confirmed by examining *in situ* databases (<http://www.brain-map.org/>), and by immunohistochemistry (**Figures 8C and 7D**). Among transcripts enriched in dNSCs (**Figure 8B**), 5 out of the top 10 (NeuroD6, Eomes, NeuroD1, Tbr1, Neurog2) are known major determinants of the glutamatergic neuronal lineage (Schuurmans et al., 2004; Hevner et al., 2006; Brill et al., 2009; Winpenny et al., 2011). In addition, a meta-analysis was performed on publicly available datasets of isolated glial cells and neurons for the characterization of TFs into defined neural lineages (Cahoy et al., 2008). Interestingly, this analysis revealed that TFs enriched in dNSCs formed at least three clusters corresponding to astroglia (18/61), neurons (15/61), and oligodendroglia (11/61; **Figure 8E**). In contrast, INSCs enriched TFs identified a single large neuronal cluster (42/51), while those of oligodendroglia were relatively fewer (3/51) and the astroglial cluster was absent (**Figure S1E**). These observations underline the greater diversity of lineages arising from the dSVZ, whereas the ISVZ generates almost exclusively interneurons (reviewed in Fiorelli et al., 2015; Azim et al., 2016).

We then focused our analysis onto HOPX, an atypical homeodomain protein, which was notably enriched in both dNSCs (rank 7; 7-fold enriched in dNSCs) and the astrocytic lineage (**Figures 8A, 8B, 8D, and 8E**). Immunodetection of HOPX confirmed that it was not expressed in migrating neuroblasts (DCX⁺) of the RMS nor in OLIG2⁺ oligodendrocytes of the corpus callosum (CC; **Figures 8F and 8G**). In contrast, HOPX was expressed by astrocytes in the CC (glial fibrillary acidic protein [GFAP]⁺; **Figure 8H**). In the dSVZ, HOPX expression was evident in astrocyte-like lineages while absent in the other lineages (**Figures S1F–S1H**), in agreement with the transcriptional meta-analysis (**Figure 8E**). Such an expression pattern supports an early expression of HOPX and its association with the astroglial lineage.

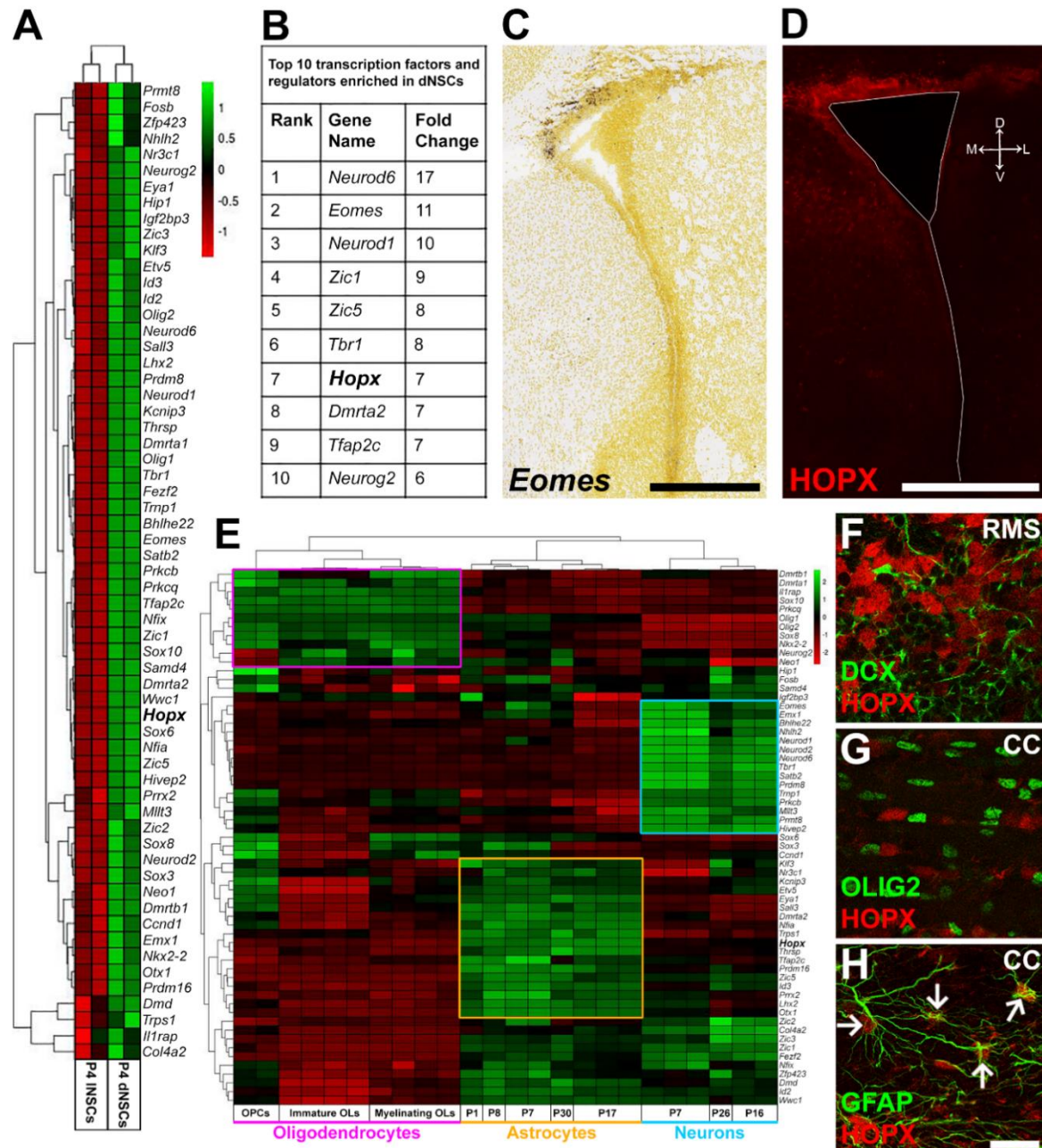


Figure 8. A Meta-Analysis of TFs Enrichment in dNSCs Highlights Their Association with Distinct Neural Lineages. (A) Heatmap showing enrichment of 61 TFs in dNSCs compared with INSCs (R1.8-fold and $p < 0.05$). (B) Top ten TFs enriched in dNSCs. (C and D): Dorsal enrichment of select transcripts was confirmed using the Allen Brain Atlas for *Eomes* (C) and by immunohistochemistry for HOPX (D). (E) Heatmap of dNSC enriched TFs reveals three clusters corresponding to defined neural lineages: oligodendrocytes (purple, 11/61); astrocytes (yellow, 18/61); neurons (turquoise, 15/61). *Hopx* (highlighted in bold) associates with the astrocytic lineage. (F–H) Confirmation of astroglial lineage-specific enrichment of HOPX by immunohistochemistry. HOPX is largely absent in neuroblasts of the RMS (DCX; F) and oligodendrocytes in the CC (OLIG2; G), but is observed in astrocytes of the CC (GFAP; H, arrows indicate double positive cells). CC, corpus callosum; dNSC, dorsal NSCs; INSC, lateral NSCs; RMS, rostral migratory stream; OPC, oligodendrocyte precursor cell; OL, oligodendrocyte. Scale bars, 500 μ m (C and D) and 25 μ m (H).

HOPX Expression Reveals Intraregional Heterogeneity within the dSVZ

We next focused our analysis on HOPX expression within the dSVZ. Using two different antibodies, HOPX protein expression was found to be restricted to the dSVZ, while it was consistently absent from its lateral counterpart (**Figure 9A**; see also **Figure S2**).

A high HOPX expression was already detectable throughout the dorsal region of the VZ/SVZ at E16. At early postnatal time points (postnatal day 1 [P1] and P4), its expression remained high but declined sharply thereafter in the young adult SVZ. Throughout its period of expression, a clear mediolateral gradient persisted, with the highest expression observed in the medial aspects of the dorsal wall and declining in its lateral aspects (i.e., high medial-to-lateral expression), which has not yet been described for any other gene (**Figure 9A**).

To further investigate HOPX expression within dNSCs we used the HES5:EGFP mouse line, which efficiently labels NSCs, as previously reported (Azim et al., 2015; Giachino et al., 2014). Quantification of HOPX expression in the dSVZ in this mouse line revealed that a large proportion ($70.1\% \pm 5.0\%$) of EGFP⁺ NSCs expressed HOPX. Due to the notable mediolateral gradient of HOPX expression in the dSVZ, quantifications of EGFP⁺/HOPX⁺ cells were performed in the medial and lateral subdomains. There was a significantly higher overlap in the medial subdomain of the dSVZ ($90.9\% \pm 6.6\%$; dmSVZ) compared with the lateral subdomain ($53.7\% \pm 6.2\%$; dlSVZ; **Figure 9B**). These results were confirmed by performing electroporations (EPOs) of a GFP-encoding plasmid into the dSVZ of pups, which were sacrificed 8 hr later. This enables labeling of cells in direct contact with the lumen of the ventricle, i.e., those with radial glia (RG) morphology, as previously described (Azim et al., 2015; Tiveron et al., 2017). Similar results were obtained with $76.0\% \pm 2.4\%$ of the electroporated (GFP⁺) cells expressing HOPX, which were significantly larger in the dorsomedial subdomain compared with its dorsolateral counterpart ($93.0\% \pm 2.4\%$ versus $69.3\% \pm 3.4\%$; **Figure 9C**).

Taken together, the gradient of HOPX expression in dNSCs demonstrates intraregional NSC heterogeneity within the dSVZ wall and proposes its regulation of NSC identity and fate.

The dSVZ Is Defined by Microdomains with Distinct Lineage Outputs

Both the astrocytic expression of *HOPX* and its regional enrichment within a subpopulation of dNSCs suggest further transcriptional heterogeneity within the dSVZ microdomains. To test this hypothesis, we took advantage of the *HES5:EGFP* mice and microdissected the medial and lateral parts of the dSVZ (dmSVZ and dlSVZ, respectively) and isolated the NSCs (dmNSCs and dlNSCs, respectively) based on their *EGFP* expression, as previously described (Azim et al., 2015). qRT-PCR was performed to compare the expression of lineage-specific markers in regional NSC populations (**Figures 10A and 10B**).

We selected known transcripts enriched in NSCs as well as in defined neural lineages (Cahoy et al., 2008; Azim et al., 2015) and compared their expression levels by qPCR. Measured transcripts were all enriched in NSCs compared with the dSVZ, thereby validating our fluorescence-activated cell sorting strategy. In addition, there was no overall regional enrichment of stem cell markers (*Hes5*, *Egfp*; Basak & Taylor 2007) and a proliferation marker (*Pcna*) within the different NSC populations, although the neuroblast marker *Dcx* was enriched in INSCs, consistent with a greater number of neuroblasts generated by this SVZ microdomain (Yang et al. 2004; **Figure 10A**, top panel). Markers for the astroglial, oligodendroglial, and neuronal lineages were confirmed using the transcriptional datasets from the Barres group (Cahoy et al. 2008; **Figure S3**). Markers that were highly specific to astrocytes (*Aqp4*, *Aldh1l1*, *Fgfr3*, *Id3*), including *Hopx*, were enriched in dmNSCs (**Figure 10B**, top panel), and those for oligodendroglial lineage (*Pdgfra*, *Plp1*, *Olig1*, *Olig2*, *Dct*) were partly enriched in dmNSCs but overall more homogeneously distributed (**Figure 10B**, middle panel). Finally, transcripts of the neuronal lineage (*Dlx2*, *Sp8*, *Eomes*, *Vax1*, *Ebf1*) were generally enriched in dlNSCs or in INSCs (**Figure 10B**, bottom panel), implying spatial segregation of lineages in the dSVZ. Taken together, *Hopx* and astroglial markers exhibit expression patterns in the dSVZ that are opposite to neuronal markers (**Figure 10C**). Interestingly, target genes for morphogens, i.e., *WNT* and *SHH*, showed that *WNT* signaling is homogeneously distributed throughout the dorsal wall (*Lef1*, *Tcf7*), whereas *Gli1* is highly expressed in INSCs (**Figure 10A**, bottom panel). Another signaling pathway target gene, *Id3*, used as a readout for bone morphogenetic protein (BMP) signaling, showed very marked enrichment in dmNSCs (**Figure 10B**, top panel). Next, to test whether NSCs harbored by those two subdomains are biased to generate specific neural progenies, we performed targeted EPO of the dmSVZ and dlSVZ (**Figure 10D**). At a short time point (i.e., 12 hr), EPO of both microdomains with a GFP-encoding plasmid resulted in efficient GFP expression in numerous RG cells. Accurate spatial targeting was assessed by measuring the GFP fluorescence intensity within 50-mm probes distributed along the mediolateral aspects of

the dSVZ at 14 days post-electroporation (dpe) (Not shown). This confirmed the precise and reliable targeting of NSCs of the dmSVZ and dISVZ. Both regions had given rise to large cohorts of progenies whose distribution and fate appeared to be strikingly different. Indeed, in agreement with the transcriptional profile of dINSCs, a large population of GFP⁺ neurons in the OB (93.3 ± 11.1 , average number of cells/section) were found following dorsolateral EPO (dIEPO), while those derived from the dorsomedial EPO (dmEPO) remained fewer (11.1 ± 1.8 ; **Figures 9E–9G**).

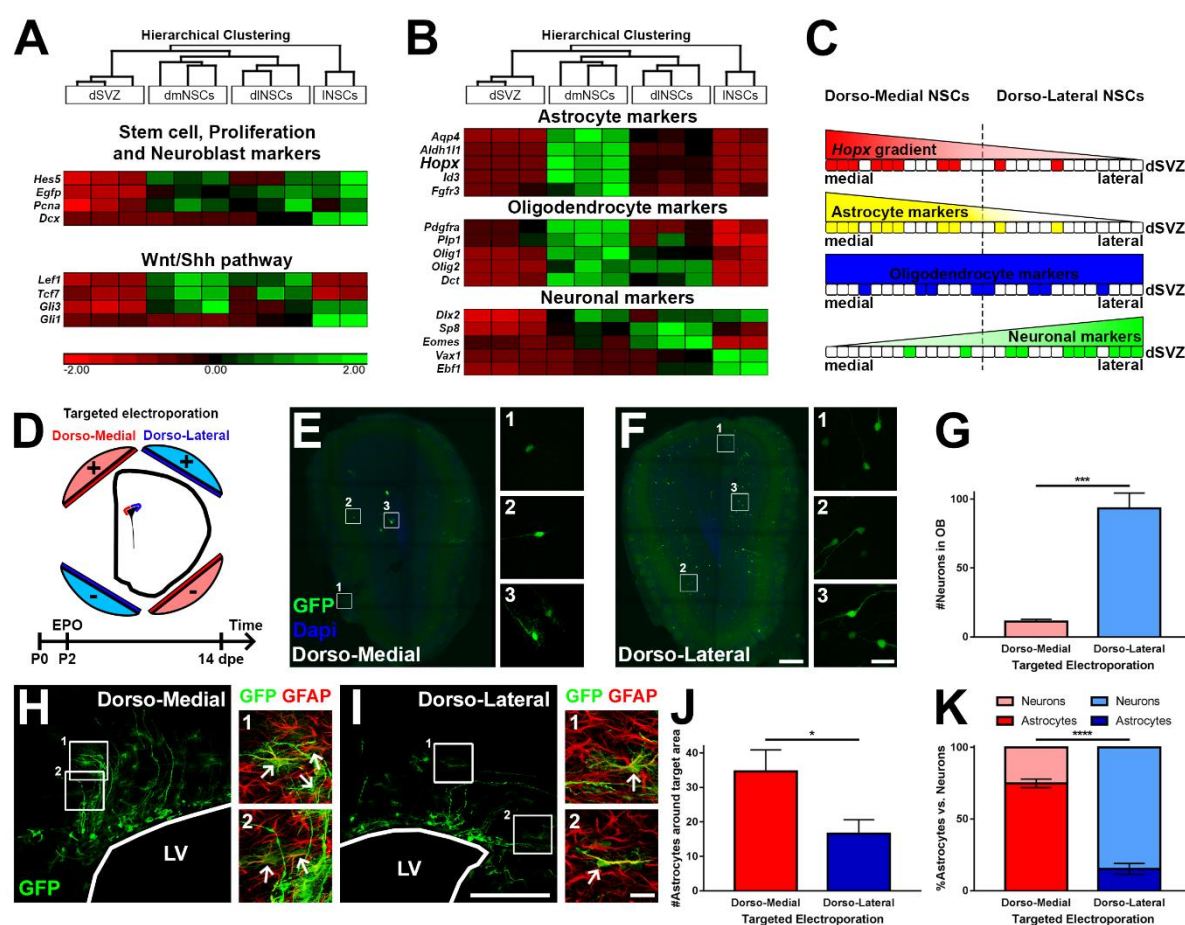


Figure 10. Lineage-Specific Markers Highlight Acquisition of Divergent Cell Fates by NSCs Located in Different dSVZ Subdomains. (A and B) Heatmaps show enrichment of transcripts in NSCs of distinct SVZ regions (dmNSCs, dINSCs, INSCs) compared with the dorsal environment (dSVZ). Transcripts of stem cell, proliferation, and neurogenesis markers (A; top panel) and selected signaling pathways. (A; bottom panel) were analyzed. Selected markers of the astroglial (B; top panel), oligodendroglial (B; middle panel), and neuronal lineage (B; bottom panel) were analyzed. Astrocyte and neuronal markers show regional enrichment in dmNSCs and dINSCs, respectively, while oligodendroglial markers show partial preference for enrichment in dmNSC. Note that HOPX transcripts were enriched in dmNSCs. (C) Scheme representing the counter gradients of the expression of Hopx (red) and astroglial

markers (yellow) against the expression of neuronal markers (green) in dNSCs. Oligodendroglial markers (blue) do not show such a clear spatial gradient. **(D)** dmEPO and dIEPO highlight divergent lineage outputs of the two dorsal subdomains. The scheme shows the orientation of the electrodes for the targeted EPOs at P2 followed by analysis at 14 dpe. **(E–G)** Representative micrographs of OB sections after dmEPO and dIEPO (E and F). Cell counts of OB neurons indicate that neurogenesis of the dSVZ mainly originates from dINSCs (G). **(H–J)** Representative micrographs of LV containing sections after dmEPO and dIEPO. Cells with an astrocytic fate were identified according to their morphology and GFAP expression (H and I, arrows indicate double positive cells). Quantification of astrocytes indicate that astrogenesis of the dSVZ is mainly provided by dmNSCs (J). **(K)** Graph showing the fractions of astroglial and neuronal progenies from NSCs of these two subdomains. It highlights that dmNSCs are primed for generating astrocytes, whilst neurons are derived from dINSCs. dpe, days post electroporation; dSVZ, dorsal SVZ; dmNSCs, dorsomedial NSCs; dINSCs, dorsolateral NSCs; INSCs, lateral NSCs; EPO, electroporation. Animals: (A) 4–5 per n; (B) dmEPO, n = 4; (B) dIEPO, n = 5. Error bars represent SEM. Scale bars in (F) and (I) represent 200 mm (overviews) and 25 mm (crops), and apply also to (E) and (H). *p < 0.05; ***p < 0.001; ****p < 0.0001.

*In contrast, the population of GFP⁺ astrocytes in the vicinity of the LV (assessed by morphology and GFAP expression; Figures 3H and 3I), was substantially larger following dmEPO than dIEPO ($34.6.5 \pm 6.3$ versus 16.5 ± 4.1 ; **Figure 10J**). Taken together, our data reveal that dmNSCs are primed to generate astrocytes ($74.9\% \pm 3.0\%$ astrocytes versus $25.1\% \pm 3.0\%$ neurons), whilst dINSCs generate largely olfactory neurons ($15.2\% \pm 3.8\%$ astrocytes versus $84.8\% \pm 3.8\%$ neurons; **Figure 10K**).*

Altogether, these findings demonstrate a high degree of heterogeneity within the dSVZ in containing specialized NSC populations that generate either astrocytes or neurons according to their location.

HOPX-Expressing dNSCs Are Biased to Acquire an Astroglial Fate

*To confirm a direct relationship between HOPX expression and the generation of distinct neural lineages by dNSCs, we fate-mapped HOPX-expressing NSCs. To this end, we co-electroporated an inducible fluorescent plasmid (pFloxPA-DsRed) with an EGFP plasmid (pCX-GFP) in the dSVZ of P1 HOPX^{CreERT2} mice and analyzed brain sections at 7 and 21 dpe (**Figures 11A and 11B**). Tamoxifen-mediated activation of the CRE-recombinase in HOPX⁺ NSCs led to DsRed/GFP co-expression (hereafter termed dsRed) in electroporated cells and their progenies, whilst the HOPX⁻ lineage expressed EGFP only (**Figure 11C**). Electroporated cell distribution and fate were assessed at both time points on serial sections encompassing the LV and the OB (**Figures 11D and 11E**). These results revealed the presence of DsRed⁺ and GFP⁺ cells at both 7 and 21 dpe (**Figure 11F**). Remarkably, while the majority of GFP⁺ cells were found in the OB (7 dpe: $66.2\% \pm 2.1\%$;*

21 dpe: $77.7\% \pm 2.5\%$) and acquired the typical morphology of granule neurons, the majority of DsRed⁺ cells remained in close proximity to the dSVZ, i.e., in the CC and the cortex (7 dpe: $64.6\% \pm 5.6\%$; 21 dpe: $63.8\% \pm 6.8\%$) at both time points (**Figure 11G**). The distinct neural fates adopted by HOPX⁺ or HOPX⁻ NSCs were examined by immunolabeling of GFAP in DsRed⁺ and GFP⁺-expressing progenies in the periventricular regions at 21 dpe. This analysis confirmed that the generation of GFAP⁺ astrocytes produced by HOPX-expressing NSCs was approximately twice as large compared with dNSCs that do not express HOPX ($59.2\% \pm 7.1\%$ versus $32.8\% \pm 4.3\%$, **Figure 11H**). These findings confirm HOPX as a marker for a subpopulation of dNSCs primed for astrogenesis.

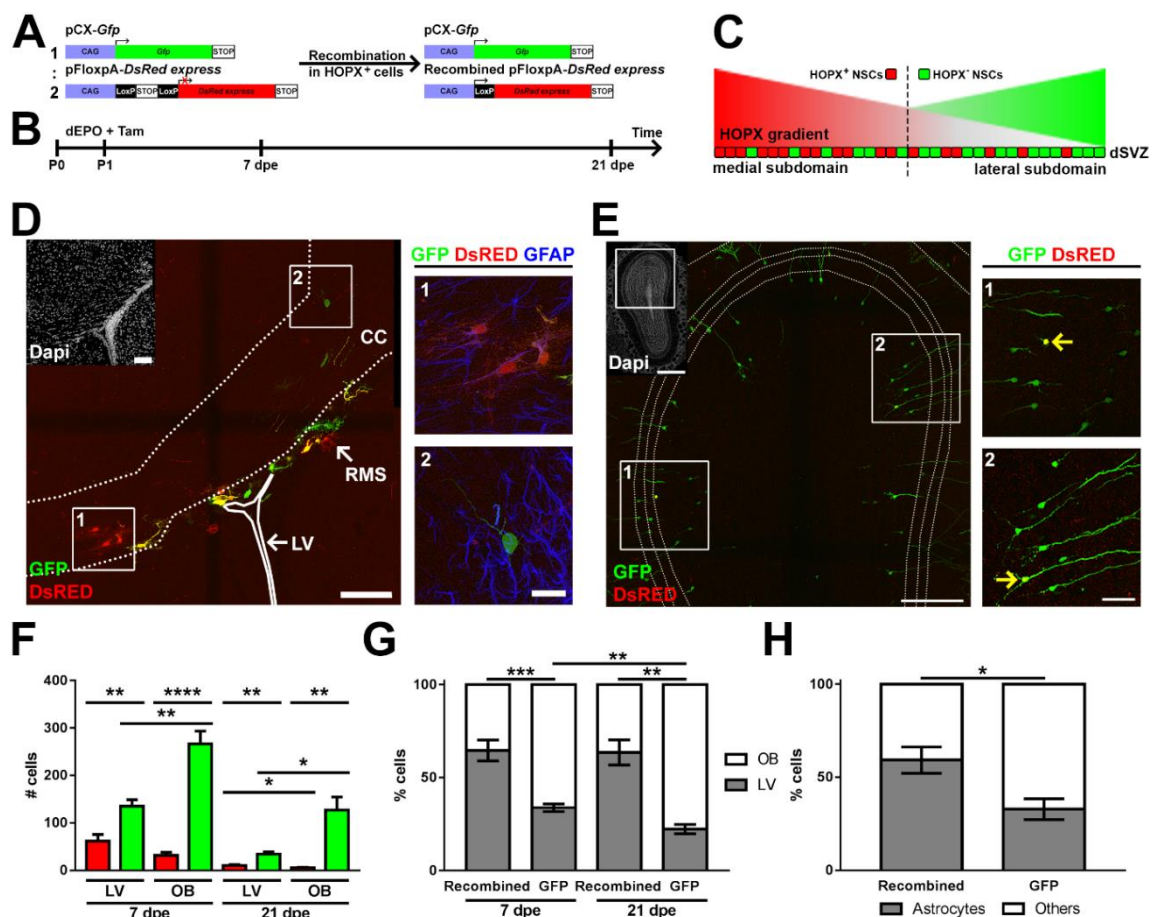


Figure 11. Conditional Fate Mapping Reveals HOPX-Expressing NSCs Are Biased to Generate Astrocytes. (A–C) Co-electroporation of a pCX-GFP and an inducible pFloxpA-DsRed plasmid (1:2; A) in HOPX^{CreERT2} mice, allows lineage tracing of HOPX⁺ and HOPX⁻ populations at short term (7 dpe) and long term (21 dpe; B). This approach results in GFP-only progenies from HOPX⁺ NSCs, whilst HOPX⁻ NSCs give rise to dsRED/GFP (termed as DsRed) progenies (C). (D and E) Representative micrographs of an LV (D) and OB (E) section

at 21 dpe. Astrocytic fate was assessed according to morphology and GFAP expression (D, crops). Neuronal fates were assessed in the OB according to morphology (E, crops; yellow arrows indicate DsRed/GFP double positive cells). (F) Graph of absolute numbers of recombined cells (red) and GFP⁺ (green) in LV and OB sections at 7 dpe and 21 dpe. (G) Graph showing the fractions of recombined DsRed⁺ and GFP⁺ cells harbored by LV and OB sections at 7 dpe and 21 dpe. (H) Graph showing the fractions of cells derived from recombined DsRed⁺ and GFP⁺ populations exhibiting astrocytic traits at 21 dpe in the vicinity of the LV. dEPO, dorsal electroporation; dpe, days post electroporation; dSVZ, dorsal SVZ; LV, lateral ventricle; NSCs, neural stem cells; OB, olfactory bulb; Tam, tamoxifen. Animals: 7 dpe, n = 5; 21 dpe, n = 4. Error bars represent SEM. Scale bars in (D) represent 100 μ m (DAPI overview and fluorescence overview) and 25 μ m (crops). Scale bars in (E) represent 500 μ m (DAPI overview), 250 μ m (fluorescence overview), and 50 μ m (crops). *p < 0.05; **p < 0.01; ***p < 0.001; ****p < 0.0001.

Hopx-expressing RGCs are Present in the Late Developing pallium and Share Transcriptional Features with adult Astrocytes

We next wondered if a subpopulation of dNSCs primed for astrogenesis is already present during the embryonic period of cortical neurogenesis. To address this question, we took advantage of two recently published single-cell RNA sequencing datasets ((Yuzwa et al., 2017; Zywitzka et al., 2018). We used the dataset of Yuzwa and colleagues, consisting of a single cell RNA sequencing analysis of cortical cells at distinct embryonic timepoints, to isolate E15.5 and E17.5 radial glia cells. We next used the dataset of Zywitzka and colleagues, consisting of a large scale single-cell RNA sequencing of the entire SVZ, to isolate the list of markers associated to niche astrocytes.

We first focused our analysis on E15.5 and E17.5 isolated cortical cells. Genes with high variance were used to compute principal components as input to visualize cells in two dimensions using t-distributed stochastic neighbor embedding (t-SNE). To identify RGCs at both time points we identified cells with Sox2 expression, representing Sox2 relative expression as a color gradient, with grey indicating no detectable mRNA and red indicating the highest mRNA level detected (**Figure 12A**). This resulted in the identification of 334 radial glial cells at E15.5 and 76 at E17.5. We combined the 2 populations together (**Figure 12B**) and identified differentially expressed genes (386 and 639 enriched genes at E15.5 and E17.5 respectively, bimod test and threshold 0.25). A functional clustering analysis was performed using the DAVID software, which revealed enrichment of cell cycle related genes (**Figure 12C**) and neuronal related genes (**Figure 12D**) in E15.5 RGCs, whereas astroglial-related genes such as Sparcl1 were enriched in E17.5 RGCs (**Figure 12E**, **Annex 3**), in agreement with the neurogenic to gliogenic switch occurring at this late embryonic timepoint. These results are consistent with the known developmental trajectories described during development.

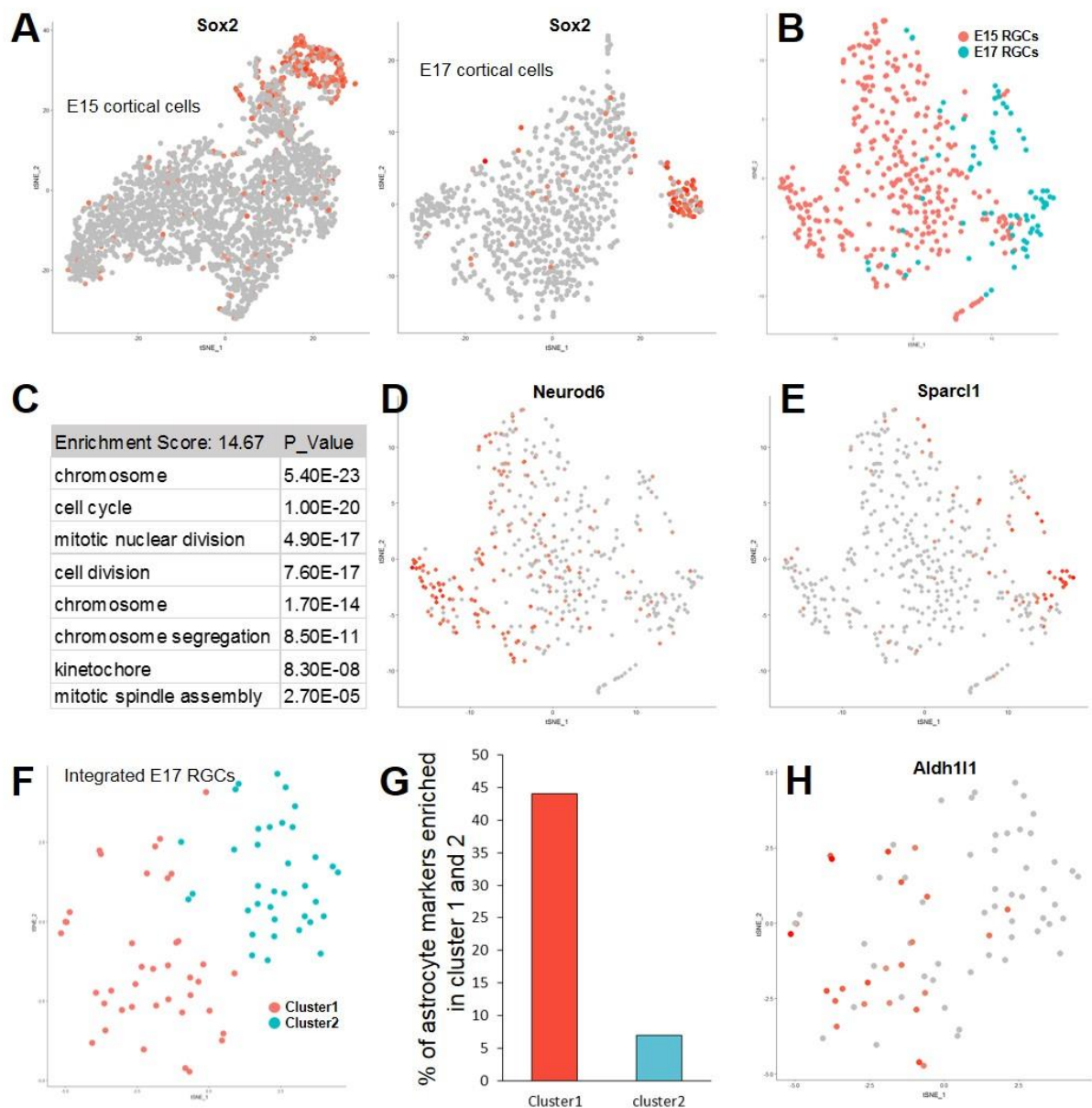


Figure 12. Single-cell RNA Sequencing Meta-analysis Reveals Hopx-expressing RGCs Share Transcriptional Features with Adult Astrocytes. (A) t-SNE of E15.5 cortical cells (left panel) and E17.5 cortical cells (right panel) generated from Yuzwa et al. raw datasets and Feature Plots showing Sox2 expression (in red) identifying the RGCs cluster at both timepoints. (B) t-SNE of E15.5 and E17.5 RGCs indicating transcriptional changes occur over embryonic development. (C-E) E15.5 RGCs show higher cell cycle activity as indicated by enrichment of cell cycle gene ontologies (C), as well as higher neurogenic potential, as illustrated by NeuroD6 expression (D). In contrast, E17.5 RGCs show astroglial potential as indicated by Sparcl1 expression (E), correlating with the neurogenic to astrogenic switch occurring at this late embryonic time point. (F-G) t-SNE of E17.5 RGCs using adult astrocytes marker from Zywitzka et al. as input genes, reveals 2 identified clusters (F). Cluster 1 contains 44% of the astrocyte markers list whereas Cluster 2 contains only 7% (G). (H) Feature Plots showing Aldh1l1 expression, a classical astrocytic marker, as illustration.

We next asked whether subpopulations of RGCs coexist at E17.5. We first attempted at identifying RGCs clusters using the graph-based clustering method from the Seurat R package. However, no significant cluster emerged through this unbiased strategy (Not shown). We next reasoned that if a subpopulation of RGCs was biased to produce astrocytes, they should share some of the genes associated with adult astrocytes. We used a list of 254 astrocytes specific genes (**Annex 4**), described in a recent single-cell RNA sequencing study of the entire SVZ (Zywitza et al., 2018) (**Figure S4A**), to visualize cells in a new t-SNE. The graph-based clustering method identified 2 clusters (**Figure 12F**). Strikingly, 44% of the Zywitza astrocyte markers were present in cluster 1 enriched genes, such as the classical astrocyte marker *Aldh1l1* (**Figure 12GH**), whereas only 7% were present in cluster 2 enriched genes. This result suggest that cluster 1 contains RGCs primed toward the astroglial lineage. Remarkably, enriched genes in cluster 1 which contains *Aqp4*, *ApoE*, *Aldoc*, *Id3*, *Clu* (**Figure S4B** and **Annex 5**) also include *Hopx*. This indicates that *Hopx* defines a subpopulation of pallial RGCs primed towards astrogenesis, as early as E17.5 a timepoint corresponding to the neurogenic to gliogenic switch.

2.4. Discussion

In this study, the expression hallmarks of TFs that regulate distinct neural lineages were further characterized for their enrichment in specific microdomains of the SVZ. By selecting one of these transcripts, we show that NSCs are spatially segregated and primed to differentiate toward specific neural fates. Our results identify *Hopx* as a gene that unravels further heterogeneity of the dSVZ in mediating aspects of astrogenesis and suggest its association with the emergence of germinal traits observed in higher-order mammals.

The diversity of neural subtypes generated by SVZ-NSCs after birth is much larger than first believed. The concept of SVZ regionalization whereby the genesis of distinct neural lineages are spatially and temporally regulated is being increasingly investigated (reviewed in Fiorelli et al. 2015; Azim et al., 2016). NSCs located in SVZ microdomains originate from specific regions of the developing forebrain (Fuentealba et al., 2015a), and generate a large diversity of neural cells, including neuronal subtypes, depending on the expression of particular transcriptional programs. Consequently, the expression of TFs directly correlates with the acquisition of defined neural fates, a concept that was explored in the present study.

We took advantage of the whole-genome transcriptome of region-specific postnatal NSCs that were recently resolved (Azim et al., 2015). A meta-analysis of TFs expressed in dorsal and lateral NSCs with datasets of isolated forebrain neuronal and glial subpopulations (Cahoy et al., 2008) highlighted transcriptional networks that correspond to microdomain-specific NSC derived lineages. Therein, we demonstrate that NSCs are primed to acquire specific fates by the early expression of lineage-specific TFs. Such an early priming is supported by a recent single-cell RNA-sequencing characterization of adult SVZ NSCs (Llorens-Bobadilla et al., 2015). Exploring the spatial heterogeneity and restricted nature of NSCs in generating specific neural lineages will be greatly facilitated by the identification of regionalized NSC markers, such as HOPX. Using two separate approaches, we demonstrate that HOPX expression is confined to a subpopulation of dNSCs whilst it is minimally expressed in INSCs. Additionally, our findings imply an association of HOPX with the astroglial lineage. Similarly, Hopx mRNA is confined to a subpopulation of E17.5 RGCs (20%) characterized by an enrichment of astrocytic markers expressed in adult SVZ niche astrocytes. This correlates with recent clonal fate mapping suggesting that this neurogenic to gliogenic transition is largely incomplete, as only a fraction of RG cells (estimated to roughly 1/6), switch to produce glial cells. Importantly, although HOPX expression is observed in a subpopulation of NSCs that mainly produces astrocytes, it cannot be considered a pan-astrocytic marker. Indeed, HOPX expression is spatially restricted and is therefore likely to be associated with the generation of a subpopulation of astrocytes. Fate-mapping studies revealed that astrocytes are allocated to spatial domains in accordance with their embryonic sites of origin in the ventricular zone (Tsai et al., 2012). Furthermore, transcriptomic analysis of astrocytes isolated from various brain regions reveals heterogeneous expression of several astrocytic markers. For instance, HOPX was shown to be enriched in astrocytes of the dorsal forebrain (cortex and hippocampus) and lowly expressed in astrocytes of subcortical regions (thalamus and hypothalamus; Morel et al., 2017). Astrocyte heterogeneity in the CNS has recently been described to influence neuronal synaptogenesis and maturation through secretion of several extracellular matrix proteins (Eroglu and Barres, 2010). In addition, the densities of astrocytes vary greatly between brain regions (Azevedo et al., 2009). The role of HOPX in influencing regional astrocytes properties and/or densities remains to be explored.

Recently, a number of key studies have reported HOPX expression in human oRG (Pollen et al., 2015; Thomsen et al., 2015b). Furthermore, ectopic overexpression of the hominoid-specific gene *Tbc1d3* into RG in rodents induces HOPX-expressing oRG that contribute to cortical folding (Ju et al., 2016). In line with these observations, our overexpression

results (not presented here, see Zweifel et al. 2018) suggest an instructive role for HOPX in oRG cell formation.

The mechanisms by which HOPX mediates its functions remain largely unknown. HOPX is an atypical TF that does not bind to DNA directly, but modulates other TFs and/or effectors of signaling pathways at the posttranscriptional level. An interaction of HOPX with SRF has been demonstrated during cardiac development (Shin et al., 2002), but is unlikely to occur in the SVZ where SRF expression remains low (data not shown). A more likely function of HOPX is the modulation of dorsally active signaling pathways, such as the BMP and WNT pathways (see also Azim et al. 2014; Azim et al. 2017), which have been demonstrated to fine-tune astrogenesis with neurogenesis during corticogenesis (Gross et al., 1996; Takizawa et al., 2001; Tiberi et al., 2012). Reciprocal signaling between BMP and WNT has been reported in multiple progenitor populations (He et al., 2004; Plikus et al., 2008; Kandyba et al., 2013; Genander et al., 2014; Song et al., 2014), and may be integrated by HOPX expression, as recently demonstrated in cardiomyoblasts (Jain et al., 2015). Future studies aimed at manipulating the activity of these two signaling pathways in HOPX KO animals may allow us to address these questions and investigate the role of extrinsic signal integration in lineage fate specification of neighboring populations of NSCs.

It is interesting to speculate that other signaling pathways may influence the pattern of HOPX expression and may be implicated in its evolution in primates. Intriguingly, HOPX expression in the mouse SVZ follows the spatiotemporal maturation of ependymal cells, which may gradually restrict RG cell contact with the cerebrospinal fluid (Mery et al., 2010). This, combined with the expression of HOPX in oRG, which lack apical processes in primates, suggests that an unknown cerebrospinal fluid-derived signal may regulate HOPX expression. Such signals might modulate SHH signaling that has been recently identified in regulating oRG cell formation (Wang et al., 2016). In agreement, SHH manipulation in mice results in oRG and gyri formation in the medialmost aspect of the cortex, where high HOPX expression is evident. Expression of HOPX in primate oRG might have evolved from this original pattern of expression for the dual coupling of oRG cells and cortex expansion. In summary, our work demonstrates that the dSVZ is much more heterogeneous than previously thought in terms of spatial segregation and early priming of NSCs in generating specific neural lineages. The abundant expression of the TF HOPX contributes to the intraregional heterogeneity of the dSVZ in rodents.

2.5. Supplementary Figures

Supplementary Figure S1

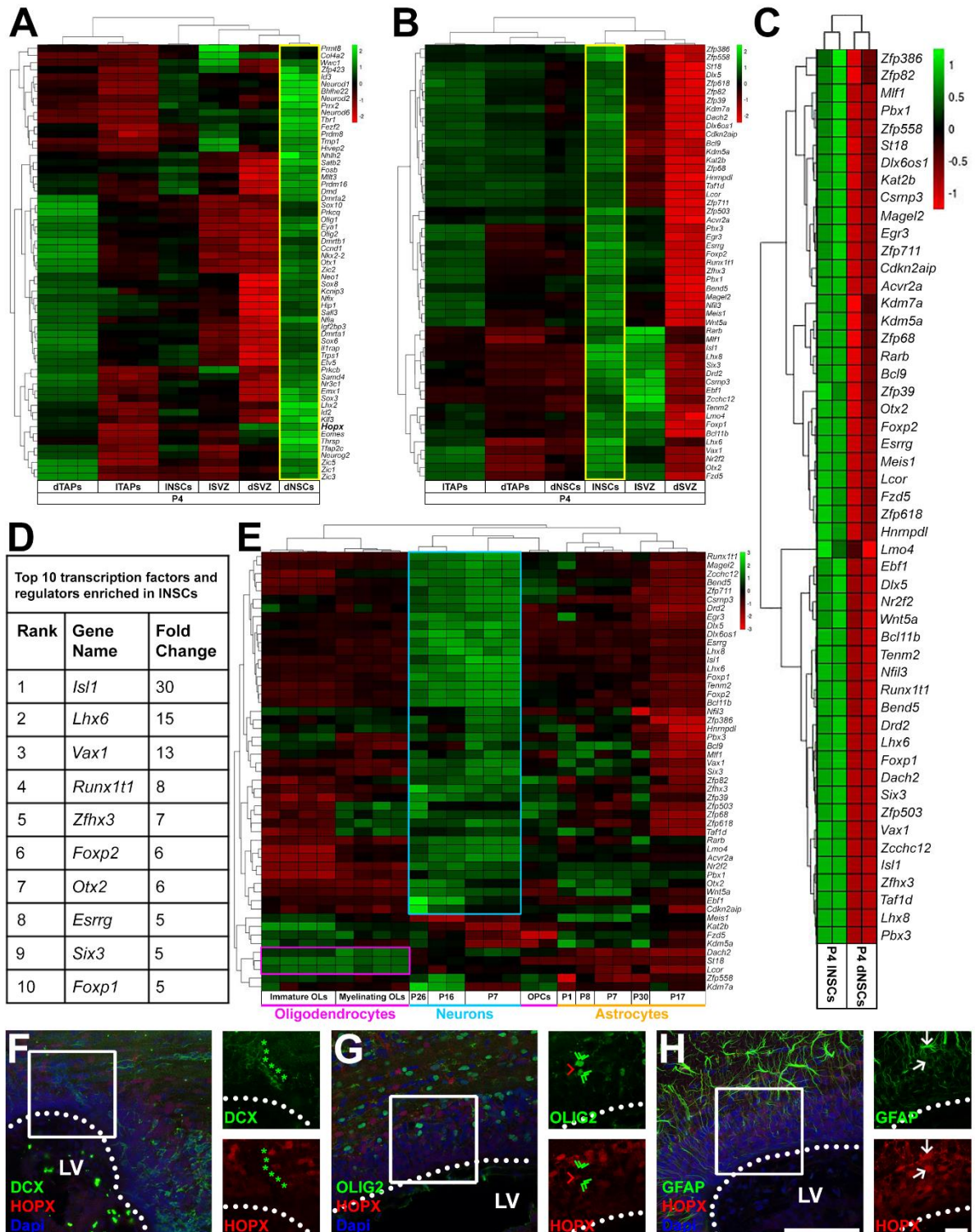


Figure S1. Analysis of TFs enriched in regionally separated NSC population. Related to Figure 8. (A, B): Heatmaps confirming the enrichment of selected TF transcripts in dNSC (vs. INSCs; A) and INSCs (vs. dNSCs; B), including the transcriptional profile in TAPs and the environment (SVZ) of those two regions. **(C):** Heatmap of in P4 INSCs enriched TFs compared to their dorsal counterparts ($\geq 1,8$ folds and p value $< 0,05$).

Supplementary Figure S2

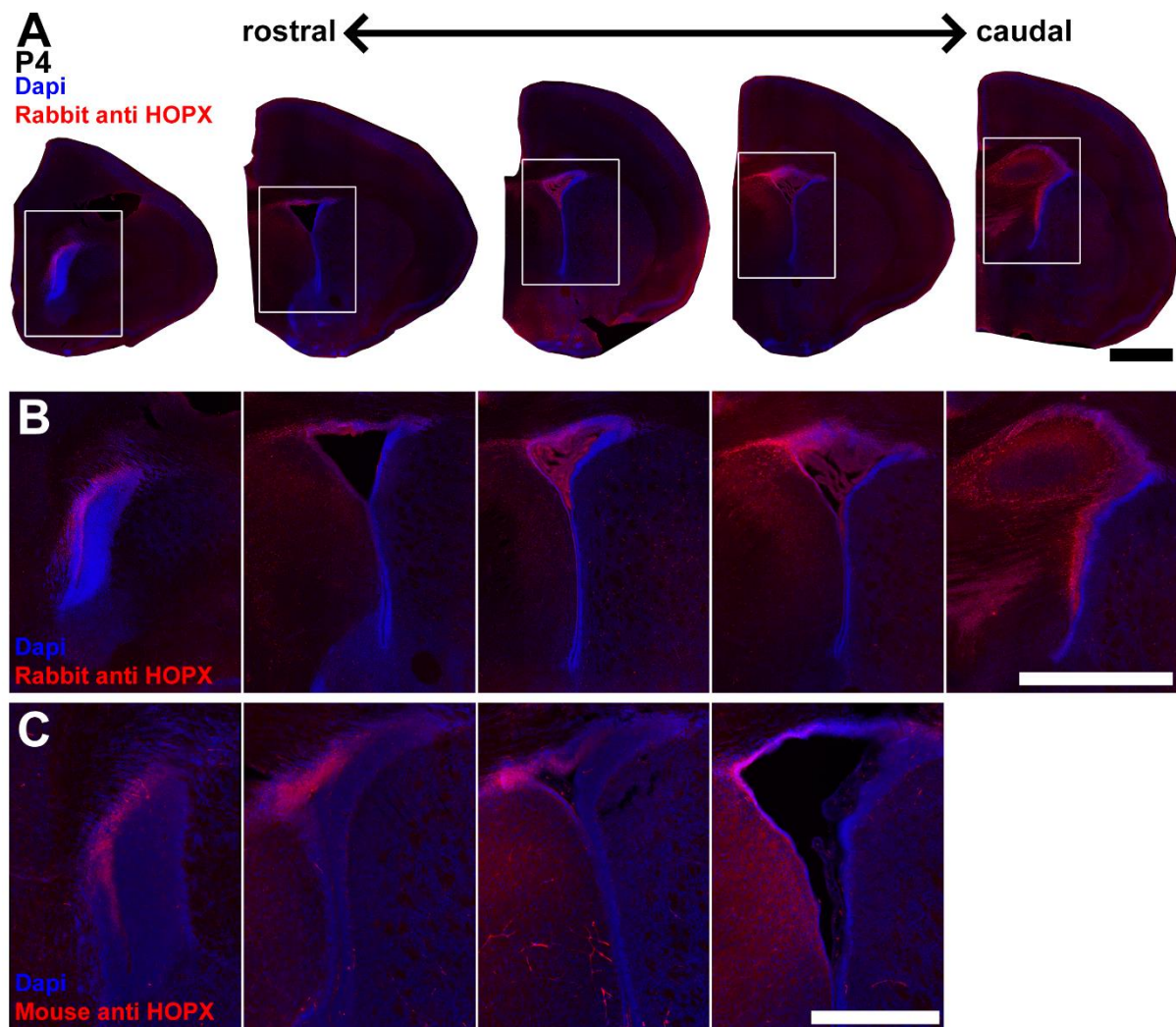


Figure S2. Spatial heterogeneity of Hopx expression at P4. Related to Figure 9. (A-C): Representative pictures demonstrate Hopx expression in a P4 animal along the rostro-caudal axis. The top and middle panel show overviews (**A**) and higher magnification pictures (**B**) of tissue stained with the rabbit anti Hopx antibody. The bottom panel shows higher magnification pictures of tissue stained with the mouse anti Hopx antibody (**C**). Note that both antibodies exhibit the same spatial pattern of Hopx expression. Scale bars: A, B = 1 mm; C = 500 μ m.

Supplementary Figure S3

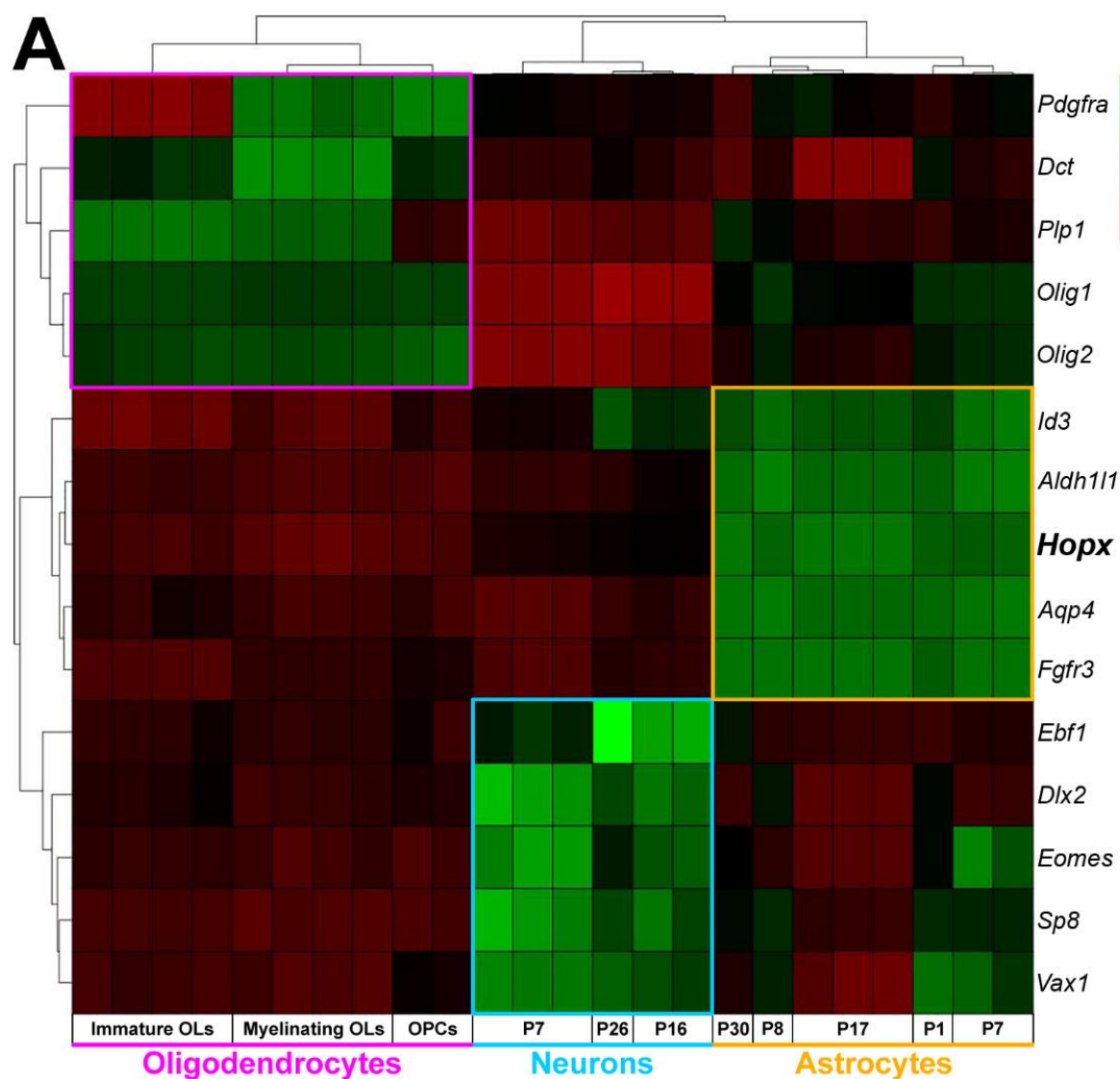


Figure S3. Confirmation of lineage specificity of selected transcripts using the dataset from the Barres group. Related to Figure 10. 5 transcripts of the oligodendrocytic lineage (*PDGFRa*, *Dct*, *Plp1*, *Olig1*, *Olig2*), 5 of the neuronal lineage (*Ebf1*, *Dlx2*, *Eomes*, *Sp8*, *Vax1*) and 5 of the astrocytic lineage (*Id3*, *Aldh1l1*, *Hopx*, *Aqp4*, *Fgfr3*) were selected.

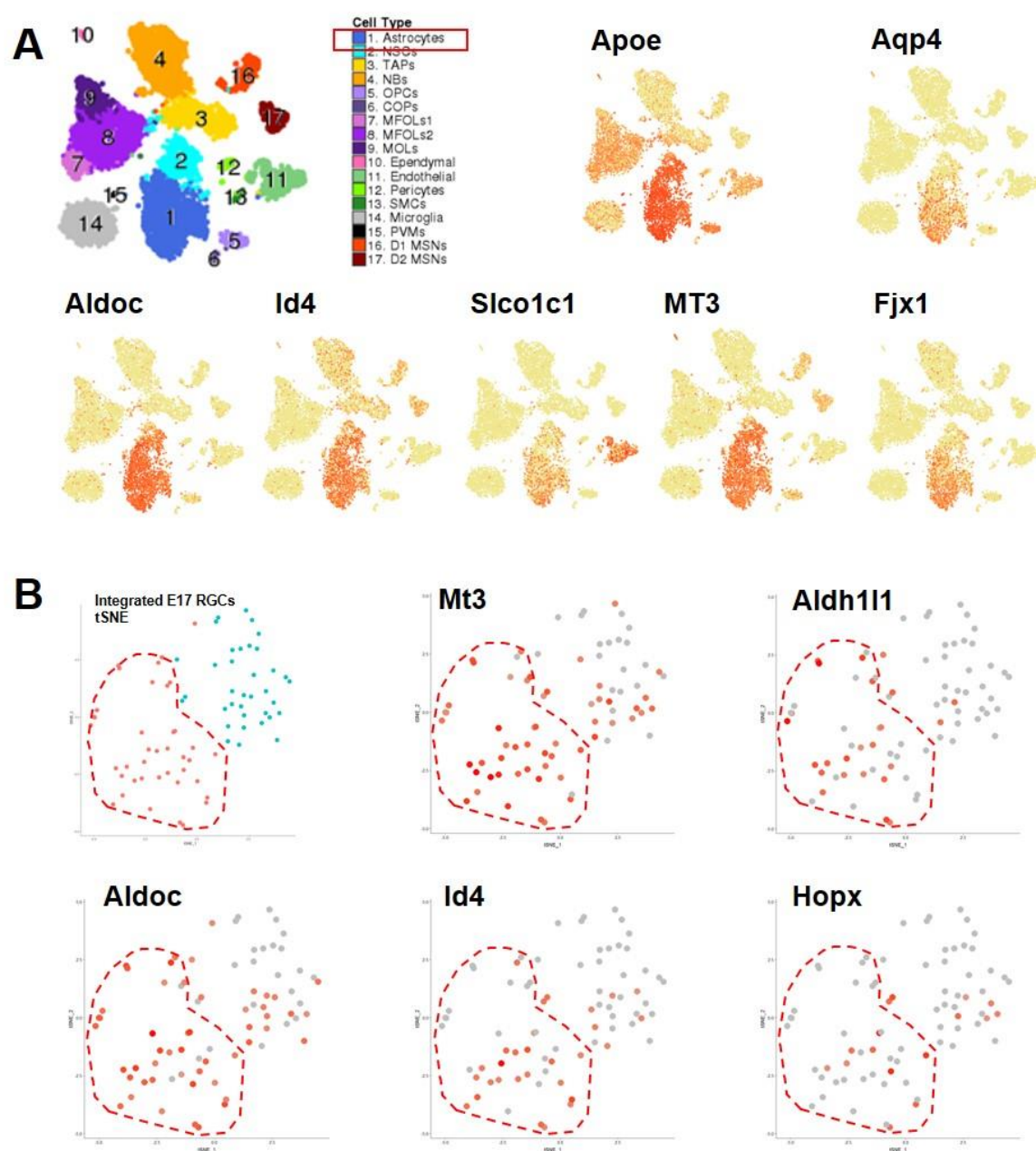


Figure S4. Hopx and astrocytic markers identified by Zywitza et al. identify a subpopulation of “astrogenic” RGCs at E17.5. Related to figure 12. (A) t-SNE plot of 9,804 cells colored by cluster annotation and t-SNE plots of cells colored by expression of selected marker genes, which were used for the identification of astrocytes (Zywitza et al. 2018). (B) Additional Feature Plots illustrating the presence of various astrocytes markers, including Hopx, in cluster 1.

3. Experimental Chapter 2: *Transcriptional Dysregulation in Postnatal Glutamatergic Progenitors Contributes to Closure of the Cortical Neurogenic Period*

The material presented in this experimental chapter was published in the following manuscript:

Vanessa Donega, **Guillaume Marcy**, Quentin Lo Giudice, Stefan Zweifel, Diane Angonin, Roberto Fiorelli, Djoher Nora Abrous, Sylvie Rival-Gervier, Muriel Koehl, Denis Jabaudon, and Olivier Raineteau (2018) *Transcriptional Dysregulation in Postnatal Glutamatergic Progenitors Contributes to Closure of the Cortical Neurogenic Period*. **Cell Reports** 22(10):2567-2574

In this second chapter, transcriptomics and fate-mapping approaches were employed to investigate the origin, transcriptional specificities and competence of postnatal glutamatergic (Glu) progenitors. I established the complete pipeline from isolating Glu progenitors from Ng2^{CreERT2} Ai14 mice – following TAM injections optimization – to single-cell RNA sequencing bioinformatics analysis using the Seurat R package. I also performed genetic manipulations in vivo in embryos as well as newborn animals to address the question of the Glu progenitors origin and competence. Our results showed that a large fraction of Glu progenitors persists in the postnatal forebrain after closure of the cortical neurogenesis period. Postnatal Glu progenitors do not accumulate during embryonic development but are produced by embryonal radial glial cells that persist after birth in the dorsal subventricular zone and continue to give rise to cortical neurons, although with low efficiency. Single-cell RNA sequencing reveals a dysregulation of transcriptional programs which correlates with the gradual decline in cortical neurogenesis observed in vivo. Rescuing experiments show that postnatal progenitors are partially permissive to genetic and pharmacological manipulations.

3.1. Introduction

During neocortical development, glutamatergic neurons are born from progenitors (Glu progenitors) located in the ventricular zone (VZ) and subventricular zone (SVZ) and assemble to form the circuits that underlie cognitive functions. It is classically accepted that the period of cortical neurogenesis closes around embryonic day (E)17.5 in the mouse, with neuronal progenitors switching fate to produce astrocytes (Li et al., 2012). However, a significant fraction of neural progenitors do not switch fate. For instance, a population of progenitors remain in the postnatal SVZ, contributing to olfactory bulb neurogenesis and parenchymal gliogenesis throughout life (Doetsch et al., 1999b). At least some of these progenitors arise from slow cycling/ quiescent embryonal radial glial cells that divide between E13.5 and E15.5 (Fuatealba et al., 2015b; Furutachi et al., 2015). Fate-mapping analysis demonstrated that they give rise to distinct neuronal and/or glial lineages, depending on their location in the SVZ (Fiorelli et al., 2015). Surprisingly, several reports suggest the persistence of Glu progenitors in the dorsal SVZ (dSVZ) until early adulthood (Brill et al., 2009; Winpenny et al., 2011). We used Neurog2^{CreERT2}/tdTom mice to permanently and specifically label synchronous cohorts of prenatal and postnatal Glu progenitors to study their lineage relationship and transcriptional specificities. Our results show that Glu progenitors continue to be produced after closure of the period of cortical neurogenesis. Single-cell RNA sequencing (scRNA-seq) reveals that postnatal Glu progenitors show dysregulation in genes involved in metabolism, differentiation, and migration, which parallels a rapid decline in their capacity to migrate and differentiate. Our data suggest that this transcriptional dysregulation in postnatal Glu progenitors may result from decreased N6-methyladenosine (m6A) methylation of certain proneural genes. Nevertheless, postnatal Glu progenitors remain partially amenable to pharmacological and genetic manipulations.

3.2. Experimental Procedures

Ethical Statement

All animal experiments were performed in accordance with international guidelines from the EU directive 2012/63/EU and approved by the Animal Care and Use Committee CELYNE (APAFIS#187 & #188).

Animals

The *Neurog2^{CreERT2}* transgenic mouse line was crossed with the reporter line *Rosa^{tdTomato}* (*tdTom*) (Madisen et al., 2010), allowing the specific labeling of Glu progenitors and their immediate progeny. For fate mapping of birthdated cohorts of Glu progenitors, tamoxifen was administered to *Neurog2^{CreERT2}/tdTom* transgenic mice at various embryonal and postnatal time points. The morning when a plug was observed was considered as E0.5, and the day of birth was defined as P0.

Tamoxifen injections

Tamoxifen (Sigma-Aldrich, T5648-16, St. Louis Missouri, USA) and progesterone (Sigma-Aldrich, P8783-1G) were dissolved in Corn oil (Sigma-Aldrich, C8267) at final concentration of 20mg/ml and 10mg/ml, respectively. Pregnant *Neurog2^{CreERT2} / tdTom* females were administered 0.5mg tamoxifen and 0.25mg progesterone by gavage at E13.5, E15.5 or E17.5. The morning when a plug was observed was considered as E0.5 and the day of birth is defined as P0. Mouse pups were injected subcutaneously with 1mg tamoxifen at P1 and were terminated at P2, P3, P5, P7, P11, P21 or P45.

In Utero Electroporation

In utero electroporation was performed at E13.5 or E15.5 to investigate the embryonal origin of postnatal Glu progenitors, using a mixture of transposon *pPB-EBFP-P2A-GFP* and hyperactive *piggyBac* transposase.

E13.5 or E15.5 timed-pregnant OF1 females were anesthetized with isoflurane (induction 4.5%; maintenance 2.5%), and the uterine horns were exposed by laparotomy. A mixture of transposon *pPB-EBFP-P2A-GFP* and hyperactive *piggyBac* transposase (1:2 with a concentration of 1.5µg/µl in PBS) together with the dye Fast Green (0.01mg/mL) (Sigma-Aldrich) to visualize the injection site, was injected into the lateral ventricles of the embryos with a pulled glass capillary. Uterine horns were soaked with PBS and embryos were held carefully between tweezer-type circular electrodes (10mm diameter, Nepa Gene, Chiba, Japan). For the electroporation, five electrical pulses (amplitude, 40V (for E13.5) or 45V (for E15.5); duration, 50ms; interval, 1sec) were delivered with an electroporation generator (CUY21 type 2, Nepa Gene). Following electroporation, uterine horns were placed back inside the abdominal cavity and the OF1 female was placed on a heating plate to recover.

Immunohistochemistry

Animals were sacrificed with an overdose of pentobarbital and fixed by transcardial perfusion with PBS followed by 4% paraformaldehyde (PFA; w/v). Brains were dissected and post-fixed in 4% PFA at 4°C. Free-floating vibratome serial sections were cut at a thickness of 50 μ m. Immunostainings were performed as described previously.

For immunostainings, sections were blocked in TNB solution for 2 hrs at room temperature and incubated overnight at 4°C with primary antibodies diluted in TNB with 0.4% Triton-X. The following primary antibodies were used: FoxP2 (rabbit, 1:1000, Millipore), Cux1 (rabbit, 1:500, Santa Cruz C-20), Ki67 (mouse, 1:1500, Abcam ab6526), Olig2 (mouse, 1:1000, EMD Millipore MABN50), PCNA (mouse, 1:400, Dako, Denmark), Satb2 (mouse, 1:200, Abcam ab51502), Tbr2 (rabbit, 1:1000, Abcam ab23345). After thorough washing, sections were incubated for 2 hrs at room temperature with the corresponding secondary antibodies conjugated to Alexa-488, Alexa-555 or Alexa-647 (1:1000, Invitrogen). Nuclear counterstaining was done with 4',6-diamidino-2-phenylindole (DAPI) (Life Technology T20932). Fate mapping Serial sections cut at a thickness of 50 μ m (with an interval of 250 μ m between sections) were stained with DAPI and images were taken on an Axio Scan.Z1 microscope (Zeiss, Cambridge) at 20x/0.8NA objective (Plan- Apochromat 20x/0.8 M27) with a resolution of 1024 μ m x 1024 μ m.

Fate mapping

Serial sections cut at a thickness of 50 μ m (with an interval of 250 μ m between sections) were stained with DAPI and images were taken on an Axio Scan.Z1 microscope (Zeiss, Cambridge) at 20x/0.8NA objective (Plan- Apochromat 20x/0.8 M27) with a resolution of 1024 μ m x 1024 μ m. Positive cells were marked on corresponding brain sections from the Allen Brain Atlas.

Quantifications

Images were taken on a Leica SPE confocal laser microscope using 10x/0.3 NA, 20x/0.75 NA, or 40x/1.25 NA oil objectives (HCPL Fluotar) and the software LAS (Leica Microsystems, v3.1.2.16221). Quantifications were performed on coronal sections by counting the number of cells either by eye from confocal images or from z stack mosaic images of the entire dSVZ on ImageJ. Depending on the analysis, quantifications were done either on an entire series of sections or on at least 3 equally spaced sections of the SVZ. Images for Sholl analysis were taken with a z-step of 0.29 μ m and a resolution of 1,024 x 1,024. Sholl analysis was performed on Neurolucida 360 software (MBF Bioscience). Images were using Photoshop (CC2015.5, Adobe Systems Software).

Statistical Analysis

Data are expressed as mean \pm SEM ($n \geq 3$). Significance was tested on GraphPad Prism 7 by using an unpaired t test or 2-way ANOVA followed by Bonferroni post hoc test.

Single cell capture, cDNA library preparation and sequencing

The brains of E15 and P2 mice were harvested and placed on ice-cold Hank's balanced salt solution (HBSS). The region of intense tdTomato expression (i.e. dorsal pallium) were then microdissected and cells were finally chemically (Trypsin-EDA 0,05%) and manually (500 μ l pipet) dissociated. After filtering on a 70 μ m cell strainer, the cell suspension was FAC-sorted on a BD® FACS Aria to isolate tdTom⁺ cells (**Annex 6**) which were confirmed to belong to the glutamatergic lineage, as expected (**Annex 7**). For each condition, tissue collection, FAC-sorting and cell isolation were performed in two independent replicates to ensure biological significance. Single cells were isolated with the C1 Single-Cell Auto Prep System, and validated by a visual check on an inverted microscope. A total of 230 cells were obtained (121 at E15.5 and 109 at P2). Reverse transcription and pre-amplification of the single-cell cDNAs were done within the integrated fluidic circuit (IFC) chip using the SMARTer Ultra Low RNA kit for Illumina (Clontech) according to the C1 protocol. Upon termination of the run, amplified cDNA was harvested, and the concentration of cDNA was assessed on a SpectraMax Gemini Fluorimeter (Molecular Devices). The typical yield of cDNA for each cell is expected to be about 0.8ng cDNA per μ l. RNA-seq libraries of the harvested cDNA were prepared using the Illumina Nextera XT DNA Sample Preparation Kit. Libraries were multiplexed and sequenced using the Illumina HiSEQ500 platform (**see pipeline in Annex 8**) as 75bp single reads using the Illumina HiSEQ500 platform at a depth of 7M reads.

Quality control, identification of outliers and analysis

The obtained RNA-seq data were prepared and analyzed as previously described (Telley et al., 2016). Briefly, sequenced reads were aligned on the latest mouse reference genome assembly (GRCm38) using STAR (Spliced Transcripts Alignment to a Reference) (Dobin et al., 2013) (See summary report in **Table 1**) and the number of reads per transcript calculated with FeatureCounts (Liao et al., 2014). For each cell, Reads per Million (RPM) are divided by the length of the gene to obtain normalized Reads Per Kilobase Million (RPKM) and transformed in log2 when necessary. Identification of progenitors, nascent neurons, and transcripts was performed using the Seurat bioinformatic pipeline as follows: We first created a "Seurat object" including cells expressing more than 500 genes and genes expressed in more than 2 cells, identifying 11.718 genes across 228 cells. We next performed a Principal Components Analysis (PCA), using the *prcomp* function of R, after

scaling and centering of the data across these genes. This ensured robust identification of the primary structures in the data. We identified statistically significant principal components and used the most significant genes for each of these PCs as input for *t*-Distributed Stochastic Neighbour Embedding (*t*-SNE, R package, “perplexity parameter” = 30). To identify clusters, a density clustering approach was used. Single-Cell Differential Expression (SCDE; Kharchenko et al. 2014) was used to identify differentially expressed genes across progenitors and nascent neurons between developmental time-points (cut off: absolute Z score ≥ 2 , corresponding to a classical *P* value ≤ 0.05).

P2	Number of Reads / Cell	% of Unique Reads	% of Assigned Reads
Average	6036057	79	43
<i>Median</i>	5660906	80	43
<i>Max</i>	10792752	87	63
<i>Min</i>	2189408	6	4
E15.5	Number of Reads / cell	% of Unique Reads	% of Assigned Reads
Average	6943141	73	41
<i>Median</i>	6806643	75	43
<i>Max</i>	11424623	82	61
<i>Min</i>	2563824	46	14

Table 1. Sequencing Report. Sequencing depth (Reads/cell) and % of assigned reads are consistent in P2 and E15.5 progenitors.

Gene ontology enrichment analyses

GO analysis were performed in identified dysregulated genes with the GO biological process complete annotation set from PANTHER (v12) (<http://pantherdb.org/>). Kegg pathway analysis was performed with a homemade R code querying the Kegg pathway database (<http://www.kegg.jp/kegg/pathway.html>). The proteinprotein interaction (PPI) analysis was performed in differentially regulated transcripts using Enrichr web-based tools (Chen et al., 2013; Wang et al., 2018) (<http://amp.pharm.mssm.edu/Enrichr/>).

Data and Software Accessibility

The accession numbers for the data reported in this paper are GEO: GSE109556 and have been posted to Mendeley at <https://doi.org/10.17632/k659jr9gvv.1>.

m6A dot blot assay

The pallium and dSVZ were isolated (*n*=4) at E15.5 and P2, respectively. mRNA was harvested using the Dynabeads mRNA Direct Purification Kit (61011, ThermoFisher, Waltham USA). 3.5 μ l and 1 μ l dots were applied to an Amersham Hybond-N⁺ membrane

(Amersham, UK) as 20ng mRNA per 1 μ L. After complete drying, the mRNA was crosslinked to the membrane by placing it at 80°C for 2hrs. The membrane was blocked with 5% skim milk (PBS-Tween20 0.1%) for 2hrs and then incubated with primary antibody m6A (mouse, 1:500, 212B11 Synaptic Systems, Goettingen Germany) diluted in blocking buffer for 2hrs at room temperature. Membranes were washed three times in PBS-T, and incubated with the secondary antibody ECL HRPconjugated (sheep-anti-mouse, 1:5000, Amersham) in blocking buffer for 2hrs at room temperature. After washing three times with PBS-T, the membrane was visualized using the Supersignal West Femto Maximum Sensitivity Substrate (34096, Thermo Scientific). Equal mRNA loading was confirmed by staining the membrane with a 0.02% methylene blue in 0.3 M sodium acetate solution (pH 5.2). m6A signal was quantified with ImageJ.

Pharmacological activation of the canonical Wnt signaling pathway

50 μ L intraperitoneal injections were given between P1-P2, twice a day (a total of four injections of 10 μ L each), with a final concentration of 5mM (dissolved in sterile PBS).

Bcl11a gain of function

Briefly, P2 mouse pups were anesthetized on ice and were fixed on a plate placed in a stereotaxic rig. A mixture of Bcl11a or control plasmid (LacZ) (final concentration 3 μ g/ μ L) and the dye Fast Green (0.2 μ L) was prepared. Injection (2 μ L) was done at the level of the right lateral ventricle at a depth of 2mm from the surface of the skull using a Hamilton syringe with a 34G needle (Nevada, USA). Successfully injected mice were subjected to five electrical pulses (95V, 50ms, separated by 950ms intervals) using the ECM CUY21 type 2 electroporator (NepaGene, Chiba, Japan).

3.3. Results

Fate Mapping of Birth-Dated Cohorts of Glutamatergic Neurons

The recombination efficiency and specificity of the Neurog2^{CreERT2}/tdTom mice was verified by injecting tamoxifen (Tam) at different embryonal time points (i.e., E13.5 and E15.5) and examining brains after 12 and 24 hr (**Figures 13A and 13B**).

The recombined cells initially expressed the Glu progenitor marker, Tbr2, and the proliferation marker Ki67, and rapidly translocated from the VZ to the cortical plate. Fate mapping of recombined cells was assessed at postnatal day (P)21. Tam injections at either

E13.5, E15.5, or E17.5 labeled neurons in subcortical and cortical brain regions in accordance with their date of birth (**Figure S5**).

To confirm the precise labeling of birth-dated cohorts of glutamatergic neurons, we performed a more detailed analysis of recombined cells in the cortex. Tam injection at E13.5 labeled neurons in the deep cortical layers (i.e., L5–L6), which expressed the deep cortical layer marker *FoxP2*, (**Figures 13C–13E**).

In contrast, recombination at E15.5 labeled neurons in L3–L4, which expressed the upper layer marker *Cux1* (**Figures 13C–13E**). Importantly, only a few glial-like cells were labeled (<1% of total *tdTom*⁺ cells) from E15.5 on. These glial cells were found in clusters, suggesting that only a very limited number of progenitors switched from a glutamatergic to an astrocytic fate (**Figure S5**). Altogether, these observations confirm that *Neurog2*^{CreERT2}/*tdTom* mice allow the specific labeling of birth-dated cohorts of glutamatergic neurons.

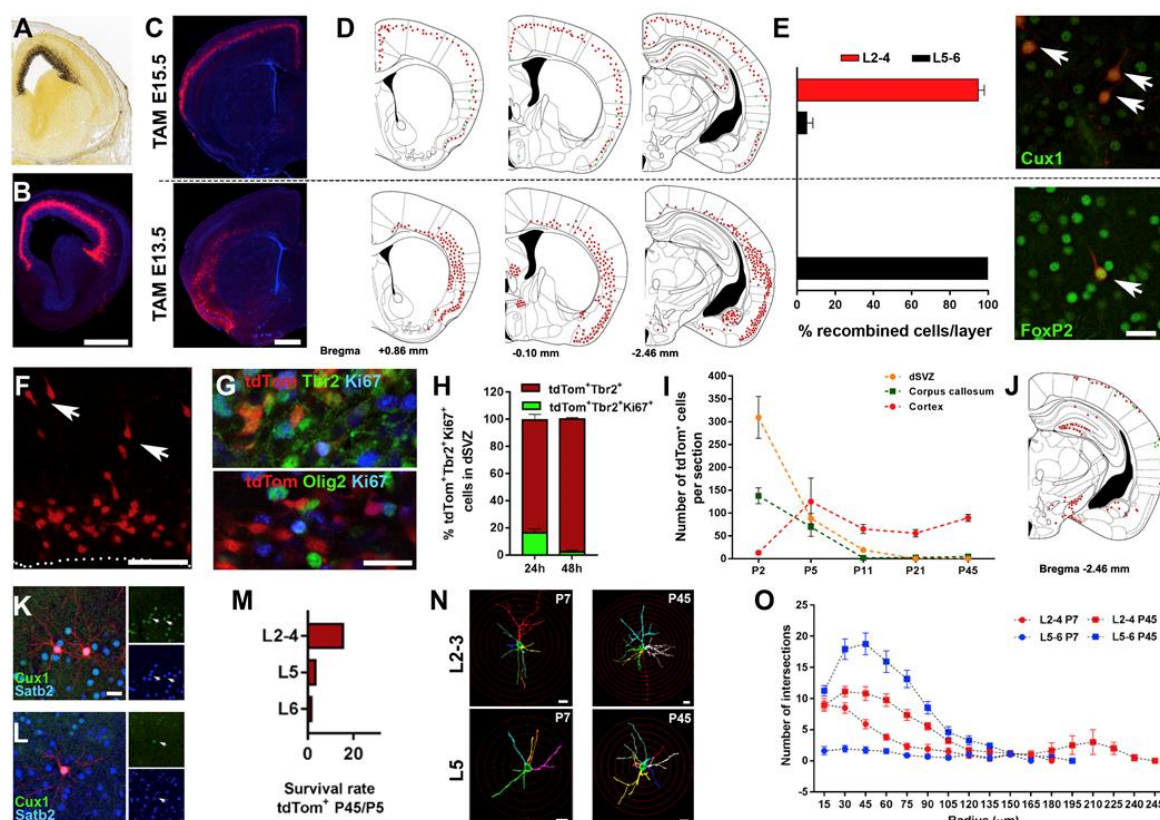


Figure 13. *Neurog2*^{CreERT2}/*tdTom* Mice Allow Fate Mapping of Birth-Dated Cohorts of Glu Progenitors and Reveal Their Persistence at Postnatal Stages. (A) In situ hybridization from the Allen Brain Atlas showing *Neurog2* expression in the VZ and SVZ at E15.5. (B)

Specific recombination of Glu progenitors in the SVZ following Tam injection at E15.5. **(C and D)** Representative coronal sections **(C)** and drawings illustrating the distribution of recombined neurons at P21 after Tam injection at E13.5 and E15.5 **(D)**. **(E)** Immunodetection and quantification of layer marker expression by recombined cortical neurons (see arrows) following Tam at E13.5 and E15.5. **(F)** Tam injection at P1 reveals a large population of Glu progenitors in the dSVZ (arrows indicate migrating cells) (see also Figures S1 and S2). **(G)** Recombined cells express the Glu progenitor marker Tbr2 but not Olig2. **(H)** Some recombined cells express the proliferative marker Ki67 24 hr post-Tam injection but exit cell cycle by 48 hr. **(I and J)** Fate mapping of P0.5 recombined cells at various postnatal time points **(I)** illustrating the disappearance of recombined cells in the dSVZ, while cortical neuron number increases and stabilizes by P21 **(J)** (see also Figure S2). **(K and L)** High-magnification image showing co-localization of tdTom⁺ cells with Cux1 and Satb2 (see arrows) in L2–L3 **(K)** or L5–L6 **(L)** at P45 (see also Figure S3). **(M–O)** Only a fraction of tdTom⁺ neurons located in upper cortical layer survive at P45 **(M)**, which correlates with their faster maturation **(N and O)** (see also Figure S4). TAM, tamoxifen. Scale bars: 500 μ m in **(B)**; 1,000 μ m in **(C)**; 50 μ m in **(F)**; 25 μ m in **(E)**, **(G)**, **(K)**, and **(L)**; and 20 μ m in **(N)**. Data are presented as mean \pm SEM. See also Figures S5, S6, S7, and S8.

A Large Population of Glu Progenitors Persist in the Postnatal SVZ

Having established the lineage and temporal specificity of recombination in the Neurog2^{CreERT2}/tdTom mice, we performed Tam injections in postnatal mice. Recombination at P0.5 revealed that a large pool of Glu progenitors persist in the early postnatal dSVZ and subcallosal zone (SCZ), despite closure of the cortical neurogenic period (Figure 13F; Figure S6A).

Recombined cells were confirmed to be Glu progenitors by their expression of Tbr2 (Figure 13G) but exclusion of other lineage markers (e.g., Olig2). Twenty-four hours following recombination, 20% of Glu progenitors were still actively cycling, but most had exited the cell cycle by P3 (Figure 13H).

To follow the long-term fate of these progenitors, we injected Tam in P0.5 pups and sacrificed them at various time points. At P2, most recombined cells were observed in the dSVZ, but their number gradually decreased with age, disappearing by P21 (Figure 13I). In parallel, Glu progenitors gave rise to a cohort of migrating neurons that transiently increased in the corpus callosum and cingulum, as they left the dSVZ and migrated toward the cortex (Figures 13I and 13J). At P21, tdTom⁺ neurons were observed in the cortex, in the dentate gyrus, and in some subcortical nuclei (Figure 13J; Figure S6B).

The number of recombined cortical neurons increased from frontal to caudal brain sections (Figure S6C), with most neurons located in sensory rather than motor regions (Figure S2D). A marked decrease in the number of recombined neurons was observed over time. Indeed, comparison of the number of tdTom⁺ cells at short and long survival times (i.e., 12

hr post-Tam injection or at P21, respectively), revealed a large decrease (81.3%) following a P0.5 Tam injection. In comparison, a marginal drop was observed in the number of cells recombined at E15.5 (11.8%), indicating that while most recombined embryonal progenitors produce neurons that efficiently survive until P21, only a fraction do so at postnatal time points.

We next looked in more detail at the location and phenotype of recombined cortical neurons. Most recombined glutamatergic neurons were located in upper cortical layers L2–L3, and a few were located in L5–L6 (**Figures S7A–S7D**). By P45, most recombined neurons expressed the marker *Satb2*. While recombined neurons located in L2–L3 also expressed the upper layer marker *Cux1*, those in L5–L6 did not express the markers of deep cortical layers, *Ctip2* or *FoxP2* (**Figures 13K and 13L; Figure S7E**).

By P45, the decrease in number of recombined neurons was more pronounced in deeper cortical layers than in superficial layers (**Figure 13M**), as around 1% of the total number of *tdTom*⁺ neurons were located in L5–L6 (i.e., 30–48 cells per brain). This decreased survival correlated with a slower maturation of surviving neurons in deep cortical layers (**Figures 13N and 13O**). Nevertheless, surviving glutamatergic neurons of both upper and deep layers developed spines (**Figure S8A**), thereby suggesting proper integration of newborn glutamatergic neurons. In contrast to neurons produced at E13.5, which formed corticofugal (i.e., internal capsule or corticospinal) projections, postnatally born neurons only formed intracortical projections, as shown by the presence of axons in the corpus callosum (**Figure S8B**).

Taken together, these results reveal that closure of the cortical neurogenic period is not due to the disappearance of Glu progenitors but rather to a gradual decline in their capacity to differentiate and survive.

ScRNA-Seq Reveals Transcriptional Dysregulation in Postnatal Glu Progenitors

We next investigated the origin and transcriptional specificities of postnatal Glu progenitors. Injection of Tam at E13.5 or E15.5 failed to label Glu progenitors at P2 (**Figures 14A–14F**). In contrast, in utero electroporation of a transposon-GFP plasmid (Siddiqi et al., 2014) at either E13.5 or E15.5 revealed a large pool of GFP⁺ cells that persisted in the postnatal dSVZ and continued generating proliferating *Tbr2*⁺ cells at P2 (**Figures 14G and 14H**) as well as at P21 (**Figures 14I and 14J**).

Together, these results indicate that postnatal Glu progenitors do not accumulate during embryonic development but are produced by embryonic radial glial cells (RGCs) that

persist after birth in the dSVZ, in accordance with recent studies (Fuentealba et al., 2015b; Furutachi et al., 2015).

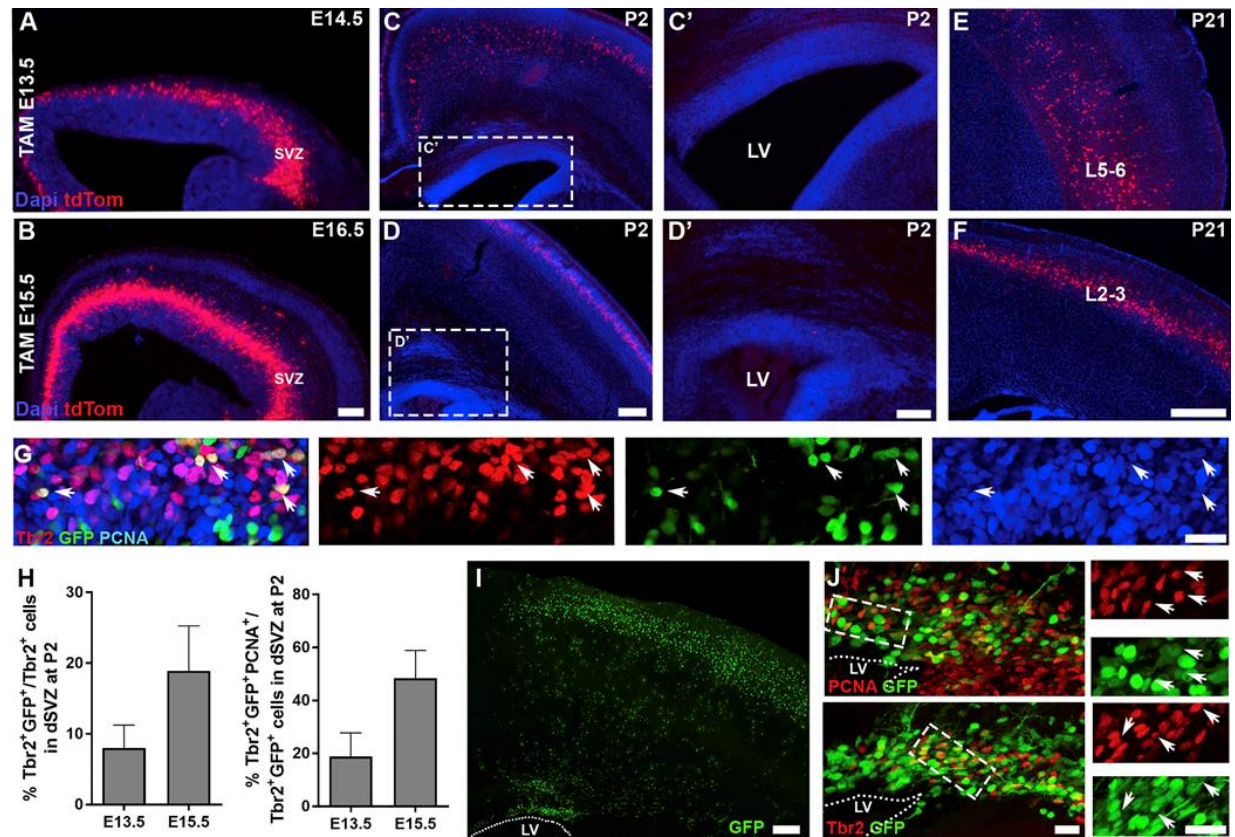


Figure 14. Postnatal Glu Progenitors Originate from a Pool of Slow-Cycling RGCs that Accumulate in the SVZ during Corticogenesis. (A–F) tdTom⁺ cells recombined at embryonal time points do not remain in the postnatal dSVZ (C–D') but generate the different Glu projection neurons embryonally. tdTom⁺ cells in the pallium 24 hr after TAM injection (A and B) and at P2 or P21 in L5–L6 (C and E) or L2–L3 (D and F) are indicated. (G–J) In utero electroporation (IUE) of transposon-GFP in the pallium at embryonal time points E13.5 (G) and E15.5 (I and J) highlight persisting RGCs (see arrows) in the dSVZ that continue giving rise to proliferating Tbr2⁺ cells at P2 (G and H) as well as at the later postnatal time point P21 (in I and J). Scale bars: 500 mm in (E) and (F); 200 mm in (C), (D), and (I); 100 mm in (A), (B), (C'), and (D'); and 25 mm in (G) and (J). Data are presented as mean ± SEM.

To explore the mechanisms of the decreased neurogenic capacity of postnatal Glu progenitors, we performed scRNA-seq of tdTom⁺ cells isolated by flow cytometry from microdissected pallium at E15.5 or P2. Unbiased clustering combined with interrogation of cell-cycle and post-mitotic markers revealed several cell clusters (Figures 15A and 15B), corresponding to actively cycling recombined cells (i.e., progenitors) and their immediate progeny (i.e., nascent neurons) (Figure 15B and Annex 9). Expression of lineage-specific

transcripts, such as *Neurog2* and *Tbr2*, confirmed their Glu identity (**Figure 15C**). Transcriptional differences increased during differentiation, with 597 (8%) and 1,425 (20%) genes being differentially regulated between E15.5 and P2 progenitors and nascent neurons, respectively (**Figures 15D and 15E**; see Table S1 in online supporting material of the article and see <https://genebrowser.lyon.inserm.fr/> for an interactive dataset). Thus, while the vast majority (90%) of E15.5 top 1,000 expressed genes were also expressed in P2 progenitors, only 40% of the E15.5 top 1,000 genes were similarly expressed in nascent neurons at P2 (**Figure 15F**).

Interestingly, transcripts enriched in Glu progenitors (i.e., *Sox2*, *Pax6*, *Neurog2*, and *Tbr2*) were upregulated at P2, suggesting a transcriptional dysregulation leading to the persistence of progenitor traits in nascent neurons (**Figure 15G**).

Knowing that m6A methylation plays a role in cortical neurogenesis by regulating the expression of proneural transcripts (Yoon et al., 2017), we assessed whether this mRNA modification was decreased in postnatal Glu progenitors. Transcriptional analysis confirmed a downregulation of transcripts coding for proteins of the methyltransferase complex, *Mettl3* and *Mettl14* (**Figure 15G**), while expression of *YTHDF2*, which has been shown to localize m6A-tagged transcripts to decay sites (Wang et al., 2015), was not changed (data not shown). To assess m6A methylation level in Glu progenitors, we performed an mRNA dot blot assay to detect m6A modifications (**Figures 15H and 15I**). Our results reveal a 65% decrease in m6A level in the postnatal dSVZ, compared to the E15.5 pallium.

All together, these data suggest that epitranscriptomic modifications participate in the transcriptional dysregulation observed in postnatal Glu progenitors and their immediate progeny.

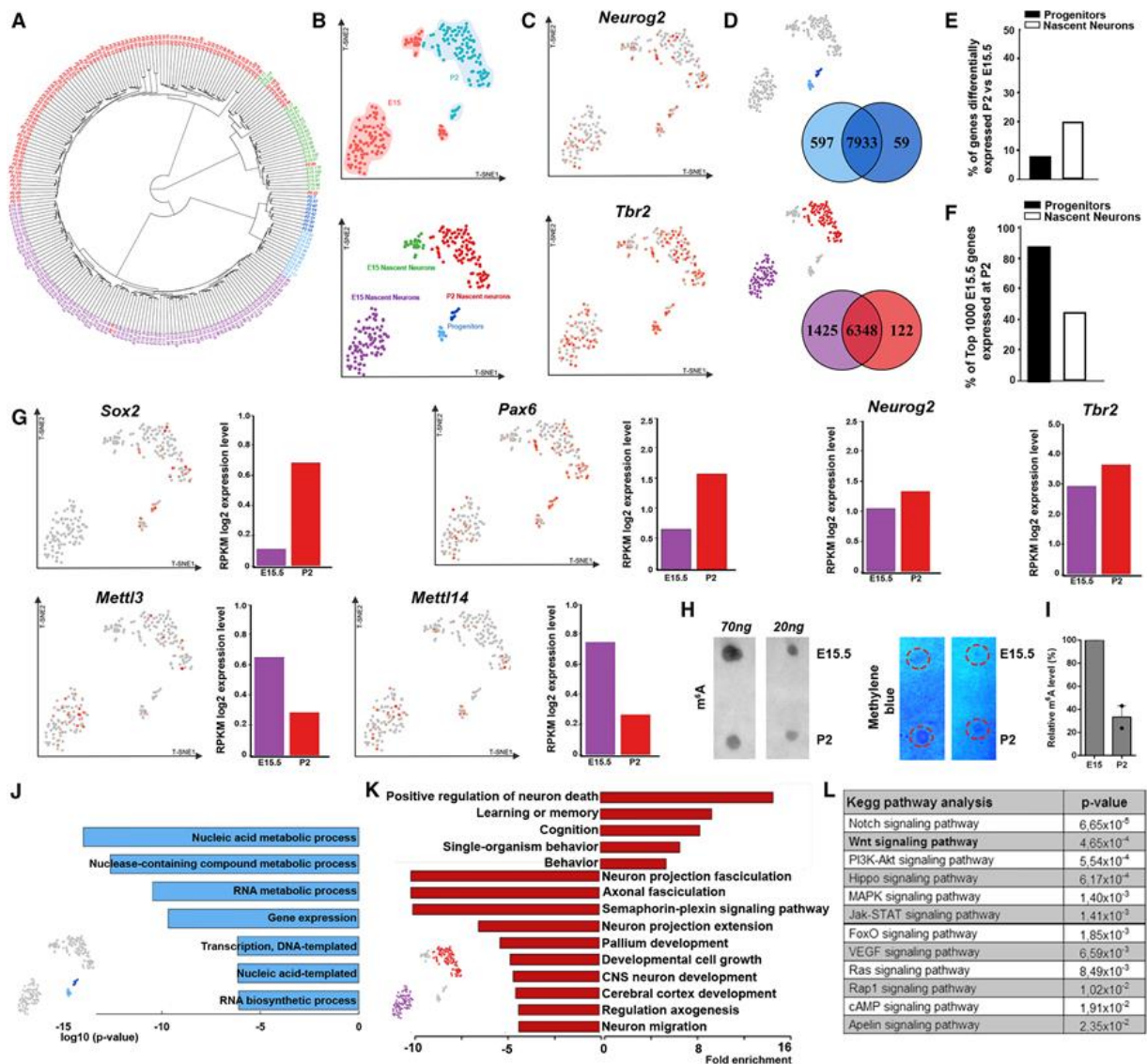


Figure 15. Dysregulation of Neurogenic Transcriptional Coding in Postnatal Glu Progenitors. (A and B) Hierarchical clustering (A) and t-SNE of individual cells recombined at E15.5 and P2 allows distinguishing 2 clusters of cells, actively cycling cells (i.e., progenitors), and their immediate progeny (i.e., nascent neurons) (B). (C) Feature plot showing the expression of transcripts of the Glu lineage. (D) Venn diagrams showing the number of differentially expressed transcripts in progenitors or nascent neurons. (E and F) Transcriptional differences increase as differentiation progresses, as reflected by the percentage of transcripts differentially expressed between E15.5 and P2 (E), as well as the gradual loss of transcripts expressed at E15.5 in P2-sorted cells (F). (G) Feature plots showing downregulation of methyltransferases Mettl3 and Mettl14 in P2 progenitors and upregulation of m6A-tagged transcripts Sox2, Pax6, Neurog2, and Tbr2. (H) Dot blot showing decreased m6A levels at P2 and methylene blue staining confirming equal mRNA loading on membrane. (I) Quantification of m6A levels. (J) GO showing downregulation in P2 progenitors of transcripts involved in transcription and metabolism. (K) GO analysis showing downregulation of migration, differentiation, and cell death in P2 nascent neurons. (L) KEGG pathway analysis highlighting dysfunctional signaling pathways. Data are presented as mean \pm SEM.

Postnatal Glu Progenitor Differentiation Can Be Partially Rescued

We next focused on the transcriptional specificities of P2 Glu progenitors and nascent neurons. Classification of transcripts differentially expressed in Glu progenitors highlighted depressed transcriptional and metabolic activities at P2 that correlates with reduced potential of Glu progenitors to differentiate postnatally (**Figure 16J**). Classification of differentially expressed transcripts in nascent neurons highlighted downregulation of generic programs of differentiation and migration, and an upregulation of genes involved in neuronal death (**Figure 16K**), in line with our histological observations. A KEGG analysis further highlighted paralleled perturbation of several key signaling pathways, such as Wnt canonical signaling (**Figure 16L**), as previously suggested (Li et al., 2012).

A more detailed analysis into downregulated GO terms, revealed a decrease in several genes, including *Ctnnb1* (i.e., β -catenin) and other Wnt signaling transcripts such as, *Fzd1* and *Lef1* (**Figures 16A and 16B**). Protein-protein interaction (PPI) analysis further emphasized the central role of β -catenin, as most of the downregulated genes at P2 encode for proteins that interact with it (**Figure 16C**).

To assess if migration and differentiation of postnatal Glu progenitors could be reactivated, we performed experiments to rescue downregulated signaling and transcriptional pathways. We first used a glycogen synthase kinase 3β (GSK 3β) inhibitor, AR-A014418, to activate the canonical Wnt signaling pathway. Our results showed increased tdTom⁺ cells in the dSVZ, which was paralleled by increased proliferation (**Figures 16D–16F**).

Next, we selected *Bcl11a* as a candidate gene for overexpression, as this transcription factor is among the top 10 differentially expressed (i.e., downregulated) transcription factors at P2 (**Figure 16G**). *Bcl11a* has been shown to regulate both migration and fate specification during embryonic development (Wiegrefe et al., 2015; Greig et al., 2016). Overexpression of *Bcl11a* increased proliferation in the dSVZ (**Figure 16H**). In addition, our results show a significant increase in migration towards the cortex and increased number of cells that adopted bipolar morphologies (**Figures 16H–16J**).

Together, these results demonstrate that Glu progenitors remain permissive to both pharmacological and genetic manipulation.

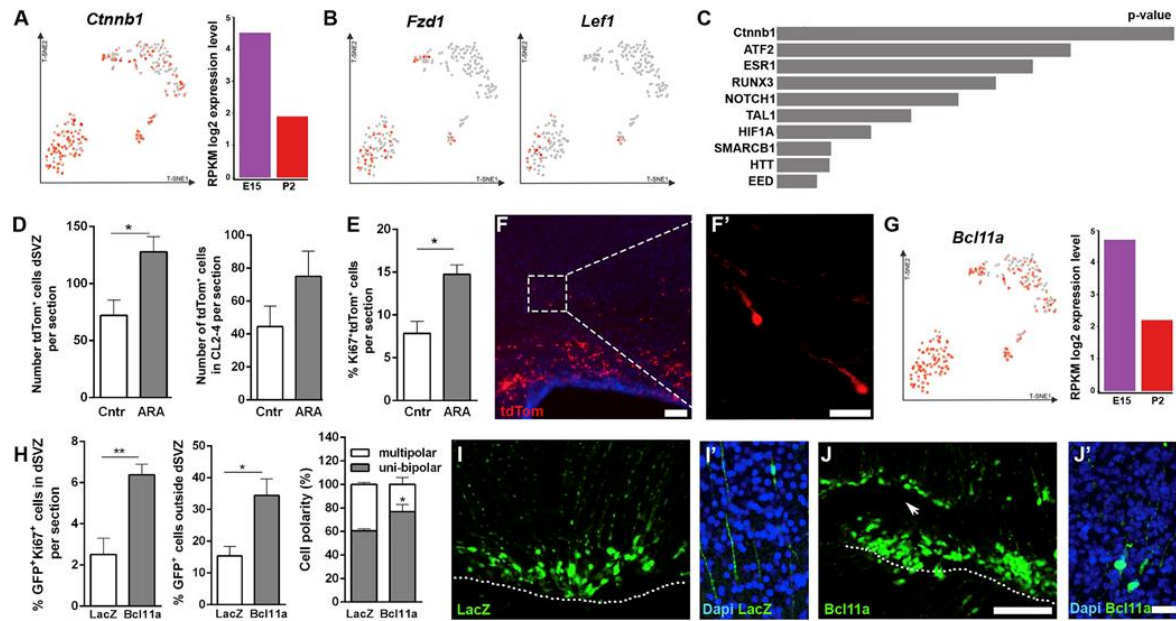


Figure 16. Partial Rescue of Impaired Migration and Differentiation of Postnatal Glu Progenitors by Pharmacological and Genetic Manipulations. (A) Feature plot showing decreased expression Ctnnb1 (β -catenin) in P2 nascent neurons. (B) Feature plots showing altered expression of two Wnt-signaling transcripts. (C) PPI analysis showing the top 10 proteins to interact with proteins coded by genes downregulated at P2. (D–F') Pharmacological activation of the Wnt canonical pathway increases the (D) number and (E) proliferation (Ki67) of tdTom⁺ cells in the dSVZ at 72 hr. (F and F') Representative images showing tdTom⁺ progenitors migrating away from the dSVZ. (G) Feature plot showing decreased expression of Bcl11a in P2 nascent neurons. (H) Overexpression of Bcl11a increases proliferation in the dSVZ while promoting cell migration and bipolar cell morphology outside the dSVZ. (I–J') Representative images after electroporation of control plasmid (LacZ) (I–I') or Bcl11a (J–J') overexpression. Scale bars: 100 μ m in (F); 50 μ m in (J); and 25 μ m in (F') and (J'). * $p < 0.05$; ** $p < 0.005$. Data are presented as mean \pm SEM.

3.4. Discussion

Our work highlights the persistence of a large population of Glu progenitors in the postnatal forebrain, after the closure of the cortical neurogenic period. Fate mapping and scRNA-seq reveal a dysregulation of transcriptional and signaling pathways that contribute to restricting the neurogenic potential of postnatal Glu progenitors early after birth. Rescuing experiments, however, show that postnatal progenitors remain partially permissive to genetic and pharmacological manipulations, suggesting that they could be recruited for cortical repair. The perinatal period has long been considered as a period of exclusive cortical gliogenesis associated with the maturation of embryonically born neurons into functional circuits. This view is currently challenged by the demonstration of neurogenesis

in specific cortical regions. Thus, GABAergic progenitors accumulate in the early postnatal white matter and give rise to a subpopulation of cortical interstitial interneurons (Frazer et al., 2017). In addition, the migration of interneurons into the frontal cortex has been shown to persist early after birth in rodents (Inta et al., 2008; Le Magueresse et al., 2012), as well as in human babies (Nogueira et al., 2017).

Our results reveal that this persisting neurogenesis is not restricted to the GABAergic lineage but also includes neurons of the glutamatergic lineage. Indeed, our work identifies a small population of cortical Satb2/Cux1⁺ neurons that are generated at birth. Surviving neurons develop spines and intracortical axonal projections, supporting their integration into cortical networks. Our results further indicate that these neurons arise from a large population of pallial RGCs that do not switch fate toward astrogenesis and persist in the dSVZ. These results are in line with recent mosaic analysis with double markers (MADM) experiments suggesting that only 1 out of 6 neurogenic RGCs produce glia (Gao et al., 2014a). Our results underline a rapid decline in the capacity of Glu progenitors to differentiate and migrate, thereby contributing to the closure of the period of cortical neurogenesis.

Our scRNAseq data shed light on the mechanisms mediating this gradual loss of neurogenic potency. Epitranscriptomic changes are emerging as key mechanisms in mediating temporal control over lineage progression. m6A is the most prevalent mRNA modification in eukaryotic cells (Desrosiers et al., 1974) and has recently been suggested to regulate transcriptional prepatterning during corticogenesis (Yoon et al., 2017). Our results identify m6A methylation as a possible mechanism leading to the transcriptional dysregulation that we observe in postnatal Glu progenitors. In addition to these epitranscriptomic modifications, KEGG pathway analysis highlights changes in several key signaling pathways, such as those involved in astrogenesis (i.e., Jak-Stat and Notch signaling pathways; Rowitch & Kriegstein 2010), suggesting that they may concomitantly affect the differentiation potential of Glu progenitors. Another signaling pathway that is dysregulated is the Wnt signaling pathway. This is in agreement with a previous study describing a gradual increase in GSK3 β activity from E15.5 on, which results in the phosphorylation of Neurog2, thereby affecting its activity (Li et al., 2012). In line with a decreased transcriptional activity of Neurog2, 64% of its target genes (Gohlke et al., 2008) are downregulated at P2, while only 2% are upregulated, despite the persistence of Neurog2 expression.

Importantly, postnatal Glu progenitors appear to be still permissive to intrinsic/extrinsic manipulation. We show that proliferation and migration of postnatal Glu progenitors can be promoted by genetic or pharmacological manipulations. Our experiments, however, reveal that these manipulations are not sufficient for promoting long-term neuron survival, suggesting that the cortex is not permissive to the integration of these newborn neurons under physiological conditions. However, recent observations suggest that permissiveness of the environment might be increased following injury, such as after neonatal chronic hypoxia, where cortical de novo neurogenesis has been observed (Fagel et al., 2009; Bi et al., 2011; Falkner et al., 2016; Azim et al., 2017). It is likely that our results will provide important information to guide future research in this context.

3.4. Supplementary Figures

Supplementary Figure S5

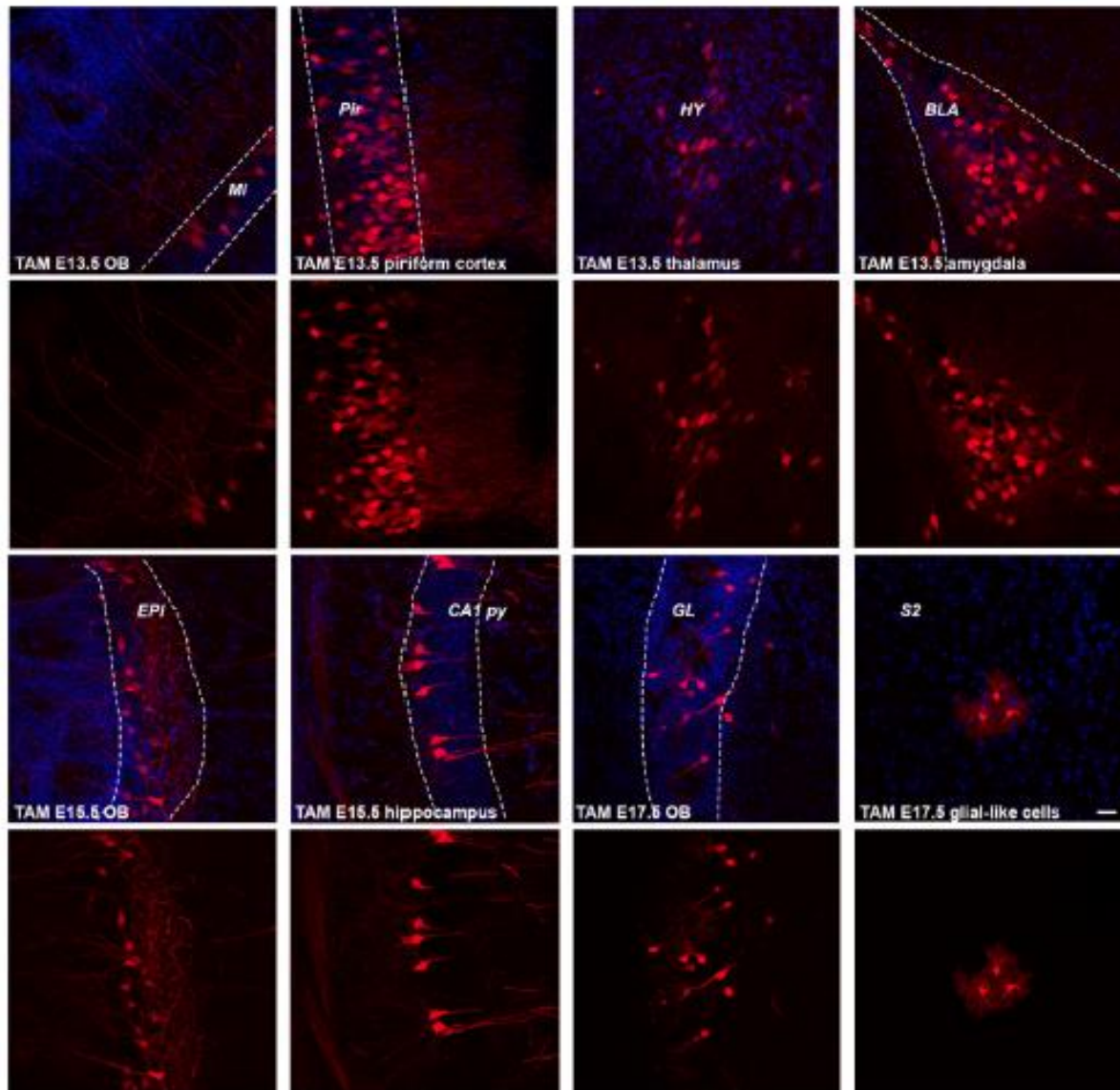


Figure S5. Related to Figure 13. Neurog2^{CreERT2}/tdTom transgenic mouse line allows detailed analyses of cell morphology. Representative high magnification images of recombined neurons following Tam injection at either E13.5, E15.5 or E17.5 and sacrificed at P21. Scale bar 25µm. Abbreviations: TAM = tamoxifen; Mi = Mitral layer; Pir = Piriform cortex; HY = Hypothalamus; BLA = Basolateral Amygdala; EPI = External Plexiform layer; CA1 pyr = Cornu Ammonis 1 pyramidal layer; GL = Glomerular layer; S2 = Somatosensory cortical region 2.

Supplementary Figure S6

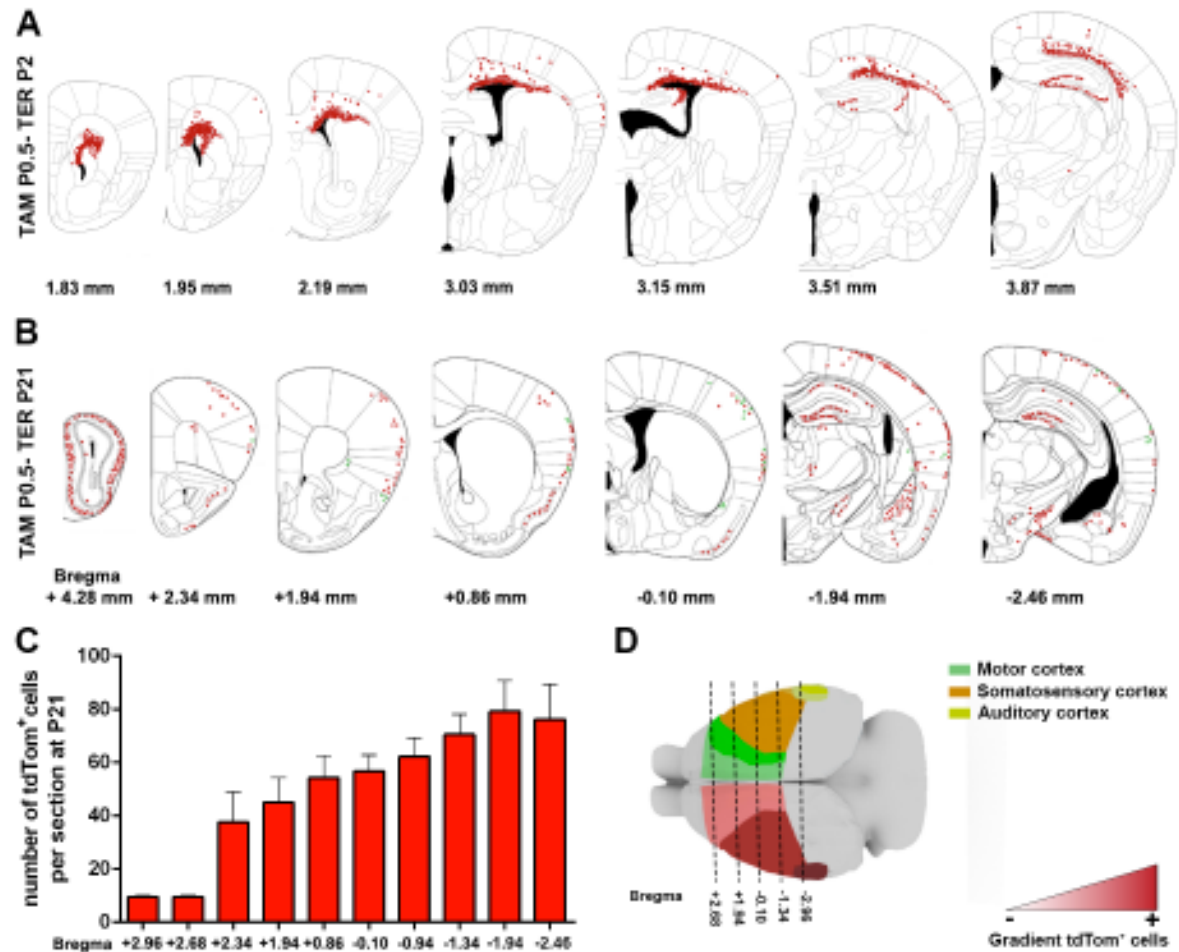


Figure S6. Related to Figure 13. Postnatal Glu progenitors mainly give rise to glutamatergic projection neurons of sensory cortical regions. (A) Drawings illustrating the distribution of recombined cells on serial sections of the forebrain following Tam injection at P0.5 and sacrificed 48hrs later. Numerous recombined cells can be seen in the dSVZ, as well as in the SCZ and SGZ. **(B)** Drawings illustrating the distribution of recombined cells following Tam injection at P0.5 and sacrificed at P21. Recombined cells are absent from the SVZ, SGZ and SCZ, but are observed in the OB and cortical regions. **(C)** The number of tdTom⁺ cells increases from frontal to caudal sections. **(D)** Schematic top view of the brain showing a heat-map distribution of tdTom⁺ cells per brain region. Note the increase from medial to lateral regions. Abbreviations: TAM = tamoxifen; TER = terminated. Data are represented as mean \pm SEM.

Supplementary Figure S7

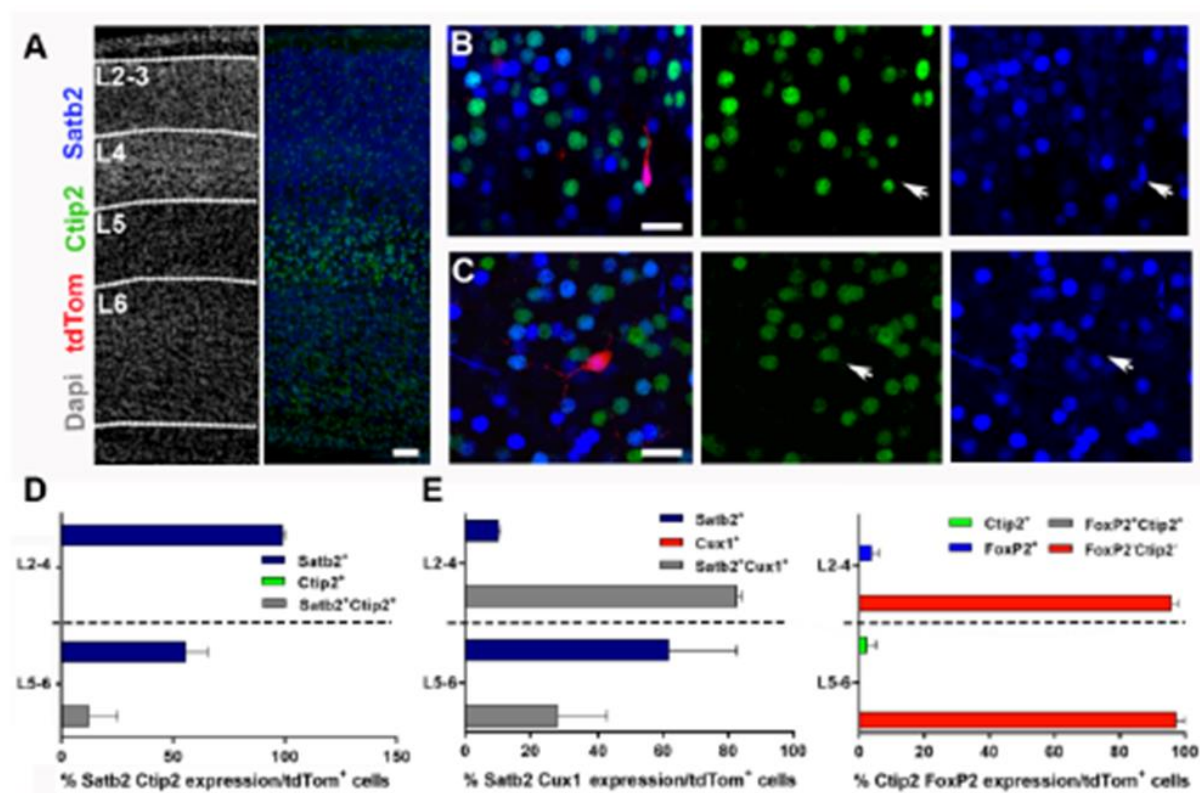


Figure S7. Related to Figure 13. Neurog2^{CreERT2}/tdTom mice reveal a late wave of corticogenesis early postnatally. (A-E) tdTom⁺ cells in both upper and deeper cortical layers express markers of glutamatergic projection neurons. (A) Overview showing the expression of Satb2 throughout cortical layers and Ctip2, which is strongly expressed in L5-6. (B-C) Examples of tdTom⁺Satb2⁺ cells. (D) The majority of tdTom⁺ cells express Satb2, but not the deep cortical layer marker Ctip2 at P7. (E) Quantification of the percentage of tdTom⁺ cells that express Cux1, Satb2, Ctip2 and FoxP2 at P45. Scale bars 75µm (A); 25µm (B-C). Data are represented as mean ± SEM.

Supplementary Figure S8

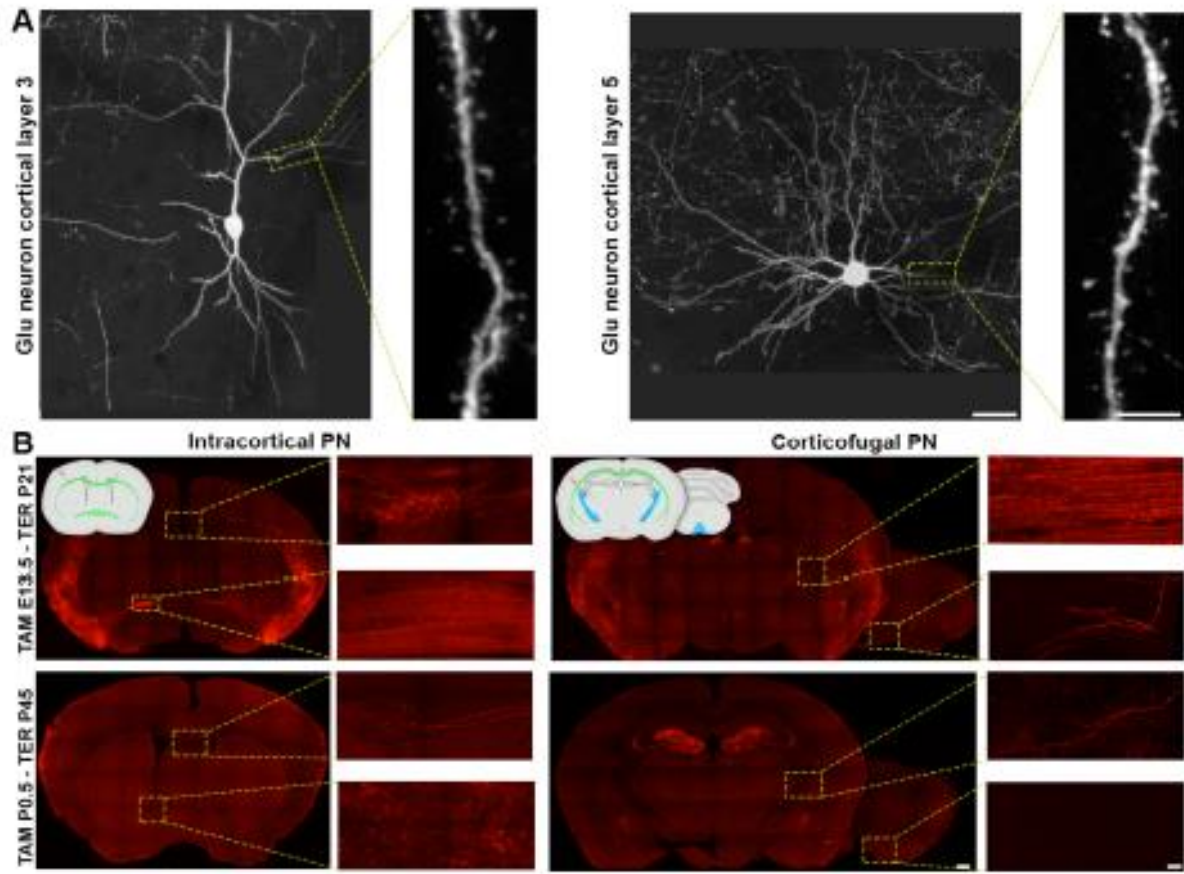


Figure S8. Related to Figure13. Postnatally born glutamatergic neurons develop intracortical projections and dendritic spines. (A) High magnification showing spine formation on postnatally born Glu neurons of both upper and deeper cortical layers at P45. **(B)** Postnatally born Glu neurons develop intracortical projections through the corpus callosum. Scale bars 1000 μ m (Tiled image B); 25 μ m (A; high magnification B); 5 μ m (high magnification A). Abbreviations: TAM = tamoxifen; TER = terminated.

GENERAL DISCUSSION

4. General Discussion

4.1. Summary and Opened Questions

Germinal regions are not homogeneous, but rather highly heterogeneous with transcriptional differences driving the production of divergent cell lineages. Recently our lab contributed to resolve this heterogeneity by demonstrating an unexpected level of transcriptional heterogeneity between the dorsal and lateral subventricular zone of the postnatal mouse forebrain, as well as in their neural stem cells and transient amplifying progenitors (Azim et al. 2015). In the first chapter of my thesis, my results contributed to describe and discuss a new level of regional and lineage-specific heterogeneity in the dorsal SVZ based on Hopx expression (Chapter 1). This work support the co-existence of lineage-biased NSC, with neighboring NSCs expressing distinct transcription factors that influence their respective behaviors and guide them through the acquisition of different fates.

In the second chapter of my thesis, I continued exploring regional and lineage-specific heterogeneity in the dorsal SVZ, by characterizing progenitors of cortical glutamatergic neurons (i.e. Glu progenitors) that we have previously shown to persist after birth (Donega et al., 2018a). Progenitors of cortical glutamatergic neurons are usually thought to switch fate before birth to produce astrocytes. My results show that this switch is largely incomplete and that a large fraction of Glu progenitors continues to be produced in the postnatal forebrain after closure of the cortical neurogenesis period. Single cell RNA-sequencing however reveals a profound transcriptional dysregulation at postnatal stages, which correlates with the gradual decline in cortical neurogenesis observed in vivo (Chapter 2).

Taken together, my work illustrates the existence of a profound NSCs heterogeneity in the postnatal SVZ, which can be explored from the regional to the single cell levels. It further highlights the benefit of transcriptional studies in exploring the diversity of NSCs heterogeneity at these different scales. It finally demonstrates the necessity of clonal analysis in histology and single cell transcriptomic in shedding new lights on our understanding of forebrain germinal activity at pre- and postnatal time points. In this general discussion, I review recent contribution of single cell approaches, including the work described in this thesis, in probing neural progenitors lineage progression and competence throughout pre- and postnatal development (concise review submitted and

under review). Finally, I conclude by discussing implication of these findings for CNS repair and propose a new experimental model to investigate the competence of postnatal neural progenitors in regenerating defined neuronal subtypes following brain injury.

4.2. Contributions of Single cell Approaches to Probe Neural Progenitor's Heterogeneity and Dynamics

The forebrain is the result of a remarkable coordination of molecular and cellular embryonic events, which transform the simple neuroepithelium (E10) into complex neural networks orchestrating sensorimotor and cognitive functions of the body. Development of the forebrain occurs in a stepwise manner. Neural progenitors (NPs) first form the pseudostratified epithelium of the ventricular zone. They initially divide symmetrically, undergoing interkinetic nuclear migration as they progress through the cell cycle, to expand their pool. Around E11.5 in the mouse, NPs acquire a radial morphology to form the Radial Glia (RG) that function as the primary neural stem cells of the developing CNS (Figure 15A). RGs have a bipolar morphology with apical and basal contacts with the surface of the ventricle and of the brain, respectively. They sequentially produce distinct subtypes of neurons before generating glial cells around birth. Later, germinal activity, including neurogenesis, persists throughout life in restricted forebrain regions, in particular the subventricular zone that lines the lateral ventricles.

Although this stepwise progression through competence states is well accepted at the population level, it is still debated if it applies to all NPs or if subpopulations of fate-biased NPs coexist. Clonal analyses in histology or transcriptomics have recently emerged as approaches to explore NPs lineage progression and competence. Here I discuss recent single cell studies made in the developing forebrain to probe the spatial and temporal neural progenitor's identity specification. I also discuss how single cell studies are contributing to our understanding of pre- and postnatal neural progenitor's changes in their competence and distribution over time.

4.2.1. Clonal Techniques in Histology and Transcriptomic

The recent single cell studies involve different set of tools which I describe in this paragraph as a technical box.

Barcoding (Golden et al., 1995)

Barcoded GFP-expressing retroviral library, in which infection of progenitor cells of a given region is achieved by local expression of an avian virus receptor (Fuentealba et al., 2015b; Mayer et al., 2018). This approach is superior to lineage tracing methods based on the use of fluorescent reporters of different colors in that it provides the complexity in tag diversity to unequivocally demonstrate that two cells in different regions are derived from a single progenitor. It may, however, underestimate clone size and/or complexity, because of viral inactivation and partial recovery of barcode sequence in laser microdissected cells.

MADM (Gao et al., 2014b; Mayer et al., 2015a; Beattie et al., 2017)

A key feature of this approach is the ability to induce clones of distinctly labeled neurons originating from a single dividing progenitor cell in a temporally defined fashion using tamoxifen. This approach also allows introduction of gene mutations allowing clonal two-color labeling with concomitant genetic manipulation. It however relies on transgenic animals and requires very low number of clones for conclusive analysis, which makes it both expensive and time consuming.

Multicolor Approaches (García-Marqués and López-Mascaraque, 2013; Roy et al., 2014; Figueres-Onãte et al., 2016)

Spectral fluorescent protein variants are stochastically expressed in cells of interest (by transgenesis, plasmid transfection or viral transduction), which both highlight cells of a tissue and differentiate them from one another when expressed in a mosaic manner. The main limitation of this approach is that juxtaposed clones labeled with a same color (due to limited number of possible colors or of their detection) cannot be distinguished and must be taken into account by modeling approaches

Single-cell RNA sequencing (Prakadan et al., 2017)

Single-cell RNA sequencing (scRNA-seq) allows the analysis of the transcriptome from individual cells, and is ideal to address the complexity and dynamics of transcriptional changes occurring during neural stem cell differentiation. There are multiple experimental approaches to capture and sequence single cells, which lead to different levels of cellular and tissue coverage. Currently, the two most popular technologies are the Drop-Seq (Yuzwa et al., 2017; Mayer et al., 2018) and the integrated fluidic circuits (IFC) (Nowakowski et al., 2017). An advantage of droplet-based approaches is their scale and speed at the expense of sequencing depth and RNA capture efficiency (Macosko et al., 2015) whereas valve-based systems (IFCs) still provide the greatest molecular efficiency and are useful for applications in which the highest-quality transcriptomes are needed at moderate scale.

Visualizing and clustering tools

Several methods have been developed to visualize the high dimensionality of the scRNA-Seq data. The two most popular data reduction methods are the Principal Component Analysis (PCA) and the t-Stochastic Neighbor Embedding (t-SNE) tools. Due to the tremendous increase number of cells analyzed, t-SNE method which puts similar cells together appears to be more suitable and has become the most common and used method. Recently, the Weighted Correlation Network Analysis (WGCNA), which analyzes relationships between co-expressed genes instead of level of expression and can be used as a clustering method as well.

4.2.2. Contributions of Single Cell Approaches to Probe Spatial Identity Specification

Following an initial period of symmetric division, neuroepithelial precursors transform into radial glial cells (i.e. RGs) around E11. RGs are heterogeneous in terms of fate, with pallial and subpallial RG generating distinct subtypes of neurons, based on the expression of defined transcription factors (TFs) (EMX1, GSH2...). In mice, inhibitory interneurons are entirely derived from the subpallium.

Original attempts at clonal RGs fate mapping made use of retroviral vectors. In the pallium, analysis of clones 1 to 3 days following viral transduction revealed that neurons migrate along clonally-related RG to form radial units. While some degree of dispersion occurs, the majority of clones populate columns thereby contributing to the functional radial organization of the neocortex (Noctor et al., 2001). Similar conclusions were reached in more recent studies relying on near clonal recombination (Magavi et al., 2012), as well as more recently by MADM clonal analysis (Gao et al., 2014a).

Similar principles are likely to apply in the subpallium. Thus, radial clusters composed of a radial cell, IPCs and newborn neurons are observed < 4 days post viral transduction at E12.5 in the MGE (Harwell et al., 2015). Subpallial RGs appear to be the primary neural stem cells, dividing asymmetrically to produce IPCs that subsequently divide symmetrically to expand their numbers, or more frequently, to produce pairs of neurons (Magavi et al., 2012; Mayer et al., 2015b). Similarities however stop there, as interneurons produced by RG from distinct ganglionic eminences then migrate tangentially rather than radially to invade distinct telencephalic regions (review Hu et al., 2017a, see also Wichterle et al., 2001). Clonal analysis in the MGE, which contributes to 60% of cortical interneuron (Miyoshi et al., 2007), reveal a dramatic dispersion of sibling interneurons. Thus, interneurons migrate to widespread regions within the telencephalon, although they do not cross the segmental boundary of the diencephalon nor the midline (Magavi et al., 2012; Mayer et al., 2015b).

scRNA-Seq studies have investigated the transcriptional identity of both pallial and subpallial RGs and the lineages they are producing. A direct comparison of results obtained in various studies is made difficult by differences in the methods of cell capture, sequencing depth, and methods of analysis (Table 2). For instance, while the VZ and SVZ are separated in some studies, this is not always the case. Important and convergent conclusions however emerge from this work.

References	Germinal zone	Age	Capture	Number of cells	Genes/cell
Mi D et al, 2018	GE	E12.5 / E14.5	C1 Fluidigm	2 003	3 200
Mayer C et al, 2018	GE	E13.5 (MGE) E14.4 (CGE + LGE)	DropSeq	20 788	> 700
Donega V et al, 2018	Pallium	E15.5 / P2	C1 Fluidigm	220	2 000
Yuzwa SA et al, 2017	Pallium	E11.5 / E13.5 / E15.5 / E17.5	DropSeq	11 000	1 000 - 1 500
Nowakowski TJ et al, 2017	Pallium	pcw 5 to 37	C1 Fluidigm	4 261	> 1 000
Telley L et al, 2016	Pallium	E14.5	C1 Fluidigm	326	3 000

Table 2. ScRNA-Seq experiments and their parameters

First, it appears that transcriptional differences between RGs that reside in distinct pallial and subpallial regions are small and rely on a rather restricted number of genes (Novotortsev et al., 2010; Mayer et al., 2018; Mi et al., 2018). For instance, only 16 TFs are differentially expressed within mitotic progenitors of MGE vs. CGE, while the majority of dynamically expressed genes follow robust and highly reproducible sequential waves of gene expression in both eminences (Mayer et al., 2018). Similarly, in the pallium, RGs from the PFC and V1 cortical areas have only 68 differentially expressed genes and share a common molecular differentiation program (Nowakowski et al., 2017). The subtle transcriptional differences which distinguish progenitors get likely superimposed onto a large pan-developmental program and therefore render the threshold of detection of progenitor subtypes rather tedious and variable between studies (Mayer et al., 2018; Mi et al., 2018). A second observation is that clearly distinctive transcriptional programs are only consistently emerging at the postmitotic level when newborn neurons from distinct germinal regions initiate migration and maturation (Nowakowski et al., 2017; Mayer et al., 2018; Mi et al., 2018).

Altogether, these observations support a model for emergence of neuronal diversity in which small differences across cycling progenitors are sufficient to drive neuronal diversity, which amplifies over time in postmitotic neurons (**Figure 17BC**). The small differences across cycling progenitors might appear disconcerting, however previous studies have

shown that swapping of individual TFs from subpallial to pallial progenitors is sufficient to re-specify them (Parras et al., 2002), illustrating the critical impact of a small number of genes on cell fate.

The introduction of an approach (i.e. flashtag) allowing labeling of isochronic cohorts of RGs and of their progeny, offers an extra level of refinement to these transcriptomic studies (Telley et al., 2016; Mayer et al., 2018). Labeled cells can be isolated at distinct time points following injection and tracked during their differentiation, thereby giving a precise overview of transcriptional waves regulating the acquisition of neuronal identity (Telley et al., 2016). This approach demonstrates the importance of the proper sequence of transcriptional waves for normal progression through neuronal differentiation and the relative high degree of their overlap. In the first hours following their labeling, RGs rapidly repress proliferation-associated transcripts while upregulating transcripts associated with protein translation. Later transcriptional waves include transcripts associated with DNA repair, revealing a critical period following mitosis during which neocortical neurons are susceptible to somatic mutations. As early as twelve hours post-labeling, differentiation programs unravel with transcriptional waves initiating late-occurring processes such as synaptogenesis. The early occurrence and overlapping nature of these transcriptional waves suggest an early priming of terminal differentiation events and provide discrete time windows during which specific transcriptional complexes are present simultaneously and can interact (Nowakowski et al., 2017). The same approach was applied by Mayer and colleagues, which conclude of common dynamics in all three eminences (Gao et al., 2014b).

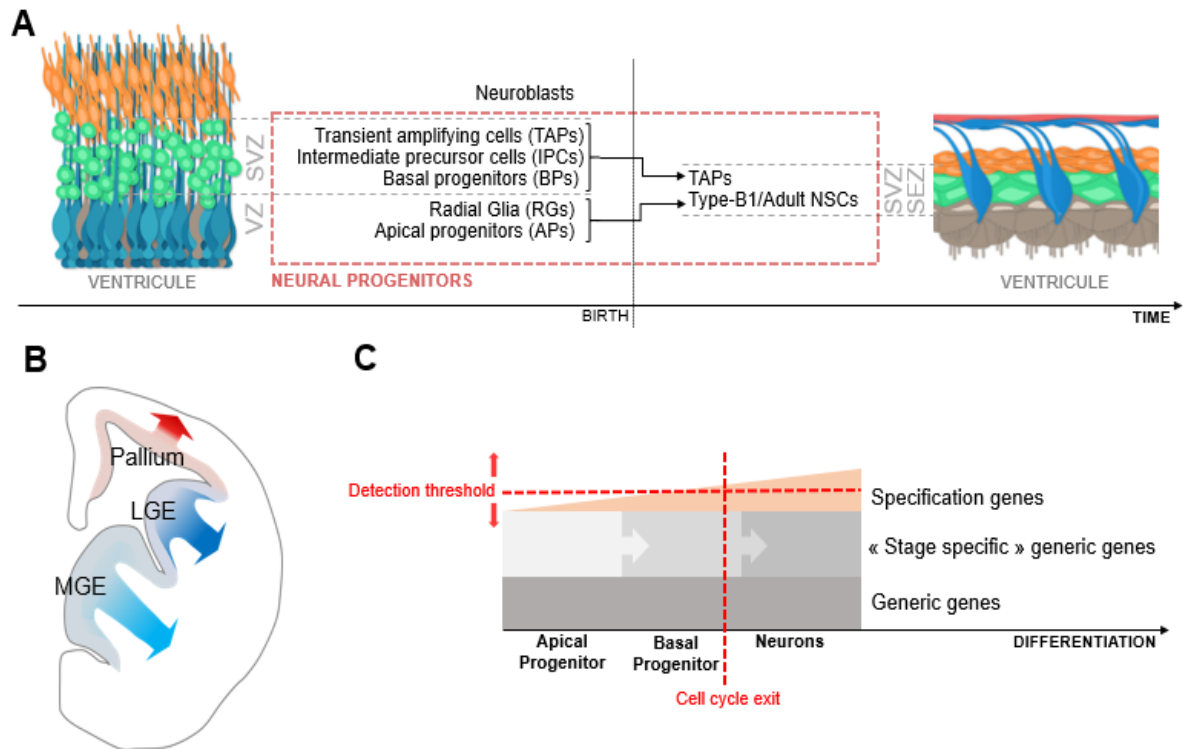


Figure 17: (A) Schematic representation of the organization of the periventricular germinal niche at pre- and postnatal timepoints. The terminology used to define neural progenitors at pre- and postnatal timepoints is summarized. The multiple layers of the embryonic periventricular germinal region merge following birth and become separated from the ventricular lumen by ependymal cells. Radial Glia (also termed basal progenitors) are the bona fide neural stem cells. They generate neurons directly or through intermediate progenitors, as well as glial cells, ependymal cells and adult neural stem cells. Different colors and shades of blue are used to illustrate their heterogeneity in term of fate and transcriptional profiles, as discussed in this review. Adapted with permission of Development.

(B) Schematic representation of the germinal regions of the embryonic forebrain. Distinct neuronal subtypes emerge from neural progenitors located in defined pallial and subpallial regions. Gradients represent the transcriptional differences observed between these neural progenitor populations. Note that transcriptional differences are minimal in neural progenitors and exacerbated during differentiation.

(C) Schematic representation of transcriptional programs superimposition during cellular differentiation. While some transcriptional programs are generic to all cells (generic genes), others are expressed at different stages of their differentiation but remain generic to all lineages (stage specific genes). Lineage specification is coded by a small number of genes which progressively increase with the acquisition of defined morphology, connectivity and functions. Clustering sensitivity following single cell RNA-Sequencing rely on differentially expressed genes which only become clearly distinctive between distinct neuronal lineages at the post-mitotic level. It is therefore highly dependent on sequencing depth and number of cells analyzed.

4.2.3. Contributions of Single cell Approaches to Probe Temporal Identity Specification

Neural progenitors change over time to contribute to the generation of cell diversity, a process termed as temporal identity specification. Thus, while RGs initially undergo proliferative divisions to amplify their pool, they later switch into a differentiating mode of division to produce specialized cells.

In the pallium, RGs progressively change their fates to sequentially produce deep-layer, then upper-layer neurons before generating glial cells at late embryonic times (Okano and Temple, 2009). While it was originally proposed that subtype of fate-biased RG cells co-exist, recent clonal studies have revealed that pallial RGs follow a deterministic behavior and unitary production of projection neurons. Thus, RGs from the neocortex appear to invariably produce combinations of layer specific subtypes of cortical neurons (Gao et al., 2014a), implying that the behavior of individual RG is remarkable predictable across developmental stages and cortical areas. RGs first undergo symmetric divisions for several rounds before transiting to asymmetrical division and producing 8 to 9 neurons in different cortical layers. Towards the end of the embryonic period, RGs then change fate and produce astrocytes that migrate to the cortex, where they amplify locally (Ge et al., 2012), to form clones (García-Marqués and López-Mascaraque, 2013) and associate to defined cortical columns (Magavi et al., 2012). Interestingly, recent clonal fate mapping suggest that this neurogenic to gliogenic transition is largely incomplete, as only a fraction of RG cells (estimated to roughly 1/6), switch to produce glial cells. Other pallial RGs appear to continue producing IPCs (*Tbr2/Neurog2* positive), whose contribution to cortical neurogenesis rapidly declines postnatally (Donega et al., 2018b), but continue producing a small population of glutamatergic interneurons in the periglomerular cell layer of the olfactory bulb for several weeks after birth (Brill et al., 2009). Finally a population of pallial RGs, identified by *Emx1* expression, change fate to contribute to the generation of calretinin-expressing GABAergic, as well as dopaminergic interneurons in the olfactory bulb (Kohwi et al., 2007; Fuentealba et al., 2015b).

The advantage but also inherent limitation of clonal fate-mapping studies is the low number of cells that can be analyzed at once. On the other hand, scRNA-Seq experiments analyze genes expression of a large number of cells across the embryonic development allowing the investigation of temporal transcriptional heterogeneity. Is transcriptional profiling using scRNA-Seq supporting clonal analysis observations? In line with clonal histology experiments, the analysis of RGs transcriptional profile at different developmental stages,

indicates a single linear trajectory of RGs from E13,5 to E17,5 (Yuzwa et al., 2017), reflecting a gradual shifting of the population of RGs, rather the co-existence of divergent fated subpopulations. In line with fate mapping studies, emergence of gliogenic related genes are observed later in the development (Novotortsev et al., 2010). Although this has not been systematically addressed in the subpallium, current evidences however support the existence of a subtle heterogeneous RGs population in the MGE from E12.5 to E14.5 whereas in the CGE RGs appear more homogeneous (Mi et al., 2018). This likely reflects the larger GABAergic neuron diversity, and sequential generation of PV and SST interneurons by the MGE. Future studies making use of the “flashmap” to label isochronic cohorts of RGs and of their progeny throughout embryonic development will be necessary to investigate in detail the transcriptional changes occurring in a population of RGs while it gives rise sequentially to distinct subtypes of neurons.

How can we explain then that relatively transcriptionally close RGs sequentially give rise to distinct neuronal subtypes? Noticeably, layer specific genes, encoding for layer specific proteins (such as Cux1 or Ctip2), are highly co-expressed in RGs throughout the neurogenic period (>70% coexpression) (Zahr et al., 2018). This situation contributes to the relative homogeneity of RGs and sheds light on a strong post-transcriptional regulation of RGs fate (Zahr et al., 2018). The authors identified 4E-T/Pum2 complex as a major player regulating fate specification of neurogenesis through post-transcriptional repression of appropriate mRNAs. In absence of this complex, aberrant specification of neurons is observed (Zahr et al., 2018). Other epitranscriptomic changes mediating temporal control over lineage progression, include m6A methylation, recently suggested to regulate transcriptional pre- patterning during corticogenesis (Yoon et al., 2017). The observation of a large decrease in m6A level in cortical progenitors persisting at birth suggest that epitranscriptomic modifications participate in the closure of the period of cortical neurogenesis (Donega et al., 2018a). Taken together, these studies highlight that the temporal production of defined neuronal subtypes is the result of numerous regulating mechanisms, not restricted to the mRNA expression revealed by scRNA-Seq, but including post-translational modifications of histones, DNA modifications and chromatin remodeling (Albert and Huttner, 2018; Sokpor et al., 2018; Stricker and Götz, 2018).

4.2.4. Contributions of Single cell Approaches to Probe Adult NSCs Origin and Biology

The persistence of a germinal activity in the ventricular zone of the postnatal and adult forebrain prompted the question of the origin of these NSCs. While original studies had suggested a continuum in the differentiation of RGs in adult NSCs at perinatal times (Tramontin et al., 2003), recent clonal fate mapping studies revealed that adult NSCs derive from embryonic RGCs, which are distinct from those contributing to the neuronal and glial lineage of the developing forebrain (**Figure 18**).

Two distinct approaches were used to demonstrate that a subpopulation of RG slow their proliferation and segregate from the rest of RG that continue proliferating. Label retaining protocols demonstrate the prevalent emergence of a slowly dividing NPC population between E14.5 and E16.5 (Fuentealba et al., 2015b; Furutachi et al., 2015). This time points coincides with cell cycle exit of a subpopulation of RG biased to generate ependymal cells (Spassky et al., 2005). While this timing coincides, it is still unclear if they are generated by a common pool of RGs. Interestingly, the level of labels retained in young adult NSCs were higher than in ependymal cells, suggesting that if NSCs and ependymal cells are produced sequentially by the same RG population, then NSCs may be produced first (Furutachi et al., 2015). Bar coding tagging of RG at distinct embryonic time points resulted in similar conclusions (Fuentealba et al., 2015b).

Interestingly, the induction of RG quiescence is not homogeneous along the lateral ventricle and is likely to explain the persistence of germinal activity to restricted regions of the lateral ventricle at adult ages. Indeed, while label-retaining cells are frequently observed in the ganglionic eminences, in particular the LGE, they are rare in the pallium (Tramontin et al., 2003). This goes in line with the different dynamics observed in the generation of pallial (i.e. *Tbr2*⁺) and subpallial (i.e. *DLX2*⁺) progenitors observed at postnatal stages. Thus, while *Tbr2* progenitors continue to be produced by pallial RGs at early postnatal timepoints (Donega et al., 2018a), their production rapidly decreases over time to become almost extinguished by P90 (Brill et al., 2009). On the contrary, *DLX2*⁺ progenitors continue being produced throughout adulthood, in agreement with the preferential accumulation of quiescent NSCs in the lateral SVZ (Furutachi et al., 2015).

In the adult, quiescent NSCs reactivate asynchronously to divide symmetrically. While 1/5th self-renew in P21 mice, the remaining population generate type C cells that cycle 3 times before generating neuroblasts that undergo one or two additional cycles (Ponti et al., 2013; Obernier et al., 2018). This results in a fast clonal expansion but limited self-renewal of

adult NSCs as demonstrated by clonal analysis (Calzolari et al., 2015). The rapid consequent depletion of activated NSCs explain the sparsity of clones containing both B1 cells and OB interneurons following bar coding tagging of RGs during embryonic development (Fuentealba et al., 2012). Thus, a population of NSCs self-renew to dampen their early depletion, while a second population reactivates to produce a progeny before rapidly extinguishing (Calzolari et al., 2015; Obernier et al., 2018). The asynchronous activation of adult NSCs allows SVZ germinal activity to persist throughout life, despite of a gradual decline. This asynchronous, gradual activation is further supported by the observation that E15.5 label retaining NSCs produce a neuronal progeny with undisguisable BrdU levels at different postnatal ages (Fuentealba et al., 2015b). It is still unclear if NSCs then produce glial cells following their final division, as the transgenic mice used in these studies did not allow discriminating between NSCs and surrounding glial cells.

Single cell transcriptomic studies revealed that RGs from the subpallium (regardless of the eminence of origin), as well as from the pallium, have different maturation statuses but no sign of fate bifurcation (Nowakowski et al., 2017; Mayer et al., 2018). A transcriptional variance is however observed across RGs, which primary origin is developmental and cell cycle progression. This likely reflects multiple modes of divisions (symmetric vs. asymmetric) at distinct embryonic stages (Mayer et al., 2018), as well as the cell cycle exit of some RGs. Analysis of a larger number of cells, indeed reveal the co-existence of mitotic vs. non-mitotic RGs within the pallium as early as E13 (Yuzwa et al., 2017). Additional analyses are required to define if these include RGs which have exited the cell cycle to engage towards specific fates, i.e. ependymal cells or adult NSCs. Detection of ependymal cells transcripts (e.g. *GemC1/Lynkeas* and *Mclidas*) may reveal early priming in a cluster of non-mitotic RGs towards this lineage, even if this might be hindered by the largely postnatal differentiation of this cell type (Tramontin et al., 2003). Detection of transcriptional similarities between slowly/non mitotic embryonic RGs from E13.15 to quiescent adult SVZ support the existence of the subpopulation of quiescent cells accumulating over development, to be reactivated in adulthood. Further investigations will reinforce the extent of transcriptional overlap of these RGs with quiescent NSCs isolated from the adult brain (Codega et al., 2014; Llorens-Bobadilla et al., 2015).

Single cell transcriptomic approaches were recently applied to adult NSCs (Llorens-Bobadilla et al., 2015) to reveal the co-existence of NSCs in multiple states of activation. Similar to the sequential transcriptional waves observed newborn neurons in the mouse neocortex (Telley et al., 2016), it reveal that NSC activation and early lineage progression

is organized as a continuum of molecular events, along which cells express sets of co-regulated genes. This work highlighted an association of NSCs quiescence with high glycolytic and lipid metabolism, as well as with the previously reported high expression of transcripts encoding membrane receptors (Codega et al., 2014). Further, NSCs activation and differentiation correlated with a progressive up-regulation of the protein synthesis machinery. Interestingly, this single cell transcriptomic analysis provides important information on the priming of individual adult NSCs towards specific lineages. Indeed, the postnatal and adult SVZ is regionalized in respect to different microdomains generating distinct neural lineages. This regionalization appears to originate from early embryonic development (Fuentelba et al., 2015b) and is intrinsically encoded by expression of selected TFs (reviewed in Fiorelli et al. 2015). Single cell analysis identified single cells exhibiting expression of oligodendroglial or neuronal subtype-specific TF combinations, thereby revealing the early priming of adult NSCs towards specific fates (Llorens-Bobadilla et al., 2015). This observation is in line with ex vivo lineage tracing of individual cells showing that neurogenic and oligodendrogenic NSCs constitute distinct lineages, while both can produce astrocytes. Recent lineage tracing of a subpopulation of dorsal NSCs expressing the TF HOPX at early postnatal timepoints, however suggests the existence of a NSCs population biased to produce astrocytes (Zweifel et al., 2018). Thus, the production of distinct cell types by adult NSCs relies on the co-existence of fate-biased NSCs, which are heterogeneously distributed along the wall of the lateral ventricle.

In conclusion, single cell approaches contribute to our understanding of NSC biology and of their specification into distinct cell types at defined developmental and postnatal stages. Future developments are likely to allow integrating emerging approaches to investigate the three-dimensional genomic organization (e.g. Chi-C mapping) or chromatin accessibility (e.g. ATAC-Seq) at the single cell level. This will provide a complete picture of transcriptional and epigenetic changes occurring in neural progenitors. Extension of these methods to pathological situations will inform on mechanisms involved in NSC activation and will guide research in their priming towards specific fate for the development of regenerative therapies.

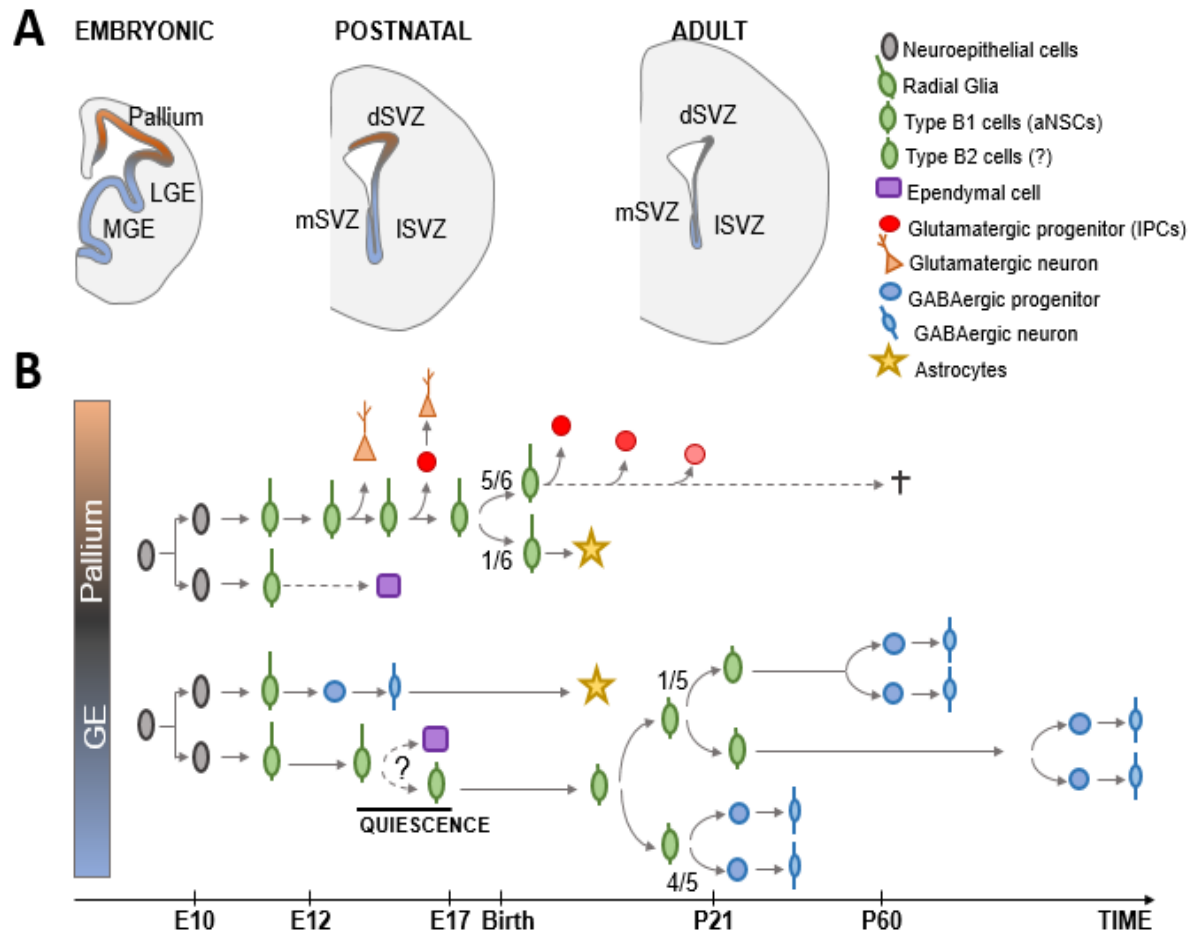


Figure 18: A unifying scheme of pre- and postnatal germinal activity, integrating single cell findings discussed in this review. (A) Schematic representation of the germinal region of the embryonic forebrain and of their evolution during postnatal life. **(B)** During development, neural progenitors from the pallium and subpallium generate distinct neuronal subtypes. Whereas the coding of this diversity is primarily spatial in the subpallium, it is temporal in the pallium with the sequential generation of deep, then upper layer neurons. Ependymal cells are produced from a subpopulation of neural progenitors around E14.5, in a time course concomitant to the generation of adult NSCs in the subpallium. Around birth, a fraction of neural progenitors change fate to produce astrocytes in both regions, while others continue generating a small population of glutamatergic neurons in the cortex. Following birth, germinal activity remains sustained in SVZ regions originating from the subpallium (i.e. mSVZ and to a larger extent ISVZ), while it gradually disappears from those derived from the pallium (dSVZ). Abbreviations: LGE: lateral ganglionic eminence; MGE: medial ganglionic eminence; dSVZ, ISVZ, mSVZ: dorsal, lateral and medial subventricular zone.

4.3. Implication for Brain Repair

4.3.1 *Are embryonic and Postnatal/adult NSCs Representing Distinct Populations in term of Diversity and Competence?*

Original studies supported a progressive restriction in the competence of NSCs in producing distinct cell lineages during forebrain development. For instance, in vitro studies demonstrated that cortical progenitors sequentially produce deep layer, then upper layer neurons, before producing glial cells (Qian et al., 2000, Shen et al., 2006) . Further, the competence of cortical progenitors appears to become increasingly restricted. Noticeably, mid-gestational progenitors can still be manipulated to generate early neuronal fates, while late-gestational progenitors have lost this competence (Shen et al., 2006). This progressive loss of competence has also been illustrated in vivo, by transplantation experiments. Early heterochronic transplantation approaches have found that the potential of different progenitor populations to generate distinct neuronal subtypes becomes gradually restricted over time (for review Gaiano and Fishell, 1998). For instance, cycling progenitors from late stages of the ferret corticogenesis, keep their intrinsic restriction, even if transplanted into an early stage environment. Indeed they keep generating upper layer neurons and fail to produce deep cortical layers, which are normally generated at this age (Frantz and McConnell, 1996). In contrast, early progenitors are able to adapt to the host environment to generate upper layer neurons, when transplanted into a late stage environment (Gümüşsoy et al., 2009). These original experiments support a gradual fate restriction of cortical progenitors during embryogenesis, a model that is still largely accepted today.

Accumulating observations however suggest that this fate restriction might not apply to postnatal and adult NSCs. For example, in vitro experiments demonstrated that adult NSCs remain bipotent, with individual clones consisting of neurons and astrocytes or oligodendrocytes and astrocytes (Ortega et al., 2013). Further, heterochronic transplantation experiments have shown that postnatal SVZ progenitors can migrate and differentiate within multiple levels of the developing neuraxis, when transplanted into embryonic mouse brain ventricles at day 15 of gestation (Lim et al., 1997). Although expression of subtype specific markers was not assessed, their acquisition of morphologies typical of resident neurons support their capacity to generate other neurons subtypes than those they normally produce within the olfactory bulb. Finally, ex vivo experiments showed that postnatal and adult SVZ explants have the capacity to generate pyramidal neurons. In these experiments, adult SVZ explants were exposed to an

embryonic environment by juxtaposing them to organotypic slices of the pallium. Neurons were produced by the SVZ explants, which invaded the pallium. Their expression of *Tbr1* suggested their acquisition of a glutamatergic phenotype, although their maturation could not be investigated at long term (Sequerre et al., 2010).

Taken together, these observations challenge the model of gradual fate restriction observed during embryogenesis. They rather suggest that embryonic and postnatal/adult NSCs represent distinct populations in term of diversity and competence to generate various cell types. The recent demonstration that postnatal/adult NSCs derive from embryonic RGCs that are distinct from those contributing to the neuronal and glial lineage of the developing forebrain, support this hypothesis (Fuentealba et al., 2015b; Furutachi et al., 2015). Further, single cell studies discussed above provide a roadmap to guide postnatal/adult NSCs to differentiate into defined cell types, and give insight in the mechanisms at play that restrict their recruitment and successful differentiation.

Unravelling the diversity and competence of postnatal/adult NSCs to produce distinct neural cell types is of major importance for further considering them as a potential source for cellular repair. Unravelling their diversity relies on the identification of markers expressed in subpopulation of NSCs biased to acquired defined fate. To this end, the identification of markers expressed in SVZ microdomains giving rise to distinct cell lineage represent a powerful approach, as illustrated in **Chapter 1**. This work resulted in the identification of *HOPX* as a marker of NSCs within the dorsal SVZ, biased to acquire an astrocytic fate. Unravelling their competence to generate diverse neural cell types relies on understanding the transcriptional changes that occur in neural progenitors over time, as illustrated in **Chapter 2**. It finally relies on testing their capacity to participate to forebrain development, or to participate to its regeneration. While the former can be achieved by heterochronic transplantation, as previously (Lim et al., 1997) the later relies on establishment of new models in which define cell types are ablated at early postnatal time points, when its regenerative potential is maximal. Please find below a description of such model.

4.3.2. Targeted Neuronal Ablation as a Model to Study Competence of Postnatal NSCs for Cortical Repair

Early brain injury following perinatal insults such as hypoxic–ischemic episodes, often result in severe neurological disabilities. The common feature of these lesions is the

massive death of various cell types including neurons and glial cells (Ferriero, 2004; Kaindl et al., 2009; Deng, 2010). The capacity of the adult mammalian cerebral cortex to compensate adequately for neuronal and glial loss appears limited. Indeed, there are only few evidences of a significant contribution of germinal regions to brain repair in the adult. Nonetheless, this situation appears to be strikingly different during the early postnatal period (Plane et al., 2004; Ong et al., 2005). Convergent observations indicate that neonatal trauma can lead to regenerative cortical neurogenesis. Newly generated neurons appear to arise from the rostral subventricular zone (SVZ), to be recruited to the damaged cortex (Jin et al., 2003; Saha et al., 2012; Thomsen et al., 2014). However, although de novo neurogenesis is well documented in newborn, fundamental questions remain to be addressed to fully appreciate the inner capacity of the neonatal forebrain to repair. In particular, the capacity of newborn neurons to specify in appropriate neuronal subtypes have not been studied in details because only generic markers have been used in most of the studies (Saha et al., 2013). Thus, do newborn neurons correctly specify in neuronal subtypes and functionally integrate? This open question is of particular interest, as an incorrectly specification and integration of these neurons may result adverse effects.

Different cortical lesion models have been developed over the years, in order to test the capacity of the neural tissue to regenerate in newborn rodents. In 2008, Kadam and colleagues, used a hypoxic-ischemia model to induce a diffuse cortical lesion (Kadam et al., 2008). In 2011, Bi and colleagues described a chronic hypoxia model in 3-days-old mice Bi et al., 2011. Other models include ischemic insults (Biran et al., 2011). Importantly, all of these models result in diffuse injuries, characterized by the loss of various cell types often accompanied by a severe disorganization of the tissue. Thus, these models are not appropriate to study the recruitment of specific progenitor populations, nor their specification and integration.

I aimed at developing a versatile injury model that circumvent most of these limitations by developing a model of targeted ablation of specific neuron populations. This approach is based on the targeting of select cohorts of cortical progenitor during embryonic development, and the control of the onset of ablation through diphtheria toxin (DT) and diphtheria toxin receptor (DTR) system (Petrenko et al., 2015). Although I did not manage to complete this project due to time constrains, I obtained encouraging data showing that DT-mediated apoptotic death of select neuronal population is efficient and sufficient to induce a proliferative response of progenitors in the dSVZ. This model present several advantages that will prove to be of interest to test repair capacity under various contexts, the spatio-temporal control of ablation and the restrained inflammation response.

Although, generation of new cortical neurons was not spontaneously observed, this model might be used to test strategies to recruit Glu progenitors, as discussed in **Chapter 2**.

Results

Diphtheria toxin is a well-characterized bacterial toxin composed of an A and a B chain. The toxin can only enter into the cell by endocytosis if a specific receptor (DTR), bound by the B chain, is expressed on the cell surface. Inside the cell the A (DTA) chain inactivates elongation factor 2 via ADP ribosylation, leading to cessation of protein synthesis and subsequent cell death. Rodent cells are naturally resistant to DT, due to the absence of DTR on their membrane (Buch et al., 2005). Sensitivity of select neuronal populations to DT can therefore be induced by selective DTR expression. We focused on layer IV cortical neurons, which integrates thalamic inputs into cortical networks. Due to the sequential generation of cortical neurons, neurons of select cortical layers can be efficiently electroporated by in utero electroporation at defined embryonic timepoints. Electroporation at E14.5 of a DTR-GFP plasmid (at 1.5 μ M) resulted in an efficient transfection of a large number of layer IV neurons, i.e. 30% of Cux1⁺ layer IV neurons in our average (**Figure 19A-D**). Electroporated neurons were distributed over a large area, covering in average 8.5 mm² of cortex. Five days following a single intraperitoneally DT injection, at the concentration of 25ng/g in P2 animals, we observed a significant 20% decrease of CUX1⁺ upper layer thickness (**Figure 19G**) which demonstrates that number of dead neurons is sufficient to induce a clear and robust phenotype. Despite an important apoptosis, our results showed a mild inflammation at the lesion site, in agreement with previous studies (Petrenko et al., 2015), as revealed by an increase of microglia (Iba1⁺) and astrocytes (GFAP⁺) in the cortex several days following the induction of the lesion (**Figure 19I-J**). Nevertheless, those cells kept a clear organization and did not form a scar as observed in more invasive injury models. The timecourse and possible persistence of this inflammation remains however to be fully assessed.

I next focused on the dorsal SVZ to investigate the consequence of the cortical ablation on cellular proliferation 5 and 12 days later. An increased proportion of Ki67⁺ cells was observed in the dorsal SVZ, five days following DT injection, when compared to controls (**Figure 20AB**). This demonstrated that the severity of the lesion was sufficient to induce a rapid proliferative response, which attenuated over time. The number of Glu progenitors, identified by Tbr2 immunolabeling, did not vary following DT injection (**Figure 20AB**). In contrast, the number of oligodendrocyte progenitors identified by Olig2 immunolabeling, increased rapidly and persistently following ablation (**Figure 20AB**). This could be due to

an important axonal degeneration following targeted cortical ablation, resulting in a reactive oligodendrogenesis.

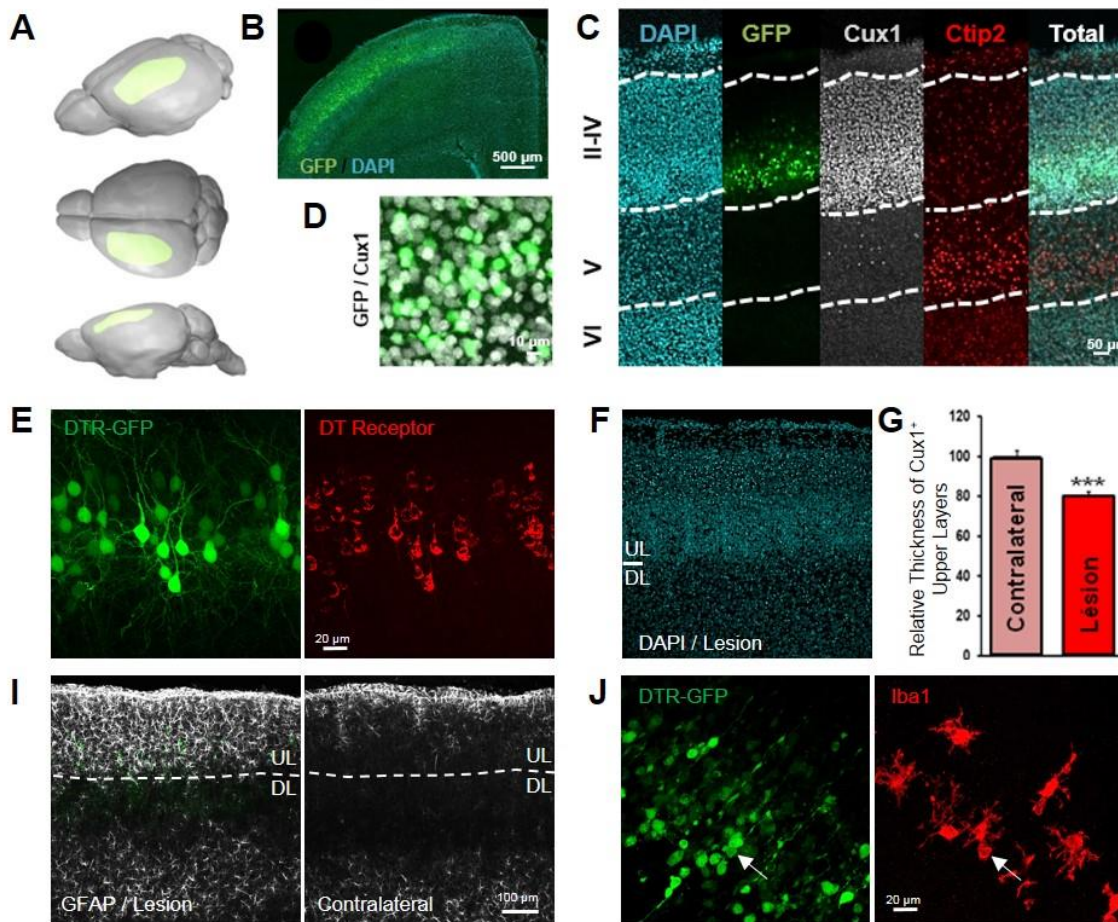


Figure 19: Specific Targeting of Layer IV Cortical Neurons induces fast and efficient neuronal ablation. (A) 3D reconstruction of DTR-GFP electroporated brains representing the average surface of the targeted area based on GFP expression. (B-C) Representative images of coronal brain sections showing localization of GFP electroporated cells at low and high magnification using epifluorescent (B) and confocal microscopy (C), respectively. In panel C, co-immunolabeling of GFP with Cux1, a upper layers marker, and Ctip2, a lower layer marker, were used to define borders of cortical layers. (D) High magnification of GFP/Cux1 immunolabeling image shows that all GFP+ cells are Cux1+ upper cortical neurons. In average, GFP+ cells represent 30% of the total number of layer IV Cux1+ neurons (Not shown). (E) Representative image of GFP targeted neurons co-expressing the Diphtheria toxin (DT) receptor detected with a HB-EGF antibody (Heparin Binding EGF-like Growth Factor). Note that all electroporated neurons express the DT receptor. (F-G) Representative image of pyknotic Dapi+ cells in targeted area (F) resulting in a 20% decrease of Cux1+ thickness 5 days following ablation induction (G) and demonstrating efficiency of the ablation approach. (I-J) Representative images of brain response 5 days following DT injection. GFAP expression, a marker of astroglial reactivity, is increased at the lesion site (I), such as Iba1+ cells number, a marker of responsive microglia (J). Arrow indicating GFP+ cells engulfed by a microglia. UL, upper layers; DL, deeper layers. Scale bars: 500 µm in (B); 50 µm in (B); 10 µm in (C), 20 µm in (E/J) and 100 µm in (I). ***p < 0.001, data are presented as mean ± SEM from n=3 animals.

I next assessed if de novo cortical neurogenesis was observed following targeted cortical ablation. The mitotic marker BrdU was administered at the time of DT injection to label the cohort of Glu progenitors and the presence of BrdU⁺/NeuN⁺ newborn neurons assessed within cortical layer 12 days post ablation. Strikingly, no BrdU⁺/NeuN⁺ newborn neurons were observed indicating that spontaneous neurogenesis does not occur in this model, although this still need to be confirmed with the use of additional neuronal markers (e.g. Dcx, Cux1...).

*I finally assessed if a pharmacological activation of canonical Wnt signaling could promote recruitment of Tbr2⁺ progenitors. The GSK3 β inhibitor AR-A014418 was then administered for 3 days in P2 control animals to confirm that the relative proportion of Ki67⁺ and Tbr2⁺ cells 5 days post-treatment efficiently increases, as previously reported (Azim et al., 2014, 2017; Donega et al., 2018a) (**Figure 20C**). Similarly, DT-injected animals were treated for 3 days following the start of ablation with AR-A014418. This resulted in a significant increase of Tbr2⁺ cells (**Figure 20D**). In parallel, a significant reduction of GFAP expression was observed around the site of neuronal ablation (**Figure 20E**). These observations support a regenerative potential for Wnt/ β -catenin stimulation following neonatal brain injuries, which remains to be fully explored. For instance, it will be interesting to study if this activation of Tbr2⁺ progenitors translate into cortical neurogenesis. If new neurons are observed, their appropriate specification in layer IV cortical neurons can then be assessed.*

Altogether this work demonstrates that DT-induced cortical ablation may prove to be an interesting model to study the competence of postnatal progenitors to produce select neuronal subtypes following injury.

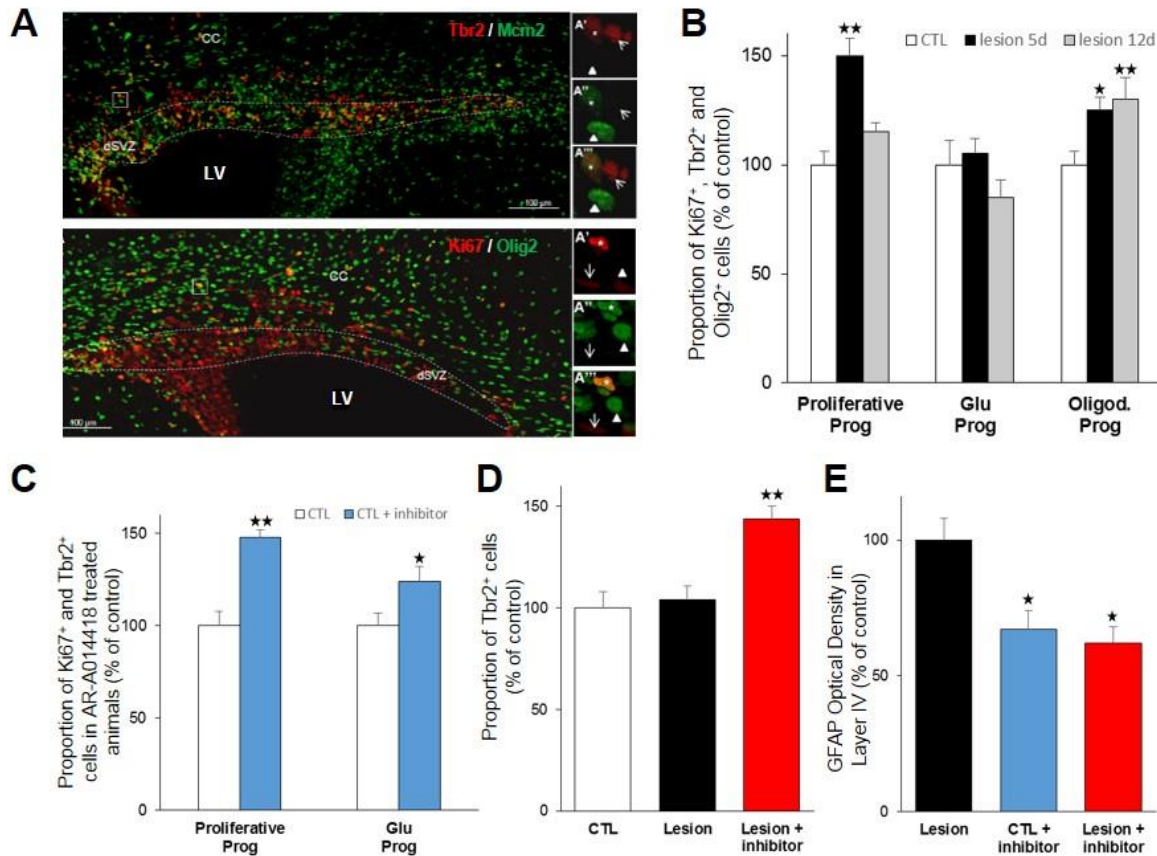


Figure 20: Targeted cortical ablation induces progenitor responses within the dSVZ. (A) Representative pictures of Tbr2 (red, top panel), Ki67 (red, bottom panel) and Olig2 (green, bottom panel) immunostaining in the dSVZ, 5 days post-ablation. (B) Histograms showing the proportion of Ki67⁺, Tbr2⁺ and Olig2⁺ cells 5 days and 12 days following ablation induction, relative to control animals. The relative numbers of proliferative progenitors (Ki67⁺) and oligodendrocyte progenitors (Olig2⁺) increase at 5 days, whereas only the Olig2⁺ increase persists at 12 days. The relative number of glutamatergic progenitor (Tbr2⁺) do not vary at any time points. (C) Administration of AR-A014418 in control animal efficiently increases the relative proportion of Ki67⁺ and Tbr2⁺ cells 5 days post-treatment, as previously described (see **experimental chapter 2**; Azim et al. 2014), thereby validating the pharmacological Wnt-signaling pathway activation. (D) Histogram showing the efficient increase of Tbr2⁺ progenitor following DT injection and AR-A014418 administration. (E) Histograms of GFAP optical density within the cortical lesion site reveal a significant decrease in GFAP⁺ reactive astrogliosis following AR-A014418 treatment, indicating a potential effect on tissue inflammation.

ANNEXES

5. Annexes

Annex 1: R Script To Run HeatMaps Generator Software Related to Figure 8 and S1

```
# library("stringr", lib.loc="/usr/local/lib/R/site-library")
## source("http://bioconductor.org/biocLite.R")
## biocLite("affy")
## biocLite("oligo")
## biocLite("limma")
library(oligo)
library(affy)
library(stringr)
library(pheatmap)
library(stringr)
library(gplots)
library(GEOquery)
library(mouse4302.db)
library(R.utils)
library(affyio)
# install.packages("/home/affxparser_1.48.0.tar.gz", repos = NULL, type="source")
# install.packages("/home/xps_1.36.1.tar.gz", repos = NULL, type="source")

##### Define Genes :

# setwd("~/Desktop/Quentin/heatmaps sur GEO gsm/")
setwd("./")
pathex = getwd()

for(w in list.files("./DataSet/")){ # Loop on file name
  # w = list.files("./DataSet/")[1]
  setwd(pathex)
  inputf = read.csv(paste0("./DataSet/",w)) # Open a dataset file containing GSM
  ### checker :
  # colnames(inputf)
  # list.dirs()
  # dir.create(paste0("./",str_split_fixed(w,".csv",2)[1]))
  # setwd(paste0("./",str_split_fixed(w,".csv",2)[1]))
  for(o in 1:dim(inputf)[2]){ ## Loop on column number
    # o = 1
    setwd(pathex)
    setwd("./temp/")
    file.remove(list.files())
    setwd("../GSM/")
    # setwd(paste0("./",str_split_fixed(w,".csv",2)[1]))
    # dir.create(paste0("./",colnames(inputf)[o]))
    # setwd(paste0("./",colnames(inputf)[o]))
    for(i in as.character(inputf[,o])){
      # i = as.character(inputf[,o])[1]
      if(nchar(i)!=0){ # If there is no empty GSM
```

```

        if(!(paste0(i,".CEL") %in% list.files())) || (paste0(i,".CEL") %in%
str_split_fixed(list.files(),"_",2)[,1])){ ## If file already here, no download
        # getGEOSuppFiles(i,makeDirectory = F)

        try(getGEOSuppFiles(i,makeDirectory = F))

        # Check file names with too many letters, select them and rename them as
        GSMxxxxxxx, looping if several
        if(length(list.files()[which(nchar(list.files())>14)])>0){
        for(s in 1:length(list.files()[which(nchar(list.files())>14)])){
        file.rename(list.files()[which(nchar(list.files())>14)][s]
        paste0(str_split_fixed(list.files()[which(nchar(list.files())>14)][s],"_",2)[1],".CEL.gz"))
        }
        }

        # gunzip(paste0(i,".CEL.gz"))
        system(paste0("gunzip ",paste0(i,".CEL.gz")))

        if (!(paste0(i,".CEL") %in% list.files())){ # If download fails, do it again
        try(getGEOSuppFiles(i,makeDirectory = F))

        # Check file names with too many letters, select them and rename them as
        GSMxxxxxxx, looping if several
        if(length(list.files()[which(nchar(list.files())>14)])>0){
        for(s in 1:length(list.files()[which(nchar(list.files())>14)])){
        file.rename(list.files()[which(nchar(list.files())>14)][s]
        paste0(str_split_fixed(list.files()[which(nchar(list.files())>14)][s],"_",2)[1],".CEL.gz"))
        }
        }
        # gunzip(paste0(i,".CEL.gz"))
        system(paste0("gunzip ",paste0(i,".CEL.gz")))
        }

        if(!(paste0(i,".CEL") %in% list.files())){ # If download still fails, error message
        cat("ERROR GSM not Downloaded : ")
        cat(i)
        cat(" \n")
        }

        #
        downl
        paste0("ftp://ftp.ncbi.nlm.nih.gov/geo/samples/",str_sub(i,1,6),"nnn/",i,"/suppl/",i,"%2ECE
L%2Egz")
        # download.file(downl,destfile = paste0("./",i,".CEL.gz")) #download files matching
        GSM
        }}

        system(paste0("gunzip ",paste0(i,".CEL.gz")))
        # gunzip(paste0(i,".CEL.gz"))
        file.copy(paste0(i,".CEL"),"./temp/")

    }

    setwd("../temp/")

```

```

# Read in the CEL files in the directory, then normalize the data
data=ReadAffy()
eset <- affy::rma(data,verbose = T)
data2 = eset @assayData$exprs

if(data@cdfName!="Mouse430_2"){
  cat("ERROR WITH GENE NAMES")
  print("ERROR WITH GENE NAMES")
}
# library("annotate")
# library("mouse4302.db", lib.loc=~ /R/x86_64-pc-linux-gnu-library/3.3")
# biocLite("mouse4302.db")
# Affymetrix Mouse Genome 430 2.0 Array annotation data (chip mouse4302)
# Verify that experiments match chip
setwd("../tables/")
if(! (paste0(colnames(inputf)[o], ".csv") %in%
list.files(paste0("../",str_split_fixed(w, ".csv",2)[1]))){
  # Test if exit table exists
  dir.create(paste0("../",str_split_fixed(w, ".csv",2)[1]))
  setwd(paste0("../",str_split_fixed(w, ".csv",2)[1]))

  namesreplace = select(mouse4302.db,rownames(data2),"SYMBOL")
  namesnondoublets = NULL
  for(i in rownames(data2)){
    namesnondoublets =
c(namesnondoublets,namesreplace[which(namesreplace$PROBEID == i)[1,2])
  }
  rownames(data2)<-namesnondoublets ## Warning : generate nbers and not names

  colnames(data2)<-
str_c(paste0(colnames(inputf)[o], "_"),as.character(1:dim(data2)[2]))
  # columns(mouse4302.db)
  write.csv(data2,paste0("../",colnames(inputf)[o], ".csv"))
}

}##End of the loop on columns
# load the affy library

## Normalize experiments
setwd(paste0("../",str_split_fixed(w, ".csv",2)[1]))
dir.create("../TablesPurif/")
tablestab = list.files(paste0("../",str_split_fixed(w, ".csv",2)[1],"/"),pattern =
".csv",include.dirs = T)
for(i in tablestab){ #lecture des tableaux crÃ©Ã©s
  # i = tablestab[1]
  if(! (i %in% list.files("../TablesPurif/"))){ # Test if file already exists
    a = read.csv(paste0("../",i))
    a = na.omit(a)

    for(z in unique(as.character(read.csv(paste0(".././genes/",w),header = F)$V1))){ #loop
on gene names
      # z = "Tcf"
      if(z %in% a[,1]){ # check if gene already exist

```

```

if(length(which(a$X == z))!=1){ ## test if genes already exist
  if(dim(a)[2]>2){
    temp = rowMeans(a[which(a$X == z),-1]) # Mean of gene expression
    names(temp) = which(a$X == z)
    indice = which(temp==max(temp)) # indice to keep, max value of the gene

    # temp = a[which(a$X == z),]
    if(length(indice)>1){# If two have same mean
      indice=indice[1]
    }
    a = a[-c(as.integer(names(temp))[-indice]),] ## remove doublet lines excluding the
    indice to keep

  }else{ # if table has one cell :
    temp = (a[which(a$X == z),-1]) # mean of gene expression
    names(temp) = which(a$X == z)
    indice = which(temp==max(temp)) # indice to keep, max value for this gene

    # temp = a[which(a$X == z),]
    if(length(indice)>1){# If two have same mean
      indice=indice[1]
    }
    a = a[-c(as.integer(names(temp))[-indice]),] ## remove doublet lines excluding the
    indice to keep
    # cat("\n#####",z,"#####\n")
    # cat("\n#####",dim(a),"#####\n")
  }
}
}
}
}
# a[which(a$X==unique(as.character(read.csv(paste0("../genes/",w),header =
F)$V1))),]
akeep=NULL
for(b in unique(as.character(read.csv(paste0("../genes/",w),header = F)$V1))){ #
loop on gene name of current table
  akeep = c(akeep,which(a$X == b))
}
a<-a[akeep,]
rownames(a)<-a$X
write.csv(a,paste0("../TablesPurif/",i))

}
}
}
ListGenes=
as.character(read.csv(paste0("../genes/",str_split_fixed(w,".csv",2)[1],".csv"),header =
F)[, 1])
# ListGenes
c("Hdac2","Emx1","Hopx","Gfap","Slc39a12","Aqp4","Slc14a1","2900052N01Rik","Chrdl1",
"Aldh1a1","S100b","2900052N01Rik-
203","Ttr","Ddn","Hpcal4","Scn4b","Syndig1l","Rasd2","Rasgef1a","Camk2a","Ernmn","Mal",
"Mog","Mobp","")

## Experiments list consitent with inputf table
setwd("../TablesPurif/")

```

```

experiences = str_c("../",colnames(inputf),".csv")

#                               ListGenes                               =
c("Neurod6","Eomes","Neurod1","Zic1","Zic5","Tbr1","Hopx","Dmrta2","Tfap2c","Neurog2")
)
results = c(1:length(ListGenes)) # initializing result
namescol = NULL
for(j in experiences){ # loop on table and combine results
  fic = read.csv(j,row.names = c(1))
  results = cbind(resultats,fic[ListGenes,-1])
  namescol=c(namescol,colnames(fic)[-1])
}

results = results[,-1] # Remove unwanted columns
colnames(results)<-namescol # cell identification of the table

results = na.omit(results)

jpeg(paste0("../..../",str_split_fixed(w,".csv",2)[1],"_heatmap.jpeg"),width = 1000,height
= 1000)
pheatmap(as.matrix(results),
  Rowv=NULL,
  Colv=NULL,
  col=redgreen(256),
  labRow="" ,border_color = "black",scale = "row",clustering_distance_cols =
'correlation')
dev.off()
}

```

Annex 2: R Scripts Used for Meta-Analysis of E17.5 Hopx Expressing RGCs. Related to Figure 12

Raw data :

1. Read counts are available in the supplementary information of Yuzwa et al. 2017
2. Astrocyte markers are available in supplementary information of Zywitza et al.

I used the R Seurat package (V2.3) for unbiased clustering and gene expression analysis

t-SNE Generation Related to Figure 12A.

```
library(Seurat)
library(dplyr)
setwd("D:/Yuzwa")

#####E15.5#####
# Load the dataset E15.5
yuzwaE15.data =
read.table("GSE107122_E155_Combined_Only_Cortical_Cells_DGE.csv", sep="," ,
header = TRUE, row.names = 1)
yuzwaE15_seurat = CreateSeuratObject(raw.data = yuzwaE15.data, min.cells = 2,
min.genes = 100, project = "YuzwaE15.5", names.field = 1)
yuzwaE15_seurat <- NormalizeData(object = yuzwaE15_seurat, normalization.method =
"LogNormalize", scale.factor = 10000)
yuzwaE15_seurat <- FindVariableGenes(yuzwaE15_seurat ,mean.function = ExpMean,
dispersion.function = LogVMR, x.low.cutoff = 0.0125, x.high.cutoff = 5, y.cutoff = 1.5)
length(yuzwaE15_seurat@var.genes)
yuzwaE15_seurat <- ScaleData(object = yuzwaE15_seurat, vars.to.regress = NULL)
yuzwaE15_seurat <- RunPCA(yuzwaE15_seurat, pc.genes =
yuzwaE15_seurat@var.genes, do.print = FALSE)
PCAPlot(object = yuzwaE15_seurat, dim.1 = 1, dim.2 = 2)
yuzwaE15_seurat <- JackStraw(object = yuzwaE15_seurat, num.replicate = 100,
display.progress = FALSE)
JackStrawPlot(yuzwaE15_seurat, PCs = 1:12)
yuzwaE15_seurat <- RunTSNE(yuzwaE15_seurat, dims.use = 1:12, do.fast = TRUE,
perplexity = 30)
TSNEPlot(yuzwaE15_seurat, do.label = FALSE, pt.size = 4)
yuzwaE15_seurat = SetAllIdent(yuzwaE15_seurat, "orig.ident")
pt.size = 3, reduction.use = "tsne")
FeaturePlot(yuzwaE15_seurat, "Sox2", pt.size = 5, cols.use = c("grey", "red"))

#####E17.5#####
# Load the dataset E17.5
yuzwaE17.data = read.table("GSM2861514_E175_Only_Cortical_Cells_DGE.csv",
sep="," , header = TRUE, row.names = 1)
yuzwaE17_seurat = CreateSeuratObject(raw.data = yuzwaE17.data, min.cells = 2,
min.genes = 100, project = "YuzwaE17.5", names.field = 1)
yuzwaE17_seurat <- NormalizeData(object = yuzwaE17_seurat, normalization.method =
"LogNormalize", scale.factor = 10000)
yuzwaE17_seurat <- FindVariableGenes(yuzwaE17_seurat ,mean.function = ExpMean,
dispersion.function = LogVMR, x.low.cutoff = 0.0125, x.high.cutoff = 5, y.cutoff = 1.8)
```



```

length(yuzwaE17_seurat@var.genes)
yuzwaE17_seurat <- ScaleData(object = yuzwaE17_seurat, vars.to.regress = NULL)
yuzwaE17_seurat <- RunPCA(yuzwaE17_seurat, pc.genes =
yuzwaE17_seurat@var.genes, do.print = FALSE)
PCAPlot(object = yuzwaE17_seurat, dim.1 = 1, dim.2 = 2)
yuzwaE17_seurat <- JackStraw(object = yuzwaE17_seurat, num.replicate = 100,
display.progress = FALSE)
JackStrawPlot(yuzwaE17_seurat, PCs = 1:12)
yuzwaE17_seurat <- RunTSNE(yuzwaE17_seurat, dims.use = 1:12, do.fast = TRUE,
perplexity = 30)
TSNEPlot(yuzwaE17_seurat, do.label = FALSE, pt.size = 4)
FeaturePlot(yuzwaE17_seurat, "Sox2", pt.size = 5, cols.use = c("grey", "red"))

```

t-SNE Generation on RGCs Related to Figure 12B.

```

yuzwaE15_seurat <- FindClusters(object = yuzwaE15_seurat, reduction.type = "pca",
dims.use = 1:12, resolution = 1.2, print.output = FALSE, save.SNN = TRUE, force.recalc
= TRUE)
TSNEPlot(yuzwaE15_seurat, do.label = FALSE, pt.size = 3)
#RP cells = cluster 4
yuzwaE17_seurat <- FindClusters(object = yuzwaE17_seurat, reduction.type = "pca",
dims.use = 1:12, resolution = 0.5, print.output = FALSE, save.SNN = TRUE, force.recalc
= TRUE)
TSNEPlot(yuzwaE17_seurat, do.label = FALSE, pt.size = 3)
#RP cells = cluster 3

#Analysis only in RGCs
RPE15.cells=WhichCells(yuzwaE15_seurat, 4)
RPE17.cells=WhichCells(yuzwaE17_seurat, 3)

```

#RPE15 vs RPE17

```

yuzwaE15RPcellsRename.data = yuzwaE15.data[,RPE15.cells]
yuzwaE17RPcellsRename.data = yuzwaE17.data[,RPE17.cells]
yuzwaAll.data = cbind(yuzwaE15RPcellsRename.data[row.names(GenesAll),],
yuzwaE17RPcellsRename.data[row.names(GenesAll),])
yuzwaAll_seurat = CreateSeuratObject(raw.data = yuzwaAll.data, min.cells = 0,
min.genes = 100, project = "YuzwaEAll", names.field = 1, names.delim = "_")
yuzwaAll_seurat <- NormalizeData(object = yuzwaAll_seurat, normalization.method =
"LogNormalize", scale.factor = 10000)
yuzwaAll_seurat <- FindVariableGenes(yuzwaAll_seurat ,mean.function = ExpMean,
dispersion.function = LogVMR, x.low.cutoff = 0.0125, x.high.cutoff = 5, y.cutoff = 1.5)
length(yuzwaAll_seurat@var.genes)
yuzwaAll_seurat <- ScaleData(object = yuzwaAll_seurat, vars.to.regress = NULL)
yuzwaAll_seurat <- RunPCA(yuzwaAll_seurat, pc.genes = yuzwaAll_seurat@var.genes,
do.print = FALSE)
PCAPlot(object = yuzwaAll_seurat, dim.1 = 1, dim.2 = 2)
yuzwaAll_seurat <- JackStraw(object = yuzwaAll_seurat, num.replicate = 100,
display.progress = FALSE)
JackStrawPlot(yuzwaAll_seurat, PCs = 1:12)
yuzwaAll_seurat <- RunTSNE(yuzwaAll_seurat, dims.use = 1:12, do.fast = TRUE,
perplexity = 30)

```

```

TSNEPlot(yuzwaAll_seurat, do.label = FALSE, pt.size = 3)
RPE17E15.markers <- FindMarkers(yuzwaAll_seurat, ident.1 = "E17", thresh.use = 0.25,
min.pct = 0.20, test.use = "bimod", only.pos = F)
write.table(RPE17E15.markers, "RPE17E15.markers.csv", sep = ",")

```

t-SNE Generation on E17.5 RGCs with Zywitza Markers Related to Figure 12.

```

##Download first astrocytes markers from Zywitza et al.
AstroGenes.data = read.table("AstroGenes.csv", sep="," , header = TRUE, row.names =
1)
yuzwaZywitza_seurat = CreateSeuratObject(raw.data = yuzwaRPE17.data, min.cells =
2, min.genes = 100, project = "yuzwaZywitza.data", names.field = 1, names.delim = "_")
yuzwaZywitza_seurat <- NormalizeData(object = yuzwaZywitza_seurat,
normalization.method = "LogNormalize", scale.factor = 10000)
yuzwaZywitza_seurat@var.genes = AstroGenes
yuzwaZywitza_seurat <- ScaleData(object = yuzwaZywitza_seurat, vars.to.regress =
NULL)
yuzwaZywitza_seurat <- RunPCA(yuzwaZywitza_seurat, pc.genes =
yuzwaZywitza_seurat@var.genes, do.print = FALSE)
PCAPlot(object = yuzwaZywitza_seurat, dim.1 = 1, dim.2 = 2)
yuzwaZywitza_seurat <- JackStraw(object = yuzwaZywitza_seurat, num.replicate = 100,
display.progress = FALSE)
JackStrawPlot(yuzwaZywitza_seurat, PCs = 1:12)
yuzwaZywitza_seurat <- RunTSNE(yuzwaZywitza_seurat, dims.use = 1:4, do.fast =
TRUE, perplexity = 25)
TSNEPlot(yuzwaZywitza_seurat, do.label = FALSE, pt.size = 3)
FeaturePlot(yuzwaZywitza_seurat, c("Sulf1"), pt.size = 6, cols.use = c("grey", "red"))
##Clustering
yuzwaZywitza_seurat <- FindClusters(object = yuzwaZywitza_seurat, reduction.type =
"pca", dims.use = 1:3, resolution = 1, print.output = FALSE, save.SNN = TRUE,
force.recalc = TRUE)
#Result: cluster 1 = "0"
TSNEPlot(yuzwaZywitza_seurat, do.label = FALSE, pt.size = 6)
##Markers
yuzwaZywitzaE17.markers <- FindMarkers(yuzwaZywitza_seurat, ident.1 = 0, thresh.use
= 0.25, min.pct = 0.20, test.use = "bimod", only.pos = F)
write.table(yuzwaZywitzaE17.markers, "yuzwaZywitzaE17.markers.csv", sep = ",")

FeaturePlot(yuzwaZywitza_seurat, c("Aldh1l1"), pt.size = 6, cols.use = c("grey", "red"))

```

Annex 3: Top Genes Enriched in E17.5 and E15.5 RGCs. Related to Figure 12

Top 200 Genes Enriched in E17.5 RGCs

Name	avg_logFC	Name	avg_logFC	Name	avg_logFC	Name	avg_logFC
Sparcl1	2.33	Mgst1	0.73	Fgfbp3	0.56	ldh1	0.45
Apoe	2.03	Sc4mol	0.73	Chic2	0.55	Ndrp2	0.45
Tnc	1.53	Asrgl1	0.72	Egr1	0.55	Mapt	0.45
Serpine2	1.53	Slc9a3r1	0.72	Cnp	0.55	Fam3c	0.45
Id3	1.49	Insig1	0.72	Acsbg1	0.55	Snx4	0.44
Olig1	1.44	Mid1ip1	0.72	Dbi	0.55	Bhlhb9	0.44
Fabp7	1.36	Clu	0.71	Cltb	0.55	Elovl5	0.44
Rpl26	1.3	Rpl38	0.71	Nim1	0.55	40057	0.44
Cst3	1.28	Smpdl3a	0.7	Nsdhl	0.55	Mageh1	0.44
Mt3	1.27	Hadha	0.69	Scd2	0.54	Sfxn5	0.44
Cpe	1.26	Id1	0.69	Pea15a	0.54	Canx	0.44
Atp1a2	1.25	Sparc	0.69	Hsd17b12	0.54	Vps37a	0.44
Slc4a4	1.23	Wipi1	0.69	Slc39a10	0.54	Cops5	0.44
Ptprz1	1.19	S100a1	0.69	Acot1	0.53	Jkamp	0.44
S100a16	1.17	Lmo4	0.68	Oxr1	0.53	D4Wsu5	0.44
Mlc1	1.17	Lamp1	0.68	Hsd12	0.53	Tpm1	0.44
Slc1a3	1.16	Sc5d	0.67	Vit	0.53	Ptpa	0.43
Lxn	1.15	Vcan	0.67	Fjx1	0.52	Gm10265	0.43
Ednrb	1.1	Qk	0.66	Bmpr1a	0.51	Rabac1	0.43
Ncan	1.04	Tspan7	0.66	Fam172a	0.5	Scg3	0.43
Hes5	1.03	Syt11	0.66	Tm9sf3	0.5	Abcd3	0.43
Cd9	1.01	Ctsl	0.65	Arhgef7	0.5	Tspan3	0.43
Bcan	1.01	Nr2f1	0.65	Pcdh10	0.5	Gpx7	0.42
Cspg5	1	Vegfa	0.65	Abhd4	0.5	Ergic3	0.42
Timp3	0.99	Vcam1	0.64	Pcdhga9	0.49	Snhg9	0.42
Lsmp	0.99	Gabbr1	0.64	App	0.49	Apbb1	0.42
Gstm1	0.98	B2m	0.64	Ctnnbip1	0.49	Specc1	0.42
Scrg1	0.96	Acadl	0.63	Cyb5	0.49	Hbb-bs	0.42
Olig2	0.95	Hmgcr	0.63	Casc4	0.48	Hsd17b4	0.42
Ptn	0.94	Gria2	0.63	Calr	0.48	Trib2	0.41
Mfge8	0.91	Tmem9b	0.63	Tmbim6	0.48	S1pr1	0.41
Slco1c1	0.89	Ntm	0.63	Rab5a	0.48	Anxa2	0.41
Phyhl1	0.88	Cyp51	0.62	Cd47	0.47	Pttg1ip	0.41
Mmd2	0.87	Ppap2b	0.62	P4hb	0.47	Stt3a	0.41
Ntrk2	0.85	Ckb	0.62	Stx4a	0.47	Lfng	0.41
Gng12	0.84	Spry2	0.62	Aldoc	0.47	4931406C	0.41
Aldh1l1	0.83	Crot	0.61	Ribp1	0.47	Lamp2	0.4
Cd81	0.83	Ttyh1	0.61	Clk1	0.46	Rnf13	0.4
Gpm6a	0.82	Dkk3	0.61	Rab6a	0.46	Prnp	0.4
Glul	0.81	Itgb1	0.61	Lrpap1	0.46	Las1l	0.4
Slc15a2	0.79	Csd2	0.61	Meg3	0.46	Spag9	0.4
Gpm6b	0.79	Fos	0.6	Rps3a3	0.46	4833439L	0.4
Fermt2	0.79	Rsu1	0.6	Arl8a	0.46	Ubl3	0.4
Hmgcs1	0.77	Rtn1	0.59	Ptad1	0.46	Tmx3	0.4
Nkain4	0.77	Ctsb	0.59	Aldoa	0.46	Itm2c	0.39
Tubb2a	0.76	Metm	0.58	37500	0.45	Gng3	0.39
Il18	0.74	Fabp5	0.57	Pmm1	0.45	Cdh4	0.39
Phlda1	0.73	Atp1b1	0.57	lgfbp5	0.45	Mest	0.39

Top 200 genes enriched in E15.5 RGCs

Name	avg_logFC	Name	avg_logFC	Name	avg_logFC	Name	avg_logFC
Neurod6	-1.32	Dek	-0.62	Zfp553	-0.54	Cdc5l	-0.49
Ube2c	-1.27	Eif4a1	-0.62	Cks1b	-0.54	H1f0	-0.49
Igfbpl1	-1.17	Tcf4	-0.62	Dnajc9	-0.54	Pax6	-0.49
Top2a	-1.11	Hirip3	-0.61	Incenp	-0.54	Mex3a	-0.48
Gm8420	-1.08	Esco2	-0.61	Smc6	-0.54	Bod1l	-0.48
Neurog2	-1.07	Tox3	-0.61	Hells	-0.53	Fkbp3	-0.48
Lig1	-1.06	Emx1	-0.61	Kif20b	-0.53	Anp32b	-0.48
Hmgb2	-1.02	Tpx2	-0.61	Lhx2	-0.53	Tsen15	-0.48
Hist1h2al	-1.02	Ppp1r7	-0.61	Supt16	-0.53	Gm9493	-0.48
Prc1	-0.92	Sgol2	-0.61	Dnph1	-0.53	Mad2l1	-0.48
Cwc22	-0.91	Smarcc1	-0.60	Cenpe	-0.53	Elavl4	-0.48
Cenpf	-0.88	Nmral1	-0.60	Smc4	-0.52	Ppa1	-0.48
Ckap2l	-0.87	Elavl2	-0.60	Pcbp2	-0.52	Psmd7	-0.48
Cenpa	-0.87	Pou3f2	-0.60	Magoh	-0.52	Dazap1	-0.47
Mpped2	-0.84	Syne2	-0.60	Pcnp	-0.52	Chaf1a	-0.47
Cdc20	-0.83	Hsp90aa	-0.59	Srsf7	-0.52	Elavl3	-0.47
2810417f	-0.83	Fen1	-0.59	Tpr	-0.52	Rsf1	-0.47
Nusap1	-0.80	Ccna2	-0.59	Atrx	-0.52	Ssb	-0.47
Kif23	-0.79	Usp1	-0.59	Ccnb1	-0.52	Mms22l	-0.47
Racgap1	-0.77	Siva1	-0.59	Pold2	-0.52	Ivns1abp	-0.47
Rrm2	-0.76	Tyms	-0.59	Trim59	-0.51	Tenm4	-0.47
Eomes	-0.75	Cdca8	-0.59	Gm4204	-0.51	Plxna2	-0.47
Tuba1b	-0.73	Grb10	-0.58	Kmt2a	-0.51	Rp9	-0.47
Birc5	-0.72	Trim2	-0.58	Wbp5	-0.51	Snrpb2	-0.47
Ezh2	-0.71	Srsf10	-0.58	Trove2	-0.51	Rnaseh2a	-0.47
Cbx1	-0.70	Pkm	-0.57	Coprs	-0.51	G2e3	-0.47
Hmgb3	-0.70	Mdk	-0.57	Fbxo5	-0.51	Timm17a	-0.47
Cdca3	-0.69	Tcerg1	-0.57	Kif5c	-0.50	Hnrnpf	-0.47
Cdca7	-0.69	Gm6104	-0.57	3110039M	-0.50	Meis2	-0.47
Kif15	-0.69	Fezf2	-0.57	Epha4	-0.50	Ewsr1	-0.46
Ezr	-0.68	Ranbp1	-0.57	Mycn	-0.50	Cenpw	-0.46
Suz12	-0.67	Pbk	-0.57	Gm17087	-0.50	Pcna	-0.46
Cenph	-0.67	Clspn	-0.56	RP23-45c	-0.50	Ckap2	-0.46
Ppil1	-0.66	Mcm7	-0.56	Clic4	-0.50	Kdm1a	-0.46
Mki67	-0.66	Tubb5	-0.56	Psip1	-0.50	Ywhaq	-0.46
Tsn	-0.65	Psmc6	-0.56	Csrp2	-0.50	261001710	-0.46
Nsmce4a	-0.65	Ptges3	-0.56	Rcbtb1	-0.50	Spc24	-0.46
Xist	-0.65	Bclaf1	-0.56	Gm10704	-0.50	Psmb5	-0.46
Auts2	-0.65	Mllt3	-0.55	Ubqln2	-0.49	Zfp91	-0.46
H2afx	-0.65	Id4	-0.55	Naa38	-0.49	Snrpa1	-0.46
Lyar	-0.64	G3bp2	-0.55	Kat6b	-0.49	Calm2	-0.46
Spc25	-0.64	Camta1	-0.55	Ift74	-0.49	Mcm4	-0.46
Dut	-0.64	Pdpf	-0.55	Shisa2	-0.49	Bnip3l	-0.46
Bub1	-0.63	Kif22	-0.55	Rfc2	-0.49	Polr3k	-0.45
Hsph1	-0.63	Trim28	-0.54	Zfp326	-0.49	Rfc3	-0.45
Nfib	-0.62	G3bp1	-0.54	Set	-0.49	Ehmt1	-0.45
2700094f	-0.62	Bub3	-0.54	H2afz	-0.49	Knstrn	-0.45
Abrac1	-0.62	Map1b	-0.54	Prrc2b	-0.49	Ptbp2	-0.45

Annex 4: Astrocyte Markers From Zywitzka et al. 2018. Figure S4

Name					
Abhd3	Clu	Fermt2	Lmo4	Prodh	Son
Acadl	Cmtm5	Fgfr3	Lsmp	Psap	Sox2
Aco2	Cnn3	Fjx1	Lxn	Ptn	Sox9
Acsbg1	Cox5a	Fut9	Macf1	Ptprz1	Spag9
Acsl3	Cox7b	Fzd2	Mertk	Rabac1	Sparcl1
Acsl6	Cox8a	Gabrb1	Mfge8	Ramp1	Suc1g1
Add3	Cpe	Gclm	Mgll	Rasa2	Tecr
Adk	Crot	Gja1	Mgst1	Rbp1	Timp3
Agpat5	Crym	Gjb6	Mid1ip1	Rcn2	Timp4
Ahcyl1	Cs	Glud1	Mif	Rgcc	Tmco1
Alcam	Cspg5	Glul	Mlc1	Rgs20	Tmed10
Aldoa	Cst3	Gm12892	Mmd2	S100a1	Tmed5
Aldoc	Ctsb	Gm14964	Mpc2	S100a13	Tmem47
Ank2	Cxcl14	Gm37376	Msi2	S100a16	Tmem59
Apoe	Cyb5a	Gm3764	Msmo1	S1pr1	Tmem9b
Appl2	Cyc1	Gnao1	Mt1	Sar1b	Tpi1
Aqp4	Cyp2j9	Gpm6a	Mt2	Saraf	Tprkb
Arhgap5	Dbi	Gpm6b	Mt3	Sat1	Tril
Arl6ip1	Dbx2	Gpr37l1	mt-Nd5	Scg3	Tsc22d3
Asrgl1	Dclk1	Gria2	Myo10	Scrg1	Tsc22d4
Atp1a2	Ddah1	Grina	Myo6	Sdc2	Tspan3
Atp1b1	Ddhd1	Grm3	Ndr2	Sdc4	Tspan7
Atp1b2	Dhrs7	Gstm1	Ndufa12	Sdf2	Ttc14
Atp5b	Dkk3	Gstm5	Ndufc2	Sepp1	Ttyh1
Atp5c1	Dtna	Hacd2	Nkain4	Serinc1	Tubb2a
Atp6v0e	Eci1	Hacd3	Nr2e1	Serpine2	Ugp2
Atraid	Eci2	Hepacam	Nrxn1	Sfxn5	Uqcrc1
AW04773	Ednrb	Hes5	Ntm	Shisa4	Uqcrfs1
Bcan	Elovl5	Hist1h2bc	Ntrk2	Slc15a2	Vcam1
Bmyc	Emc7	Hmgn3	Ntsr2	Slc1a2	Vegfa
Btbd17	Enho	Hsd17b1	Oat	Slc1a3	Vimp
Cadm1	Eno1	Htra1	Omg	Slc25a3	Xist
Cadm2	Etfa	Id2	Pantr1	Slc25a4	
Cd47	Etfb	Id3	Phgdh	Slc25a5	
Cd63	Eva1a	Id4	Phkg1	Slc27a1	
Cd63-ps	Ezr	Il18	Phyhip1	Slc38a3	
Cd81	F3	Itm2b	Pla2g7	Slc39a12	
Chchd10	Fabp5	Itm2c	Plcd4	Slc3a2	
Chmp4b	Fabp7	Ivd	Pmm1	Slc4a4	
Chpt1	Fam107a	Kcnk1	Pnir	Slc6a1	
Chst1	Fam171b	Klf9	Pou3f3	Slc6a11	
Chst2	Fam213a	Lamp2	Ppap2b	Slc7a10	
Cisd1	Fbxo2	Lap3	Prdx1	Slc9a3r1	
Ckb		Laptm4a	Prdx6	Slco1c1	
Cldn10		Ldhd	Prnp	Smpd13a	

Annex 5: List of Genes Differentially Expressed in Clusters 1 and 2. Related to Figure 12

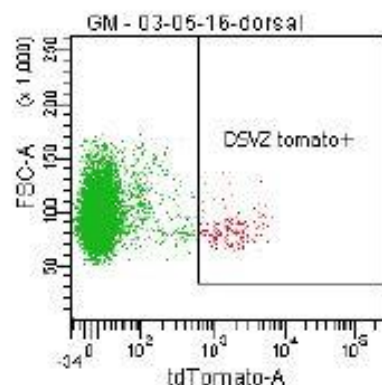
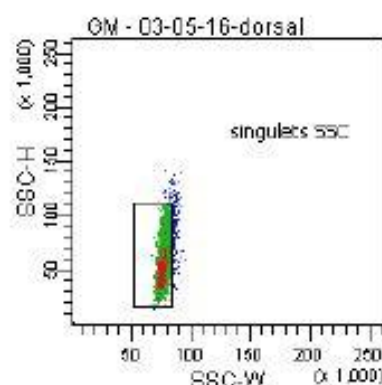
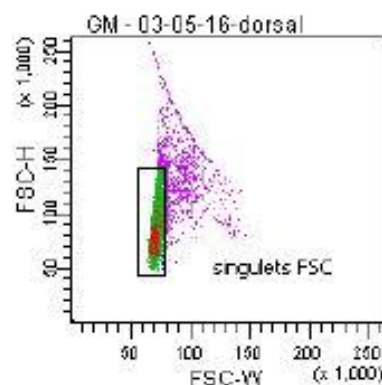
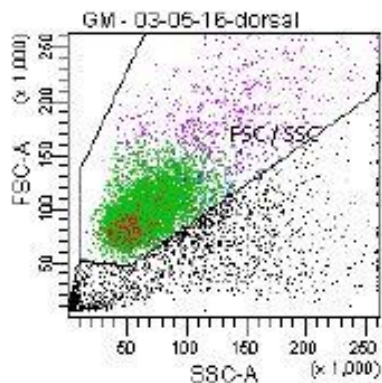
Primed E17.5 RGCs (cluster 1)

Name	avg_logFC	Name	avg_logFC	Name	avg_logFC	Name	avg_logFC	Name	avg_logFC
Apoe	2.029	Atp1a2	0.915	Hmgcs1	0.743	Klf7	0.642	Dtx3	0.578
Slc9a3r1	1.602	Ptpz1	0.914	Plekho1	0.742	Csnk1d	0.641	Aacs	0.578
Lxn	1.570	Clptm1	0.907	Sp3	0.741	Acss1	0.638	1700011J10F	0.577
Smpdl3a	1.530	Hes5	0.901	Dcll1	0.740	Arfrp1	0.637	Camta1	0.576
Slc4a4	1.508	Pdlim4	0.898	Kcnk2	0.739	Cyfp1	0.634	Tbrg1	0.575
Gstm1	1.411	Tmx3	0.892	Sirt2	0.739	Tpp1	0.634	Fads2	0.571
Aldoc	1.393	Hsd12	0.887	Selm	0.735	Nrarp	0.632	Rfc1	0.570
Sparcl1	1.391	Cd9	0.884	Itga6	0.734	Mras	0.631	Ppp1r12a	0.570
Ttyh1	1.384	Dtna	0.882	Nfe2l2	0.732	Vegfa	0.625	Tmem47	0.569
Mt3	1.329	Gpt2	0.881	Ppap2b	0.730	Ufl1	0.624	1810058I24R	0.568
Nkain4	1.301	Micu1	0.879	Uba5	0.727	Rab10	0.621	Fuz	0.567
Mgst1	1.273	Arhgef26	0.876	Asrgl1	0.722	Ostm1	0.619	Cuedc2	0.562
Cpe	1.263	S100a16	0.872	Hepacarr	0.719	Appl2	0.618	Chmp2b	0.561
Cyp51	1.250	Clu	0.872	Acot1	0.712	Trappc2l	0.618	Osgep	0.557
Csdc2	1.237	Ptn	0.863	Dars	0.710	Leprot	0.617	Ppp1r9a	0.557
Psat1	1.219	Pygb	0.863	Suco	0.708	Ctnna2	0.617	Fads1	0.557
Aldh1l1	1.216	Abhd4	0.862	Polr3f	0.706	Magi1	0.616	Faim	0.557
Sc4mol	1.196	Snx4	0.852	Aamdc	0.701	Immt	0.614	Ilk	0.554
Paqr7	1.176	Fgf13	0.847	Tspan13	0.698	Clpp	0.614	Tmem176b	0.553
Slc15a2	1.172	Adhfe1	0.843	Ndr2	0.697	Mier1	0.612	Kcnj10	0.553
Glul	1.166	Trim9	0.831	Ifitm2	0.696	Dbi	0.611	BC031181	0.552
Aqp4	1.163	Glud1	0.830	Pdpn	0.695	Pih1d1	0.611	Tmem167b	0.549
Fgfbp3	1.157	Scg3	0.829	Erp44	0.691	Klf15	0.609	Brnp3l	0.548
Myo6	1.145	Emc3	0.827	Sat1	0.689	Mbnl2	0.608	Glt8d1	0.548
Klf21a	1.131	Alcam	0.827	Rsu1	0.686	Rab9	0.608	Hopx	0.547
Emp2	1.124	Ppp2r2b	0.826	Lrng	0.686	Id1	0.606	Hexb	0.547
Mlc1	1.102	Fmo1	0.826	Gm1775	0.685	Cxadr	0.605	Macf1	0.545
Atp1b2	1.101	Car2	0.824	Zfand2b	0.682	Anxa2	0.605	Prdx3	0.545
Vcan	1.084	Ndufs4	0.820	Smc5	0.682	Crot	0.605	Polb	0.544
Tnc	1.078	Acsbg1	0.807	Stard4	0.678	Ntm	0.604	Magt1	0.542
Ak3	1.072	Kbtbd11	0.805	Mpst	0.674	Mrps28	0.602	4931406C07f	0.542
Cst3	1.063	Timp3	0.804	Larp7	0.670	Lrrc42	0.601	Prkag1	0.541
Fabp7	1.063	Kcne1l	0.800	Malsu1	0.668	Il18	0.596	Thap3	0.541
Id4	1.054	Gpr19	0.800	Cenpc1	0.661	Pmm1	0.596	Plxbn1	0.540
40057.000	1.041	Elovl5	0.796	Grb2	0.661	Tiprl	0.594	Mff	0.540
Fam13c	1.022	Fbln2	0.794	Hsd17b4	0.659	Maf1	0.593	Atp6v1e1	0.537
Med31	1.019	Gdpd2	0.789	Mid1ip1	0.657	Taf7	0.592	Atxn10	0.537
Ncan	1.018	Usf2	0.788	Fxyd6	0.656	Ctsd	0.592	Fam76a	0.536
Prdx6	1.011	Cetn2	0.782	Stoml2	0.656	Mphosph	0.590	Tspan7	0.536
Id3	1.010	Ap3s1	0.782	Htra1	0.655	Fkbp8	0.590	Itm2b	0.532
Cntnap2	1.003	Rhoc	0.781	Nudt16l1	0.647	Eid2b	0.585	Grcc10	0.531
Oat	0.994	Fgfr1	0.780	Nim1	0.647	Pld3	0.585	Polr3h	0.531
Plat	0.991	Plxnc1	0.780	Fjx1	0.646	Camk2n1	0.584	Dcaf8	0.529
Bcan	0.971	Kdelr1	0.778	Klf13	0.646	Pqbp1	0.583	Zcchc18	0.528
Phyhipl	0.967	Plgrkt	0.765	Mapre2	0.646	Tm7sf2	0.583	Aldh2	0.528
Scd2	0.960	Mmp14	0.764	Lgmn	0.646	Nelfcd	0.582	Mpv17	0.526
Slc1a3	0.955	Aldoa	0.764	Lamp2	0.645	Nsdhl	0.582	Golim4	0.525
Vimp	0.946	Cd63	0.763	Gpm6b	0.644	Lman1	0.581	Deb1	0.524
Fstl5	0.923	Npdc1	0.756	Msi2	0.644	Aplp2	0.578	Ccni	0.524

Non Primed E17.5 RGCs (cluster 2)

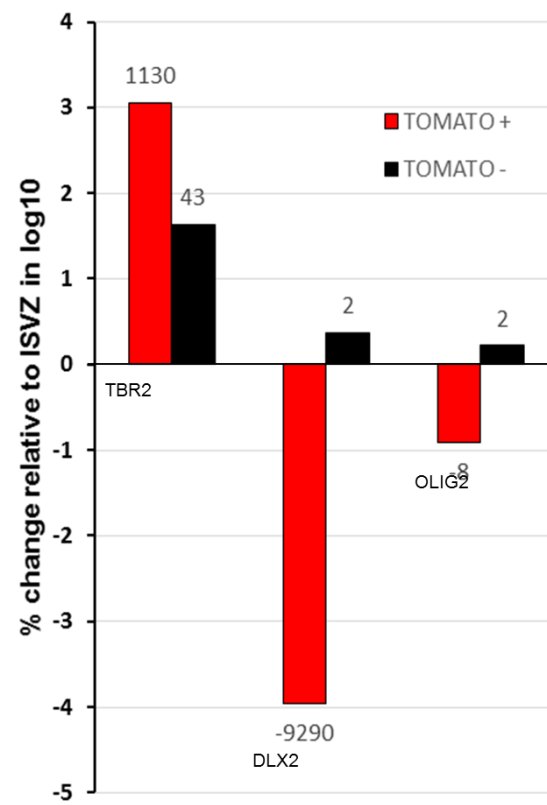
Name	avg_logFC	Name	avg_logFC	Name	avg_logFC	Name	avg_logFC	Name	avg_logFC
Gadd45g	-1.899	Ppp2r2d	-0.695	Fam92a	-0.622	Mcm3	-0.576	Erh	-0.537
Pdgfra	-1.196	Taf1	-0.693	Cops8	-0.621	Nap1l4	-0.573	Hnrnpa3	-0.535
Gnl3	-1.084	Lmnbl1	-0.691	Pthr2	-0.619	Prmt1	-0.573	Atp5j	-0.533
Erb2ip	-1.064	Eny2	-0.687	Tfap2c	-0.618	Hmgbl2	-0.573	Gm10263	-0.533
Tpm1	-1.063	Ubal2	-0.686	Hnrnpm	-0.618	Glyr1	-0.572	Ppil2	-0.533
Lima1	-1.038	Hnrnpab	-0.686	2610017l	-0.617	Ctnnb1	-0.570	Eif3m	-0.532
Gas1	-1.019	Cdon	-0.684	Trp53	-0.617	Cct8	-0.569	Glod4	-0.532
Hes6	-0.988	Rps19	-0.683	Crbn	-0.613	Aimp2	-0.568	Tial1	-0.531
Ppp1r14b	-0.980	Smim7	-0.682	Cox5a	-0.612	Snrnp48	-0.567	Rpp30	-0.530
Ccnd1	-0.973	Akirin2	-0.680	Usp22	-0.608	Eef1d	-0.567	Dek	-0.530
Olig2	-0.945	Rps3	-0.680	Gtf3c6	-0.606	Mthfd1	-0.566	H2afy2	-0.530
Rpl31	-0.903	Gtf2h5	-0.676	Rps26	-0.606	Polr2j	-0.566	Rpl36	-0.530
Smadca5	-0.902	Rplp0	-0.676	Heatr3	-0.606	Yars	-0.565	Trpm7	-0.529
Cdca8	-0.867	Gspt1	-0.675	Rrs1	-0.605	Gars	-0.565	Rplp1	-0.528
Tbl1x	-0.825	Mcm6	-0.674	Nsg2	-0.605	Dctpp1	-0.563	Phlda1	-0.528
Serpine2	-0.819	Pak1ip1	-0.673	Set	-0.604	Denr	-0.561	Got2	-0.527
Dync1li1	-0.812	Chd7	-0.672	Clns1a	-0.604	Gas5	-0.560	Mettl10	-0.527
Cdk2ap1	-0.812	Ddb1	-0.668	Rcor2	-0.603	Pes1	-0.560	Gripap1	-0.527
Ebna1bp2	-0.812	Golm1	-0.668	Nhp2l1	-0.603	Gpx1	-0.560	Elf2	-0.527
Mycn	-0.811	Ascl1	-0.668	Abhd14a	-0.602	Hp1bp3	-0.559	Pa2g4	-0.526
Ddx39	-0.809	Nfix	-0.668	Cct3	-0.602	B3gat2	-0.556	Wdr12	-0.525
Ckap5	-0.808	Ptma	-0.666	Pam	-0.602	Tmsb10	-0.556	Rps21	-0.524
Nop14	-0.800	Xrcc6	-0.665	Nop56	-0.602	Rplp2	-0.553	Atp5f1	-0.523
Nop58	-0.797	Cdca7	-0.662	Dync1h1	-0.601	Cxxc1	-0.553	Adsl	-0.517
Slc7a6os	-0.796	Sfpq	-0.661	Naca	-0.601	Lias	-0.553	Actr1a	-0.517
1700025G04Rik	-0.777	Whsc1	-0.660	Rrm1	-0.600	Ddx52	-0.553	Eef1e1	-0.516
Sf3b2	-0.771	Med4	-0.659	Fam32a	-0.597	Eef1b2	-0.551	mt-Rnr1	-0.514
Serf1	-0.770	1500012f	-0.656	Cd164	-0.596	Mrpl33	-0.550	Pbdc1	-0.514
Lpcat1	-0.759	Eif5b	-0.655	Rbm25	-0.593	Tsnax	-0.550	Hnrnp1	-0.513
Hmgbl1	-0.756	Pttg1	-0.654	Lsm12	-0.593	Hist1h2bc	-0.549	Ptp4a2	-0.513
Ypel3	-0.749	Ddx21	-0.651	Atp5k	-0.591	Ppa1	-0.548	Aplp1	-0.512
Trim28	-0.748	Hint1	-0.650	Gm1027f	-0.589	Ezh2	-0.547	Ranbp3	-0.511
Las1l	-0.747	Bzw1	-0.650	Rpl38	-0.589	Dkc1	-0.547	Stmn3	-0.509
Lig3	-0.744	Kpna4	-0.647	Setd8	-0.588	Rps5	-0.545	Fscn1	-0.508
Ncl	-0.742	Rps26-ps	-0.644	Yme1l1	-0.587	Kif5b	-0.545	Psmc8	-0.507
Rps3a3	-0.736	Hdgf	-0.644	Pou6f1	-0.587	Wdr77	-0.543	Zmynd8	-0.507
Ccar1	-0.733	Eef1a1	-0.643	Ash1l	-0.585	Ankrd11	-0.543	Rps28	-0.507
Paics	-0.725	Zcchc17	-0.635	Miat	-0.584	Clip3	-0.542	Rpl37	-0.507
C1qbp	-0.725	Nol12	-0.635	Uchl5	-0.584	Pcna-ps2	-0.540	Ddx42	-0.506
Eif3e	-0.718	Npm1	-0.634	Tnpo3	-0.584	A430005L	-0.539	Immp1l	-0.506
Midn	-0.717	Hdgfrp3	-0.634	Dpm3	-0.583	Usp10	-0.539	Gm16286	-0.505
Epb4.1	-0.712	Sox4	-0.632	Srrt	-0.583	Gm3940	-0.539	Hnrnpc	-0.505
Ssrp1	-0.712	Tipin	-0.631	Slc25a39	-0.582	Exosc8	-0.538	Asnsd1	-0.505
Olig1	-0.708	Gm1028f	-0.629	Ran	-0.582	Arhgef2	-0.538	Ak2	-0.502
Tle1	-0.707	Mif	-0.628	Pou3f2	-0.579	Mrpl2	-0.537	Lbh	-0.502
Rps11	-0.706	Gm8730	-0.628	Epha4	-0.578	Kpnb1	-0.537	Alyref	-0.502
Eid2	-0.705	Upf3a	-0.627	Sar1b	-0.578	Tcp1	-0.537	Fam50a	-0.501
Smadcc1	-0.701	Gm1007f	-0.626	Ccp110	-0.577	Bzw2	-0.537	Mios	-0.501
Lsm2	-0.700	Snrpe	-0.624	Scpep1	-0.576	Hdac2	-0.537	Snhg5	-0.500

Annex 6: FAC-sorting of Tomato⁺ Glu Progenitors



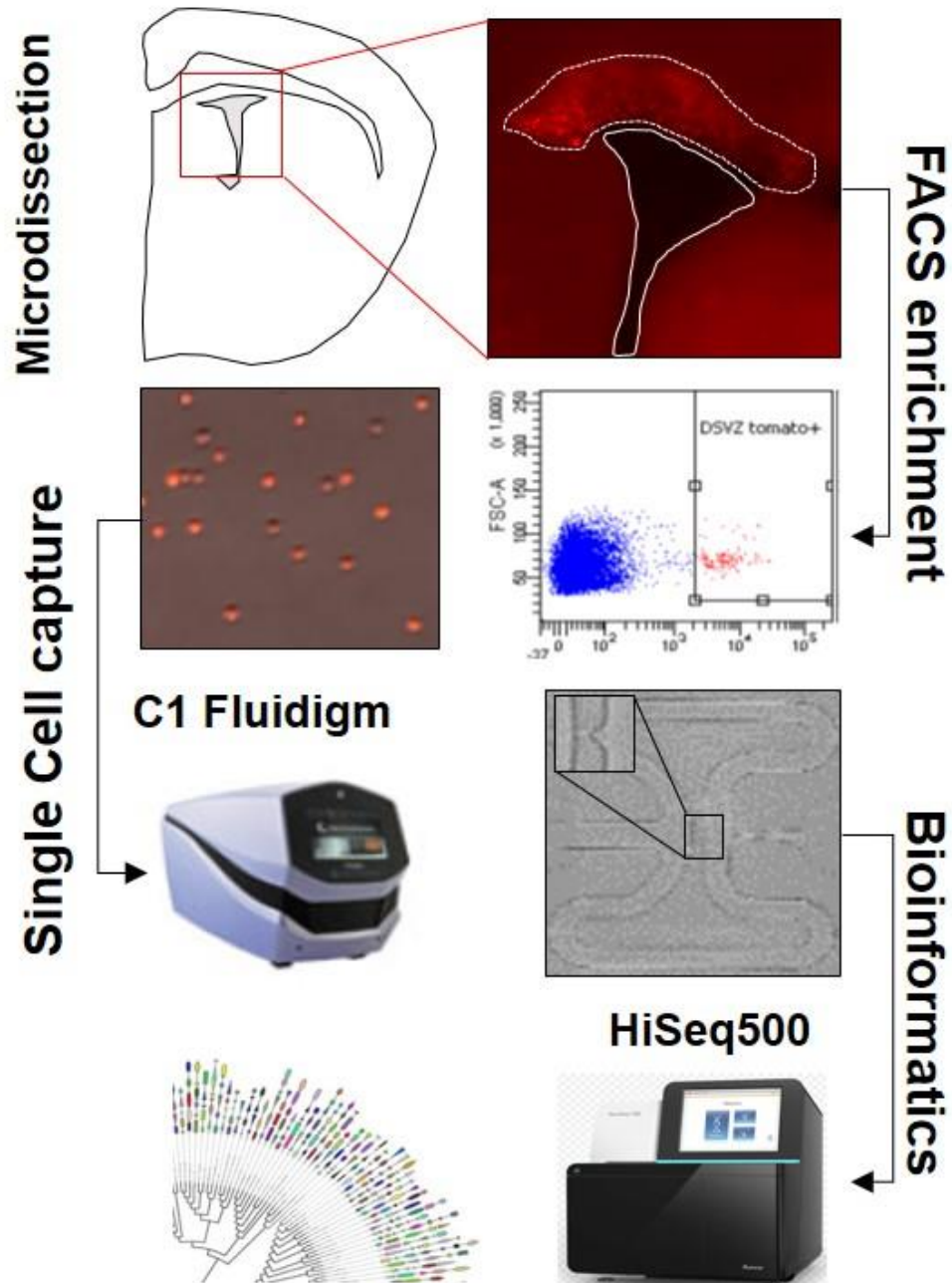
Tube: dorsal			
Population	#Events	%Parent	%Total
All Events	11,769	###	100.0
FSC / SSC	10,000	85.0	85.0
singlets FSC	9,163	91.6	77.9
singlets SSC	9,030	98.5	76.7
DSVZ tomato+	149	1.7	1.3

Annex 7: QPCR Validation of Isolated Tomato⁺ Progenitors



Annex 8: Bioinformatics Pipeline

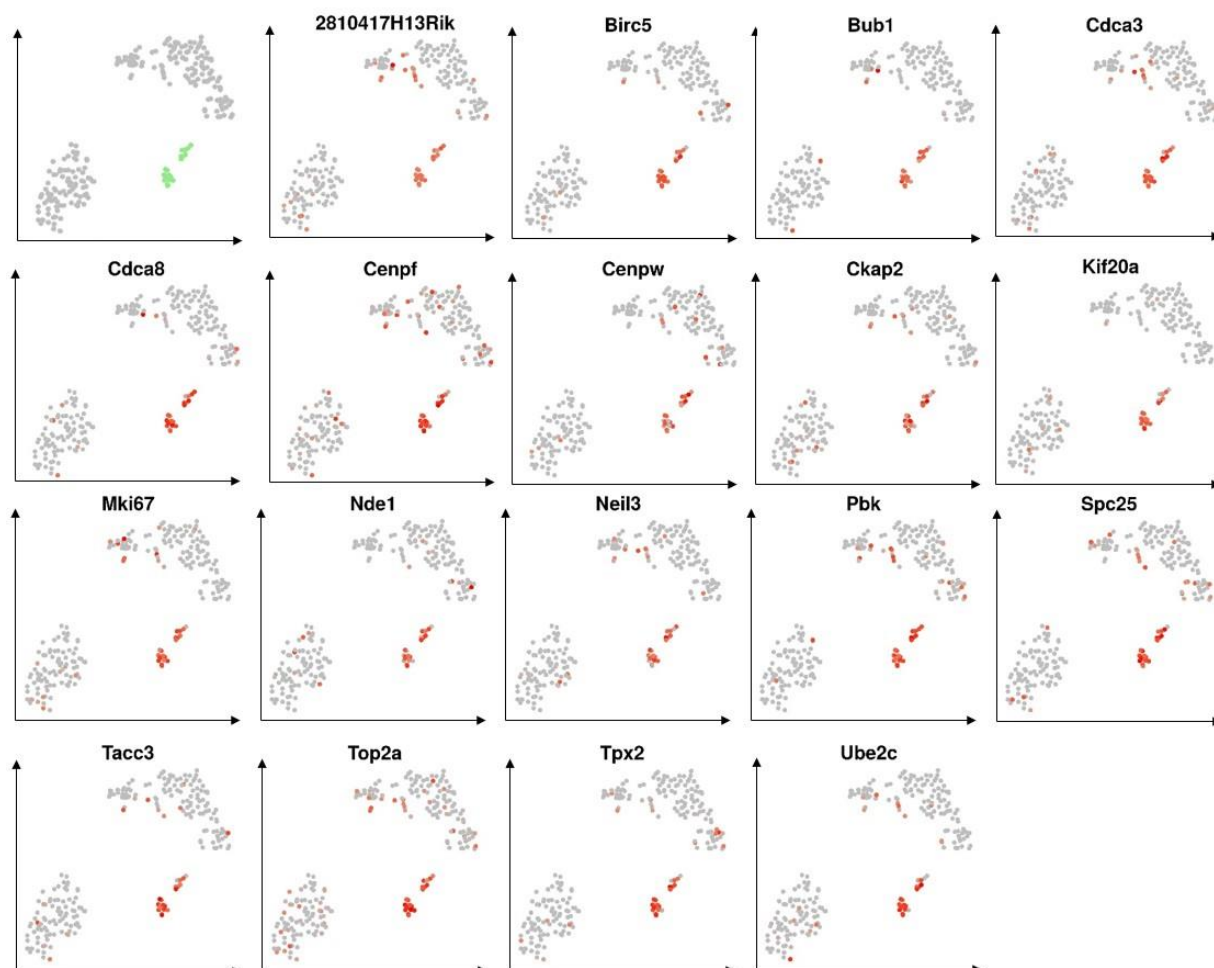
Experimental Workflow



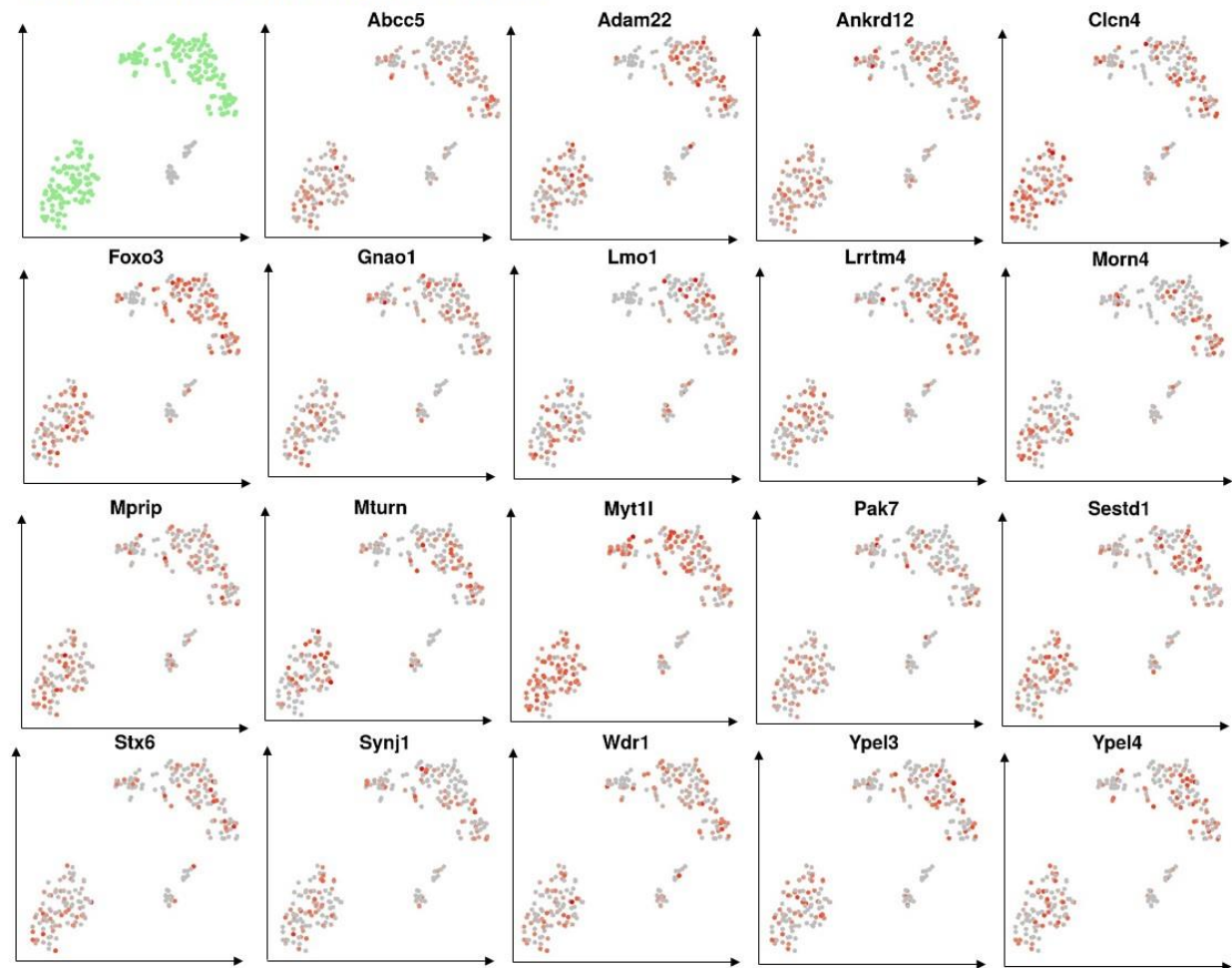
Annex 9: Feature Plots of E15 and P2 progenitors

Generic Progenitor Markers

Generic Progenitor Markers

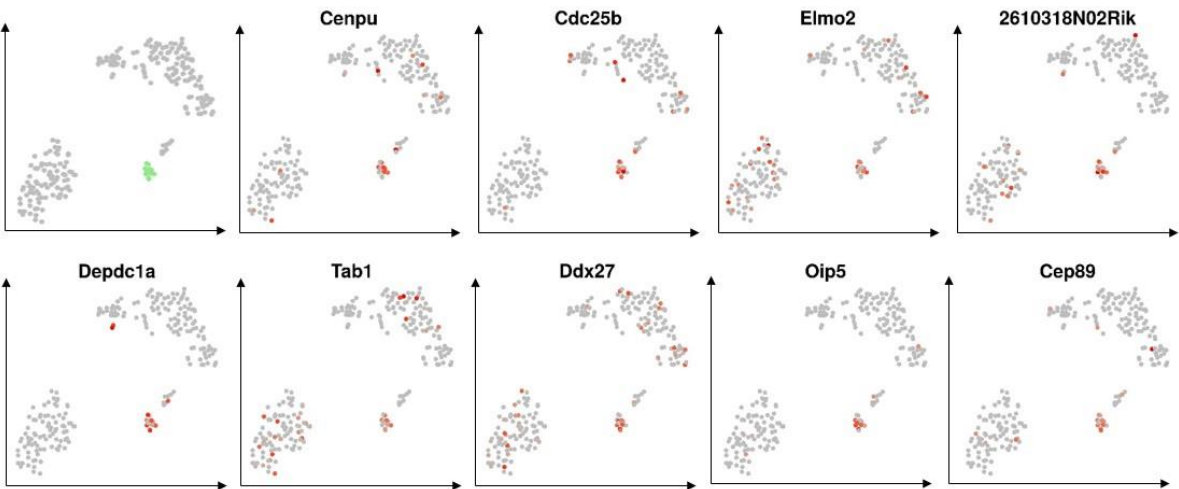


Generic Nascent Neurons Markers

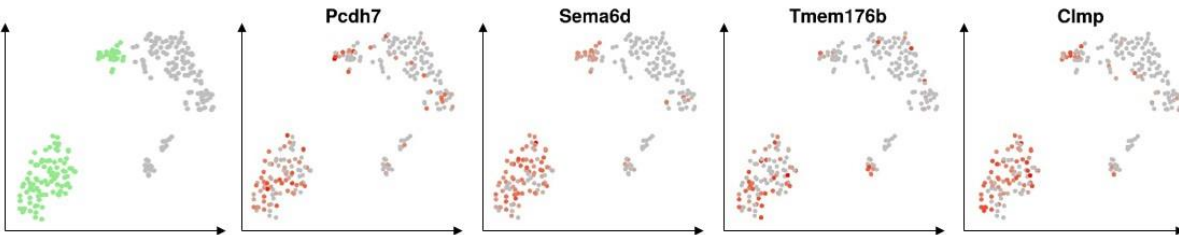


Identity Markers (1)

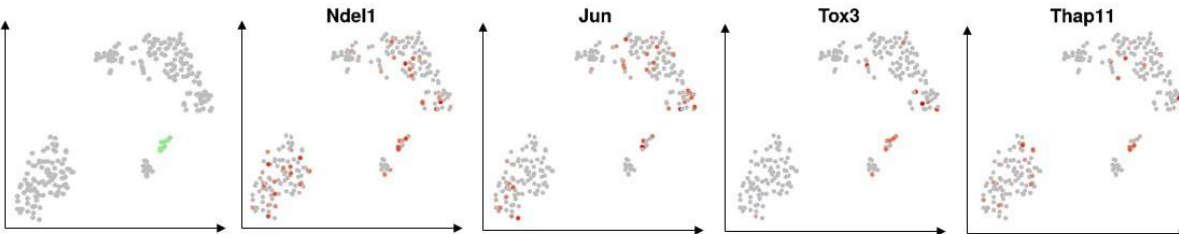
Identity Marker – Glu Progenitors E15



Identity Marker – Nascent Neurons E15



Identity Marker – Glu Progenitors P2

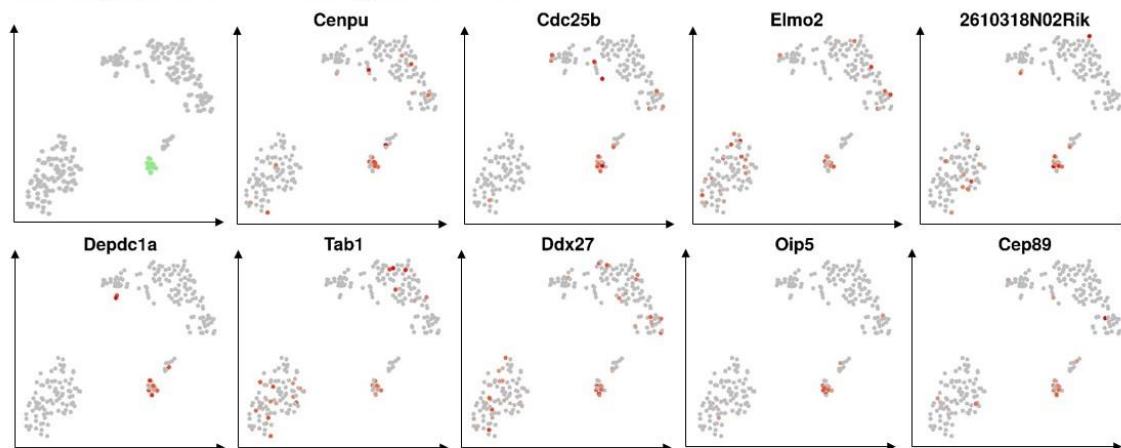


Identity Marker – Nascent Neurons P2

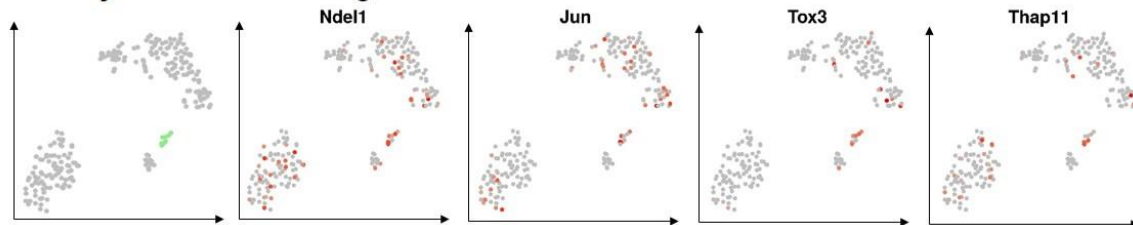


Identity Markers (2)

Identity Marker – *Glu Progenitors E15*

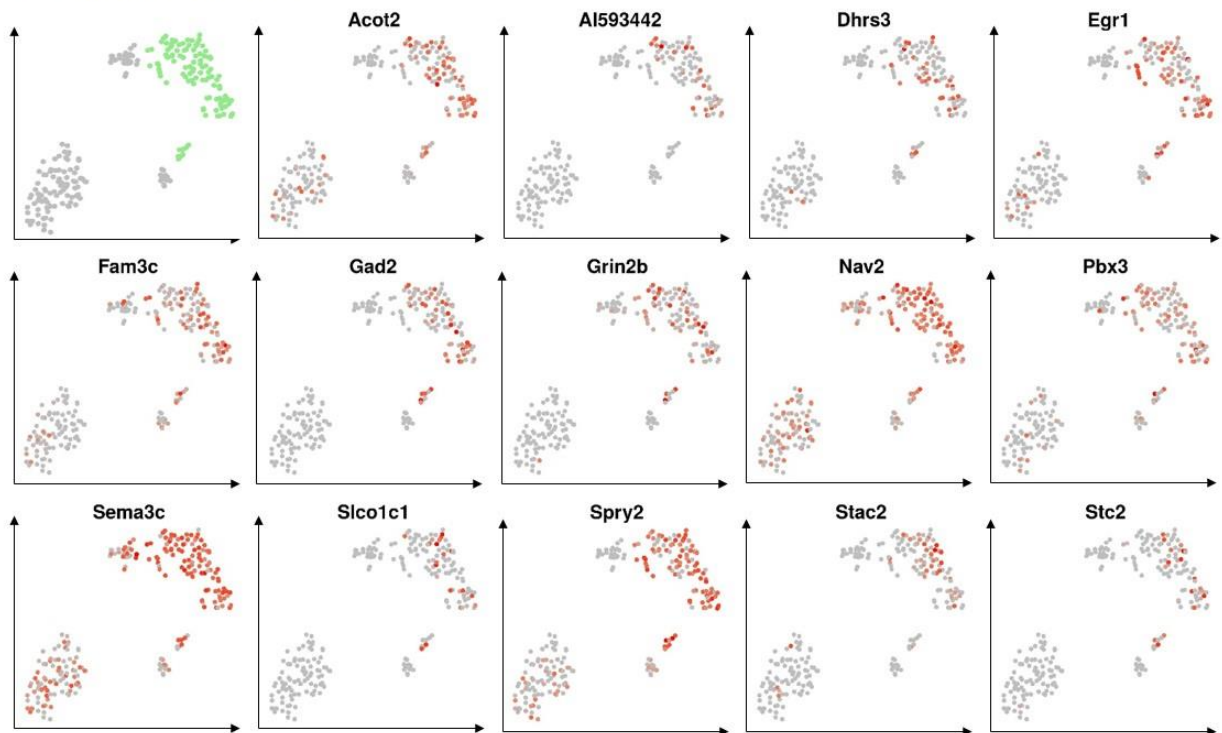


Identity Marker – *Glu Progenitors P2*



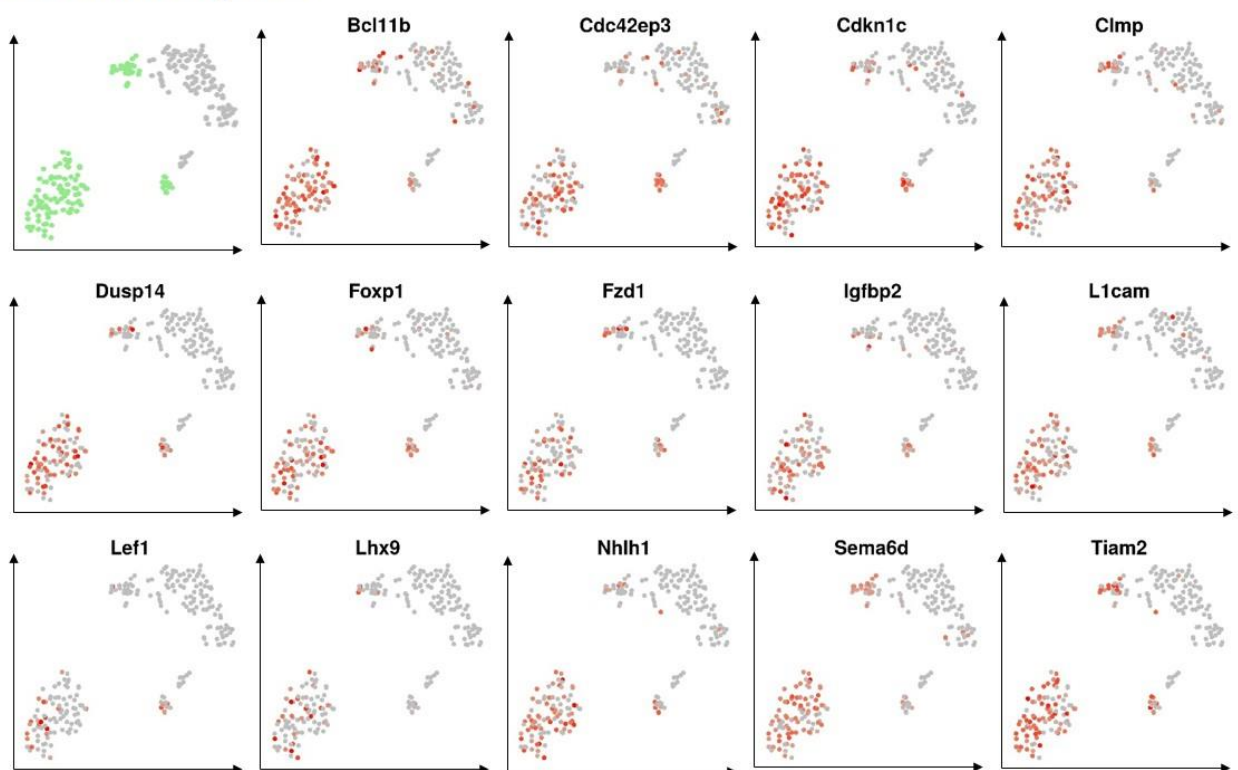
P2 Enriched Genes

P2 enriched genes



E15 Enriched Genes

E15 enriched genes



REFERENCES

6. References

- Agirman G, Broix L, Nguyen L (2017) Cerebral cortex development: an outside-in perspective. *FEBS Lett* 591:3978–3992
- Agoston Z, Heine P, Brill MS, Grebbin BM, Hau A-C, Kallenborn-Gerhardt W, Schramm J, Gotz M, Schulte D (2014) Meis2 is a Pax6 co-factor in neurogenesis and dopaminergic periglomerular fate specification in the adult olfactory bulb. *Development* 141:28–38
- Aguirre A, Rubio ME, Gallo V (2010) Notch and EGFR pathway interaction regulates neural stem cell number and self-renewal. *Nature* 467:323–327.
- Albert M, Huttner WB (2018) Epigenetic and transcriptional pre-patterning-An emerging theme in cortical neurogenesis. *Front Neurosci* 12.
- Alvarez-Buylla A, Kohwi M, Nguyen TM, Merkle FT (2008) The heterogeneity of adult neural stem cells and the emerging complexity of their niche. In: *Cold Spring Harbor Symposia on Quantitative Biology*, pp 357–365.
- Anderson SA, Marín O, Horn C, Jennings K, Rubenstein JL (2001) Distinct cortical migrations from the medial and lateral ganglionic eminences. *Development* 128:353–363
- Angevine JB, Sidman RL (1961) Autoradiographic study of cell migration during histogenesis of cerebral cortex in the mouse. *Nature* 192:766–768
- Arlotta P, Molyneaux BJ, Chen J, Inoue J, Kominami R, MacKlis JD (2005) Neuronal subtype-specific genes that control corticospinal motor neuron development in vivo. *Neuron* 45:207–221.
- Azevedo FAC, Carvalho LRB, Grinberg LT, Farfel JM, Ferretti REL, Leite REP, Filho WJ, Lent R, Herculano-Houzel S (2009) Equal numbers of neuronal and nonneuronal cells make the human brain an isometrically scaled-up primate brain. *J Comp Neurol* 513:532–541.
- Azim K, Angonin D, Marcy G, Pieropan F, Rivera A, Donega V, Cantù C, Williams G, Berninger B, Butt AM, Raineteau O (2017) Pharmacogenomic identification of small molecules for lineage specific manipulation of subventricular zone germinal activity. *PLoS Biol* 15.
- Azim K, Berninger B, Raineteau O (2016) Mosaic subventricular origins of forebrain oligodendrogenesis. *Front Neurosci* 10.
- Azim K, Fiorelli R, Zweifel S, Hurtado-Chong A, Yoshikawa K, Slomianka L, Raineteau O (2012a) 3-Dimensional Examination of the Adult Mouse Subventricular Zone Reveals Lineage-Specific Microdomains. *PLoS One* 7:e49087
- Azim K, Fischer B, Hurtado-Chong A, Draganova K, Cantù C, Zemke M, Sommer L, Butt A, Raineteau O (2014) Persistent Wnt/ β -catenin signaling determines dorsalization of the postnatal subventricular zone and neural stem cell specification into oligodendrocytes and glutamatergic neurons. *Stem Cells* 32:1301–1312
- Azim K, Hurtado-Chong A, Fischer B, Kumar N, Zweifel S, Taylor V, Raineteau O (2015) Transcriptional hallmarks of heterogeneous neural stem cell niches of the subventricular zone. *Stem Cells* 33:2232–2242.
- Azim K, Raineteau O, Butt AM (2012b) Intraventricular injection of FGF-2 promotes generation of oligodendrocyte-lineage cells in the postnatal and adult forebrain. *Glia* 60:1977–1990.

Backman M, Machon O, Mygland L, van den Bout CJ, Zhong W, Taketo MM, Krauss S (2005) Effects of canonical Wnt signaling on dorso-ventral specification of the mouse telencephalon. *Dev Biol* 279:155–168

Baek JH (2006) Persistent and high levels of *Hes1* expression regulate boundary formation in the developing central nervous system. *Development* 133:2467–2476

Bai CB, Auerbach W, Lee JS, Stephen D, Joyner AL (2002) *Gli2*, but not *Gli1*, is required for initial *Shh* signaling and ectopic activation of the *Shh* pathway. *Development* 129:4753–4761

Basak O, Giachino C, Fiorini E, MacDonald HR, Taylor V (2012) Neurogenic Subventricular Zone Stem/Progenitor Cells Are Notch1-Dependent in Their Active But Not Quiescent State. *J Neurosci* 32:5654–5666

Basak O, Taylor V (2007) Identification of self-replicating multipotent progenitors in the embryonic nervous system by high Notch activity and *Hes5* expression. *Eur J Neurosci* 25:1006–1022.

Basak O, Taylor V (2009) Stem cells of the adult mammalian brain and their niche. *Cell Mol Life Sci* 66:1057–1072.

Bauer S, Patterson PH (2006) Leukemia Inhibitory Factor Promotes Neural Stem Cell Self-Renewal in the Adult Brain. *J Neurosci* 26:12089–12099

Beattie R, Postiglione MP, Burnett LE, Laukoter S, Streicher C, Pauler FM, Xiao G, Klezovitch O, Vasioukhin V, Ghashghaei TH, Hippenmeyer S (2017) Mosaic Analysis with Double Markers Reveals Distinct Sequential Functions of *Lgl1* in Neural Stem Cells. *Neuron* 94:517–533.e3.

Beckervordersandforth R, Tripathi P, Ninkovic J, Bayam E, Lepier A, Stempfhuber B, Kirchhoff F, Hirrlinger J, Haslinger A, Lie DC, Beckers J, Yoder B, Irmeler M, Götz M (2010) In vivo fate mapping and expression analysis reveals molecular hallmarks of prospectively isolated adult neural stem cells. *Cell Stem Cell* 7:744–758.

Benner EJ, Luciano D, Jo R, Abdi K, Paez-Gonzalez P, Sheng H, Warner DS, Liu C, Eroglu C, Kuo CT (2013) Protective astrogenesis from the SVZ niche after injury is controlled by Notch modulator *Thbs4*. *Nature* 497:369–373.

Bi B, Salmaso N, Komitova M, Simonini M V., Silbereis J, Cheng E, Kim J, Luft S, Ment LR, Horvath TL, Schwartz ML, Vaccarino FM (2011) Cortical Glial Fibrillary Acidic Protein-Positive Cells Generate Neurons after Perinatal Hypoxic Injury. *J Neurosci* 31:9205–9221

Biran V, Heine VM, Verney C, Sheldon RA, Spadafora R, Vexler ZS, Rowitch DH, Ferriero DM (2011) Cerebellar abnormalities following hypoxia alone compared to hypoxic-ischemic forebrain injury in the developing rat brain. *Neurobiol Dis*.

Borello U, Cobos I, Long JE, Murre C, Rubenstein JLR (2008) FGF15 promotes neurogenesis and opposes FGF8 function during neocortical development. *Neural Dev* 3:17

Bracko O, Singer T, Aigner S, Knobloch M, Winner B, Ray J, Clemenson GD, Suh H, Couillard-Despres S, Aigner L, Gage FH, Jessberger S (2012) Gene Expression Profiling of Neural Stem Cells and Their Neuronal Progeny Reveals IGF2 as a Regulator of Adult Hippocampal Neurogenesis. *J Neurosci* 32:3376–3387

Brill MS, Ninkovic J, Winpenny E, Hodge RD, Ozen I, Yang R, Lepier A, Gascón S, Erdelyi F, Szabo G, Parras C, Guillemot F, Frotscher M, Berninger B, Hevner RF, Raineteau O, Götz M (2009) Adult generation of glutamatergic olfactory bulb interneurons. *Nat Neurosci* 12:1524–1533

- Brill MS, Snapyan M, Wohlfrom H, Ninkovic J, Jawerka M, Mastick GS, Ashery-Padan R, Saghatelian A, Berninger B, Gotz M (2008) A *Dlx2*- and *Pax6*-Dependent Transcriptional Code for Periglomerular Neuron Specification in the Adult Olfactory Bulb. *J Neurosci*.
- Bulfone A, Martinez S, Marigo V, Campanella M, Basile A, Quaderi N, Gattuso C, Rubenstein JLR, Ballabio A (1999) Expression pattern of the *Tbr2* (*Eomesodermin*) gene during mouse and chick brain development. *Mech Dev* 84:133–138.
- Bulfone A, Puelles L, Porteus MH, Frohman MA, Martin GR, Rubenstein JLR (1993) Spatially restricted expression of *Dlx-1*, *Dlx-2* (*Tes-1*), *Gbx-2*, and *Wnt-3* in the embryonic day 12.5 mouse forebrain defines potential transverse and longitudinal segmental boundaries. *J Neurosci* 13:3155–3172.
- Bulfone A, Smiga SM, Shimamura K, Peterson A, Puelles L, Rubenstein JLR (1995) *T-Brain-1*: A homolog of *Brachyury* whose expression defines molecularly distinct domains within the cerebral cortex. *Neuron* 15:63–78.
- Butt SJB, Fuccillo M, Nery S, Noctor S, Kriegstein A, Corbin JG, Fishell G (2005) The temporal and spatial origins of cortical interneurons predict their physiological subtype. *Neuron* 48:591–604.
- Cadigan KM (2012) TCFs and Wnt/ β -catenin Signaling. More than One Way to Throw the Switch. In: *Current Topics in Developmental Biology*, pp 1–34
- Cahoy JD, Emery B, Kaushal A, Foo LC, Zamanian JL, Christopherson KS, Xing Y, Lubischer JL, Krieg PA, Krupenko SA, Thompson WJ, Barres BA (2008) A Transcriptome Database for Astrocytes, Neurons, and Oligodendrocytes: A New Resource for Understanding Brain Development and Function. *J Neurosci* 28:264–278
- Calzolari F, Michel J, Baumgart EV, Theis F, Götz M, Ninkovic J (2015) Fast clonal expansion and limited neural stem cell self-renewal in the adult subependymal zone. *Nat Neurosci* 18:490–492.
- Capela A, Temple S (2002) *LeX/ssea-1* is expressed by adult mouse CNS stem cells, identifying them as nonependymal. *Neuron* 35:865–875.
- Caronia-Brown G, Yoshida M, Gulden F, Assimacopoulos S, Grove EA (2014) The cortical hem regulates the size and patterning of neocortex. *Development* 141:2855–2865
- Casarosa S, Fode C, Guillemot F (1999) *Mash1* regulates neurogenesis in the ventral telencephalon. *Development* 126:525–534.
- Cecchi GA, Petreanu LT, Alvarez-Buylla A, Magnasco MO (2001) Unsupervised learning and adaptation in a model of adult neurogenesis. *J Comput Neurosci* 11:175–182.
- Cederquist GY, Azim E, Shnyder SJ, Padmanabhan H, Macklis JD (2013) *Lmo4* Establishes Rostral Motor Cortex Projection Neuron Subtype Diversity. *J Neurosci* 33:6321–6332
- Chambers CB, Peng Y, Nguyen H, Gaiano N, Fishell G, Nye JS (2001) Spatiotemporal selectivity of response to *Notch1* signals in mammalian forebrain precursors. *Development* 128:689–702
- Chavali M, Klingener M, Kokkosis AG, Garkun Y, Felong S, Maffei A, Aguirre A (2018) Non-canonical Wnt signaling regulates neural stem cell quiescence during homeostasis and after demyelination. *Nat Commun* 9:36

- Chen EY, Tan CM, Kou Y, Duan Q, Wang Z, Meirelles G V., Clark NR, Ma'ayan A (2013) Enrichr: Interactive and collaborative HTML5 gene list enrichment analysis tool. *BMC Bioinformatics* 14.
- Chen F, Kook H, Milewski R, Gitler AD, Lu MM, Li J, Nazarian R, Schnepf R, Jen K, Biben C, Runke G, Mackay JP, Novotny J, Schwartz RJ, Harvey RP, Mullins MC, Epstein JA (2002) Hop is an unusual homeobox gene that modulates cardiac development. *Cell* 110:713–723.
- Chev  e M, Robertson JDJ, Cannon GH, Brown SP, Goff LA (2018) Variation in Activity State, Axonal Projection, and Position Define the Transcriptional Identity of Individual Neocortical Projection Neurons. *Cell Rep* 22:441–455.
- Chmielnicki E (2004) Adenovirally Expressed Noggin and Brain-Derived Neurotrophic Factor Cooperate to Induce New Medium Spiny Neurons from Resident Progenitor Cells in the Adult Striatal Ventricular Zone. *J Neurosci* 24:2133–2142
- Codega P, Silva-Vargas V, Paul A, Maldonado-Soto AR, DeLeo AM, Pastrana E, Doetsch F (2014) Prospective Identification and Purification of Quiescent Adult Neural Stem Cells from Their In Vivo Niche. *Neuron* 82:545–559.
- Cohen E, Meininger V (1987) Ultrastructural analysis of primary cilium in the embryonic nervous tissue of mouse. *Int J Dev Neurosci* 5:43–51
- Colak D, Mori T, Brill MS, Pfeifer A, Falk S, Deng C, Monteiro R, Mummery C, Sommer L, Gotz M (2008) Adult Neurogenesis Requires Smad4-Mediated Bone Morphogenic Protein Signaling in Stem Cells. *J Neurosci* 28:434–446
- Daynac M, Pineda JR, Chicheportiche A, Gauthier LR, Morizur L, Boussin FD, Mouthon MA (2014) TGF   lengthens the G1 phase of stem cells in aged mouse brain. *Stem Cells* 32:3257–3265.
- de Chevigny A, Core N, Follert P, Wild S, Bosio A, Yoshikawa K, Cremer H, Beclin C (2012) Dynamic expression of the pro-dopaminergic transcription factors Pax6 and Dlx2 during postnatal olfactory bulb neurogenesis. *Front Cell Neurosci*
- de la Pompa JL, Wakeham A, Correia KM, Samper E, Brown S, Aguilera RJ, Nakano T, Honjo T, Mak TW, Rossant J, Conlon RA (1997) Conservation of the Notch signalling pathway in mammalian neurogenesis. *Development* 124:1139–1148
- De Toni A, Zbinden M, Epstein JA, Altaba ARI, Prochiantz A, Caill   I (2008) Regulation of survival in adult hippocampal and glioblastoma stem cell lineages by the homeodomain-only protein HOP. *Neural Dev* 3.
- Deng W (2010) Neurobiology of injury to the developing brain. *Nat Rev Neurol*.
- Desrosiers R, Friderici K, Rottman F (1974) Identification of Methylated Nucleosides in Messenger RNA from Novikoff Hepatoma Cells. *Proc Natl Acad Sci* 71:3971–3975 Available at: <http://www.pnas.org/cgi/doi/10.1073/pnas.71.10.3971>.
- D           E, Pignatelli J, Nieto-Est  vez V, Vicario-Abej  n C (2013) Transcriptional regulation of olfactory bulb neurogenesis. *Anat Rec* 296:1364–1382.
- Dobin A, Davis CA, Schlesinger F, Drenkow J, Zaleski C, Jha S, Batut P, Chaisson M, Gingeras TR (2013) STAR: Ultrafast universal RNA-seq aligner. *Bioinformatics* 29:15–21.
- Doetsch F, Alvarez-Buylla A (1996) Network of tangential pathways for neuronal migration in adult mammalian brain. *Proc Natl Acad Sci* 93:14895–14900
- Doetsch F, Caille I, Lim DA, Garcia-Verdugo JM, Alvarez-Buylla A (1999a) Subventricular zone astrocytes are neural stem cells in the adult mammalian brain. *Cell* 97:703–716

Doetsch F, García-Verdugo JM, Alvarez-Buylla A (1999b) Regeneration of a germinal layer in the adult mammalian brain. *Proc Natl Acad Sci* 96:11619–11624

Doetsch F, García-Verdugo JM, Alvarez-Buylla A (1997a) Cellular composition and three-dimensional organization of the subventricular germinal zone in the adult mammalian brain. *J Neurosci* 17:5046–5061

Donega V, Marcy G, Lo Giudice Q, Zweifel S, Angonin D, Fiorelli R, Abrous DN, Rival-Gervier S, Koehl M, Jabaudon D, Raineteau O (2018) Transcriptional Dysregulation in Postnatal Glutamatergic Progenitors Contributes to Closure of the Cortical Neurogenic Period. *Cell Rep* 22:2601–2614.

Draganova K, Zemke M, Zurkirchen L, Valenta T, Cantù C, Okoniewski M, Schmid MT, Hoffmans R, Götz M, Basler K, Sommer L (2015) Wnt/ β -catenin signaling regulates sequential fate decisions of murine cortical precursor cells. *Stem Cells* 33:170–182

Echelard Y, Epstein DJ, St-Jacques B, Shen L, Mohler J, McMahon JA, McMahon AP (1993) Sonic hedgehog, a member of a family of putative signaling molecules, is implicated in the regulation of CNS polarity. *Cell* 75:1417–1430

Ehm O, Goritz C, Covic M, Schaffner I, Schwarz TJ, Karaca E, Kempkes B, Kremmer E, Pfrieger FW, Espinosa L, Bigas A, Giachino C, Taylor V, Frisen J, Lie DC (2010) RBPJ -Dependent Signaling Is Essential for Long-Term Maintenance of Neural Stem Cells in the Adult Hippocampus. *J Neurosci* 30:13794–13807

Englund C (2005) Pax6, Tbr2, and Tbr1 Are Expressed Sequentially by Radial Glia, Intermediate Progenitor Cells, and Postmitotic Neurons in Developing Neocortex. *J Neurosci* 25:247–251

Eroglu C, Barres BA (2010) Regulation of synaptic connectivity by glia. *Nature* 468:223–231.

Evsyukova I, Plestant C, Anton ES (2013) Integrative Mechanisms of Oriented Neuronal Migration in the Developing Brain. *Annu Rev Cell Dev Biol* 29:299–353

Fagel DM, Ganat Y, Cheng E, Silbereis J, Ohkubo Y, Ment LR, Vaccarino FM (2009) Fgfr1 Is Required for Cortical Regeneration and Repair after Perinatal Hypoxia. *J Neurosci* 29:1202–1211

Falkner S, Grade S, Dimou L, Conzelmann KK, Bonhoeffer T, Götz M, Hübener M (2016) Transplanted embryonic neurons integrate into adult neocortical circuits. *Nature* 539:248–253.

Fernandes M, Gutin G, Alcorn H, McConnell SK, Hebert JM (2007) Mutations in the BMP pathway in mice support the existence of two molecular classes of holoprosencephaly. *Development* 134:3789–3794

Fernández ME, Croce S, Boutin C, Cremer H, Raineteau O (2011) Targeted electroporation of defined lateral ventricular walls: A novel and rapid method to study fate specification during postnatal forebrain neurogenesis. *Neural Dev* 6:13

Ferriero DM (2004) Neonatal brain injury. *N Engl J Med*.

Figueres-Onãte M, García-Marqués J, López-Mascaraque L (2016) UbC-StarTrack, a clonal method to target the entire progeny of individual progenitors. *Sci Rep* 6.

Fiorelli R, Azim K, Fischer B, Raineteau O (2015) Adding a spatial dimension to postnatal ventricular-subventricular zone neurogenesis. *Development* 142:2109–2120

Flames N, Pla R, Gelman DM, Rubenstein JLR, Puelles L, Marin O (2007) Delineation of Multiple Subpallial Progenitor Domains by the Combinatorial Expression of

Transcriptional Codes. J Neurosci 27:9682–9695

Frantz GD, McConnell SK (1996) Restriction of late cerebral cortical progenitors to an upper-layer fate. *Neuron* 17:55–61

Frazer S, Prados J, Niquille M, Cadilhac C, Markopoulos F, Gomez L, Tomasello U, Telley L, Holtmaat A, Jabaudon D, Dayer A (2017) Transcriptomic and anatomic parcellation of 5-HT3AR expressing cortical interneuron subtypes revealed by single-cell RNA sequencing. *Nat Commun* 8.

Fuccillo M (2004) Temporal requirement for hedgehog signaling in ventral telencephalic patterning. *Development* 131:5031–5040

Fuentealba LC, Obernier K, Alvarez-Buylla A (2012) Adult neural stem cells bridge their niche. *Cell Stem Cell* 10:698–708

Fuentealba LC, Rompani SB, Parraguez JI, Obernier K, Romero R, Cepko CL, Alvarez-Buylla A (2015a) Embryonic Origin of Postnatal Neural Stem Cells. *Cell* 161:1644–1655.

Fuentealba LC, Rompani SB, Parraguez JI, Obernier K, Romero R, Cepko CL, Alvarez-Buylla A (2015b) Embryonic Origin of Postnatal Neural Stem Cells. *Cell* 161:1644–1655 Available at: <http://dx.doi.org/10.1016/j.cell.2015.05.041>.

Furuta Y, Piston DW, Hogan BLM (1997) Bone morphogenetic proteins (BMPs) as regulators of dorsal forebrain development. *Development* 124:2203–2212

Furutachi S, Miya H, Watanabe T, Kawai H, Yamasaki N, Harada Y, Imayoshi I, Nelson M, Nakayama KI, Hirabayashi Y, Gotoh Y (2015) Slowly dividing neural progenitors are an embryonic origin of adult neural stem cells. *Nat Neurosci* 18:657–665.

Fuzik J, Zeisel A, Mate Z, Calvigioni D, Yanagawa Y, Szabo G, Linnarsson S, Harkany T (2016) Integration of electrophysiological recordings with single-cell RNA-seq data identifies neuronal subtypes. *Nat Biotechnol* 34:175–183.

Gaiano N, Fishell G (1998) Transplantation as a tool to study progenitors within the vertebrate nervous system. *J Neurobiol* 36:152–161

Gaiano N, Fishell G (2002) The Role of Notch in Promoting Glial and Neural Stem Cell Fates. *Annu Rev Neurosci* 25:471–490

Gan Q, Lee A, Suzuki R, Yamagami T, Stokes A, Nguyen BC, Pleasure D, Wang J, Chen HW, Zhou CJ (2014) Pax6 mediates β -catenin signaling for self-renewal and neurogenesis by neocortical radial glial stem cells. *Stem Cells* 32:45–58

Gao P, Postiglione MP, Krieger TG, Hernandez L, Wang C, Han Z, Streicher C, Papusheva E, Insolera R, Chugh K, Kodish O, Huang K, Simons BD, Luo L, Hippenmeyer S, Shi SH (2014a) Deterministic progenitor behavior and unitary production of neurons in the neocortex. *Cell* 159:775–788

García-Marqués J, López-Mascaraque L (2013) Clonal identity determines astrocyte cortical heterogeneity. *Cereb Cortex* 23:1463–1472.

Ge WP, Miyawaki A, Gage FH, Jan YN, Jan LY (2012) Local generation of glia is a major astrocyte source in postnatal cortex. *Nature* 484:376–380.

Genander M, Cook PJ, Ramsköld D, Keyes BE, Mertz AF, Sandberg R, Fuchs E (2014) BMP signaling and its pSMADS1/5 target genes differentially regulate hair follicle stem cell lineages. *Cell Stem Cell* 15:619–633.

Givogri MI, de Planell M, Galbiati F, Superchi D, Gritti A, Vescovi A, de Vellis J, Bongarzone ER (2006) Notch Signaling in Astrocytes and Neuroblasts of the Adult

Subventricular Zone in Health and after Cortical Injury. Dev Neurosci 28:81–91

Gohlke JM, Armant O, Parham FM, Smith M V., Zimmer C, Castro DS, Nguyen L, Parker JS, Gradwohl G, Portier CJ, Guillemot F (2008) Characterization of the proneural gene regulatory network during mouse telencephalon development. *BMC Biol* 6.

Golden JA, Fields-Berry SC, Cepko CL (1995) Construction and characterization of a highly complex retroviral library for lineage analysis. *Proc Natl Acad Sci* 92:5704–5708

Gomes WA, Mehler MF, Kessler JA (2003) Transgenic overexpression of BMP4 increases astroglial and decreases oligodendroglial lineage commitment. *Dev Biol* 255:164–177

Graef W, Beimler HJ (1979) Zahnkariesfrequenz Bei Jugendlichen in Gemeinden Mit Natürlich Erhohtem Und Geringem Trinkwasserfluoridgehalt. *Zentralblatt für Bakteriologie Hygiene Krankenhaushygiene Betriebs-hygiene Prav Medizin - Abt 1 Orig B* 169:409–426

Gratton M-O, Torban E, Jasmin SB, Theriault FM, German MS, Stifani S (2003) Hes6 Promotes Cortical Neurogenesis and Inhibits Hes1 Transcription Repression Activity by Multiple Mechanisms. *Mol Cell Biol* 23:6922–6935

Greig LC, Woodworth MB, Galazo MJ, Padmanabhan H, Macklis JD (2013) Molecular logic of neocortical projection neuron specification, development and diversity. *Nat Rev Neurosci* 14:755–769.

Greig LC, Woodworth MB, Greppi C, Macklis JD (2016) Ctip1 Controls Acquisition of Sensory Area Identity and Establishment of Sensory Input Fields in the Developing Neocortex. *Neuron* 90:261–277.

Gross RE, Mehler MF, Mabie PC, Zang Z, Santschi L, Kessler JA (1996) Bone morphogenetic proteins promote astroglial lineage commitment by mammalian subventricular zone progenitor cells. *Neuron* 17:595–606.

Gümüşsoy M, Atmaca S, Bilgici B, Ünal R (2009) Changes in IGF-I, IGFBP-3 and ghrelin levels after adenotonsillectomy in children with sleep disordered breathing. *Int J Pediatr Otorhinolaryngol* 73:1653–1656.

Gutin G (2006) FGF signalling generates ventral telencephalic cells independently of SHH. *Development* 133:2937–2946

Han W, Kwan KY, Shim S, Lam MMS, Shin Y, Xu X, Zhu Y, Li M, Sestan N (2011) TBR1 directly represses Fezf2 to control the laminar origin and development of the corticospinal tract. *Proc Natl Acad Sci* 108:3041–3046

Han Y, Kebschull JM, Campbell RAA, Cowan D, Imhof F, Zador AM, Mrsic-Flogel TD (2018) The logic of single-cell projections from visual cortex. *Nature* 556:51–56.

Han YG, Spassky N, Romaguera-Ros M, Garcia-Verdugo JM, Aguilar A, Schneider-Maunoury S, Alvarez-Buylla A (2008) Hedgehog signaling and primary cilia are required for the formation of adult neural stem cells. *Nat Neurosci* 11:277–284.

Harrison-Uy SJ, Pleasure SJ (2012) Wnt signaling and forebrain development. *Cold Spring Harb Perspect Biol* 4:1–11

Harwell CC, Fuentealba LC, Gonzalez-Cerrillo A, Parker PRL, Gertz CC, Mazzola E, Garcia MT, Alvarez-Buylla A, Cepko CL, Kriegstein AR (2015) Wide Dispersion and Diversity of Clonally Related Inhibitory Interneurons. *Neuron* 87:999–1007

Haubensak W, Attardo A, Denk W, Huttner WB (2004) From The Cover: Neurons arise in the basal neuroepithelium of the early mammalian telencephalon: A major site of neurogenesis. *Proc Natl Acad Sci* 101:3196–3201

- He XC, Zhang J, Tong WG, Tawfik O, Ross J, Scoville DH, Tian Q, Zeng X, He X, Wiedemann LM, Mishina Y, Li L (2004) BMP signaling inhibits intestinal stem cell self-renewal through suppression of Wnt- β -catenin signaling. *Nat Genet* 36:1117–1121.
- Hébert JM, Fishell G (2008) The genetics of early telencephalon patterning: Some assembly required. *Nat Rev Neurosci*.
- Hébert JM, Mishina Y, McConnell SK (2002) BMP signaling is required locally to pattern the dorsal telencephalic midline. *Neuron* 35:1029–1041
- Herrera DG, Garcia-Verdugo JM, Alvarez-Buylla A (1999) Adult-derived neural precursors transplanted into multiple regions in the adult brain. *Ann Neurol* 46:867–877.
- Hippenmeyer S (2014) Molecular pathways controlling the sequential steps of cortical projection neuron migration. In: *Advances in Experimental Medicine and Biology*, pp 1–24
- Hirabayashi Y (2004) The Wnt/ β -catenin pathway directs neuronal differentiation of cortical neural precursor cells. *Development* 131:2791–2801
- Hu JS, Vogt D, Sandberg M, Rubenstein JL (2017a) Cortical interneuron development: a tale of time and space. *Development* 144:3867–3878
- Hu P, Fabianic E, Kwon DY, Tang S, Zhou Z, Wu H (2017b) Dissecting Cell-Type Composition and Activity-Dependent Transcriptional State in Mammalian Brains by Massively Parallel Single-Nucleus RNA-Seq. *Mol Cell* 68:1006–1015.e7.
- Huang X, Xu X, Bringas P, Hung YP, Chai Y (2010) Smad4-Shh-Nfic signaling cascade-mediated epithelial-mesenchymal interaction is crucial in regulating tooth root development. *J Bone Miner Res* 25:1167–1178.
- Ihrie RA, Álvarez-Buylla A (2011) Lake-Front Property: A Unique Germinal Niche by the Lateral Ventricles of the Adult Brain. *Neuron* 70:674–686
- Ihrie RA, Shah JK, Harwell CC, Levine JH, Guinto CD, Lezameta M, Kriegstein AR, Alvarez-Buylla A (2011) Persistent Sonic Hedgehog Signaling in Adult Brain Determines Neural Stem Cell Positional Identity. *Neuron* 71:250–262
- Ille F, Sommer L (2005) Wnt signaling: Multiple functions in neural development. *Cell Mol Life Sci* 62:1100–1108.
- Imayoshi I, Isomura A, Harima Y, Kawaguchi K, Kori H, Miyachi H, Fujiwara T, Ishidate F, Kageyama R (2013) Oscillatory control of factors determining multipotency and fate in mouse neural progenitors. *Science* (80-) 342:1203–1208
- Imayoshi I, Sakamoto M, Ohtsuka T, Takao K, Miyakawa T, Yamaguchi M, Mori K, Ikeda T, Itohara S, Kageyama R (2008) Roles of continuous neurogenesis in the structural and functional integrity of the adult forebrain. *Nat Neurosci* 11:1153–1161
- Imayoshi I, Sakamoto M, Yamaguchi M, Mori K, Kageyama R (2010) Essential Roles of Notch Signaling in Maintenance of Neural Stem Cells in Developing and Adult Brains. *J Neurosci* 30:3489–3498
- Imura T, Nakano I, Kornblum HL, Sofroniew M V. (2006) Phenotypic and functional heterogeneity of GFAP-expressing cells in vitro: Differential expression of LeX/CD15 by GFAP-expressing multipotent neural stem cells and non-neurogenic astrocytes. *Glia* 53:277–293.
- Inoue F, Kurokawa D, Takahashi M, Aizawa S (2012) Gbx2 Directly Restricts Otx2 Expression to Forebrain and Midbrain, Competing with Class III POU Factors. *Mol Cell Biol* 32:2618–2627

Inta D, Alfonso J, von Engelhardt J, Kreuzberg MM, Meyer AH, van Hooft JA, Monyer H (2008) Neurogenesis and widespread forebrain migration of distinct GABAergic neurons from the postnatal subventricular zone. *Proc Natl Acad Sci* 105:20994–20999

Ishibashi M, Ang SL, Shiota K, Nakanishi S, Kageyama R, Guillemot F (1995) Targeted disruption of mammalian hairy and Enhancer of split homolog-1 (HES-1) leads to up-regulation of neural helix-loop-helix factors, premature neurogenesis, and severe neural tube defects. *Genes Dev* 9:3136–3148

Itoh M, Kim CH, Palardy G, Oda T, Jiang YJ, Maust D, Yeo SY, Lorick K, Wright GJ, Ariza-McNaughton L, Weismann AM, Lewis J, Chandrasekharappa SC, Chitnis AB (2003) Mind bomb is a ubiquitin ligase that is essential for efficient activation of notch signaling by delta. *Dev Cell* 4:67–82

Jain R, Li D, Gupta M, Manderfield LJ, Ifkovits JL, Wang Q, Liu F, Liu Y, Poleshko A, Padmanabhan A, Raum JC, Li L, Morrissey EE, Lu MM, Won KJ, Epstein JA (2015) Integration of Bmp and Wnt signaling by Hopx specifies commitment of cardiomyoblasts. *Science* (80-) 348.

Jiang X, Nardelli J (2015) Cellular and molecular introduction to brain development. *Neurobiol Dis* 92:3–17

Jin K, Sun Y, Xie L, Peel A, Mao XO, Batteur S, Greenberg DA (2003) Directed migration of neuronal precursors into the ischemic cerebral cortex and striatum. *Mol Cell Neurosci*.

Ju XC, Hou QQ, Sheng AL, Wu KY, Zhou Y, Jin Y, Wen T, Yang Z, Wang X, Luo ZG (2016) The hominoid-specific gene *TBC1D3* promotes generation of basal neural progenitors and induces cortical folding in mice. *Elife* 5.

Kadam SD, Mulholland JD, McDonald JW, Comi AM (2008) Neurogenesis and neuronal commitment following ischemia in a new mouse model for neonatal stroke. *Brain Res*.

Kageyama R, Ohtsuka T, Kobayashi T (2008) Roles of Hes genes in neural development. *Dev Growth Differ* 50 Suppl 1:S97-103

Kaindl AM, Favrais G, Gressens P (2009) Molecular mechanisms involved in injury to the preterm brain. *J Child Neurol*.

Kandyba E, Leung Y, Chen Y-B, Widelitz R, Chuong C-M, Kobiela K (2013) Competitive balance of intrabulge BMP/Wnt signaling reveals a robust gene network ruling stem cell homeostasis and cyclic activation. *Proc Natl Acad Sci* 110:1351–1356

Kang W, Wong LC, Shi S-H, Hebert JM (2009) The Transition from Radial Glial to Intermediate Progenitor Cell Is Inhibited by FGF Signaling during Corticogenesis. *J Neurosci* 29:14571–14580

Kepecs A, Fishell G (2014) Interneuron cell types are fit to function. *Nature* 505:318–326.

Kessaris N, Fogarty M, Iannarelli P, Grist M, Wegner M, Richardson WD (2006) Competing waves of oligodendrocytes in the forebrain and postnatal elimination of an embryonic lineage. *Nat Neurosci* 9:173–179.

Kharchenko P V., Silberstein L, Scadden DT (2014) Bayesian approach to single-cell differential expression analysis. *Nat Methods* 11:740–742.

Kobayashi D, Kobayashi M, Matsumoto K, Ogura T, Nakafuku, Shimamura K (2002) Early subdivisions in the neural plate define distinct competence for inductive signals. *Development* 129:83–93

- Kohwi M, Petryniak MA, Long JE, Ekker M, Obata K, Yanagawa Y, Rubenstein JLR, Alvarez-Buylla A (2007) A Subpopulation of Olfactory Bulb GABAergic Interneurons Is Derived from Emx1- and Dlx5/6-Expressing Progenitors. *J Neurosci* 27:6878–6891
- Kokovay E, Wang Y, Kusek G, Wurster R, Lederman P, Lowry N, Shen Q, Temple S (2012) VCAM1 is essential to maintain the structure of the SVZ niche and acts as an environmental sensor to regulate SVZ lineage progression. *Cell Stem Cell* 11:220–230.
- Kriegstein A, Alvarez-Buylla A (2009) The Glial Nature of Embryonic and Adult Neural Stem Cells. *Annu Rev Neurosci* 32:149–184
- Kumamoto T, Hanashima C (2014) Neuronal subtype specification in establishing mammalian neocortical circuits. *Neurosci Res* 86:37–49
- Lagutin O V., Zhu CC, Kobayashi D, Topczewski J, Shimamura K, Puellas L, Russell HRC, McKinnon PJ, Solnica-Krezel L, Oliver G (2003) Six3 repression of Wnt signaling in the anterior neuroectoderm is essential for vertebrate forebrain development. *Genes Dev* 17:368–379.
- Langseth AJ, Munji RN, Choe Y, Huynh T, Pozniak CD, Pleasure SJ (2010) Wnts Influence the Timing and Efficiency of Oligodendrocyte Precursor Cell Generation in the Telencephalon. *J Neurosci* 30:13367–13372
- Le Magueresse C, Alfonso J, Bark C, Eliava M, Khrulev S, Monyer H (2012) Subventricular zone-derived neuroblasts use vasculature as a scaffold to migrate radially to the cortex in neonatal mice. *Cereb Cortex* 22:2285–2296.
- Lee JE (1997) Basic helix-loop-helix genes in neural development. *Curr Opin Neurobiol* 7:13–20.
- Lehtinen MK, Walsh CA (2011) Neurogenesis at the Brain–Cerebrospinal Fluid Interface. *Annu Rev Cell Dev Biol* 27:653–679
- Lehtinen MK, Zappaterra MW, Chen X, Yang YJ, Hill AD, Lun M, Maynard T, Gonzalez D, Kim S, Ye P, D’Ercole AJ, Wong ET, LaMantia AS, Walsh CA (2011) The Cerebrospinal Fluid Provides a Proliferative Niche for Neural Progenitor Cells. *Neuron* 69:893–905
- Lepanto P, Badano JL, Zolessi FR (2016) Neuron’s little helper: The role of primary cilia in neurogenesis. *Neurogenesis* 3:e1253363
- Li D, Takeda N, Jain R, Manderfield LJ, Liu F, Li L, Anderson SA, Epstein JA (2015) Hopx distinguishes hippocampal from lateral ventricle neural stem cells. *Stem Cell Res* 15:522–529.
- Li S, Mattar P, Zinyk D, Singh K, Chaturvedi C-P, Kovach C, Dixit R, Kurrasch DM, Ma Y-C, Chan JA, Wallace V, Dilworth FJ, Brand M, Schuurmans C (2012) GSK3 Temporally Regulates Neurogenin 2 Proneural Activity in the Neocortex. *J Neurosci* 32:7791–7805
- Li YL, Wang XL, Xiao D, Liu MY, Du Y, Deng J (2018) Organocatalytic Biomimetic Decarboxylative Aldol Reaction of Fluorinated β -Keto Acids with Unprotected Isatins. *Adv Synth Catal* 17:5820–5829
- Liao Y, Smyth GK, Shi W (2014) FeatureCounts: An efficient general purpose program for assigning sequence reads to genomic features. *Bioinformatics* 30:923–930.
- Lim DA, Alvarez-Buylla A (2016) The adult ventricular–subventricular zone (V-SVZ) and olfactory bulb (OB) neurogenesis. *Cold Spring Harb Perspect Biol* 8:a018820
- Lim DA, Fishell GJ, Alvarez-Buylla A (1997) Postnatal mouse subventricular zone

neuronal precursors can migrate and differentiate within multiple levels of the developing neuraxis. *Proc Natl Acad Sci U S A*.

Lim DA, Tramontin AD, Trevejo JM, Herrera DG, García-Verdugo JM, Alvarez-Buylla A (2000) Noggin antagonizes BMP signaling to create a niche for adult neurogenesis. *Neuron* 28:713–726.

Lledo PM, Merkle FT, Alvarez-Buylla A (2008) Origin and function of olfactory bulb interneuron diversity. *Trends Neurosci* 31:392–400.

Llorens-Bobadilla E, Zhao S, Baser A, Saiz-Castro G, Zwadlo K, Martin-Villalba A (2015) Single-Cell Transcriptomics Reveals a Population of Dormant Neural Stem Cells that Become Activated upon Brain Injury. *Cell Stem Cell* 17:329–340

Lodato S, Arlotta P (2015) Generating Neuronal Diversity in the Mammalian Cerebral Cortex. *Annu Rev Cell Dev Biol* 31:699–720

Lodato S, Molyneaux BJ, Zuccaro E, Goff LA, Chen HH, Yuan W, Meleski A, Takahashi E, Mahony S, Rinn JL, Gifford DK, Arlotta P (2014) Gene co-regulation by *Fezf2* selects neurotransmitter identity and connectivity of corticospinal neurons. *Nat Neurosci* 17:1046–1054.

Lois C, Alvarez-Buylla A (1994) Long-distance neuronal migration in the adult mammalian brain. *Science* (80-) 264:1145–1148.

López-Juárez A, Howard J, Ullom K, Howard L, Grande A, Pardo A, Waclaw R, Sun YY, Yang D, Kuan CY, Campbell K, Nakafuku M (2013) *Gsx2* controls region-specific activation of neural stem cells and injury-induced neurogenesis in the adult subventricular zone. *Genes Dev* 27:1272–1287.

Louvi A, Yoshida M, Grove EA (2007) The derivatives of the *Wnt3a* lineage in the central nervous system. *J Comp Neurol* 504:550–569.

Lutolf S, Radtke F, Aguet M, Suter U, Taylor V (2002) *Notch1* is required for neuronal and glial differentiation in the cerebellum. *Development* 129:373–385

Macosko EZ, Basu A, Satija R, Nemesh J, Shekhar K, Goldman M, Tirosh I, Bialas AR, Kamitaki N, Martersteck EM, Trombetta JJ, Weitz DA, Sanes JR, Shalek AK, Regev A, McCarroll SA (2015) Highly parallel genome-wide expression profiling of individual cells using nanoliter droplets. *Cell* 161:1202–1214.

Magavi S, Friedmann D, Banks G, Stolfi A, Lois C (2012) Coincident Generation of Pyramidal Neurons and Protoplasmic Astrocytes in Neocortical Columns. *J Neurosci* 32:4762–4772

Mason I (2007) Initiation to end point: The multiple roles of fibroblast growth factors in neural development. *Nat Rev Neurosci* 8:583–596

Mayer C, Hafemeister C, Bandler RC, Machold R, Batista Brito R, Jaglin X, Allaway K, Butler A, Fishell G, Satija R (2018) Developmental diversification of cortical inhibitory interneurons. *Nature* 555:457–462

Mayer C, Jaglin XH, Cobbs L V., Bandler RC, Streicher C, Cepko CL, Hippenmeyer S, Fishell G (2015a) Clonally Related Forebrain Interneurons Disperse Broadly across Both Functional Areas and Structural Boundaries. *Neuron* 87:989–998.

Menn B, Garcia-Verdugo JM, Yaschine C, Gonzalez-Perez O, Rowitch D, Alvarez-Buylla A (2006) Origin of Oligodendrocytes in the Subventricular Zone of the Adult Brain. *J Neurosci* 26:7907–7918

Mercier F, Kitasako JT, Hatton GI (2002) Anatomy of the brain neurogenic zones revisited: Fractones and the fibroblast/macrophage network. *J Comp Neurol* 451:170–188

Merkle FT, Fuentealba LC, Sanders TA, Magno L, Kessarar N, Alvarez-Buylla A (2014) Adult neural stem cells in distinct microdomains generate previously unknown interneuron types. *Nat Neurosci* 17:207–214.

Merkle FT, Mirzadeh Z, Alvarez-Buylla A (2007a) Mosaic organization of neural stem cells in the adult brain. *Science* (80-) 317:381–384

Mery F, Zárate A, Fadic R, Lorenzoni J, Elgueta F, Villanueva P, Rojas R, Tagle P (2010) Resección de lesiones cerebrales con asistencia de mapeo cortical intraoperatorio. *Rev Chil Neuropsiquiatr* 48:184–196.

Mi D, Li Z, Lim L, Li M, Moissidis M, Yang Y, Gao T, Hu TX, Pratt T, Price DJ, Sestan N, Marín O (2018) Early emergence of cortical interneuron diversity in the mouse embryo. *Science* (80-) 360:81–85.

Mich JK, Signer RAJ, Nakada D, Pineda A, Burgess RJ, Vue TY, Johnson JE, Morrison SJ (2014) Prospective identification of functionally distinct stem cells and neurosphere-initiating cells in adult mouse forebrain. *Elife* 2014.

Mirzadeh Z, Merkle FT, Soriano-Navarro M, Garcia-Verdugo JM, Alvarez-Buylla A (2008) Neural Stem Cells Confer Unique Pinwheel Architecture to the Ventricular Surface in Neurogenic Regions of the Adult Brain. *Cell Stem Cell* 3:265–278.

Miyata T (2004) Asymmetric production of surface-dividing and non-surface-dividing cortical progenitor cells. *Development* 131:3133–3145

Miyoshi G, Butt SJB, Takebayashi H, Fishell G (2007) Physiologically Distinct Temporal Cohorts of Cortical Interneurons Arise from Telencephalic Olig2-Expressing Precursors. *J Neurosci* 27:7786–7798

Mizutani KI, Yoon K, Dang L, Tokunaga A, Gaiano N (2007) Differential Notch signalling distinguishes neural stem cells from intermediate progenitors. *Nature* 449:351–355

Molyneaux BJ, Arlotta P, Fame RM, MacDonald JL, MacQuarrie KL, Macklis JD (2009) Novel Subtype-Specific Genes Identify Distinct Subpopulations of Callosal Projection Neurons. *J Neurosci* 29:12343–12354

Molyneaux BJ, Goff LA, Brettler AC, Chen HH, Brown JR, Hrvatin S, Rinn JL, Arlotta P (2015) DeCoN: Genome-wide analysis of invivo transcriptional dynamics during pyramidal neuron fate selection in neocortex. *Neuron* 85:275–288.

Morel L, Chiang MSR, Higashimori H, Shoneye T, Iyer LK, Yelick J, Tai A, Yang Y (2017) Molecular and Functional Properties of Regional Astrocytes in the Adult Brain. *J Neurosci*:3956–16

Moreno N, González A, Rétaux S (2009) Development and evolution of the subpallium. *Semin Cell Dev Biol* 20:735–743

Morita M, Kozuka N, Itofusa R, Yukawa M, Kudo Y (2005) Autocrine activation of EGF receptor promotes oscillation of glutamate-induced calcium increase in astrocytes cultured in rat cerebral cortex. *J Neurochem* 95:871–879.

Morizur L, Chicheportiche A, Gauthier LR, Daynac M, Boussin FD, Mouthon MA (2018) Distinct Molecular Signatures of Quiescent and Activated Adult Neural Stem Cells Reveal Specific Interactions with Their Microenvironment. *Stem Cell Reports*.

Mühlfriedel S, Kirsch F, Gruss P, Stoykova A, Chowdhury K (2005) A roof plate-dependent enhancer controls the expression of Homeodomain only protein in the developing cerebral cortex. *Dev Biol* 283:522–534.

Munji RN, Choe Y, Li G, Siegenthaler JA, Pleasure SJ (2011) Wnt Signaling Regulates Neuronal Differentiation of Cortical Intermediate Progenitors. *J Neurosci*

Nam H song, Benezra R (2009) High Levels of *Id1* Expression Define B1 Type Adult Neural Stem Cells. *Cell Stem Cell* 5:515–526.

Noctor SC, Flint AC, Weissman TA, Dammerman RS, Kriegstein AR (2001) Neurons derived from radial glial cells establish radial units in neocortex. *Nature* 409:714–720.

Noctor SC, Martinez-Cerdeño V, Ivic L, Kriegstein AR (2004) Cortical neurons arise in symmetric and asymmetric division zones and migrate through specific phases. *Nat Neurosci* 7:136–144.

Nogueira AB, Nogueira AB, Veiga JCE, Teixeira MJ (2017) Letter: Extensive Migration of Young Neurons into the Infant Human Frontal Lobe. *Neurosurgery* 81:E16–E18.

Nowakowski TJ, Bhaduri A, Pollen AA, Alvarado B, Mostajo-Radji MA, Di Lullo E, Haeussler M, Sandoval-Espinosa C, Liu SJ, Velmeshev D, Ounadjela JR, Shuga J, Wang X, Lim DA, West JA, Leyrat AA, Kent WJ, Kriegstein AR (2017) Spatiotemporal gene expression trajectories reveal developmental hierarchies of the human cortex. *Science* (80-) 358:1318–1323

Nyfeler Y, Kirch RD, Mantei N, Leone DP, Radtke F, Suter U, Taylor V (2005a) Jagged1 signals in the postnatal subventricular zone are required for neural stem cell self-renewal. *EMBO J* 24:3504–3515

Obermair FJ, Fiorelli R, Schroeter A, Beyeler S, Blatti C, Zoerner B, Thallmair M (2010) A novel classification of quiescent and transit amplifying adult neural stem cells by surface and metabolic markers permits a defined simultaneous isolation. *Stem Cell Res* 5:131–143.

Obernier K, Cebrian-Silla A, Thomson M, Parraguez JI, Anderson R, Guinto C, Rodas Rodriguez J, Garcia-Verdugo JM, Alvarez-Buylla A (2018) Adult Neurogenesis Is Sustained by Symmetric Self-Renewal and Differentiation. *Cell Stem Cell*:221–234.e8.

Okano H, Temple S (2009) Cell types to order: temporal specification of CNS stem cells. *Curr Opin Neurobiol* 19:112–119.

Ong J, Plane JM, Parent JM, Silverstein FS (2005) Hypoxic-ischemic injury stimulates subventricular zone proliferation and neurogenesis in the neonatal rat. *Pediatr Res*.

Ortega F, Gascón S, Masserdotti G, Deshpande A, Simon C, Fischer J, Dimou L, Chichung Lie D, Schroeder T, Berninger B (2013) Oligodendroglial and neurogenic adult subependymal zone neural stem cells constitute distinct lineages and exhibit differential responsiveness to Wnt signalling. *Nat Cell Biol* 15:602–613.

Parras CM, Schuurmans C, Scardigli R, Kim J, Anderson DJ, Guillemot F (2002) Divergent functions of the proneural genes *Mash1* and *Ngn2* in the specification of neuronal subtype identity. *Genes Dev* 16:324–338.

Pastrana E, Cheng L-C, Doetsch F (2009) Simultaneous prospective purification of adult subventricular zone neural stem cells and their progeny. *Proc Natl Acad Sci* 106:6387–6392

Paterson JA, Privat A, Ling EA, Leblond CP (1973) Investigation of glial cells in semithin sections. III. Transformation of subependymal cells into glial cells, as shown by radioautography after ³H-thymidine injection into the lateral ventricle of the brain of young rats. *J Comp Neurol* 149:83–102

- Peretto P, Cummings D, Modena C, Behrens M, Venkatraman G, Fasolo A, Margolis FL (2002) BMP mRNA and protein expression in the developing mouse olfactory system. *J Comp Neurol* 451:267–278.
- Petreaanu L, Alvarez-Buylla A (2002) Maturation and Death of Adult-Born Olfactory Bulb Granule Neurons: Role of Olfaction. *J Neurosci* 22:6106–6113
- Petrenko V, Mihhailova J, Salmon P, Kiss JZ (2015) Apoptotic neurons induce proliferative responses of progenitor cells in the postnatal neocortex. *Exp Neurol* 273:126–137 Available at: <http://dx.doi.org/10.1016/j.expneurol.2015.08.010>.
- Plane JM, Liu R, Wang TW, Silverstein FS, Parent JM (2004) Neonatal hypoxic-ischemic injury increases forebrain subventricular zone neurogenesis in the mouse. *Neurobiol Dis*.
- Plikus M V., Mayer JA, De La Cruz D, Baker RE, Maini PK, Maxson R, Chuong CM (2008) Cyclic dermal BMP signalling regulates stem cell activation during hair regeneration. *Nature* 451:340–344.
- Pollen AA, Nowakowski TJ, Chen J, Retallack H, Sandoval-Espinosa C, Nicholas CR, Shuga J, Liu SJ, Oldham MC, Diaz A, Lim DA, Leyrat AA, West JA, Kriegstein AR (2015) Molecular Identity of Human Outer Radial Glia during Cortical Development. *Cell* 163:55–67.
- Ponti G, Obernier K, Guinto C, Jose L, Bonfanti L, Alvarez-Buylla A (2013) Cell cycle and lineage progression of neural progenitors in the ventricular-subventricular zones of adult mice. *Proc Natl Acad Sci* 110:E1045–E1054
- Prakadan SM, Shalek AK, Weitz DA (2017) Scaling by shrinking: Empowering single-cell “omics” with microfluidic devices. *Nat Rev Genet* 18:345–361.
- Puelles L, Kuwana E, Puelles E, Bulfone A, Shimamura K, Keleher J, Smiga S, Rubenstein JLR (2000) Pallial and subpallial derivatives in the embryonic chick and mouse telencephalon, traced by the expression of the genes *Dlx-2*, *Emx-1*, *Nkx-2.1*, *Pax-6*, and *Tbr-1*. *J Comp Neurol* 424:409–438.
- Qian X, Shen Q, Goderie SK, He W, Capela A, Davis AA, Temple S (2000) Timing of CNS cell generation: A programmed sequence of neuron and glial cell production from isolated murine cortical stem cells. *Neuron* 28:69–80.
- Raballo R, Rhee J, Lyn-Cook R, Leckman JF, Schwartz ML, Vaccarino FM (2000) Basic Fibroblast Growth Factor (*Fgf2*) Is Necessary for Cell Proliferation and Neurogenesis in the Developing Cerebral Cortex. *J Neurosci* 20:5012–5023
- Radakovits R, Barros CS, Belvindrah R, Patton B, Muller U (2009) Regulation of Radial Glial Survival by Signals from the Meninges. *J Neurosci* 29:7694–7705
- Rash BG, Grove EA (2006) Area and layer patterning in the developing cerebral cortex. *Curr Opin Neurobiol* 16:25–34.
- Rash BG, Tomasi S, Lim HD, Suh CY, Vaccarino FM (2013) Cortical Gyrification Induced by Fibroblast Growth Factor 2 in the Mouse Brain. *J Neurosci* 33:10802–10814
- Richardson WD, Kessaris N, Pringle N (2006) Oligodendrocyte wars. *Nat Rev Neurosci* 7:11–18.
- Rowitch DH, Kriegstein AR (2010) Developmental genetics of vertebrate glial-cell specification. *Nature* 468:214–222.
- Roy E, Neufeld Z, Livet J, Khosrotehrani K (2014) Concise review: Understanding clonal dynamics in homeostasis and injury through multicolor lineage tracing. *Stem Cells* 32:3046–3054.

- Rudy B, Fishell G, Lee SH, Hjerling-Leffler J (2011) Three groups of interneurons account for nearly 100% of neocortical GABAergic neurons. *Dev Neurobiol*.
- Saha B, Jaber M, Gaillard A (2012) Potentials of endogenous neural stem cells in cortical repair. *Front Cell Neurosci* 6:1–10
- Saha B, Peron S, Murray K, Jaber M, Gaillard A (2013) Cortical lesion stimulates adult subventricular zone neural progenitor cell proliferation and migration to the site of injury. *Stem Cell Res* 11:965–977
- Sahara S, O’Leary DDM (2009) Fgf10 Regulates Transition Period of Cortical Stem Cell Differentiation to Radial Glia Controlling Generation of Neurons and Basal Progenitors. *Neuron* 63:48–62
- Sakamoto M, Kageyama R, Imayoshi I (2014) The functional significance of newly born neurons integrated into olfactory bulb circuits. *Front Neurosci*.
- Scott JA (2006) Loan officer turnover and credit availability for small firms. *J Small Bus Manag* 44:544–562.
- Sequerre EB, Miyakoshi LM, Fróes MM, Menezes JRL, Hedin-Pereira C (2010) Generation of glutamatergic neurons from postnatal and adult subventricular zone with pyramidal-like morphology. *Cereb Cortex* 20:2583–2591
- Shakèd M, Weissmüller K, Svoboda H, Hortschansky P, Nishino N, Wölfl S, Tucker KL (2008) Histone deacetylases control neurogenesis in embryonic brain by inhibition of BMP2/4 signaling Chan-Ling T, ed. *PLoS One* 3:e2668
- Shen Q, Wang Y, Dimos JT, Fasano CA, Phoenix TN, Lemischka IR, Ivanova NB, Stifani S, Morrissey EE, Temple S (2006) The timing of cortical neurogenesis is encoded within lineages of individual progenitor cells. *Nat Neurosci* 9:743–751.
- Shen Q, Wang Y, Kokovay E, Lin G, Chuang SM, Goderie SK, Roysam B, Temple S (2008) Adult SVZ Stem Cells Lie in a Vascular Niche: A Quantitative Analysis of Niche Cell-Cell Interactions. *Cell Stem Cell* 3:289–300
- Shimamura K, Rubenstein JL (1997) Inductive interactions direct early regionalization of the mouse forebrain. *Development* 124:2709–2718
- Shin CH, Liu ZP, Passier R, Zhang CL, Wang DZ, Harris TM, Yamagishi H, Richardson JA, Childs G, Olson EN (2002) Modulation of cardiac growth and development by HOP, an unusual homeodomain protein. *Cell* 110:725–735.
- Shinya M, Koshida S, Sawada A, Kuroiwa A, Takeda H (2001) Fgf signalling through MAPK cascade is required for development of the subpallial telencephalon in zebrafish embryos. *Development* 128:4153–4164
- Siddiqi F, Chen F, Aron AW, Fiondella CG, Patel K, LoTurco JJ (2014) Fate mapping by piggybac transposase reveals that neocortical glast+ progenitors generate more astrocytes than nestin+ progenitors in rat neocortex. *Cereb Cortex* 24:508–520.
- Silva-Vargas V, Maldonado-Soto AR, Mizrak D, Codega P, Doetsch F (2016) Age-Dependent Niche Signals from the Choroid Plexus Regulate Adult Neural Stem Cells. *Cell Stem Cell* 19:643–652
- Simeone A, Acampora D, Pannese M, D’Esposito M, Stornaiuolo A, Gulisano M, Mallamaci A, Kastury K, Druck T, Huebner K (1994) Cloning and characterization of two members of the vertebrate Dlx gene family. *Proc Natl Acad Sci U S A* 91:2250–2254.
- Sokpor G, Castro-Hernandez R, Rosenbusch J, Staiger JF, Tuoc T (2018) ATP-dependent chromatin remodeling during cortical neurogenesis. *Front Neurosci* 12.

- Song J, McColl J, Camp E, Kennerley N, Mok GF, McCormick D, Grocott T, Wheeler GN, Munsterberg AE (2014) Smad1 transcription factor integrates BMP2 and Wnt3a signals in migrating cardiac progenitor cells. *Proc Natl Acad Sci* 111:7337–7342
- Spassky N, Merkle FT, Flames N, Tramontin AD, García-Verdugo JM, Alvarez-Buylla A (2005) Adult ependymal cells are postmitotic and are derived from radial glial cells during embryogenesis. *J Neurosci* 25:10–18
- Srinivas S, Watanabe T, Lin CS, William CM, Tanabe Y, Jessell TM, Costantini F (2001) Cre reporter strains produced by targeted insertion of EYFP and ECFP into the ROSA26 locus. *BMC Dev Biol* 1:1–8.
- Stricker SH, Götz M (2018) DNA-methylation: Master or slave of neural fate decisions? *Front Neurosci* 12.
- Stump G, Durrer A, Klein AL, Lütolf S, Suter U, Taylor V (2002) Notch1 and its ligands Delta-like and Jagged are expressed and active in distinct cell populations in the postnatal mouse brain. *Mech Dev* 114:153–159
- Tabata H (2015) Diverse subtypes of astrocytes and their development during corticogenesis. *Front Neurosci* 9:10.3389/fnins.2015.00114.
- Tabata H, Kanatani S, Nakajima K (2009) Differences of migratory behavior between direct progeny of apical progenitors and basal progenitors in the developing cerebral cortex. *Cereb Cortex* 19:2092–2105
- Takeda N, Jain R, LeBoeuf MR, Wang Q, Lu MM, Epstein JA (2011) Interconversion between intestinal stem cell populations in distinct niches. *Science* (80-) 334:1420–1424.
- Takizawa T, Nakashima K, Namihira M, Ochiai W, Uemura A, Yanagisawa M, Fujita N, Nakao M, Taga T (2001) DNA Methylation Is a Critical Cell-Intrinsic Determinant of Astrocyte Differentiation in the Fetal Brain. *Dev Cell* 1:749–758.
- Tasic B et al. (2016) Adult mouse cortical cell taxonomy revealed by single cell transcriptomics. *Nat Neurosci* 19:335–346.
- Tasouri E, Willaredt MA, Tucker KL (2013) Primary cilia and brain development. *Cilia Nerv Syst Dev Funct* 9789400758:83–104
- Tavazoie M, Van der Veken L, Silva-Vargas V, Louissaint M, Colonna L, Zaidi B, Garcia-Verdugo JM, Doetsch F (2008) A Specialized Vascular Niche for Adult Neural Stem Cells. *Cell Stem Cell* 3:279–288
- Telley L, Govindan S, Prados J, Stevant I, Nef S, Dermitzakis E, Dayer A, Jabaudon D (2016) Sequential transcriptional waves direct the differentiation of newborn neurons in the mouse neocortex. *Science* (80-) 351:1443–1446.
- Thomsen ER, Mich JK, Yao Z, Hodge RD, Doyle AM, Jang S, Shehata SI, Nelson AM, Shapovalova N V., Levi BP, Ramanathan S (2015a) Fixed single-cell transcriptomic characterization of human radial glial diversity. *Nat Methods* 13:87–93.
- Thomsen ER, Mich JK, Yao Z, Hodge RD, Doyle AM, Jang S, Shehata SI, Nelson AM, Shapovalova N V., Levi BP, Ramanathan S (2015b) Fixed single-cell transcriptomic characterization of human radial glial diversity. *Nat Methods* 13:87–93
- Thomsen GM, Le Belle JE, Harnisch JA, Mc Donald WS, Hovda DA, Sofroniew M V., Kornblum HI, Harris NG (2014) Traumatic brain injury reveals novel cell lineage relationships within the subventricular zone. *Stem Cell Res* 13:48–60
- Tiberi L, Vanderhaeghen P, van den Aamele J (2012) Cortical neurogenesis and morphogens: Diversity of cues, sources and functions. *Curr Opin Cell Biol* 24:269–

Tong CK, Alvarez-Buylla A (2014) SnapShot: Adult Neurogenesis in the V-SVZ. *Neuron* 81:220–220.e1.

Tong CK, Fuentealba LC, Shah JK, Lindquist RA, Ihrie RA, Guinto CD, Rodas-Rodriguez JL, Alvarez-Buylla A (2015) A dorsal SHH-dependent domain in the V-SVZ produces large numbers of oligodendroglial lineage cells in the postnatal brain. *Stem Cell Reports* 5:461–470.

Tozer S, Baek C, Fischer E, Gojame R, Morin X (2017) Differential Routing of Mindbomb1 via Centriolar Satellites Regulates Asymmetric Divisions of Neural Progenitors. *Neuron* 93:542–551.e4

Tramontin AD, García-Verdugo JM, Lim DA, Alvarez-Buylla A (2003) Postnatal development of radial glia and the ventricular zone (VZ): A continuum of the neural stem cell compartment. *Cereb Cortex* 13:580–587.

Tremblay R, Lee S, Rudy B (2016) GABAergic Interneurons in the Neocortex: From Cellular Properties to Circuits. *Neuron* 91:260–292

Tropepe V, Sibilio M, Ciruna BG, Rossant J, Wagner EF, Van Der Kooy D (1999) Distinct neural stem cells proliferate in response to EGF and FGF in the developing mouse telencephalon. *Dev Biol* 208:166–188.

Tsai HH, Li H, Fuentealba LC, Molofsky A V., Taveira-Marques R, Zhuang H, Tenney A, Murnen AT, Fancy SPJ, Merkle F, Kessaris N, Alvarez-Buylla A, Richardson WD, Rowitch DH (2012) Regional astrocyte allocation regulates CNS synaptogenesis and repair. *Science* (80-) 337:358–362.

Ventura RE, Goldman JE (2007) Dorsal Radial Glia Generate Olfactory Bulb Interneurons in the Postnatal Murine Brain. *J Neurosci* 27:4297–4302

Wachowiak M, Shipley MT (2006) Coding and synaptic processing of sensory information in the glomerular layer of the olfactory bulb. *Semin Cell Dev Biol* 17:411–423

Wamsley B, Fishell G (2017) Genetic and activity-dependent mechanisms underlying interneuron diversity. *Nat Rev Neurosci* 18:299–309.

Wang L, Hou S, Han YG (2016) Hedgehog signaling promotes basal progenitor expansion and the growth and folding of the neocortex. *Nat Neurosci* 19:888–896

Wang X, Guan Z, Sheng Y, Tian Y (2018) Real-time quantitative description of gas invasion in deepwater drilling. *J Eng Res* 6:232–243.

Wichterle H, Turnbull DH, Nery S, Fishell G, Alvarez-buylla A (2001) In utero fate mapping reveals distinct migratory pathways and fates of neurons born in the mammalian basal forebrain. *Development*.

Wiegrefe C, Simon R, Peschkes K, Kling C, Strehle M, Cheng J, Srivatsa S, Liu P, Jenkins NA, Copeland NG, Tarabykin V, Britsch S (2015) Bcl11a (Ctip1) Controls Migration of Cortical Projection Neurons through Regulation of Sema3c. *Neuron* 87:311–326.

Willaime-Morawek S, Seaberg RM, Batista C, Labbé E, Attisano L, Gorski JA, Jones KR, Kam A, Morshead CM, Van Der Kooy D (2006) Embryonic cortical neural stem cells migrate ventrally and persist as postnatal striatal stem cells. *J Cell Biol* 175:159–168.

Willaime-Morawek S, Van Der Kooy D (2008) Cortex- and striatum- derived neural stem cells produce distinct progeny in the olfactory bulb and striatum. *Eur J Neurosci* 27:2354–2362.

- Winpenny E, Lebel-Potter M, Fernandez ME, Brill MS, Götz M, Guillemot F, Raineteau O (2011) Sequential generation of olfactory bulb glutamatergic neurons by Neurog2-expressing precursor cells. *Neural Dev* 6:12
- Wrobel CN, Mutch CA, Swaminathan S, Taketo MM, Chenn A (2007) Persistent expression of stabilized β -catenin delays maturation of radial glial cells into intermediate progenitors. *Dev Biol* 309:285–297
- Yabut OR, Fernandez G, Huynh T, Yoon K, Pleasure SJ (2015) Suppressor of Fused Is Critical for Maintenance of Neuronal Progenitor Identity during Corticogenesis. *Cell Rep* 12:2021–2034
- Yang HKC, Sundholm-Peters NL, Goings GE, Walker AS, Hyland K, Szele FG (2004) Distribution of Doublecortin Expressing Cells Near the Lateral Ventricles in the Adult Mouse Brain. *J Neurosci Res* 76:282–295.
- Ying QL, Nichols J, Chambers I, Smith A (2003) BMP induction of *Id* proteins suppresses differentiation and sustains embryonic stem cell self-renewal in collaboration with STAT3. *Cell* 115:281–292
- Yoon KJ et al. (2017) Temporal Control of Mammalian Cortical Neurogenesis by m6A Methylation. *Cell* 171:877–889.e17.
- Yoon KJ, Koo BK, Im SK, Jeong HW, Ghim J, Kwon M chul, Moon JS, Miyata T, Kong YY (2008) Mind Bomb 1-Expressing Intermediate Progenitors Generate Notch Signaling to Maintain Radial Glial Cells. *Neuron* 58:519–531
- Young KM, Fogarty M, Kessar N, Richardson WD (2007) Subventricular Zone Stem Cells Are Heterogeneous with Respect to Their Embryonic Origins and Neurogenic Fates in the Adult Olfactory Bulb. *J Neurosci* 27:8286–8296
- Yun K, Potter S, Rubenstein JL (2001) *Gsh2* and *Pax6* play complementary roles in dorsoventral patterning of the mammalian telencephalon. *Development* 128:193–205
- Yuzwa SA, Borrett MJ, Innes BT, Voronova A, Ketela T, Kaplan DR, Bader GD, Miller FD (2017) Developmental Emergence of Adult Neural Stem Cells as Revealed by Single-Cell Transcriptional Profiling. *Cell Rep* 21:3970–3986.
- Zahr SK, Yang G, Kazan H, Borrett MJ, Yuzwa SA, Voronova A, Kaplan DR, Miller FD (2018) A Translational Repression Complex in Developing Mammalian Neural Stem Cells that Regulates Neuronal Specification. *Neuron*.
- Zeisel A, M̂oz-Manchado AB, Codeluppi S, Lönnerberg P, Manno G La, Juréus A, Marques S, Munguba H, He L, Betsholtz C, Rolny C, Castelo-Branco G, Hjerling-Leffler J, Linnarsson S (2015) Cell types in the mouse cortex and hippocampus revealed by single-cell RNA-seq. *Science* (80-) 347:1138–1142.
- Zhang R, Engler A, Taylor V (2018) Notch: an interactive player in neurogenesis and disease. *Cell Tissue Res* 371:73–89
- Zheng W, Nowakowski RS, Vaccarino FM (2004) Fibroblast growth factor 2 is required for maintaining the neural stem cell pool in the mouse brain subventricular zone. *Dev Neurosci* 26:181–196.
- Zhong YF, Butts T, Holland PWH (2008) HomeoDB: A database of homeobox gene diversity. *Evol Dev* 10:516–518.
- Zhong YF, Holland PWH (2011) HomeoDB2: Functional expansion of a comparative homeobox gene database for evolutionary developmental biology. *Evol Dev* 13:567–568.

Zweifel S, Marcy G, Lo Guidice Q, Li D, Heinrich C, Azim K, Raineteau O (2018) *HOPX Defines Heterogeneity of Postnatal Subventricular Zone Neural Stem Cells*. *Stem Cell Reports* 11:770–783.

Zywitz V, Misios A, Bunatyan L, Willnow TE, Rajewsky N (2018) *Single-cell transcriptomics characterizes cell types in the subventricular zone and uncovers molecular defects underlying impaired adult neurogenesis*. *Cell Reports* 25, 2457-2469

7. CV

Guillaume MARCY
Married, 2 kids
27/12/1982

PhD candidate

PhD school : Ecole Pratique des Hautes Etudes (EPHE)
PSL University
Thesis Director : Giovanni Stevanin
Thesis co Director : Olivier Raineteau
Postnatal brain development and plasticity lab
INSERM U1208 / Stem Cell and Brain Research Institute
guillaume.marcy@inserm.fr

WORK EXPERIENCE

October 2014 – Présent

INSERM U1208 Lyon, France
O. Raineteau
G. Stevanin

PhD candidate

- Heterogeneity and competence of postnatal SVZ in the mouse forebrain

October 2013 – October 2014

INSERM U846 Lyon, France
O. Raineteau

Research Assistant

- Heterogeneity and competence of postnatal SVZ in the mouse forebrain

May 2009 – September 2013

Duke-NUS graduate medical school
Singapore
E.Goh

Research Assistant/Associate

- Rett Syndrome modeling using hIPSCs
- Rett Syndrome associated genes screening
- Regulation of proliferation and differentiation of NSCs

November 2006 – March 2009

INSERM U846 Lyon, France
C. Dehay

Research Assistant

- G1 phase regulation in mouse corticogenesis

September 2003 - Nov 2006

INSERM U846 Lyon, France
C. Dehay

EPHE internship

- Cell cycle features of primate ES cells
- Establishing hES cells culture

8. List of Publications

From PhD work

Marcy G and Raineteau O. (2018). Contributions of single cell approaches to probe neural progenitor's heterogeneity and dynamics. Concise Review. *Stem Cells*, **Under Review**.

Zweifel S, **Marcy G**, Lo Giudice Q, Li D, Heinrich C, Azim K and Raineteau O (2018). HOPX Defines Heterogeneity of Postnatal Subventricular Zone Neural Stem Cells. *Stem Cell Reports*, 11(3):770-783.

Donega V, **Marcy G**, Lo Giudice Q, Zweifel S, Angonin D, Fiorelli R, Abrous N, Rival-Gervier S, Koehl M, Jabaudon D and Raineteau O (2018). Transcriptional dysregulation in postnatal glutamatergic progenitor contributes to closure of the cortical neurogenic period. *Cell Reports*, 22(10):2567-2574.

Azim K, Angonin D, **Marcy G**, Pieropan F, Rivera A, Donega V, Cantù C, Williams G, Berninger B, Butt AM, Raineteau O (2017). Pharmacogenomic identification of small molecules for lineage specific manipulation of subventricular zone germinal activity. *Plos Biology*, 15(3):e2000698.

Angonin D, **Marcy G** and Raineteau O (2015). Postnatal Subventricular zone regionalization by morphogens. *Médecine Sciences: M/S*, 11:968-70.

From previous work

*Chin EW, ***Marcy G**, *Yoon SI, Ma D, Rosales FJ, Augustine GJ and Goh EL (2016). Choline Ameliorates Disease Phenotypes in Human iPSC Models of Rett Syndrome. *Neuromolecular Medicine*, 3:364-77 (IF 3,6).

Aksoy I, **Marcy G**, Chen J, Divakar U, Kumar V, John-Sanchez D, Rahmani M, Buckley NJ and Stanton LW (2016). A Role for RE-1-Silencing Transcription Factor in Embryonic Stem Cells Cardiac Lineage Specification. *Stem Cells*, 4:860-72.

Ma DL, Yoon SI, Yang CH, **Marcy G**, Zhao N, Leong WY, Ganapathy V, Han J, Van Dongen AMJ, Hsu KS, Ming GL, Augustine GL and Goh ELK (2014). Rescue of MeCP2 dysfunction-induced defects in newborn neurons by pentobarbital. *Neurotherapeutics*, 2:477-90.

*Su CTE, *Yoon SI, ***Marcy G**, Chin EWM, Augustine G and Goh ELK (2014). An optogenetic approach for assessing formation of neuronal connections in a co-culture system. *JOVE*, 96:e52408.

Fan Y, **Marcy G**, Lee ES, Rozen S, Mattar CN, Waddington SN, Goh EL, Choolani M, Chan JK (2014). Regionally specified second trimester fetal neural stem cells reveals differential neurogenic programming. *Plos One*, 9:e105985.

Mattu SC, **Marcy G**, Low G, Ryu JR, Zhao X, Rosales R and Goh E (2012). Taurine induces proliferation of neural stem cells and synapse development in the developing mouse brain. *Plos One*, 8:e42935.

Moe AAK, Suryana M, **Marcy G**, Lim SK, Ankam S, Goh JZW, Jing J, Teo BKK, Law JBK, Low HY, Goh E, Sheetz MP and Yim EKF (2012). Microarray with micro- and nanotopographies enables identification of optimal topography to direct differentiation of primary murine neural progenitor cells. *Small*, 19:3050-3061.

Cao H, **Marcy G**, Goh EL, Wang F, Wang J, Chew SY (2012). The Effects of Nanofiber Topography on Astrocyte Behavior and Gene Silencing Efficiency. *Macromolecular Bioscience*, 12(5):666-74.

Low WC, Yau WW, Stanton LW, **Marcy G**, Goh E and Chew SY (2012). Directing neuronal differentiation of primary neural progenitor cells by gene knockdown approach, *DNA and Cell Biology*, 7:1148-1160.

Handarmin, Tan GJY, Sundaray B, **Marcy G**, Goh E and Chew SY (2011). Nanofibrous scaffold with incorporated protein gradient for directing neurite outgrowth. *Drug delivery and translational research*, 1:147-160.

Pilaz LJ, Patti D, **Marcy G**, Olier E, Pfister S, Douglas RJ, Betizeau M, Gautier E, Cortay V, Doerflinger N, Kennedy H and Dehay C (2009). Forced G1-phase reduction alters mode of division, neuron number, and laminar phenotype in the cerebral cortex. *PNAS*, 51:21924-21929.

Wianny F, Bernat A, Huissoud C, **Marcy G**, Markossian S, Cortay V, Giroud P, Leviel V, Kennedy H, Savatier P, and Dehay C (2008). Derivation and cloning of a novel rhesus embryonic stem cell line stably expressing tau-green fluorescent protein. *Stem Cells*, 6:1444-1453.

*Fluckiger A. C, ***Marcy G**, Marchand M, Negre D, Cosset FL, Mitalipov S, Wolf D, Savatier P, and Dehay C (2006). Cell cycle features of primate embryonic stem cells. *Stem Cells*, 3:547-556.

9. Additional Publications

Publications referred below were not discussed in this manuscript but were part of my PhD projects. They are attached.

Azim K, Angonin D, **Marcy G**, Pieropan F, Rivera A, Donega V, Cantù C, Williams G, Berninger B, Butt AM, Raineteau O (2017). Pharmacogenomic identification of small molecules for lineage specific manipulation of subventricular zone germinal activity. **Plos Biology**, 15(3):e2000698.

Angonin D, **Marcy G** and Raineteau O (2015). Postnatal Subventricular zone regionalization by morphogens. **Médecine Sciences: M/S**, 11:968-70.

Résumé

Lors du développement, la coordination d'événements moléculaires et cellulaires mène à la production du cortex cérébral. Son développement s'effectue par étapes : les cellules gliales radiales (RGs), cellules souches neurales (NSCs) du cerveau en développement, génèrent séquentiellement des nouveaux neurones qui formeront les couches corticales. Autour de la naissance, les RGs changent de devenir et produisent des cellules gliales. Cependant, une fraction persiste tout au long de la vie dans la zone sous ventriculaire (SVZ) bordant le ventricule et produisent ensuite les différents interneurons du bulbe olfactif ainsi que des cellules gliales en fonction de leur origine spatiale.

Ces observations soulèvent d'importantes questions non résolues sur 1) le codage transcriptionnel régulant la régionalisation de la SVZ, 2) le potentiel des NSCs postnatales dans la réparation cérébrale, et 3) le lignage et les spécificités transcriptionnelles entre les NSCs et leurs descendants.

J'ai développé des approches bio-informatiques pour connecter l'expression de facteurs de transcription avec la genèse régionale de lignages neuraux distincts et pour comparer des progéniteurs pré et postnataux à l'échelle de la cellule unique.

Ces résultats soulignent le potentiel des études transcriptomiques à résoudre des questions fondamentales comme les changements moléculaires intervenant dans une population de progéniteurs au cours du temps et participant aux changements de leur destinée. Cette connaissance sera la clé d'approches novatrices pour recruter et promouvoir des types cellulaires spécifiques, incluant les sous-types neuronaux dans un contexte pathologique.

Mots Clés

Cellules souches neurales, Progéniteurs, Zone sous-ventriculaire, Séquençage d'ARN sur cellule unique, Lésion corticale, Etude transcriptomique

Abstract

During development, remarkable coordination of molecular and cellular events leads to the generation of the cortex, which orchestrates most sensorimotor and cognitive functions. Its development occurs in a stepwise manner: radial glia cells (RGs) - the neural stem cells (NSCs) of the developing brain - sequentially give rise to distinct waves of nascent neurons that form cortical layers. Around birth, RGs switch fate to produce glial cells. A fraction of neurogenic RGs however persists throughout postnatal life in the subventricular zone (SVZ) that lines the lateral ventricles. These NSCs give rise to different subtypes of olfactory bulb interneurons and glial cells, according to their spatial origin within the postnatal SVZ.

These observations raise important unresolved questions on 1) the transcriptional coding of postnatal SVZ regionalization, 2) the potential of postnatal NSCs for cellular regeneration and brain repair, and 3) the lineage relationship and transcriptional specificities of postnatal NSCs and of their progenies.

I developed bioinformatics approaches to relate expression of defined transcription factors to the regional generation of distinct neural lineages and to explore and compare select populations of pre- and postnatal progenitors at the single cell level.

These data highlight the potential of transcriptomic studies to unravel fundamental questions such as transcriptional changes occurring in a population of progenitors over time and participating to changes in their fate potential. This knowledge will be key in developing innovative approaches to recruit and promote the generation of specific cell types, including neuronal subtypes in pathologies.

Keywords

Neural stem cells, Progenitors, Subventricular zone, Single-cell RNA sequencing, Cortical lesion, Transcriptional profiling